



University of
Nottingham
UK | CHINA | MALAYSIA

Novel insights into ascorbic acid skin permeation

Jatin Mistry MChem

Thesis submitted to the University of Nottingham
for the degree of Doctor of Philosophy

School of Pharmacy

September 2019

Abstract

Ascorbic acid (vitamin C) is a popular topically applied cosmeceutical due to its antioxidative, photoprotective, antiaging and antipigmentary effects. Despite these beneficial effects to the skin, instability of ascorbic acid in aqueous solution has directed formulation scientists to focus on stable ascorbic acid derivatives that can be used in topical preparations. However, these derivatives are required to be metabolised by the skin to the active, free-acid form to observe efficacy. Accordingly, current knowledge regarding skin permeation of ascorbic acid is limited, with *in vivo* human skin permeation data unavailable.

The aim of this work was to use imaging techniques, specifically time of flight-secondary ion mass spectrometry (ToF-SIMS), to visualise the spatial distribution of topically applied ascorbic acid in the skin without the requirement for chemical labelling. This was performed in conjunction with established analytical techniques, such as high performance liquid chromatography (HPLC), that are traditionally used for skin permeation studies to obtain absolute quantitative information but with no spatial component. This dual approach provides the opportunity to reveal new insights into ascorbic acid skin permeation that would not be possible with one analytical technique alone.

A comprehensive study comparing ascorbic acid and caffeine permeation, believed to be the first of its kind, shows how a gel formulation can retard the permeation of ascorbic acid but enhance the permeation of caffeine through *ex vivo* porcine skin tissue. The gel formulations were rubbed into the skin, to mimic in use conditions. When examining the spatial distribution, ascorbic acid and caffeine were found to be non-uniformly distributed and primarily localised to the epidermis. Contrary to previous reports that the follicular route contributes approximately 50% of the total *in vitro* skin permeation, no localisation of caffeine was observed in the hair follicle.

Nanostructured lipid carrier (NLC) formulations have been intensively investigated as topical formulation vehicles. Herein an NLC formulation, and a

comparator cream formulation, were developed and tested on human skin *in vivo* for permeation. Analysis of tape strip samples by HPLC analysis showed the cream formulation to deliver the most ascorbic acid into the *stratum corneum*. However, analysis of tape strip samples from cream-treated skin, by ToF-SIMS, showed the ascorbic acid was mainly localised in the furrows of the skin. A direct correlation between ToF-SIMS and HPLC, performed for the first time, showed that for the NLC formulation, ascorbic acid was more laterally distributed over the corneocytes at all concentrations, and not just localised to skin furrows, than the cream formulation.

An ideal topical preparation should deliver the active ingredient into the corneocytes. Uncovering the spatial distribution, and localisation, of the permeant in the skin barrier has facilitated identification of the NLC formulation to be the most suitable topical preparation for ascorbic acid; and therefore, have the potential to increase the therapeutic effects observed in the skin. Dependence on the established analytical techniques, used for skin permeation studies would have resulted in an altogether different conclusion being reached.

The standard approach of using HPLC, as advised by regulatory bodies, provides limited information about skin permeation due to a lack of imaging capability. The application of imaging techniques, such as ToF-SIMS, in this work has shown unequivocally permeation behaviour different from current literature understanding and a permeation profile different from conventional chromatography based methodology. It was therefore demonstrated that information regarding spatial distribution of the permeant in the skin barrier is essential to gaining a more holistic understanding of the mechanisms and routes of skin permeation when evaluating the effectiveness of topically applied formulations.

Acknowledgements

I would like to sincerely thank Dr David Scurr, my primary supervisor, for his support, dedication, advice and long discussions which guided the PhD work and preparation of the thesis. I am also grateful to Prof David Barrett, Dr Jake Hicks (of Walgreens Boots Alliance) and Dr Nichola Starr for their supervision and guidance. I would like also to extend my gratitude to Prof Bruno Sarmiento, Dr Marta de Oliveira Ferreira and Ana Rita Matias, of Inovapotek, for making me feel most welcome in Portugal and their assistance with the clinical trial. I am deeply grateful to all my supervisors for their patience and their sharing of knowledge and experience imparted to me.

I would also like to thank the examiners, Prof Jon Heylings and Dr Mischa Zelzer, for their helpful suggestions and advice.

Technical assistance and training received from all university staff is truly appreciated, especially Paul Cooling, Dr Chris Parmenter, Denise Mclean and John Corbett.

I am indebted to all my friends with whom I had a pleasure and honour to work with during this research progression. I wish to thank Akmal Bin Sabri, Dr Yogeeta Rocha and Cláudia Martins in particular for scientific and non-scientific discussions. Hooi May Teoh and Jennie Chang are also thanked for their assistance in the lab.

I would like to acknowledge funding received by the EPSRC under grant no. EP/L01646X (CDT in Advanced Therapeutics and Nanomedicines) and the Horizon 2020 MSCA-RISE programme under grant no. 691128 (FutForm) from the University of Nottingham.

A heartfelt thank you to my mum, dad and brother Jay for their love, support, understanding and unwavering belief in me.

Lastly, to you all and many others included but unmentioned, thank you for your support and encouragement however small or not our interaction may have been.

Table of Contents

Chapter 1: General Introduction	1
1.1 Skin structure and function	1
1.1.1 Epidermis	1
1.1.2 Dermis.....	2
1.1.3 Hypodermis.....	3
1.1.4 Skin appendages	3
1.2 Monitoring skin permeation	3
1.2.1 Routes of permeation	4
1.2.2 Physicochemical properties of compounds affecting permeation ..	5
1.2.3 <i>In vitro</i> permeation studies	5
1.2.4 <i>In vivo</i> permeation studies	10
1.2.5 Dose applied to skin.....	14
1.3 Analytical techniques for studying skin permeation	15
1.3.1 Liquid chromatography and spectrophotometry methods	15
1.3.2 Imaging spectrophotometry methods	17
1.3.3 Imaging mass spectrometry methods.....	18
1.4 Skin permeation enhancement	25
1.4.1 Physical and chemical skin permeation enhancement strategies	25
1.4.2 Topical preparations	27
1.5 Topical delivery of ascorbic acid	30
1.5.1 Skin benefits	31
1.5.2 Summary of efficacy studies	32
1.5.3 Summary of skin permeation studies.....	33
1.5.4 Topical formulations.....	35
1.6 Topical delivery of caffeine	38
1.6.1 Skin benefits	38
1.6.2 Existing skin permeation data.....	38
1.7 Aims of this thesis	40

Chapter 2: Optimisation of the experimental approach to study skin permeation of ascorbic acid and caffeine.....	41
2.1 Introduction.....	41
2.2 Chapter aims	42
2.3 Materials and methods	43
2.3.1 Materials	43
2.3.2 Porcine ear skin collection and preparation.....	43
2.3.3 Franz diffusion cell permeation experiment.....	44
2.3.4 Freezing and cryo-ultramicrotome of skin tissue	44
2.3.5 Tape stripping of <i>stratum corneum</i>	46
2.3.6 UV-Vis analysis.....	46
2.3.7 HPLC analysis	46
2.3.8 ToF-SIMS analysis	47
2.3.9 CRM analysis	48
2.3.10 Protein quantification of tape strip samples	48
2.3.11 Statistics.....	50
2.4 Results and discussion	51
2.4.1 Analysis of skin cross sections without embedding material	51
2.4.2 Investigating the permeation of ascorbic acid and caffeine by imaging techniques	53
2.4.3 Assessing stability of ascorbic acid in aqueous solution.....	61
2.4.4 Method development for extraction of ascorbic acid from tape strip samples	68
2.4.5 Quantification of protein on tape strip samples collected after ascorbic acid skin permeation.....	70
2.5 Conclusions.....	74
 Chapter 3: Comparative study of ascorbic acid and caffeine permeation into <i>ex vivo</i> porcine skin.....	 75
3.1 Introduction.....	75
3.2 Chapter aims	76
3.3 Materials and methods.....	77

3.3.1	Materials	77
3.3.2	Preparation of ascorbic acid and caffeine formulations	77
3.3.3	Formulation stability.....	78
3.3.4	<i>Ex vivo</i> skin permeation experiment.....	78
3.3.5	UV-Vis spectroscopy and ToF-SIMS Analysis.....	79
3.3.6	Statistics.....	79
3.4	Results and discussion	80
3.4.1	Stability of cosolvent and gel formulations.....	80
3.4.2	Effect of receptor fluid pH on skin permeation	83
3.4.3	Transdermal permeation of ascorbic acid and caffeine	84
3.4.4	Amount of permeant detected in epidermis and dermis of excised skin and intact skin permeation experiments.....	88
3.4.5	Permeation distribution of ascorbic acid and caffeine in porcine skin <i>ex vivo</i>	90
3.4.6	Statistical analysis of ascorbic acid and caffeine permeation into epidermis and dermis by ToF-SIMS.	94
3.4.7	Variability in ascorbic acid and caffeine ion intensity in epidermis of skin cross sections.	96
3.5	Conclusions.....	98
Chapter 4: Preparation and characterisation of ascorbic acid lipid nanoparticle formulations		100
4.1	Introduction.....	100
4.2	Chapter aims	100
4.3	Materials and methods.....	101
4.3.1	Materials	101
4.3.2	Preparation of NLC formulation.....	101
4.3.3	Preparation of cream formulation.....	103
4.3.4	Dynamic light scattering.....	103
4.3.5	Association efficiency	103
4.3.6	Formulation stability testing.....	104
4.3.7	Cryo-transmission electron microscopy	105
4.3.8	Laser diffraction particle size analysis	105

4.3.9	Rheology.....	106
4.3.10	ToF-SIMS analysis of formulations	106
4.3.11	Statistics.....	106
4.4	Results and discussion	107
4.4.1	NLCs with composition suitable for topical use.....	107
4.4.2	Characterisation of particle/droplet size, and charge, of NLCs and cream.....	107
4.4.3	Association efficiency of NLCs.....	111
4.4.4	Stability of emulsion and ascorbic acid in the formulations.....	113
4.4.5	Imaging of NLC nanoparticles using Cryo-TEM.....	116
4.4.6	Rheological properties of lipid nanoparticle and cream formulations.....	118
4.4.7	Identifying secondary ions in ToF-SIMS spectra of the formulation that could be used to monitor skin permeation.....	120
4.5	Conclusions.....	125
Chapter 5: <i>In vivo</i> and <i>ex vivo</i> assessment of ascorbic acid permeation amount and distribution in the <i>stratum corneum</i> from lipid nanoparticle formulation		
126		
5.1	Introduction.....	126
5.2	Chapter aims	127
5.3	Materials and Methods.....	128
5.3.1	<i>Ex vivo</i> tape stripping test.....	128
5.3.2	<i>In vivo</i> tape stripping test.....	129
5.3.3	Analysis of tape strip samples	130
5.3.4	Statistics.....	131
5.4	Results and Discussion	132
5.4.1	Depth of <i>stratum corneum</i> removed by tape stripping	132
5.4.2	Amount of formulation topically applied	133
5.4.3	Amount of ascorbic acid skin permeation	134
5.4.4	Distribution and localisation of ascorbic acid in the <i>stratum corneum</i>	140

5.4.5	HPLC and ToF-SIMS analytical method correlation	147
5.4.6	Formulation effects on skin hydration.....	151
5.5	Conclusions.....	154
Chapter 6:	Conclusions and general discussion	156
6.1	General conclusions	156
6.2	Future work and recommendations.....	160
Chapter 7:	References.....	165
Chapter 8:	Appendix I - Supplementary figures.....	185
Chapter 9:	Appendix II - <i>In vivo</i> study ethical approval.....	196

Figures

<i>Figure 1-1 Schematic diagram of skin structure.</i>	1
<i>Figure 1-2 Schematic diagram of epidermis.</i>	2
<i>Figure 1-3 Schematic of drug penetration routes across the stratum corneum.</i>	4
<i>Figure 1-4 Schematic diagram of a vertical Franz-type static diffusion cell.</i>	6
<i>Figure 1-5 Confocal laser scanning microscopy image of excised human skin in (A) Franz diffusion cell and (B) Saarbruecken model.</i>	8
<i>Figure 1-6 Schematic representation of the tape-stripping process.</i>	11
<i>Figure 1-7 Schematic diagram showing tape stripping over a skin furrow.</i>	12
<i>Figure 1-8 Methods to assess follicular permeation. (A) Follicular closing technique and (B) differential tape stripping.</i>	16
<i>Figure 1-9 Schematic diagram of ToF-SIMS instrument and collision cascade (yellow arrows) caused by primary ion bombardment of sample surface.</i>	20
<i>Figure 1-10 ToF-SIMS images of various chlorhexidine digluconate specific ions on tape strips from untreated and chlorhexidine treated ex vivo porcine skin.</i>	24
<i>Figure 1-11 Localisation of topically applied carvacrol in the eccrine sweat gland (yellow circle) of ex vivo porcine skin.</i>	25
<i>Figure 1-12 Skin occlusion effect of lipid nanoparticles depending on their size.</i>	29
<i>Figure 1-13 Oxidation and degradation pathway for ascorbic acid.</i>	30
<i>Figure 1-14 Caffeine molecular structure and physiochemical properties.</i>	38
<i>Figure 1-15 Comparison of mean absorption of applied caffeine in vivo (blue) and in vitro (red).</i>	39
<i>Figure 2-1 Schematic of liquid nitrogen vapour freezing method.</i>	45
<i>Figure 2-2 Normalised ToF-SIMS intensity of (A) $C_2H_3O^+$ ($m/z = 43$) and (B) $C_2H_3O_2^-$ ($m/z = 59$), which are OCT compound associated fragment ions, from the epidermis region of interest (ROI).</i>	52
<i>Figure 2-3 Optical profilometer image of porcine skin cross sections with (A) and without (B) OCT embedding.</i>	53
<i>Figure 2-4 Ascorbic acid and caffeine ToF-SIMS reference spectra.</i>	54
<i>Figure 2-5 Negative-ion ToF-SIMS images (B-D) of an untreated porcine ear skin cross section.</i>	56

<i>Figure 2-6 Positive-ion ToF-SIMS images (B-D) of an untreated porcine ear skin cross section.</i>	57
<i>Figure 2-7 ToF-SIMS ion images of (A) untreated porcine skin and (B) ascorbic acid treated skin.</i>	58
<i>Figure 2-8 Confocal Raman spectra of ascorbic acid (AA), untreated stratum corneum and AA treated stratum corneum of porcine skin cross section.</i>	59
<i>Figure 2-9 ToF-SIMS data for an example skin tape strip sample showing the thresholding process from original (A) to post-threshold (F).</i>	61
<i>Figure 2-10 UV-Vis absorbance spectra of (A) ascorbic acid, dehydroascorbic acid and (B) caffeine in 25 mM MPA solution.</i>	62
<i>Figure 2-11 Stability of ascorbic acid and caffeine in PBS buffer and MPA solution at 36.5 °C.</i>	63
<i>Figure 2-12 HPLC chromatogram of ascorbic acid (A), caffeine (B) and untreated porcine skin Franz cell receptor fluid (A and B).</i>	65
<i>Figure 2-13 HPLC chromatogram of untreated porcine skin tape strip (A), untreated human skin tape strip (B), and ascorbic acid (A and B).</i>	66
<i>Figure 2-14 Stability of ascorbic acid in MPA solution (25 mM, pH 2.4) at ambient temperature (18-22 °C).</i>	67
<i>Figure 2-15 Percent recovery of ascorbic from spiked tape strips by extraction methods A-C.</i>	69
<i>Figure 2-16 Evaluation of Pierce™ 660 nm Protein Assay Kit for determining protein content of tape strips.</i>	71
<i>Figure 2-17 Protein content of tape strip samples, with increasing tape strip number, determined by infrared densitometry.</i>	72
<i>Figure 2-18 Optical profilometer image of human and porcine corneocytes on Corneofix® tape.</i>	73
<i>Figure 3-1 Schematic diagram of ex vivo porcine ear skin permeation experiment with intact and excised skin.</i>	78
<i>Figure 3-2 Stability of ascorbic acid and caffeine cosolvent formulations made with varying ethanol concentrations.</i>	81
<i>Figure 3-3 Stability of ascorbic acid and caffeine gel formulations made with varying PG concentrations.</i>	82
<i>Figure 3-4 Skin permeation of caffeine, from cosolvent formulation, with different Franz cell receptor fluid.</i>	84

<i>Figure 3-5 (A) Thickness of skin used and (B) weight of formulation applied in ex vivo permeation experiment.</i>	85
<i>Figure 3-6 Concentration of ascorbic acid and caffeine in Franz cell receptor compartment after application of cosolvent and gel formulations.</i>	85
<i>Figure 3-7 Comparing ToF-SIMS ion intensity from excised skin and intact skin cross section regions of interest (ROI) after ex vivo permeation experiment.</i>	89
<i>Figure 3-8 Representative ToF-SIMS secondary ion images of excised skin and intact skin cross sections, highlighting the spatial distribution of ascorbic acid</i>	91
<i>Figure 3-9 Representative ToF-SIMS secondary ion images of excised skin and intact skin cross sections, highlighting the spatial distribution of caffeine.</i>	92
<i>Figure 3-10 Exported ToF-SIMS data showing average secondary ion intensities for ascorbic acid and caffeine in epidermis and upper dermis ROI (A and C) and lower dermis ROI (B and D).</i>	95
<i>Figure 3-11 Change in average secondary ion intensity, of (A) ascorbic acid and (B) caffeine, with number of cross sections analysed.</i>	97
<i>Figure 4-1 Schematic of double-emulsion NLC preparation by solvent emulsification-evaporation method.</i>	102
<i>Figure 4-2 Size distribution of ascorbic acid encapsulated NLC with ultrasonication time of 3 minutes (NLC B) and 1 minute (NLC D).</i>	109
<i>Figure 4-3 Droplet size distribution of cream formulation, measured by laser diffraction.</i>	110
<i>Figure 4-4 Stability photographs of positive control, NLC and cream formulations.</i>	114
<i>Figure 4-5 Ascorbic acid concentration of positive control, lipid nanoparticle and cream formulation over time at (A) 4 °C, (B) 18 °C and (C) 40 °C.</i>	115
<i>Figure 4-6 Representative cryo-TEM images of ascorbic acid loaded lipid nanoparticle formulation</i>	117
<i>Figure 4-7 Oscillatory amplitude sweep versus the shear stress τ, of cream and lipid nanoparticle formulation.</i>	119
<i>Figure 4-8 Shear-rate dependent viscosity curves of cream and lipid nanoparticle formulation at 32 °C.</i>	120

<i>Figure 4-9 ToF-SIMS normalised ion intensities of lipid nanoparticle formulation made with and without ascorbic acid in negative polarity.</i>	121
<i>Figure 4-10 Overlay of ingredient ToF-SIMS spectra in negative polarity, normalised to total ion intensity.</i>	122
<i>Figure 4-11 Normalised ion intensities of positive control, lipid nanoparticle and cream formulation measured on silicon wafer</i>	123
<i>Figure 5-1 Depth of the stratum corneum (SC) reached after removal of 30 sequential tape strips on ex vivo porcine skin (A) and after removal of 15 sequential tape strips on in vivo human skin (B).</i>	132
<i>Figure 5-2 Weight of formulation applied to skin test sites ex vivo (C) and in vivo (D).</i>	133
<i>Figure 5-3 Ascorbic acid stratum corneum permeation profile in ex vivo porcine skin (A) and in vivo human skin (B).</i>	135
<i>Figure 5-4 Statistical analysis of in vivo human stratum corneum ascorbic acid permeation by taking the area under the curve (method 1) or the sum of tape strips 3 through to 15 (method 2).</i>	137
<i>Figure 5-5 Ascorbic acid recovered in sponge wipe and superficial tapes (A) and unrecovered ascorbic acid (B).</i>	140
<i>Figure 5-6 Normalised intensity of ascorbic acid [M-H]⁻ ion (A), sum of ascorbic acid associated ions (B), lauric acid [M-H]⁻ ion (C) and sum of excipient associated ions (D) with increasing tape strip depth.</i>	141
<i>Figure 5-7 ToF-SIMS ion images of porcine tape strips collected at a SC depth of approximately 3.2 μm.</i>	143
<i>Figure 5-8 ToF-SIMS ion images of human tape strips collected at a SC depth of approximately 2.1 μm.</i>	144
<i>Figure 5-9 ToF-SIMS ion images pre and post thresholding to select corneocyte containing areas on tape strips</i>	145
<i>Figure 5-10 Ascorbic acid human stratum corneum penetration profile determined by HPLC analysis (A) and ToF-SIMS analysis (B) of tape strip samples.</i>	148
<i>Figure 5-11 HPLC quantification of ascorbic acid correlation with ToF-SIMS ascorbic acid [M-H]⁻ ion intensity from tape strip samples from human skin</i>	149

Figure 5-12 TEWL increase 60 minutes after product application (A) and after removal of 15 sequential tape strip layers (B) from in vivo human skin.....152

Tables

<i>Table 1-1 Comparison of imaging mass spectrometry techniques</i>	19
<i>Table 1-2 Previous ToF-SIMS studies on skin samples.</i>	22
<i>Table 1-3 Summary of ascorbic acid skin permeation studies.</i>	34
<i>Table 1-4 Summary of recent nanoparticles encapsulating ascorbic acid in the literature.</i>	37
<i>Table 2-1 Intra-day (n=6) and inter-day (n=11) precision and accuracy of ascorbic acid HPLC method.</i>	67
<i>Table 2-2 HPLC method matrix effect of ascorbic acid in skin tape extraction matrix.</i>	68
<i>Table 2-3 Extraction recovery of ascorbic acid, from tape strip samples and sponge, based on a formulation application of 10 mg/cm² containing 5% w/w ascorbic acid.</i>	70
<i>Table 4-1 Hydrodynamic diameter, polydispersity index (PDI) and zeta potential of NLCs A-E and cream.</i>	108
<i>Table 4-2 Association efficiency (AE) and drug loading (DL) of NLCs A-E and cream.</i>	112
<i>Table 5-1 Composition of test formulations (% w/w).</i>	128
<i>Table 5-2 Comparison of test formulations for their delivery of ascorbic acid into human stratum corneum by taking the area under the curve from 0.7 to 3.5 μm (units of $\mu\text{m}.$% ascorbic acid applied).</i>	138

Abbreviations

[M+H] ⁺	Molecular ion in positive ionisation mode
[M-H] ⁻	Molecular ion in negative ionisation mode
AE	Association efficiency
AG	Ascorbyl glucoside
ANOVA	Analysis of variance
AOAC	Association of Official Analytical Chemists
AP	Ascorbyl palmitate
BCA	Bicinchoninic acid
BSA	Bovine serum albumin
CIR	Cosmetic Ingredient Review
CLSM	Confocal laser scanning microscopy
CRM	Confocal Raman microspectroscopy
Da	Dalton
DESI-MS	Desorption electrospray ionisation mass spectrometry
DL	Drug loading
DLS	Dynamic light scattering
EAC	3-O-Ethyl ascorbate
EC	European Commission
EDXS	Energy dispersive x-ray spectroscopy
EU	European Union
FDA	USA Food and Drug Administration
GRAS	Generally recognised as safe
H&E	Haemotoxylin and eosin
HPLC	High performance liquid chromatography
HPMC	Hydroxyl methylcellulose
logP	Partition coefficient (octanol: water)
LOQ	Limit of quantification
m/z	Mass-to-charge
MALDI-MS	Matrix assisted laser desorption ionisation mass spectrometry
MAP	Magnesium ascorbyl phosphate
mAU	Milliabsorption unit
MMPs	Matrix metalloproteins
MPA	Metaphosphoric acid
MW	Molecular weight
NLC	Nanostructured lipid carrier
O/W	Oil in water
°C	Degree centigrade
OCT	Optimal cutting temperature
OECD	Organisation for Economic Cooperation and Development

PAMPA	Parallel artificial membrane-permeability assay
PBS	Phosphate buffered saline
PDI	Polydispersity index
PEG	Polyethylene glycol
PG	Propylene glycol
PVA	polyvinyl alcohol
q.s.	<i>quantum satis</i>
RE	Relative error
ROI	Region of interest
ROS	Reactive oxygen species
RSD	Relative standard deviation
S: N	Signal: noise
SCCS	Scientific Committee on Consumer Safety
SD	Standard deviation
SEM	Standard error of the mean
SLN	Solid lipid nanoparticle
TEER	Transepidermal electrical resistance
TEM	Transmission electron microscopy
TEWL	Transepidermal water loss
ToF-SIMS	Time of flight-secondary ion mass spectrometry
TWF	Transepidermal water flux
UV	Ultraviolet
UV-Vis	Ultraviolet-visible
v/v	Volume by volume
W/O	Water in oil
W/O/W	Water in oil in water
w/v	Weight by volume
w/w	Weight by weight
WHO	World Health Organisation
XRF	X-ray fluorescence

Chapter 1: General Introduction

1.1 Skin structure and function

The skin is the largest organ of the human body. It accounts for about 10% of total body weight and covers a body surface area of approximately 1.7 m² for the average adult. The main function of the skin is to provide a protective barrier between the body and the external environment. The barrier protects against the permeation of ultraviolet (UV) radiation, chemicals, allergens and microorganisms, and the loss of moisture and body nutrients. The skin also plays a key role in regulation of body temperature and acts as a sensory organ.¹ The skin is a complex, multi-layered structure that can be divided into three layers: epidermis, dermis and hypodermis (subcutaneous tissue). In addition, the skin contains appendages such as hair follicles, sweat glands and sebaceous glands as shown in Figure 1-1.²

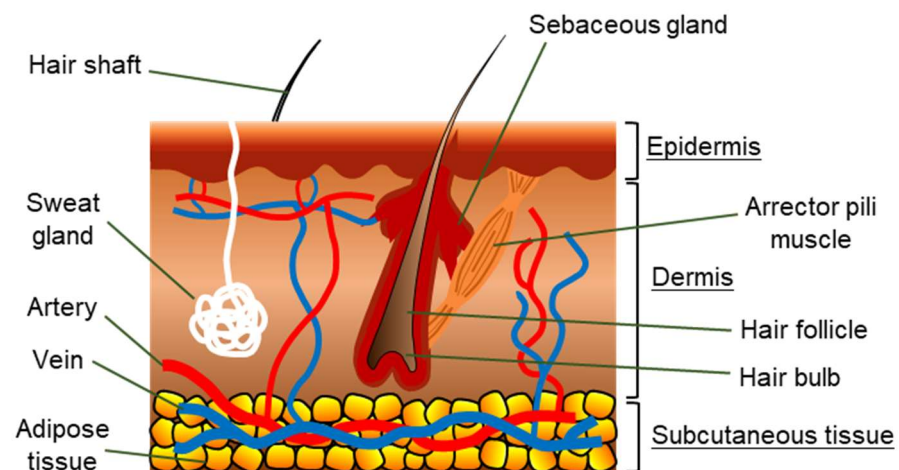


Figure 1-1 Schematic diagram of skin structure. Adapted from Ng et al.²

1.1.1 Epidermis

The epidermis is the outermost, avascularised layer of the skin, and varies in thickness from 0.06 mm on the eyelids to about 0.8 mm on the palms of the hands. The epidermis consists predominantly of keratinocytes (approximately 95% of cells), which are at various stages of differentiation progressing from the most inward layer of the epidermis (*stratum basale*) upwards to the *stratum corneum*, as shown in Figure 1-2.¹

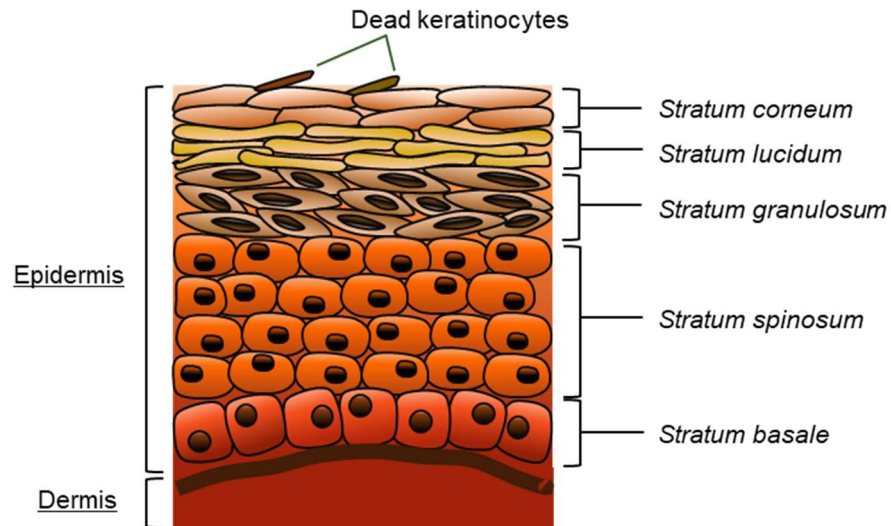


Figure 1-2 Schematic diagram of epidermis. Adapted from Maibach et al.³

Keratinocytes differentiate terminally into elongated (40-60 μm wide), flattened (about 0.2-0.8 μm thick), non-nucleated, non-viable cells called corneocytes.⁴⁻⁶ The *stratum corneum* is typically 10-20 μm thick and composed of 10-20 layers of corneocytes which are embedded in an extracellular lipid matrix. This organisation of the *stratum corneum* is commonly referred to as the ‘brick and mortar’ model where the corneocytes and extracellular matrix are likened to bricks and mortar respectively.^{7,8} The corneocytes are connected by structural protein links, called desmosomes, which are enzymatically digested in a process called desquamation. Desquamation results in the sloughing of corneocytes at the skin surface with the *stratum corneum* typically renewing in 14 days.⁹

The *stratum corneum* contains 15-20% water that is primarily associated with the keratin in the corneocytes.¹⁰ The extracellular matrix is composed of cholesterol, free fatty acids and ceramides. These lipids adopt a highly ordered, 3-dimensional structure of stacked densely packed lipid layers (lamellae).^{11,12} The structural properties of the *stratum corneum* are pivotal to its role as the major barrier to permeation of exogenous molecules.²

1.1.2 Dermis

The dermis is approximately 2-5 mm in thickness and consists primarily of fibroblast cells embedded in an extracellular matrix of structural proteins,

mainly collagen and elastin, which give strength and elasticity to the skin. The dermis also contains hair follicles, sweat glands, sebaceous glands, sensory nerve endings, lymphatic vessels and blood capillaries. The blood supply provides oxygen and nutrients to and removes toxins and waste products from the dermis. The blood supply also removes permeated molecules into systemic circulation.^{1,10}

1.1.3 Hypodermis

The hypodermis, or subcutaneous tissue layer, consists of a layer of fat cells. The primary function of the hypodermis is heat insulation and protection against physical shock.¹

1.1.4 Skin appendages

Skin appendages consist of hair follicles, sweat, and sebaceous glands. Hair follicles cover around 0.1% of the skin surface area except on the palms of the hands and soles of the feet.¹ Hair follicles produce hair fibres in a regular cycle. Hair performs several functions such as protection from environmental influences (allergens, UV radiation, cold temperature) and aiding sensory perception.¹³ The sebaceous glands, which are associated with hair follicles, secrete sebum, which consists of triglycerides, fatty acids and waxes, to lubricate the skin surface and maintain skin surface pH at around 5. The sweat glands secrete sweat in response to heat and emotional stress.¹

1.2 Monitoring skin permeation

The skin is not optimised to favour the permeation of substances from the external environment, but rather, to provide a protective barrier. This makes the delivery of drugs to and through the skin challenging for pharmaceutical and formulation scientists.¹⁴ Topical drug delivery, however, can be advantageous over oral administration since it bypasses the harsh conditions of the gastrointestinal tract and hepatic first-pass metabolism. In addition due to the easy accessibility of the skin, and non-invasive nature of topical drug delivery, it is considered as more patient compliant compared to parenteral administration which is associated with pain and and/ or a requirement for

trained personnel.^{15,16} For topically applied pharmaceuticals and cosmetics, permeation through the skin barrier is essential for developing their effects.

1.2.1 Routes of permeation

Molecules can permeate the *stratum corneum* via either the transepidermal pathway or the appendageal pathway as illustrated in Figure 1-3.

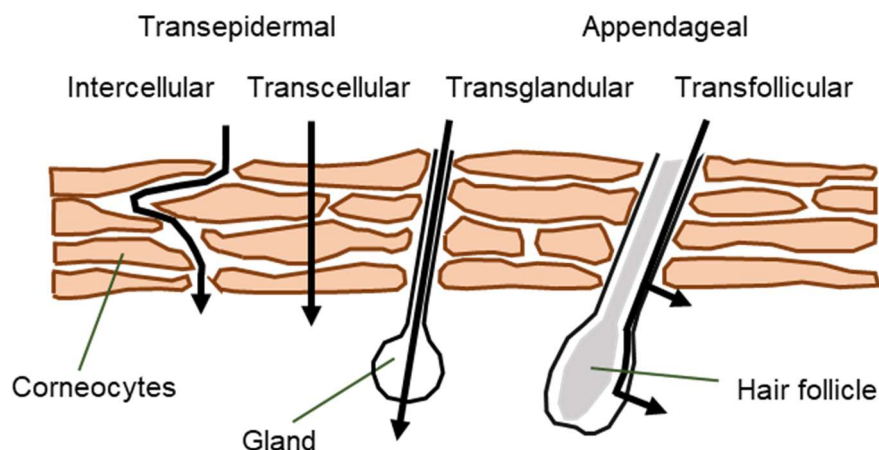


Figure 1-3 Schematic of drug penetration routes across the *stratum corneum*.
Adapted from Trommer et al.¹⁷

1.2.1.1 Transepidermal pathway

Molecules can permeate the *stratum corneum* either intercellularly, by going around the corneocytes through the lipid matrix, or transcellularly, by taking the route across alternating layers of corneocytes and lipid matrix. The transcellular route is the shortest route, however, molecules are required to partition multiple times between the lipophilic intercellular domain and the more hydrophilic corneocytes. On the other hand, the lipid matrix is the only continuous domain in the *stratum corneum* and so the view of most skin scientists is that the intercellular route is the most predominant route of permeation.¹ This view is supported by empirical data which demonstrates chemical penetration enhancers which disrupt lipid organisation enhance skin permeation¹⁸, lipid extraction reduces *stratum corneum*'s barrier function¹⁹, and using multiphoton laser scanning microscopy skin permeation of gold nanoparticles (15 nm in size) was found to occur predominantly via the lipid matrix²⁰. This is despite the diffusional pathlength estimated for intercellular

route to be around 300-900 μm , much longer than the thickness of the *stratum corneum* (20 μm).¹⁴ It is thought that small hydrophilic molecules may generally favour the transcellular route over the intercellular route.²

1.2.1.2 Appendageal pathway

Skin appendageal routes, where drug molecules are transported via sweat glands (transglandular) or hair follicles (transfollicular), circumvent penetration through the *stratum corneum*.²¹ The skin appendages occupy $\sim 0.1\%$ of the total human skin area and so the appendageal routes are considered to make only a small or insignificant contribution to drug penetration.¹⁷ The transfollicular route may be important for the permeation of very high molecular weight substances with low diffusion coefficients, e.g. nanoparticles²², and hydrophilic molecules, e.g. caffeine.^{23,24} Advantages of transfollicular route include enhanced permeation depth and prolonged residence duration of drug in the hair follicle.²⁵

1.2.2 Physiochemical properties of compounds affecting permeation

The relative contribution to the different routes of skin permeation will depend on the physiochemical properties of the drug and the formulation.¹ Molecules with intermediate lipophilicity can partition between the lipid and polar microenvironments of the intercellular route. A partition coefficient (log P) of 1-3 is considered to be optimum for skin permeation.^{26,27} Skin permeation is inversely proportional to the size of the molecule, with permeants less than 500 Da considered suitable for topical delivery.²⁸ The permeant should also exhibit reasonable aqueous solubility so it can partition into the viable epidermis by the aqueous pores. An organic molecule, with a melting point below 200 $^{\circ}\text{C}$, is predicted to have suitable aqueous solubility for topical delivery.²⁹

1.2.3 *In vitro* permeation studies

In vitro skin permeation studies are typically performed with Franz diffusion cells, as illustrated in Figure 1-4. In this cell, excised skin is mounted between an upper (donor) chamber and a lower receptor (acceptor) chamber and the permeation of compounds through the skin tissue section is monitored. Franz

cell permeation experiments can provide a platform for the initial assessment of topical drugs and formulations.³⁰ Quick and large scale investigations can be carried out on multiple repeat samples without the need to recruit large numbers of subjects.

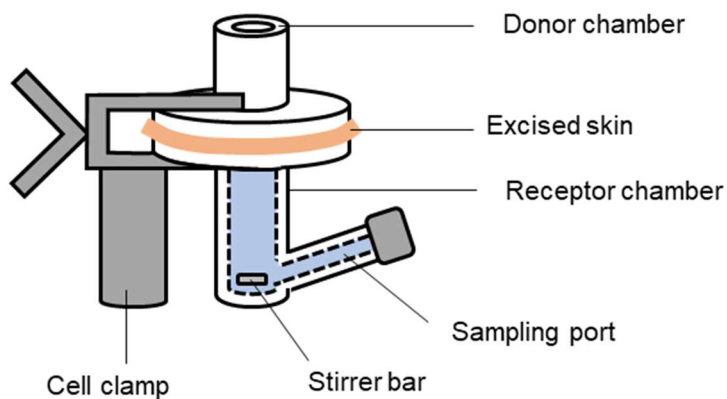


*Figure 1-4 Schematic diagram of a vertical Franz-type static diffusion cell.
Adapted from Finnin et al.³⁰*

Franz cell experiments are widely performed to assess permeation of cosmetic, agrochemical and industrial chemical products that come into contact with the skin and is a key part of human risk assessment.³¹ The Organisation for Economic Cooperation and Development (OECD) has published guidance documents to assist in performing dermal absorption studies (2004, 2011).³²⁻³⁴ The European Commission Scientific Committee on Consumer Safety (SCCS) has provided additional guidance for cosmetic products and dermal absorption testing (2010, 2016).^{35,36} The OECD and SCCS do not provide a specific “one size fits all” protocol as it cannot be appropriate for all test substances however it does require a full justification of the test system experimental parameters.³⁰ Experimental parameters which require justification include, but not limited to, skin species, receptor fluid, integrity testing, test vehicle, dose applied, experimental duration and analytical method validation.^{32,34}

1.2.3.1 Human vs animal tissue

Although *ex vivo* human skin is considered the best surrogate for *in vivo* human skin, it is not readily available and has large variability due to age, gender, race and anatomical site differences.³⁰ *Ex vivo* animal skin can be used

instead to evaluate permeation with porcine ear skin reported to be the most histologically similar to human skin.³⁷

Porcine ear skin has comparable *stratum corneum* thickness of 20 μm , viable epidermis thickness of 70 μm , and dermis thickness of approximately 1.86 mm to human skin. Porcine ear skin also averages 20 hairs/ cm^2 in contrast to humans 14-32 vellus hairs/ cm^2 excepting the forehead. The structure of the hair follicles is also similar to human appendages since they both have an outer root sheet – this is the layer of keratinocytes that are continuous with the interfollicular epidermis (skin). However, the orifices of porcine hair follicles show a diameter of approximately 200 μm , two to three times higher than those on human forearm (78 μm).^{37,38}

Porcine and human *stratum corneum* are described to have similar lipids in the form of ceramides, cholesterol and free fatty acids however the compositions between species are different. Whilst porcine and human *stratum corneum* lipids show similar lamellar organisation, there is a substantial difference in their lateral packing. Porcine *stratum corneum* lipids are arranged predominantly in a hexagonal lattice whereas human lipids are arranged in the denser orthorhombic lattice.^{37,39} Despite this, a range of studies show the permeability of pig skin to be more similar to human skin, for both lipophilic and hydrophilic drugs, than dog or rodent skin.⁴⁰⁻⁴²

There is also the option of using artificial membranes which range from simple homogenous polymer materials, for example poly(dimethoxysilane), through to lipid-based parallel artificial membrane-permeability assay (PAMPA).

Whilst artificial membranes are convenient and more reproducible than animal tissue, they are not capable of representing all *in vivo* skin properties.⁴³

Reconstructed skin models, with layers of human epidermal cells laid in a polymer matrix, may also be used but these are significantly more permeable than human skin but could be used for toxicological screening.³⁷

1.2.3.2 Limitations of Franz diffusion cells

Despite the wide use of Franz cells for *in vitro* permeation studies, they do not fully represent the *in vivo* situation. An alternative to the Franz diffusion cell,

is the Saarbrücken penetration model, where excised skin is mounted on soaked filter paper which sits above a Teflon bloc. In the Saarbrücken model, nonphysiological hydration of the skin is avoided due to the absence of a liquid acceptor medium. Wagner *et al.* (2000)⁴⁴ demonstrated that 5(6)-carboxyfluorescein, loaded into the Franz cell acceptor compartment, permeated upwards into the dermis as shown in Figure 1-5 A. This resulted in an overhydration of the skin tissue, measured by the change in skin thickness, more than would occur under physiological conditions as shown in Figure 1-5 B. The authors reported more flufenamic acid (logP 5.25) permeation in the skin layers when using Franz cell, and this was much greater than the *in vivo* situation. In contrast skin in the Saarbrücken model showed lower permeation consistent with the *in vivo* situation.⁴⁴

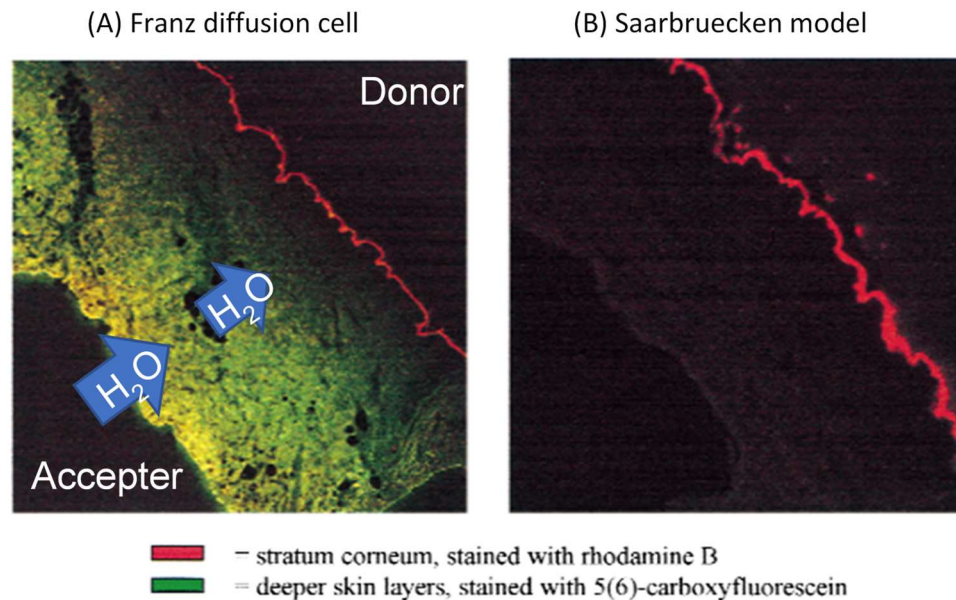


Figure 1-5 Confocal laser scanning microscopy image of excised human skin in (A) Franz diffusion cell and (B) Saarbrücken model. Adapted from Wagner *et al.*⁴⁴

More recently the use of whole pig ears, with the skin left attached to the underlying cartilage, has been proposed as an alternative permeation model by Patzelt *et al.* (2008)⁴⁵. Since the skin is fixed to the underlying cartilage, the elastic fibres do not contract. When skin is resected, the close network of elastic fibres surrounding the hair follicle contract and close the hair follicle. In addition, the elastic fibres between the hair follicles, which are straighter and

more parallel and contribute to skin elasticity, also contract but can also be expanded by stretching the skin out again. Patzelt *et al.*⁴⁵ found the permeation of curcumin into hair follicles was significantly reduced for *in vitro* excised skin compared to *in vivo* situation. D'Alvise *et al.* (2014) reported the permeation of Lidocaine into porcine hair follicles for the first time when using whole pig ears with the underlying cartilage.⁴⁶

1.2.3.3 Skin integrity testing

To avoid unsuitable overprediction of the skin permeation by the use of impaired skin, OECD Guideline 428³⁴ requires a skin integrity check. This can be done by a visual examination of the skin followed by measuring transepidermal electrical resistance (TEER), transepidermal water loss (TEWL) or transepidermal water flux (TWF) of a reference compound.⁴⁷

TWF involves application of an infinite dose of water, with the reference compound, to the skin before and/or after permeation experiment.

Measurement of TWF before could lead to increased tissue hydration and permeability whereas measurement of TWF after could lead to rejection of previously intact skin samples. TWF could be measured concurrently but the additional compound may influence absorption of the test compound.⁴⁷

TEER is also measured before and/or after skin permeation experiment and involves application of an infinite dose of saline solution to acceptor and donor chambers. Once the Franz cell has been equilibrated, for > 30 minutes, TEER can be measured. Measurement of TEER experiences the same limitations as TWF. Despite these concerns, measurement of intact skin barrier function is very important to *in vitro* skin permeation studies.^{47,48}

TEWL is an established technique to evaluate skin barrier function *in vivo* and unlike TWF and TEER no solutions have to be added to perform the barrier integrity test.⁴⁹ However, TEWL is not a well-accepted test *in vitro* since the validity of this method to predict skin permeability is unclear. More recently Zhang *et al.*⁵⁰ determined a TEWL of > 10 g/m²/h should be used as exclusion criteria for *in vitro* permeation studies.

1.2.4 *In vivo* permeation studies

According to the Cosmetics Regulation, European Commission (EC) Regulation No. 1223/2009, it is prohibited in the European Union (EU) to test cosmetic products and ingredients on animals so only human volunteers may be used for *in vivo* permeation studies.⁵¹ Since topical products are designed for human use, clinical trials with human volunteers represents the most clinically relevant situation. However clinical trials are expensive, time-consuming and limited by ethical constraints because the study protocol must be submitted for consideration and approval by a research ethics committee in accordance with the World Medical Association's 1964 Declaration of Helsinki.⁵² *In vivo* human skin permeation may be assessed by tape stripping, micro dialysis, skin biopsy and confocal Raman spectroscopy (discussed later in section 1.3.2).⁵³

1.2.4.1 *Tape stripping*

Tape stripping is a minimally non-invasive procedure for *stratum corneum* removal and sampling. It involves the sequential application and removal of an adhesive tape strip from the skin surface in order to collect layers of corneocyte cells, as shown in Figure 1-6. The procedure is acceptable to human subjects because it is relatively painless and not particularly invasive, because only dead cells embedded in the lipid matrix are removed. Tape stripping can be used to evaluate skin barrier function, pathologies of the skin and local bioavailability of drugs whose target is the *stratum corneum*.⁵⁴

A large number of intrinsic and extrinsic factors can affect the amount of *stratum corneum* removed by a single adhesive tape strip.⁵⁵ Intrinsic factors relate to the size of the corneocytes which is influenced by the anatomical site, the age and the thickness of the *stratum corneum*. Extrinsic factors include the type of adhesive tape, force of removal from the skin and also the topically applied substance.⁵⁵ In order to assess permeation of drugs, and therefore bioavailability, variability caused by intrinsic and extrinsic factors should be minimised in the study design.

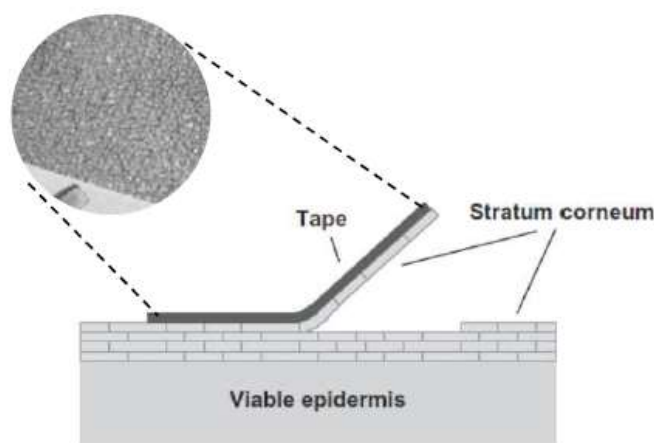


Figure 1-6 Schematic representation of the tape-stripping process. Adapted from Wiedersberg et al.⁵⁴

Since the *stratum corneum* is in most cases the main barrier to the penetration of topically applied drugs, it has been argued that drug level therein should be correlated with those attained in the viable epidermis and dermis.⁵⁴ This hypothesis was tested by Rougier *et al.* (1983)⁵⁶ who found a linear correlation between the amount of chemical (sodium benzoate, caffeine, benzoic acid, acetyl salicylic acid) absorbed across the skin following a 30 minute application and the quantity recovered in the *stratum corneum* by tape stripping after an identical, but independent, administration procedure. Therefore, if there is a correlation between drug levels in the *stratum corneum* and drug levels in the underlying tissues, then the tape stripping technique can be theoretically used to determine the bioavailability of all topical drugs. This would also be true for cosmetic ingredients.

In 1998, a draft tape stripping guidance was issued by the USA Food and Drug Administration (FDA) to assess bioequivalence of topical dermatological drug products. This draft was withdrawn in 2002 due to inter-laboratory comparative studies on the same products were found to have conflicting and opposite results. The reproducibility of the method was a concern because the application area was not delimited in one of the studies.⁵⁷

However recently Au *et al.* (2010)⁵⁸ demonstrated the potential of a standardised tape stripping study as an option for the assessment of bioequivalence of topical corticosteroid formulations. The authors found data

from the tape stripping study correlated well with data from the human skin blanching assay – which is the only acceptable bioequivalence method approved by the USA Food and Drug Administration. The standardised tape stripping study recommendations include the careful removal of residual formulation prior to skin stripping, controlled systematic stripping orientation of each site (rotate 90° after every tape strip), normalisation of individual skin thickness and careful control of the dose and application of doses to demarcated skin sites. The authors also recommend avoidance of areas on the volar aspect of the forearm where increased variability in uptake may exist such as areas near the wrist and elbows and careful control of the temperature and humidity of the environment where the study is being conducted.

When evaluating tape strip data, it should be viewed from the perspective that corneocytes on one tape strip of the *stratum corneum* may be derived from different layers, depending on the position of the tape strip in relation to the slope of the furrows in the skin as illustrated in Figure 1-7. Van der Molen *et al.*⁵⁹ found that a TiO₂ containing compound, applied to the skin and subsequently tape-stripped, was persistently present but restricted to the rims of the furrows on the tape strip by x-ray microprobe analysis and scanning electron microscopy. With the spatial resolution of the techniques, it could be concluded that the TiO₂ containing compound did not penetrate the *stratum corneum* barrier.

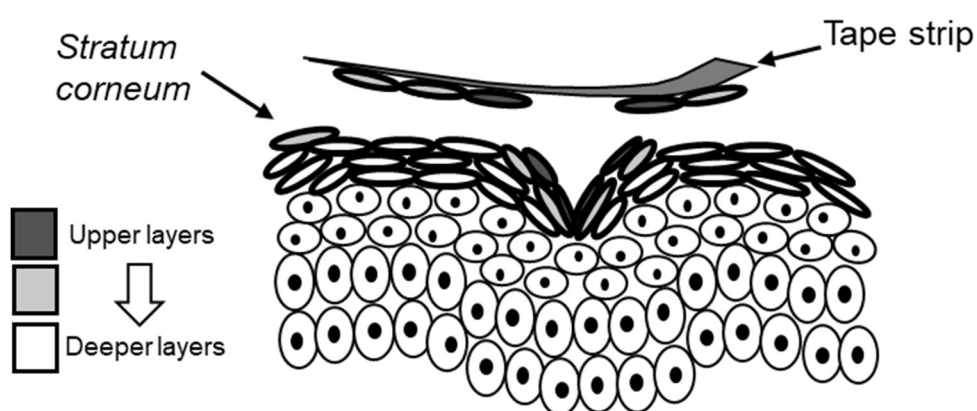


Figure 1-7 Schematic diagram showing tape stripping over a skin furrow.
Adapted from Van der Molen *et al.*⁵⁹

To minimise the influence of skin furrows, it is advised that the adhesive tape is pressed onto the skin using a roller to stretch the skin surface.⁵⁵ Where a roller is too large for the skin test site, it has been suggested to apply pressure with the thumb in a rolling movement.⁶⁰ Nonetheless the effect of skin furrows on removal of corneocytes cannot be entirely avoided and the roller method may have the disadvantage that the force of stretching to flatten the surface of the skin can influence the architecture of the skin and thus the penetration of compounds.⁵⁹

1.2.4.2 Microdialysis

Dermal microdialysis, involves superficially implanting a thin semipermeable hollow tube, into the dermis parallel to the skin surface. The implanted probe, perfused with a physiological solution at a low flow rate, collects free unbound drug that has permeated across the epidermis. Microdialysis technique allows *in vivo* real-time sampling of the permeation of drugs to obtain a pharmacokinetic profile. This approach is considered more appropriate than taking blood samples if the pharmacological target is the skin.⁵³ However, this technique is more invasive than tape stripping, which makes recruitment of willing volunteers more challenging. Probe insertion can lead to tissue trauma, increased blood flow and histamine release, which diminishes after 40-135 minutes, so equilibration time also needs to be factored in. Probe implantation is also technically challenging, and requires specialised training, to insert the probe at a consistent depth.⁶¹

1.2.4.3 Skin Biopsy

Skin biopsies offer the capability to see drug deposition in the different skin layers. This is an invasive procedure, that results in a permanent change to the skin appearance, so is restricted to skin tissue that would be removed during surgical operation (for example removal of small tumours). The availability of human volunteers, undergoing surgery, and willing to participate for *in vivo* skin permeation studies is very limited so this approach is best suited to animal and *in vitro* studies.⁵³

1.2.5 Dose applied to skin

1.2.5.1 *Infinite vs finite dosing*

In infinite dose skin permeation studies, the applied dose of formulation is so large that depletion of the permeant in the donor chamber, caused by evaporation or diffusion into the *stratum corneum*, is negligibly small. Infinite doses reach a constant rate of absorption, i.e. steady state, which simplifies analysis of the compound's permeability. In contrast finite dose studies involve application of a limited amount of the donor formulation. Finite doses best resemble the *in vivo* situation, i.e. not steady state, due to the influence of evaporation of excipients on permeation.⁶²

On the other hand, infinite dose application may exert an occlusive effect and thus lead to an increased permeability of the skin for example with ointment formulations.⁶³ Large volumes of water in the donor formulation could also increase the hydration of the skin and lead to swelling of the corneocytes in the *stratum corneum* barrier. Extended water exposure for 4 to 24 hours has been reported to lead to extensive disruption of *stratum corneum* intercellular lipid lamellae and increase in skin permeability.^{64,65} Therefore, infinite dose regimes would not be representative of the *in vivo* situation for hydrophilic permeants.

OECD guideline 428,³⁴ and the guidance document 28,³³ states a finite dose application to be $\leq 10 \mu\text{L}/\text{cm}^2$ of a liquid formulation and between 1 to 10 mg/cm^2 for semisolid and solid formulations. The definition of a finite dose does however vary in previous studies with investigators assuming finite dose conditions if donor depletion was observed during the experiment. Recent studies discuss volumes as large as 16 – 39 $\mu\text{L}/\text{cm}^2$ ($\sim 16\text{-}39 \text{ mg}/\text{cm}^2$) being finite dose applications but this will depend on the volatility of the excipients.

The SCCS Notes of Guidance for the Testing of Cosmetic Ingredients states a formulation dose of 1-5 mg/cm^2 is typically applied to the skin by consumers.^{35,36} Investigations with very low doses can be problematic regarding analytical method sensitivity, so for sunscreen risk assessment 3 mg/cm^2 is recommended to study sunscreen penetration.⁶⁶ In a recent study by Benson *et al.*⁶⁷, participants were asked to apply sunscreen as they normally

would on the beach. The average amount of formulation applied was 20 mg/cm², almost double the definition provided by the OECD.

1.2.5.2 In-use conditions

It is common practise to rub or massage a topical product onto the skin however OECD guideline 428³⁴ (*in vitro*) and 427⁶⁸ (*in vivo*) do not discuss how the formulation should be applied to the skin. Rubbing of formulation into the skin was reported to increase the skin permeability of entrapped drug in ointment.⁶⁹ Recently Nguyen *et al.*⁷⁰ investigated different techniques such as using glass rod, rheometer, and gloved finger for rubbing gel formulation on *in vitro* porcine skin. They reported that rubbing the formulation resulted in a uniform gel thickness on the skin and rubbing with gloved finger significantly increased the amount of drug delivered into the skin layers. Skin permeation studies, both *in vitro* and *in vivo*, should look to simulate rubbing formulation as would occur in clinical practise. It is also necessary to ensure that the amount of formulation applied does not vary significantly between the test sites.

1.3 Analytical techniques for studying skin permeation

In vitro and *in vivo* skin permeation experiments can be followed up with a wide variety of analytical techniques. This can include established analytical methods, such as high performance liquid chromatography (HPLC), and spectrophotometry methods to more advanced imaging analytical techniques such as confocal Raman microspectroscopy (CRM) and various imaging mass spectrometry techniques. Each technique has their own advantages and disadvantages and the choice of technique used will depend on what is being investigated.

1.3.1 Liquid chromatography and spectrophotometry methods

The conventional approach for studying skin permeation involves HPLC with UV-Visible (UV-Vis) spectroscopy or mass spectrometer detectors. HPLC analysis generates a quantitative result so absolute concentrations are deduced. This data is vital for dermal absorption risk assessment work.^{32,35} A UV-Vis spectrophotometer may also be used alone for detection of the analyte, as it is

less expensive, more portable and measurement is quicker. It is particularly useful for kinetic studies.⁷¹ However, the spectrophotometer does not separate interfering compounds, so control samples would have to be carefully acquired to subtract the background signal and to obtain quantitative results.

The analyte is required to be in solution, so an extraction step is required. The Franz cell receptor liquid is already in the correct state for analysis; however, tape strip samples must be extracted into solution.⁷² The remaining skin tissue can also be cut into smaller pieces for extraction (i.e. full recovery experiment), however, this is dextrous work and care must be taken to avoid sample contamination.⁷³ The disadvantage of this approach is loss of the spatial resolution of the analyte in the skin tissue layers.

Nevertheless, sophisticated approaches can be taken to study the route of permeation. For example, follicular closing/ plugging technique can be used to study follicular permeation. A wax is applied to the hair follicles to seal their pathway and skin permeation experiments can be performed with and without plugging to deduce the contribution of follicular route (Figure 1-8 A).⁷⁴ However, because the analyte was not visualised in the hair follicle, it can only be assumed that follicular permeation took place.

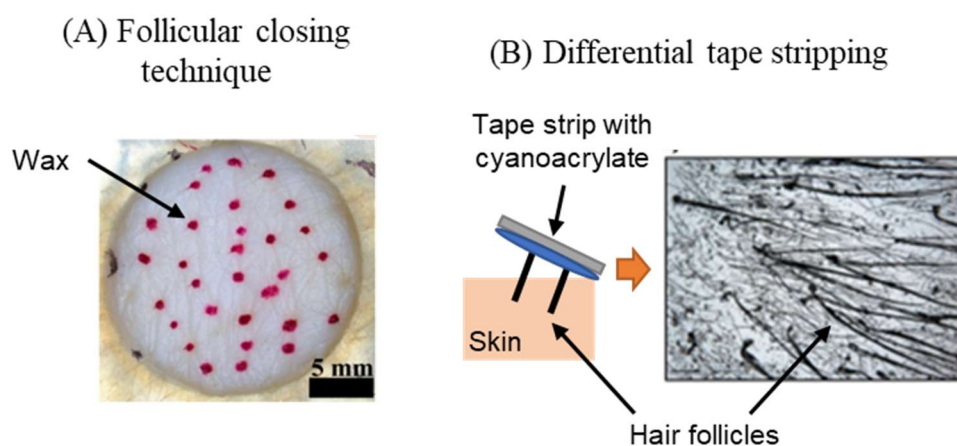


Figure 1-8 Methods to assess follicular permeation. (A) Follicular closing technique and (B) differential tape stripping. Adapted from Mohd et al.⁷⁴ and Tampucci et al.⁷⁵

Differential tape stripping, which involves application of cyanoacrylate glue to the skin surface to remove follicular casts, can also be used to determine

follicular permeation (Figure 1-8 B).⁷⁵ The analyte from the follicular casts can be subsequently extracted into solution. Differential tape stripping may be performed *in vivo* however it is likely to be uncomfortable.

Skin tape strip samples extracted into solution may overestimate skin permeation depth if the permeant is found localised in the furrows of the skin. To overcome this problem, Lademann *et al.*⁷⁶ used a roller (on the tape strips) to stretch the porcine skin, which removed the furrow structures of the stratum corneum, and resulted in the removal of a homogenous layer of corneocytes. In consequence, no fluorescent dye from the topical product was left in the skin furrows. A more accurate permeation profile of the permeant was therefore obtained since any formulation trapped in the furrows was removed with the initial tape strips and thus not considered to have permeated. However, a severe drawback of this approach is that the distribution of the formulation is disturbed during rolling of the skin surface which may also influence penetration into the corneocytes. In contrast, tape strips which are pressed onto the skin site does not disturb the furrows and formulation distribution

For some drugs, usually with low permeation, HPLC methods may not be sensitive enough so isotopically labelled (radiolabeled) drugs or fluorescently tagged drugs may be used. Analysis can then be performed using liquid scintillation counting, which measures the ionising radiation, or spectrofluorometry, which measures the fluorescence from the analyte.^{77,78} However, the former requires additional safety controls in the laboratory whilst the latter changes the physicochemical properties of the permeant.

1.3.2 Imaging spectrophotometry methods

Imaging techniques can give important information about the spatial distribution of the drug inside the different skin layers or explain the mechanism of penetration. Confocal laser scanning microscopy (CLSM) has been widely used to visualise fluorescent compounds in the skin. CLSM is non-invasive and so has been used *in vivo* and *in vitro* to obtain 3D images of fluorescent permeants in the skin and skin appendages.⁷⁹⁻⁸¹ Fluorescent tagging could influence drug permeation, so this technique is best restricted to drugs which are fluorophores.⁸²

CRM, is a vibrational spectroscopy technique, that can monitor the permeation distribution of drugs, as well as endogenous molecules, label-free, in 3D, in real-time, and non-invasively including in human skin *in vivo*.^{83,84} Saar *et al.*⁸⁵ was able to visualise the permeation of ketoprofen, ibuprofen, and propylene glycol into mouse skin at different time intervals. They were able to detect the permeant in hair follicles as well as the intercellular pathway across the *stratum corneum*. Chrit *et al.*^{86,87} was able to determine the water concentration profile with depth in the *stratum corneum*, after the application of moisturising agents to human skin *in vivo*. These studies show 3D chemical information can be obtained at a depth up to 100 μm , with a depth resolution of $\sim 2 \mu\text{m}$ and lateral resolution of 1 μm .^{82,85-87}

However, since the Raman signal is generally a weak signal, a prerequisite is that the molecule of interest is present at sufficient concentration, and possess spectral features of sufficient intensity, to permit its differentiation from those of the skin. Therefore, the number of substances that can be analysed is limited and furthermore only relative concentrations can be determined. Another technical problem is the high level of biological tissue fluorescence which can mask the much weaker Raman signal so computational methods are required to subtract the fluorescence interference in the Raman spectra.^{82,88-90}

1.3.3 Imaging mass spectrometry methods

1.3.3.1 Comparison of imaging mass spectrometry techniques

A range of imaging mass spectrometry techniques have been used to investigate skin samples including ambient mass spectrometry methods, matrix assisted laser desorption ionisation mass spectrometry (MALDI-MS) and time of flight-secondary ion mass spectrometry (ToF-SIMS). Important technical parameters to consider include lateral resolution, limits of detection and the sample preparation involved. The National Physical Laboratory (Teddington, UK) published said parameters for their imaging mass spectrometry techniques, in 2015⁹¹, and are noted in Table 1-1. It is important to note that instrument manufacturers are continually improving the capability of their instruments however the below comparison gives a good perspective on the

strengths of each technique. In general, mass spectrometry techniques have high chemical specificity compared to spectroscopy techniques.

*Table 1-1 Comparison of imaging mass spectrometry techniques.*⁹¹

	Ambient mass spectrometry	MALDI-MS	ToF-SIMS
X-Y resolution	100-200 μm	10-200 μm	<1 μm
Z depth resolution	N/A	N/A	5 nm
Sensitivity	fM	fM	<0.1 μM
Sample Preparation	Not required	Matrix application	Vacuum compatible

Desorption electrospray ionisation mass spectrometry (DESI-MS), is an ambient mass spectrometry technique, so analysis of biological samples can be performed in their native state. D'Alvise *et al.*⁴⁶ was able to show the spatial distribution of permeated lidocaine in *ex vivo* porcine skin tissue using DESI-MS. The lidocaine could be mapped with a spatial resolution of 50 μm , so that localisation in hair follicles could be observed. With this spatial resolution, the distribution of the permeant at the corneocyte level (30 μm diameter) would not be possible so its application to tape strip samples is limited.

MALDI-MS is a preferred technique for the analysis of biological samples due to its ability to detect high mass ions, such as lipids and proteins. MALDI-MS has been used to analyse skin tissue samples⁹²⁻⁹⁴, as well as more recently tape strip samples.⁹⁵ Hochart *et al.*⁹⁵ was able to visualise the distribution of endogenous molecules on tape strip samples collected from the cheek and volar forearm of human volunteers. Data analysis was performed by excluding the regions of the tape with no corneocytes at a spatial resolution of 20 μm . Whilst this was effective, other techniques such as ToF-SIMS (Section 1.3.3.2) have sub-micron resolution and therefore better sensitivity when it comes to excluding data from non-corneocyte regions on the tape strip samples.

MALDI-MS requires the application of a thin layer of matrix onto the sample surface therefore the sample cannot be analysed in its native state. One advantage of this is that the matrix peaks can be used as an external standard, to quantify drug concentration in the tissue.⁹⁶ However, the matrices typically show an abundance of fragment ions below 500 m/z which would make quantification of small molecule drugs more difficult due to the matrix ion noise.⁹⁷ Consequently, at the present time the application of MALDI-MS is more suited to higher mass molecules, that would not typically be ideal candidates for dermal permeation.

1.3.3.2 ToF-SIMS

ToF-SIMS is more suitable for the study of small mass molecules (< 1000 m/z)⁹⁸ than MALDI-MS and has far superior spatial resolution (Table 1-1) and is therefore more applicable to studying skin permeation. ToF-SIMS is an ultra-high vacuum technique that uses a highly focussed primary ion beam to bombard the sample surface, which induces a collision cascade resulting in the ejection of secondary atomic and molecular species, as shown schematically in Figure 1-9. The ionised species are received in the detector, whilst the neutral species, which represent the vast majority of the sputtered material (> 99%), is not analysed.⁹⁹ ToF-SIMS instrument has the ability to map each detected ion, in 2D as well as in 3D, such that an individual mass spectrum is obtained for each pixel in the image (ion map).

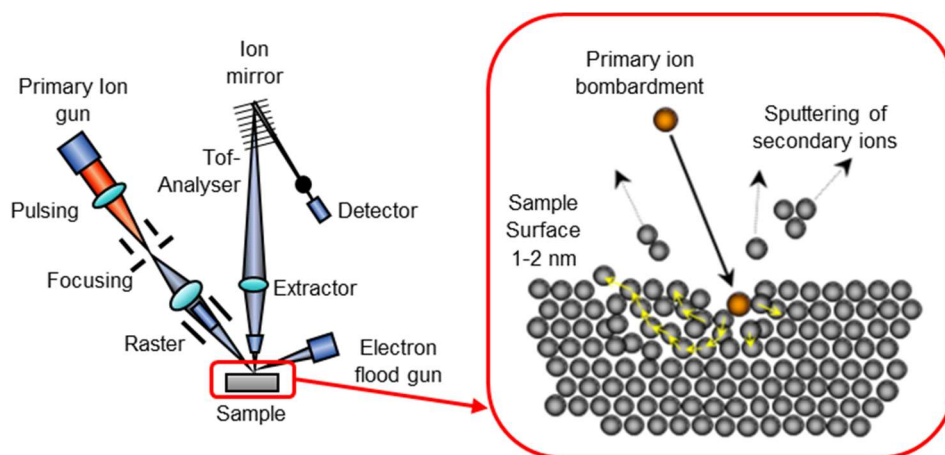


Figure 1-9 Schematic diagram of ToF-SIMS instrument and collision cascade (yellow arrows) caused by primary ion bombardment of sample surface.

Adapted from NIST.¹⁰⁰

In order to analyse only the surface (top 1-2 nm) of a sample, and not sputter ions from further below, analysis is performed under the ‘static’ limit which is a primary ion dose of $\leq 10^{12}$ ions/cm². It has been estimated that one primary ion imparts an area on the surface of 10 nm² and therefore it would require 10¹³ ions/cm² to damage all the sample surface.⁹⁹ Keeping within the ‘static’ limit ensures that statistically no area on the sample is bombarded twice. In this way, a 2D surface analysis is performed. The analysis of the samples is performed under ultra-high vacuum conditions ($\sim 10^{-7}$ Torr) to keep the ion beam focussed and thus achieve high spatial resolution.

The development of cluster ion or polyatomic ion sources, such as Bi_n⁺ or Ar_n⁺ or C₆₀⁺, led to an increase in biological samples being analysed by ToF-SIMS. The large size and low energy per atom of polyatomic ions, results in an energy deposition that remains closer to the sample surface (i.e. softer impact), hence increasing desorption of ions from the surface. In addition, this reduces the damage caused to the sample.^{99,101} The increased secondary ion yield was useful for the analysis of organic and biological materials which do not ionise as readily as inorganic materials.

1.3.3.3 Application of ToF-SIMS to skin samples

ToF-SIMS can be used to visualise the spatial distribution of endogenous skin compounds, and exogenous compounds label-free, with high spatial resolution and chemical specificity. This research topic first started in 2008, and since then there have been several publications in this field, all of which are presented in Table 1-2. Sample types analysed mainly include cross-sections and tape strip samples since they have quicker vacuum evacuation (pump down) times due to their low moisture content.

Table 1-2 Previous ToF-SIMS studies on skin samples.

Researcher	Skin sample	Main topic
Okamoto <i>et al.</i> (2008) ¹⁰²	<i>Ex vivo</i> porcine skin cross sections	<ul style="list-style-type: none"> Permeation of synthetic pseudo-ceramides into the <i>stratum corneum</i>.
Judd <i>et al.</i> (2013) ¹⁰³	<i>Ex vivo</i> porcine skin cross sections and tape strips	<ul style="list-style-type: none"> Chlorhexidine digluconate permeation was mainly localised to the <i>stratum corneum</i>. Non-uniform permeation distribution.
Kezutyte <i>et al.</i> (2013) ¹⁰⁴	<i>Ex vivo</i> human skin cross sections	<ul style="list-style-type: none"> Oleic acid enhanced permeation of tolnaftate. Interestingly the permeation profile of oleic acid did not correlate with tolnaftate.
Kubo <i>et al.</i> (2013) ¹⁰⁵	<i>In vivo</i> mouse skin cross sections	<ul style="list-style-type: none"> Permeation of metal ions into mouse <i>stratum corneum</i> revealed three distinct layers.
Sjovall <i>et al.</i> (2014) ¹⁰⁶	<i>In vivo</i> mouse skin cross sections	<ul style="list-style-type: none"> Permeation of roflumilast, tofacitinib and ruxolitinib primarily distributed into <i>stratum corneum</i> only. Endogenous skin components imaged.
Starr <i>et al.</i> (2016) ¹⁰⁷	<i>In vivo</i> human tape strips	<ul style="list-style-type: none"> Spatial distribution of endogenous <i>stratum corneum</i> lipids determined. Age-related increase and change in spatial distribution of cholesterol sulphate observed.
Cizinauskas <i>et al.</i> (2017) ¹⁰⁸	<i>Ex vivo</i> human skin cross sections	<ul style="list-style-type: none"> Permeation of fatty acids and dihydroquercetin monitored simultaneously however no direct relationship between permeation profiles observed.
Cizinauskas <i>et al.</i> (2017) ¹⁰⁹	<i>Ex vivo</i> human skin cross sections	<ul style="list-style-type: none"> Permeation of topically applied fatty acids induce redistribution of native fatty acids in the skin.
Holmes <i>et al.</i> (2017) ¹¹⁰	<i>Ex vivo</i> porcine skin cross sections and tape strips	<ul style="list-style-type: none"> Dendrimer pretreatment increased permeation depth of chlorhexidine digluconate. Uniform permeation across epidermis observed with no increased co-localisation in skin appendages.

Sjovall <i>et al.</i> (2018) ¹¹¹	<i>Ex vivo</i> human skin tissue cross sections	<ul style="list-style-type: none"> • Spatial distribution of lipids, ceramides and cholesterol sulphate in skin layers determined. • Carvacrol permeation was localised to tri-glyceride rich structures in the dermis.
Starr <i>et al.</i> (2019) ¹¹²	<i>Ex vivo</i> porcine skin tissue	<ul style="list-style-type: none"> • Supramolecular gel formulation increased the permeation of ascorbic acid and ascorbyl glucoside. • 3D depth profile of permeation obtained. • Breakdown of ascorbyl glucoside to ascorbic acid occurred with increased skin depth.
Al-Mayahy <i>et al.</i> (2019) ¹¹³	<i>Ex vivo</i> porcine skin cross sections and tape strips	<ul style="list-style-type: none"> • Microneedle pretreatment led to increased imiquimod permeation. • Co-localisation of imiquimod in microneedle channels and lateral permeation observed.

The uptake of ToF-SIMS analysis in this area has been quite slow. This could be due to the large cost involved in buying and operating the instrument and inability to produce inherently quantitative results. The intensity of the detected secondary ions is influenced by the surrounding matrix material, referred to as matrix effects. Consequently, some of the reported permeation studies use chromatography methods to support their ToF-SIMS findings. Some of the earlier studies were performed with the aim of highlighting the capability of the ToF-SIMS instrument, so large number of replicate samples were not analysed. Therefore ToF-SIMS analysis of skin samples is still a novel research area. More importantly though, the use of ToF-SIMS has generated unprecedented findings by the ability to map the ion distribution in skin cross sections and tape strip samples, so its application will only continue to grow. Two examples are highlighted in Figure 1-10 and 1-11 below.

Judd *et al.*¹⁰³ was the first to report distribution of a topically applied substance on tape strip samples by ToF-SIMS. ToF-SIMS had a high level of sensitivity to detect the permeant, chlorhexidine, in the 20th tape strip layer of the *stratum corneum* as shown in Figure 1-10. It was noted that tape strip samples contained areas of lower total ion count that corresponded to non-corneocyte

containing regions of the tape. The authors therefore demonstrated that the data could be thresholded to selectively analyse the corneocyte containing regions of the tape strip sample. A non-uniform permeation distribution of chlorhexidine was observed across the tape strip samples but was generally co-localised with the corneocyte material.

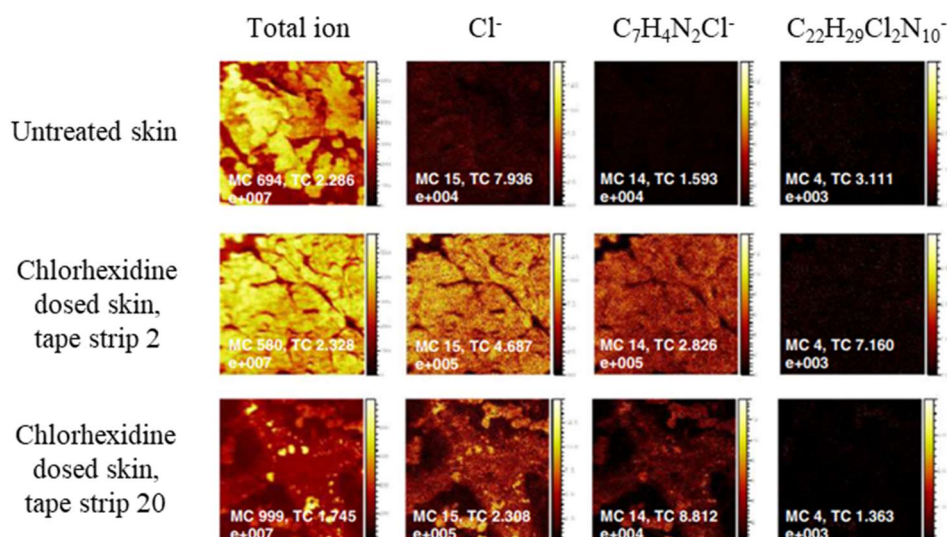


Figure 1-10 ToF-SIMS images of various chlorhexidine digluconate specific ions on tape strips from untreated and chlorhexidine treated ex vivo porcine skin. Field of view is 500 × 500 μm. Adapted from Judd et al.¹⁰³

Sjovall *et al.*¹¹¹ imaged the distribution of carvacrol, from topically applied thyme oil, in porcine skin cross sections. As shown in Figure 1-11 C, the sweat gland location could be chemically identified by secondary ions diagnostic of triglycerides. The authors observed the carvacrol M-H⁻ secondary ion (Figure 1-11 B) was co-localised in these triglyceride rich regions of the skin and therefore suggested a follicular permeation route. The low intensity of the carvacrol M-H⁻ secondary ion at the epidermis suggests very little to none transepidermal penetration. It should be noted however that only one cross section was presented in the publication, and this may not be a reliable indicator of the overall permeation behaviour.

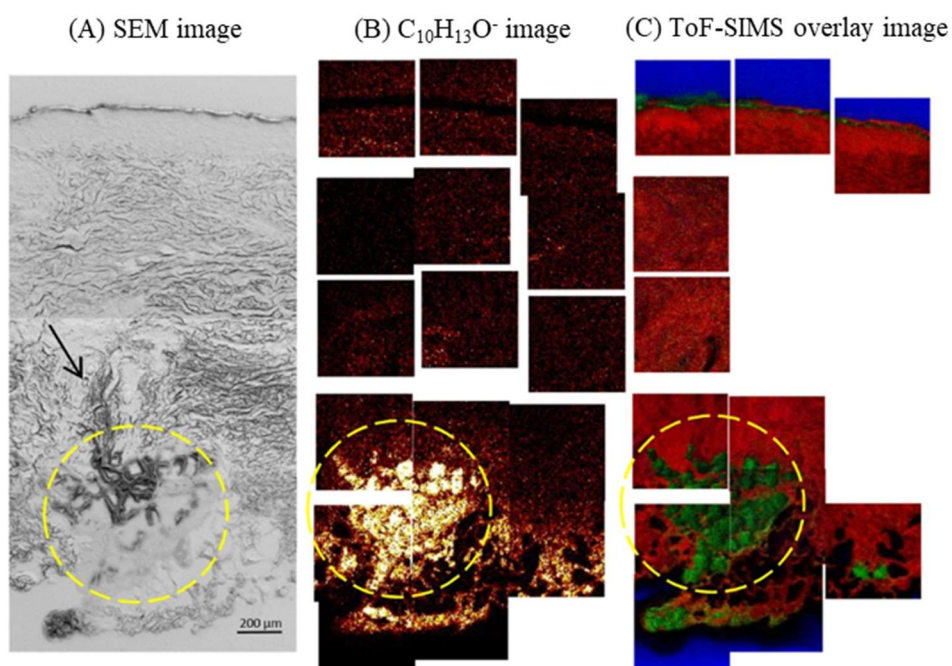


Figure 1-11 Localisation of topically applied carvacrol in the eccrine sweat gland (yellow circle) of ex vivo porcine skin. (A) Large area SEM image (stitched) of skin cross section (the arrow indicates a hair follicle). (B) Carvacrol M-H ToF-SIMS image. (C) ToF-SIMS overlay image showing diacylglycerides (m/z (575–579)+(601–605), green), representing triglycerides, Phosphatidylcholine fragments (m/z 86 + 184, red) and silicon (m/z 28, blue). Each ToF-SIMS image has a field of view of $500 \times 500 \mu\text{m}$.

Adapted from Sjovall et al.¹¹¹

1.4 Skin permeation enhancement

1.4.1 Physical and chemical skin permeation enhancement strategies

Dermal delivery of cosmetic and pharmaceutical ingredients is limited by the poor permeation through the *stratum corneum* barrier.⁵ Various strategies have been developed to modify the *stratum corneum* structure to increase skin permeation; these can be divided into physical and chemical enhancement strategies. Physical penetration enhancement strategies include the use of electroporation, iontophoresis, ultrasound, laser radiation, microneedle-based devices, skin abrasion and thermophoresis. Whilst these approaches have been successful in increasing dermal and transdermal delivery of a variety of drugs,

more research is required to show the skin is not damaged with long-term use that would be contrary to the purpose of applying cosmetic and skin care ingredients to the skin.^{10,114,115} Physical penetration enhancement strategies may also have low consumer acceptability if they cause discomfort, for example microneedles can cause mild to moderate skin irritation¹¹⁶, so their applicability to cosmetic and skin care ingredients is limited.

Currently topical formulations widely use excipients that can be regarded as chemical penetration enhancers such as alcohols, amides, esters, ether alcohols, fatty acids, glycols, sulphoxides, surfactants and terpenes. Each chemical penetration enhancer will have, where known, a mechanism of action. Ideal skin penetration enhancers should be pharmacologically inert, non-toxic, non-irritating, non-allergenic and ideally should have a reversible action on the skin.^{14,18,117}

Water can also be classified as a chemical penetration enhancer and is frequently the first ingredient listed on topical formulations. In general, increased skin hydration appears to increase permeation of both hydrophilic and lipophilic permeants.¹⁸ Thermal analysis reveals that 20 to 35% of the water present in the *stratum corneum* is 'bound', i.e. is associated with structures within the tissue. The other 65 to 80% 'unbound' water in the *stratum corneum*, more if the skin is hydrated, is available to act as a solvent for the permeant.¹¹⁸

But water alone cannot be used in topical preparations due to its short residence time, by evaporation or run-off, on the skin. Therefore, viscosity thickening agents, resulting in a gel formulation, and lipids and surfactants which are less volatile, resulting in an emulsion (lotion/cream), are commonly incorporated in topical preparations to increase residence time on the skin surface. However, Bucks and Maibach¹¹⁹ state that occlusion by a formulation, which also leads to increased skin hydration, may not consistently increase percutaneous absorption but warn that occlusion may cause local skin irritation.

1.4.2 Topical preparations

1.4.2.1 Gel formulation

Gels are a two-component system consisting of water or hydroalcoholic solution entrapped in a continuous polymer network structure. They are semi-solids, with acceptable skin-feel and texture for consumers. Gels are popular in cosmetic skin care, where they may be referred to as serums, as they are convenient to apply, handle, and wash off.^{120,121} Polymers can be synthetic (e.g. Carbopol) or natural (xanthan gum, alginate, guar gum) and function as binders, emulsion stabilisations, surfactant-emulsifying agent as well as viscosity increasing agent.¹²² Xanthan gum, in particular, is stable in a wide range of pH values (2-12).¹²³

1.4.2.2 Emulsions

Creams and lotions are emulsions of water in oil (W/O) or oil in water (O/W). O/W emulsions are most common for topical formulations as they feel less greasy than W/O emulsions, which can be of utmost importance to the consumer. O/W emulsions are best suited for water-soluble drugs.¹²⁴ Cheng *et al.*¹²⁵ define a basic cream formulation having a composition of emollients (10-40%), surfactants (1-6%), humectants (1-5%), thickeners (0.1-0.5%) to give a consistency desirable for topical application and preservatives (0.01-0.5%).

Creams and lotions are popular formulations in cosmetic skin care due to their moistening and emollient properties, spreadability, are conveniently applied to all body parts, and as the aqueous phase evaporates, they have a cooling sensation on the skin.¹²⁴ As we age, lipid production in the skin declines, which can result in rough skin texture, tightness, and loss of suppleness, hence topical application of creams and lotions which contain lipids, can be beneficial to the skin by keeping it hydrated and maintaining the skin's natural barrier.^{126,127}

1.4.2.3 Lipid nanoparticle formulations

Lipid nanoparticles are an oil-in-water nanoemulsion colloidal dispersion with mean size between 40 and 1000 nm. Lipid nanoparticles have been intensively studied for cutaneous application due to their advantageous characteristics such

as entrapment of both hydrophilic and lipophilic active ingredients, controlled release of the active, good tolerability, a narrow contact with *stratum corneum* and an increase in skin hydration. Additionally, lipid nanoparticles are able to increase chemical stability of active ingredients against light, oxidation and hydrolysis.¹²⁸

Nanostructured lipid carriers (NLC) contain a combination of solid and liquid lipids in ratio 70:30 up to 99.9:0.1 whereas solid lipid nanoparticles (SLN) contain solid lipid only. NLCs have several advantages over SLNs because liquid lipid molecules lead to the formation of imperfections in the lipid matrix structure. The less ordered solid lipid matrix can accommodate more drug molecules and therefore has higher drug loading capacity. NLCs can be loaded with hydrophobic and hydrophilic ingredients.¹²⁹ Single emulsion NLCs (O/W) have limited loading for hydrophilic drugs so double emulsion water in oil in water (W/O/W) can be prepared to overcome this.¹³⁰ The lipids used for the preparation of lipid nanoparticles are GRAS (Generally Recognised As Safe) therefore no problems of biocompatibility or toxicity are associated.¹³¹ There is also interest in using lipid nanoparticles as delivery systems for sunscreen formulations since these nanoparticles have protective effect from the sun.¹³²

Lipid nanoparticles applied onto skin have shown enhanced and/or altered drug penetration of a wide variety of dermatological agents such as ascorbyl palmitate¹³³, hydroquinone¹³⁴, coenzyme Q10¹³⁵, retinol¹³⁶, isotretinoin¹³⁷, prednicarbate¹³⁸, and acyclovir¹³⁹ through the *stratum corneum* with applications in hyperpigmentation, acne, dermatitis, herpes labialis and aesthetic (cosmetic) medicine. Where it has been studied, lipid nanoparticles have been shown to lead to an accumulation of the embedded active into the upper skin layers whilst reducing transdermal drug flux. Lipid nanoparticle containing formulations have been previously tested *in vivo* on human volunteers with no reported side effects^{133,135,138,140,141}.

1.4.2.4 Nanoparticle skin permeation mechanisms

Various mechanisms of drug permeation, into skin, from nanoparticle formulations are discussed.^{142,143} These include fusion of nanoparticles with

stratum corneum lipids and release of active into the skin, intact penetration of nanoparticles through the *stratum corneum* and/or hair follicles, and furrow deposition of nanoparticles and release of active into the skin.^{142,143}

Enhanced drug permeation is generally considered not to be due to the result of penetrating particles unless the nanoparticles are < 20 nm and/or the *stratum corneum* barrier is damaged.¹⁴⁴ More recently, Dreier *et al.*¹⁴⁵ used super resolution optical microscopy and raster image correlation spectroscopy, with optical resolution low enough to resolve 100 nm liposomes in the skin, to find virtually none of the liposomes (nanosized vesicles) remained intact beneath the skin surface. The results suggest that nanoparticles do not permeate intact.

Lipid nanoparticles have been demonstrated to show occlusive action, and increase in skin hydration, which is thought to be the mechanism of enhanced drug permeation into the skin. The small size of NLCs ensures a close contact to the *stratum corneum*. Lipid nanoparticles with diameter of < 500 nm are reported to lead to a dense film formation on the skin surface and subsequent occlusion effect.¹²⁸ Regarding lipid nanoparticles, it was shown that approximately 4% of lipid nanoparticles with a diameter of approximately 200 nm should form theoretically a monolayer film when c. 4 mg of formulation is applied per cm².¹⁴⁶ This monolayered dense film retards the loss of moisture caused by evaporation as illustrated in Figure 1-12.^{129,147}

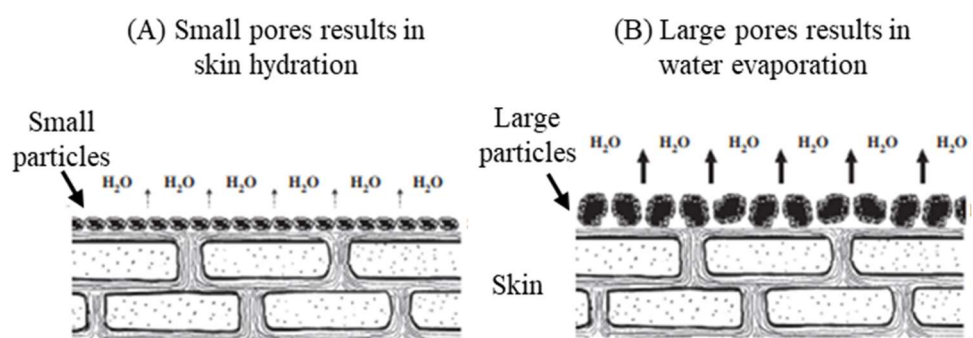


Figure 1-12 Skin occlusion effect of lipid nanoparticles depending on their size. Adapted from Souto and Muller.¹⁴⁷

1.5 Topical delivery of ascorbic acid

Ascorbic acid (Vitamin C; L-ascorbic acid) is the body's major aqueous-phase antioxidant and is the most abundant antioxidant in human skin.¹⁴⁸ Unlike plants and some animals, humans are unable to synthesize ascorbic acid due to absence of the enzyme L-glucono-gamma-lactone oxidase therefore ascorbic acid can only be obtained by supplementation.¹⁴⁹

Developing ascorbic acid formulations is challenging due to its instability in aqueous solution. Ascorbic acid readily oxidises to dehydroascorbic acid in aqueous solution, as shown in Figure 1-13. The rate of oxidation, and subsequent degradation, is increased at high pH or temperature, and in the presence of dissolved oxygen and metal ions. Degradation of ascorbic acid is accompanied by a yellow discoloration which very quickly shortens the shelf-life of the formulation.¹⁵⁰

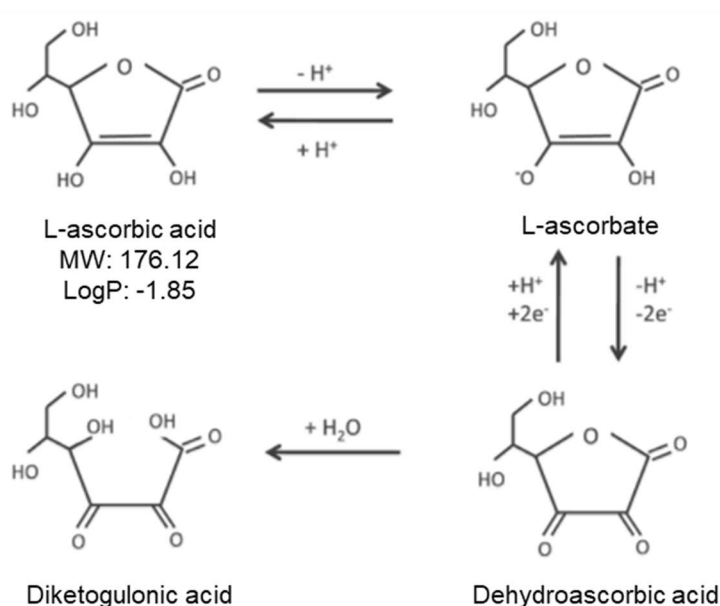


Figure 1-13 Oxidation and degradation pathway for ascorbic acid. Adapted from Robitaille et al.¹⁵¹

Formulation scientists have therefore developed more stable ascorbic acid derivatives such as magnesium ascorbyl phosphate (MAP), ascorbyl palmitate (AP), ascorbyl glucoside (AG) and 3-O-Ethyl ascorbate (EAC). These derivatives are required to be converted back to ascorbic acid, in the skin, to observe therapeutic effect. MAP and AG have been shown to convert to

ascorbic acid *in vitro* in keratinocytes but none of the aforementioned derivatives have yet been shown to convert to ascorbic acid *in vivo*. Ascorbic acid, on the other hand, does not require conversion, and its therapeutic effects (Section 1.5.1) have been demonstrated with *in vivo* efficacy studies (Section 1.5.2).¹⁵⁰

1.5.1 Skin benefits

Extrinsic aging (caused by solar UV radiation and air pollutants) and intrinsic aging increases the production of reactive oxygen species (ROS) in the skin and lowers the level of antioxidants. Generation of ROS is thought to play a major role in the ageing process. Increased levels of ROS in the skin up-regulates the expression of matrix-metalloproteins (MMPs) which are enzymes responsible for degradation of type I collagen found in the skin. Healthy collagen levels give the skin its strength, durability and youthful appearance.^{152–154} Antioxidants can reduce ROS and so their inclusion into topical products can be described to reduce, mask or prevent signs of aging.¹⁵⁵

Antioxidants for skin care are termed cosmeceuticals, a hybrid between cosmetic and pharmaceutical, since they incorporate biologically active ingredients.¹⁵⁶ Ascorbic acid is a popular topically applied cosmeceutical due to its antioxidative, photoprotective, antiaging and antipigmentary effects.¹⁵⁷ The mechanisms by which ascorbic acid work in the skin are currently well understood.

Ascorbic acid, as an antioxidant, deactivates UV-induced free radicals and decreases UVB erythema. It was found that treatment with topical 10% ascorbic acid decreases the number of abnormal “sunburn cells” by 40–60% and reduces UV damage to DNA 8-hydroxydeoxyguanosine by 62%.¹⁵⁸

Ascorbic acid is an essential cofactor for the two enzymes required for collagen synthesis: prolyl hydroxylase (to stabilize the collagen molecule) and lysyl hydroxylase (to give structural strength cross-linking). Enhanced collagen production can reduce the appearance of fine lines and wrinkles.¹⁵⁹ Ascorbic acid is also a depigmenting agent due to its inhibition of the enzyme tyrosinase and subsequent reduction in melanin production.¹⁶⁰

1.5.2 Summary of efficacy studies

In order to claim a skin care product is more efficacious than another, *in vivo* clinical trials are performed with participants instructed to apply the formulation for a period of time. At study end, non-invasive biometric measurements are taken to evaluate, for example, the reduction in the appearance of wrinkles or increase in skin hydration.¹⁶¹

Typical concentrations of AA in cosmetic products vary from 0.5 – 20%^{162,163}. A number of efficacy studies on ascorbic acid formulations have been performed on human subjects *in vivo*. A double-blind, placebo-controlled study by Fitzpatrick *et al.* (2002)¹⁶⁴ on 10 subjects using 10% topical ascorbic acid over a 12-week period showed a statistically significant reduction in photoaged scores and improvement in wrinkles in ascorbic acid-treated subjects as compared to placebo.

Humbert *et al.* (2005)¹⁶⁵ tested the efficacy of a 5% ascorbic acid cream on skin aging induced by repeated UVA irradiation over three months. The study on 20 women, with facial heliodermatitis, involved daily application of cream to the face and volunteers were irradiated with UVA 3 times per week over 3 months, with increasing doses (up to 20 J/cm²). The study shows efficacy of the cream against photo aging by a significant increase in skin hydration (measured by corneometry), increase in skin elasticity (measured by cutometry) and a decrease in wrinkles (measured by fringe projection).

A recent clinical trial by Crisan D *et al.* (2015)¹⁶⁶ shows that topically applied ascorbic acid (concentration of 5% and a pH of 5.5 in a novel complex with rosa moschata oil and proteoglycans) is highly efficient as a rejuvenation therapy, inducing significant collagen synthesis in all age groups with minimal side effects. *In vivo* ultrasonographic images (Dermascan C, 20 MHz) were taken at 40 and 60 days.¹⁶⁶

Ascorbic acid is a GRAS substance. The Cosmetic Ingredient Review (CIR) expert panel believe ascorbic acid to be a safe ingredient based on the following studies: An opaque cream containing 5% ascorbic acid did not induce dermal sensitization in 103 human subjects. A product containing 10%

ascorbic acid was nonirritant in a 4-day minicumulative patch assay on human skin. A repeat-insult patch test using 5% ascorbic acid gave negative results therefore ascorbic acid does not present a risk of skin sensitization.¹⁶⁷ Thus high levels of topical ascorbic acid are not associated with harmful pro-oxidant effects.

The efficacy studies do not investigate permeation of ascorbic acid but there is an assumption that in order to observe efficacy, ascorbic acid must penetrate the skin barrier. The general conclusion that can be made is that topical formulations require around 5% ascorbic acid concentration to observe efficacy. *In vivo* efficacy studies are both expensive and time-consuming to organise, and positive therapeutic effects are not always guaranteed to be observed. To speed up the development of more efficacious formulations, skin permeation studies can be performed but these must mimic as close as possible the clinical situation.

1.5.3 Summary of skin permeation studies

In an oral supplement study, human volunteers were required to take 3g/day ascorbic acid for six weeks. After this time, buccal keratinocytes were collected, and ascorbic acid concentration was found to increase 2-fold compared to the native level. Buccal keratinocytes are proposed to be a good model for skin keratinocytes.^{168,169} The dosage was significantly higher than the World Health Organisation (WHO) recommended daily intake of 60 mg/day so blood plasma saturation would have been achieved. As with many other tissues, it is likely that skin ascorbic acid levels respond to increases in plasma supply.^{169,170} However dietary supplementation, to raise skin ascorbic acid levels, is expected to be only effective in individuals with below-saturation plasma levels.¹⁶⁸ In contrast, In an *in vivo* porcine skin permeation study, a 15% ascorbic acid solution was applied to the skin via a Hill Top Chamber. After 24 hours, ascorbic acid concentration in the skin was found to increase 20-fold compared to the native level.¹⁷¹ Therefore, topical delivery achieves skin concentration higher than would be achieved by oral supplementation.

The number of ascorbic acid skin permeation studies is limited due to formulation scientists focussing on stable ascorbic acid derivatives.¹⁵⁰ All previous ascorbic acid permeation studies are presented in Table 1-3 below.

Table 1-3 Summary of ascorbic acid skin permeation studies.

	Species	Dose and time	Formulation	Analytical technique
Darr <i>et al.</i> (1992) ¹⁵⁸	<i>Ex vivo</i> porcine	8.88 mg/cm ² , finite, 48h	[¹⁴ C] ascorbic acid in gel	Liquid scintillation counter
Lee <i>et al.</i> (1998) ¹⁷²	<i>Ex vivo</i> mouse	Not specified, 48 h	[¹⁴ C] ascorbic acid in aqueous solution	Liquid scintillation counter
Pinnell <i>et al.</i> (2001) ¹⁷¹	<i>In vivo</i> porcine	200 µL under a hill-top chamber, infinite, 24 h	Aqueous solution	HPLC
Leveque <i>et al.</i> (2004) ¹⁷³	<i>Ex vivo</i> human	2 mg/cm ² , finite, 24h	Serum with silylated ascorbic acid (m/z 575)	GCMS
Lee <i>et al.</i> (2003) ¹⁷⁴	<i>Ex vivo</i> mouse	649.5 µL/cm ² , infinite, 24h	Aqueous solution with lasers and skin micro-dermabrasion	HPLC
Heber <i>et al.</i> (2006) ¹⁷⁵	<i>Ex vivo</i> human	20.4 mg/cm ² occluded with parafilm, 48 h	Anhydrous oil vehicle	Indirectly by immunocytochemistry of collagen
Zhou <i>et al.</i> (2014) ¹⁷⁶	<i>Ex vivo</i> mouse	564.9 µL/cm ² , infinite, 24h	Liposomal	UV-Vis
Duarah <i>et al.</i> (2017) ¹⁷⁷	<i>Ex vivo</i> goat	393.7 mg/cm ² , infinite, 8h	Polymer nanoparticle	UV-Vis
Maione-Silva <i>et al.</i> (2018) ¹⁷⁸	<i>Ex vivo</i> porcine	107.5 µL/cm ² , infinite, 24h	Liposomal	HPLC
Starr <i>et al.</i> (2019) ¹¹²	<i>Ex vivo</i> porcine	312.5 mg/cm ² , infinite, 24h	Supramolecular hydrogel	ToF-SIMS

As Table 1-3 shows, most skin permeation studies were performed with large infinite dose of formulation. Infinite dose conditions are likely to lead to an overestimation of the utility of the formulation due to occlusion and/ or evaporation of volatiles not occurring (Section 1.2.5.1).¹⁴ Leveque *et al.*¹⁷³ performed finite dose permeation studies on *ex vivo* human tissue using microdialysis technique. However, to be able to detect low ascorbic acid concentrations, the authors derivatised the ascorbic acid with a silyating agent, so the molecular weight of ascorbic acid was significantly increased. This is likely to have influenced permeation behaviour.

Due to ascorbic acid's hydrophilicity, permeation of ascorbic acid across the skin might be expected to be poor. Nevertheless, increased levels of ascorbic acid in the skin was found after topical application. Lee *et al.*¹⁷² reported ascorbic acid to penetrate mouse skin well, despite its hydrophilicity, and observed ascorbic acid to have a higher skin permeation compared with other hydrophilic drugs. However, mouse skin is no longer accepted as a suitable model for human skin permeation due to a thinner *stratum corneum* and being generally more permeable than human skin across a range of permeants.³⁸ No *in vivo* human skin permeation study has previously been reported according to the Cosmetic Ingredient Review expert panel¹⁶⁷ and Stamford *et al.*¹⁵⁰

One of the studies, Starr *et al.*¹¹², used ToF-SIMS to visualise the distribution of ascorbic acid in porcine skin tissue. The authors reported a supramolecular hydrogel to increase the depth and amount of permeation of ascorbic acid. ToF-SIMS analysis was performed in 3D by use of a second ion beam to sputter the tissue sample. The distribution of ascorbic acid across the *stratum corneum* and epidermis looked uniform, but this may have been due to a large infinite dose application which is unlikely to represent the clinical situation. All other studies in Table 1-3 used analytical techniques which do not have the ability to image the spatial distribution of ascorbic acid label-free.

1.5.4 Topical formulations

Work done by Pinnell *et al.* (2001)¹⁷¹ found that the pH of the formulation influences the penetration of ascorbic acid across the *stratum corneum*. Pinnell *et al.* investigated permeation of ascorbic acid at pH levels between 2.0 and 5.0

on *in vivo* porcine skin using a semi-occlusive Hill Top Chamber. It was reported that at pH <3.5, ascorbic acid is transported well across the *stratum corneum*¹⁵⁵. At this pH, the ionic charge on the molecule is removed (pKa for ascorbic acid is 4.2)¹⁵⁵. Low pH formulation is also preferred for ascorbic acid stability (see Figure 1-13).

As a result of this finding, Zielinski and Pinnell (2005)¹⁷⁹ obtained a patent for a single-phase ascorbic acid solution, with a pH of 2.5 and 3.0, and containing other antioxidants (namely cinnamic acid derivatives such as ferulic acid) to stabilise ascorbic acid in solution. Gel formulations and serums that contain ascorbic acid at the optimum pH 2.5 – 3.0, with and without other antioxidants, would infringe on this patent. However ascorbic acid formulations with emulsions and particles would not infringe the patent and can be formulated at low pH 2.5 – 3.0 for increased ascorbic acid stability.

Nanoparticles have been shown to enhance stability of encapsulated drugs (Section 1.4.2.3) so previous attempts of encapsulating ascorbic acid can be found in the literature and these are summarised in Table 1-4 below.

Only one of the nanoparticle examples in Table 1-4 was designed for topical application. Duarah *et al.* (2017)¹⁷⁷ prepared ascorbic acid encapsulated polymeric nanoparticles however a final ascorbic acid concentration of 0.2% w/v would be too small to observe therapeutic effect on the skin. Furthermore the polymer used does not have the same skin benefits as lipids (Section 1.4.2.2). Guney *et al.* (2014)¹⁸⁰ on the other hand prepared ascorbic acid encapsulated SLNs using a hot homogenisation method. This involved heating the lipid matrix to 80 °C to which ascorbic acid was added. This high temperature would degrade ascorbic acid during manufacture and is therefore considered not suitable.

Table 1-4 Summary of recent nanoparticles encapsulating ascorbic acid in the literature. ND = not documented. Red shaded boxes indicate properties considered not suitable for topical ascorbic acid formulations.

	Duarah <i>et al.</i> (2017) ¹⁷⁷	Lin <i>et al.</i> (2015) ¹⁸¹	Guney <i>et al.</i> (2014) ¹⁸⁰	Britto <i>et al.</i> (2014) ¹⁸²	Cho <i>et al.</i> (2012) ¹⁸³
pH	4.89 ± 0.5	2.1 – 2.6	ND	ND	ND
Entrapment efficiency (%)	87.3 ± 0.84	ND	90	17.1 (chi) 6.3 (TMC)	55 - 67
Zeta potential (mV)	+ 9.30	ND	-19.5 – 25.4	30.7 ± 3.7 mV (chi) 10.3 ± 6.4 mV (TMC)	+5.9 to +18.4
Polydispersity index	0.265	0.164 – 0.353	0.321 – 0.387	ND	ND
Particle size (nm)	258 ± 12	150 - 300	200 -250	325 ± 24 nm (chi) 338 ± 74 nm (TMC)	215.6 - 288.2
Final ascorbic acid concentration	0.2% w/v	ND but states 10% of gelatine weight	ND but states 5% of lipid weight	0.067 % w/v	ND but states 4% of N-acyl chitosan weight
Preparation method	Solvent emulsification	Double desolvation	Hot homogenisation	Homogenisation	Ultrasonication
Type	Polymeric	Gelatine	SLN	Polymeric; chitosan (chi) and N,N,N-trimethyl chitosan (TMC)	Polymeric
<i>In vivo/In vitro</i> testing	<i>Ex vivo</i> skin permeation study on excised goat skin membrane	Cell uptake studies with NCTC Clone 929 Cell line (murine)	Anti-tumour efficacy on Rat H-Ras 5RP7 cells and NIH/3T3 cells	None (food grade nanoparticle)	<i>In vitro</i> release studies in PBS and HCl solution

The number of reported ascorbic acid encapsulated nanoparticles is quite low (Table 1-4), in part due to the difficulty in encapsulating a hydrophilic ingredient. Nanoparticles for oral or parenteral administration require high encapsulation efficiencies (70 – 90%)¹⁸⁴ whereas for topical administration it could be argued encapsulation efficiency is less important as the particles do not permeate intact (Section 1.4.2.4). Therefore, there is scope to develop ascorbic acid nanoparticle formulation specifically for topical delivery.

1.6 Topical delivery of caffeine

1.6.1 Skin benefits

Caffeine (Figure 1-14) is being increasingly used in skin care products due to its wide range of therapeutic effects. Caffeine is an anti-cellulite by stimulating the degradation of fats during lipolysis through inhibition of phosphodiesterase. It also increases microcirculation of blood in the skin and stimulates hair growth through inhibition of 5- α -reductase. Caffeine is also an antioxidant so has a protective effect against UV-radiation. Commercially available topical formulations normally contain 3% caffeine.^{185,186}

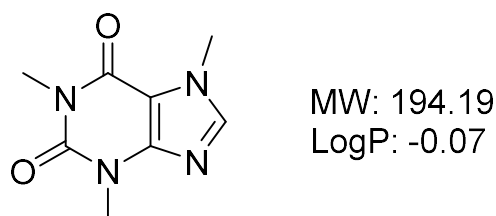


Figure 1-14 Caffeine molecular structure and physicochemical properties.

1.6.2 Existing skin permeation data

Caffeine is recommended as a model hydrophilic compound by the OECD Guidance notes on dermal absorption No. 156³². Due to inter and intra-laboratory variability for *in vitro* skin permeation experimental data, some countries suggest data from a reference compound is obtained at the same time, or close to the dates of the study to increase confidence in the results.³²

Caffeine skin permeation has been studied extensively *in vitro* and *in vivo*.¹⁸⁶ Previous studies by Otberg *et al.* (2008)¹⁸⁷, Trauer *et al.* (2009)²⁴ and Liu *et al.*

(2011)²³ point to an important role for the follicular pathway in caffeine skin permeation. The authors applied a formulation containing polyethylene glycol (PEG) and ethanol as a finite dose with no occlusive covering of the skin. The authors used a follicular closing technique (Figure 1-8) to study caffeine permeation. The amount of formulation applied *in vivo* was significantly less than in the *in vitro* experiments because a more sensitive analytical method was used for the *in vivo* samples. The authors reported the follicular penetration pathway contributed 50% of the total penetration *in vitro*, and 34% of the total penetration *in vivo* in human skin permeation experiments, as shown in Figure 1-15.

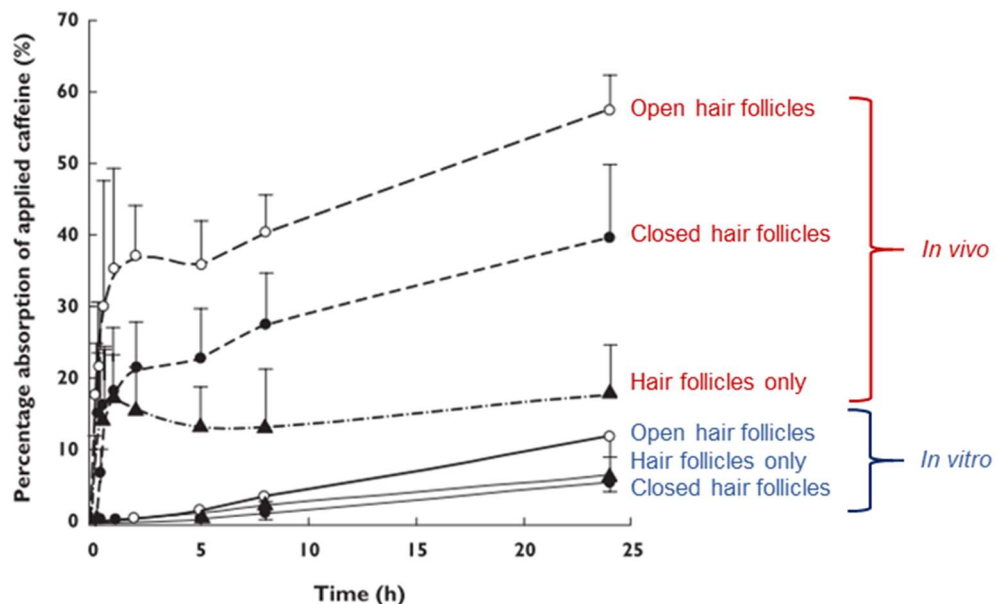


Figure 1-15 Comparison of mean absorption of applied caffeine *in vivo* (blue) and *in vitro* (red). Data shown as mean \pm SD ($n=6$). Taken from Liu et al.²³

Follicular closing technique combined with chromatography analytical method does not allow the permeation of caffeine into hair follicles to be visualised. Follicular penetration is assumed to occur in unblocked hair follicles but not in blocked hair follicles. In their unblocked hair follicle experiments, the authors applied wax to the area of the skin without hair follicle present to compensate for the skin surface area lost when blocking hair follicles. Being able to see the spatial distribution of the active ingredient is important in being able to understand the mechanism of permeation.

1.7 Aims of this thesis

This thesis looks to address the current limited understanding of ascorbic acid skin permeation, by using ToF-SIMS, to visualise the spatial distribution in the skin. Comparison will also be made to established analytical techniques that are traditionally used for skin permeation studies.

The first aim of this thesis is to compare the skin permeation of ascorbic acid and caffeine, which is an extensively studied hydrophilic molecule, and their distribution in the skin tissue. The experimental approach and analytical parameters will be first optimised for monitoring ascorbic acid and caffeine. Formulations, with clinically relevant dosage, will then be prepared and applied to *in vitro* porcine skin to closely match real-life topical application. Following this, skin cross sections will be analysed to obtain information about the permeation distribution of the active ingredients into the epidermis and hair follicles of the skin. This knowledge would enable an understanding of the principal routes of permeation into the skin and inform formulation development to observe improved permeation.

The second aim of this thesis is to develop enhanced ascorbic acid permeation into the *stratum corneum* layer of the skin by using emerging and classic topical formulation strategies, specifically lipid nanoparticle containing formulation and oil-in-water emulsion. Lipid nanoparticle formulations will be prepared and extensively characterised to evaluate their suitability for topical application. A tape stripping procedure will be used to monitor the permeation of ascorbic acid for *in vitro* porcine skin and *in vivo* human skin. The tape strip samples will be analysed by ToF-SIMS to visualise the distribution of ascorbic acid, and excipients, in layers of the *stratum corneum*. This data will be evaluated with a conventional chromatography approach to analysing tape strips. Analysis by two independent analytical methods will help determine whether the formulations have enhanced ascorbic acid permeation but also reveal novel insights about ascorbic acid permeation.

Chapter 2: Optimisation of the experimental approach to study skin permeation of ascorbic acid and caffeine

2.1 Introduction

Skin permeation cannot be monitored unless there is an identified analytical method that is specific to the compound(s) of interest and has measurement sensitivity with physiologically relevant concentration/ dosages applied to the skin. Imaging techniques, such as ToF-SIMS and CRM, do not provide absolute quantitative results due to matrix-related effects, whereas established analytical techniques, such as UV-Vis spectroscopy and HPLC, do not provide imaging capability (Section 1.3). Therefore, to study skin permeation, imaging techniques require the support of established analytical methods to cross-validate findings.

Following *ex vivo* skin permeation experiments, imaging techniques can be used to analyse skin cross sections. When obtaining biological tissue cross sections, it is common practise to use an embedding medium to preserve tissue morphology and to provide support during sectioning.¹⁸⁸ However, there is concern that the use of embedding agents could interfere with the permeant distribution in the skin, particularly at the skin surface (*stratum corneum*) and this may not reflect the actual permeant distribution.

Ascorbic acid is known to oxidise in aqueous solution. High pH and temperatures can also increase the rate of oxidation (Section 1.5). This provides a challenge when interpreting ascorbic acid concentration that has reached the Franz cell acceptor compartment or been extracted from tape strip samples into solution. Ascorbic acid stability therefore needs to be evaluated over time so that its permeation is not underestimated.

Tape stripping is a popular technique to assay the amount of active that has permeated or is localised in the *stratum corneum* barrier (Section 1.2.4.1). There is no standardised protocol for the extraction of tape stripped *stratum corneum* samples, with researchers using different extraction receptacles, extraction solvents, extraction solvent volumes, incubation time and sonication

and/or vortex mixing time. This can make comparisons with other studies difficult particularly if extraction efficiency/recovery was not measured.

Tape stripping of the *stratum corneum* results in a variable amount of corneocytes lifted by the adhesive tape due to a range of intrinsic and extrinsic factors (Section 1.2.4.1). It is therefore important to normalise for this when determining penetration depth of active ingredients. This can be achieved by weighing the tape strips or determining protein content. Topically applied formulation may be stuck to the tape strips, resulting in an additional weight increase, so weighing the tape strips is not reliable.¹⁸⁹ For quantification of *stratum corneum* proteins, a bicinchoninic acid (BCA) assay, a copper-reduction based protein assay, is typically used.¹⁹⁰ However, the BCA assay is not compatible with ascorbic acid since it can also reduce Cu^{2+} to Cu^{+} , so the BCA assay cannot be used in this work.

2.2 Chapter aims

The aim of this chapter is to optimise the experimental approach for studying ascorbic acid and caffeine permeation using both imaging techniques and established analytical methods. An alternative approach to obtaining skin cross sections will be investigated to avoid interference from embedding agents. The stability of ascorbic acid in aqueous solution (i.e. Franz cell acceptor compartment and tape strip extraction solutions) was evaluated over time to avoid underestimation of ascorbic acid concentration. The method for extracting ascorbic acid from tape strip samples was also assessed to ensure complete extraction recovery. Alternative approaches to quantifying protein from tape stripped *stratum corneum* was also investigated to normalise for depth of *stratum corneum* removed.

2.3 Materials and methods

2.3.1 Materials

Ascorbic acid and caffeine were purchased from Sigma-Aldrich (Haverhill, UK). Phosphate buffered saline (PBS) tablets were purchased from Fischer Scientific (Loughborough, UK). Metaphosphoric acid (MPA) was purchased from VWR International (Lutterworth, UK). Ultrapure water was prepared in-house with a conductivity of 0.055 $\mu\text{S}/\text{cm}$ and a resistivity of 18.2 $\text{M}\Omega\cdot\text{cm}$, using Milli-Q station from Millipore Corp. (Watford, UK). All reagents were of analytical grade, unless otherwise stated.

2.3.2 Porcine ear skin collection and preparation

Porcine ears were obtained from a local abattoir from six month old pigs. The pigs were specifically reared for food, and not experimentation, and was therefore a secondary use of the animal in accordance with the NC3R framework on the replacement, reduction and refinement of animals used in research. Porcine ears were taken immediately after slaughter and prior to any cleaning (by scalding tank). The ears were washed with distilled water and dried using tissue. The ear skin was not detached from the underlying cartilage and was wrapped in aluminium foil and stored at $-20\text{ }^{\circ}\text{C}$. Ear skin was used within 6 months of being frozen.

All *ex vivo* porcine skin permeation experiments were performed with the inner side of the ear. The inner ear skin is protected from external contact, so the skin is usually less damaged than the outer side. Therefore, a number of large test site areas ($n > 6$) could be delineated from one ear skin. In addition, the inner ear skin is more strongly attached to the underlying cartilage so limits the shrinkage or expansion of the skin layer with freezing. Lastly Meyer and Zschemisch¹⁹¹ determined the ear skin thickness layer of domesticated pigs and found no significant difference in *stratum corneum* thickness between outer and inner sides. They did however find that the outer side had a larger dermis thickness, but this is not the principle barrier to skin permeation.

2.3.3 Franz diffusion cell permeation experiment

Porcine ear was defrosted at 4 °C overnight before use. The hair was carefully trimmed by scissors to avoid any damage to the *stratum corneum*. The ear was then cut, using scalpel blade, to generate samples that could fit the Franz cell. The skin was also detached from the underlying cartilage to give full thickness skin samples. Excess subcutaneous fat was also carefully removed using a scalpel blade. The skin samples were mounted, epidermis facing upwards, in Franz-type static diffusion cells (PermeGear, Inc., Hellertown, PA, USA) with an exposed diameter of 11 mm (exposed surface area = 0.95 cm²).

To measure skin integrity, the acceptor and donor chamber were filled with 3 mL and 1 mL of 0.9% w/v sodium chloride solution respectively. The Franz cells were equilibrated for approximately 30 minutes, at 36.5 °C, placed in a stirring water bath (Clever Scientific Ltd, UK). TEER was measured using an EVOM2 Voltohmmeter (World Precision Instruments, U.S.A) with one electrode in the acceptor solution and the other in the donor solution. Skin samples passed the integrity test if they showed resistance ≥ 1.57 k Ω /cm².⁴⁸

The acceptor chamber (3 mL capacity) was filled with PBS solution (100 mM, pH 7.4) or MPA solution (25 mM, pH 2.4) and a stirrer bar. The Franz cells were carefully inverted to remove air bubbles in the acceptor solution. The donor chamber side of the skin received a ~ 20 mg/cm² dose of formulation (5% w/w ascorbic acid in water, pH 2.4). The Franz cells were then placed upright in a stirring water bath for 24 hours at 36.5 °C - this was measured to give a skin surface temperature of 32 °C. After the allotted time, the skin sample was removed from the Franz cell and frozen (Section 2.3.4). The receptor fluid was withdrawn using syringe luer, and filtered through 0.22 μ m membrane filter (Merck Millipore Ltd, Ireland). Receptor fluid samples were stored at – 20 °C until further analysis.

2.3.4 Freezing and cryo-ultramicrotome of skin tissue

Skin samples, after permeation experiment, were carefully handled to avoid disturbing the epidermis. The skin application sites were cut into square size, with an area of approximate 1 cm \times 1 cm. The liquid nitrogen vapour freezing

method was chosen to freeze the skin tissue as this avoids any contact with liquids (e.g. ethane, isopentane) that could disturb the active ingredient distribution in the skin. A styrofoam box – freezing chamber was filled with an appropriate level of liquid nitrogen (Figure 2-1 A). The skin tissue, placed in individual Cryomold® moulds, was then frozen by the nitrogen vapour. The frozen skin tissue was then firmly mounted in a vertical position using a small level of optimal cutting temperature (OCT) compound (VWR Chemicals, UK) in the cryomold (Figure 2-1 B). The OCT was immediately frozen by placing the cryomold on the cold metal block in the freezing chamber. This was done so that the skin tissue could be mounted perpendicular to the cryo-sectioning blade. All skin tissue was stored in a freezer at -80 °C.

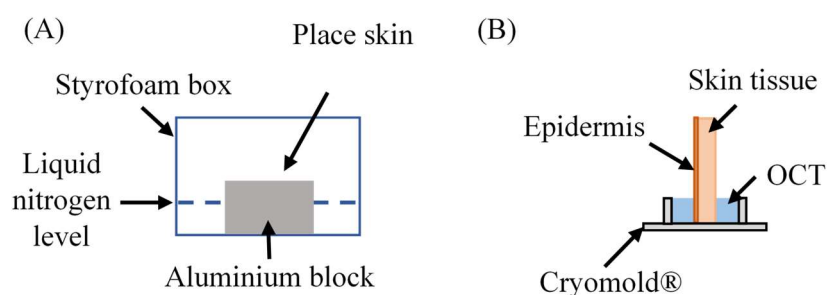


Figure 2-1 Schematic of liquid nitrogen vapour freezing method. (A) Diagram indicating the appropriate level of liquid nitrogen relative to the metal block. (B) Mounting of skin tissue in OCT embedding medium.

Vertical skin cross sections (20 μm thick) were taken using a cryostat (Leica CM3050, Leica Biosystems GmbH, Wetzlar, Germany). An object temperature of -30 °C and chamber temperature of -24 °C was used. Approximately 10-16 cross sections were collected from each skin sample. Intact skin cross sections, that showed a hair follicle at or close to the skin surface, and at least 200 μm apart were selected for ToF-SIMS analysis (n=2 per skin sample). An optical profiling microscope (Zeta-20, KLA-Tencor Corporation, Milpitas, CA, USA) was used to inspect the cross sections. Where required, haematoxylin and eosin (H&E) staining was performed with the standard protocol.¹⁹²

2.3.5 Tape stripping of *stratum corneum*

Untreated *ex vivo* porcine ear skin and *in vivo* human volar forearm skin was tape stripped using Corneofix® F 20 adhesive tape strips (Courage + Khazaka electronic GmbH, Cologne, Germany). Clausen *et al.* (2016)¹⁹³ reported no significant difference in the amount of corneocytes lifted when 5 or 10 seconds of pressure was applied on the tape strip on human skin. Tape strips was therefore pressed onto the skin test site by thumb pressure, for 10 seconds, and removed from the skin in one quick motion. Each skin test site was tape stripped taking up to 15 consecutive tape strip layers. The direction of stripping was altered by 90 degrees after every tape to ensure even removal of the *stratum corneum*.

2.3.6 UV-Vis analysis

A UV-Vis spectrophotometer, Varian Cary®50 UV-Vis Spectrophotometer (Agilent Technologies, Santa Clara, CA, USA), was used to measure the absorbance of ascorbic acid (254 nm) and caffeine (275 nm) in Franz receptor fluid. A Quartz cuvette for used for all measurements. Calibration curve of ascorbic acid and caffeine was established from 0 to 20 µg/mL. All samples were filtered as specified in Section 2.3.3.

2.3.7 HPLC analysis

2.3.7.1 Extraction of ascorbic acid from tape strip samples

To determine extraction efficiency, blank tape strips (with no corneocytes) were spiked with 48 mg of ascorbic acid formulation (5% w/w in water). The tape strip was briefly placed on a hotplate, set to 40 °C, for the evaporation of the water. The tape strip was then extracted. The final optimum extraction protocol is detailed here. Tape strips were extracted in individual microcentrifuge tubes (Eppendorf®, 1.5 mL) with 1 mL of extraction solvent. Sponges were extracted in individual centrifuge tubes (BD Falcon™, 50 mL) with 10 mL of extraction solvent. Extraction solvent was composed of 75:25 v/v 25 mM MPA (pH 2.4): methanol. Tape strips were extracted overnight (12-14 hrs) at ambient temperature and darkness with 10 minutes sonication at the

start and end of extraction (total 20 minutes sonication). Clausen *et al.* (2016)¹⁹³ found no significant difference in the retrieved amount of protein (and therefore corneocytes) in PBS solution when using 10 mins or 15 mins sonication time at the start and end of extraction. Therefore, ultrasonication time did not require further optimisation. Once extraction was complete, the tape or sponge was removed from the centrifuge tubes and extraction samples centrifuged at 10,000 rpm for 10 minutes (Centrifuge 5430, Eppendorf® AG, Germany). Extraction samples were analysed by HPLC on the same day.

2.3.7.2 Detection of ascorbic acid

The HPLC method used to quantify ascorbic acid is based on the validated method by Maia *et al.* (2007)¹⁹⁴. This method had not been used to study skin permeation previously. Chromatographic analysis was performed in an Agilent 1100 series instrument (Agilent Technologies, Santa Clara, CA, USA) equipped with inline degasser, quaternary pump, column thermostat, autosampler and variable wavelength UV detector (G1314A). System control and data acquisition were performed using Chemstation software. A GraceSmart™ RP C18 (5 µm, 250 mm × 4.60 mm) was used.

The adapted chromatographic conditions consisted of a mobile phase of 95:5 v/v 25 mM MPA (pH 2.4): methanol, flow rate of 1.0 mL min⁻¹, ambient column temperature (20 °C), injection volume of 20 µL and detection wavelength of 254 nm. Ascorbic acid had a retention time of 3.4 minutes. The mobile phase solvents were filtered through a pore 0.7 µm diameter glass microfibre filter (VWR International bvba, Leuven, Belgium) and degassed using an in-line degasser. The mobile phase solvents were combined using individual pump lines in the HPLC.

2.3.8 ToF-SIMS analysis

Analysis was performed using a ToF-SIMS IV instrument (IONToF, GmbH) with a Bi₃⁺ cluster primary ion source and a single-stage reflectron analyzer. A primary ion energy of 25 keV, a pulsed target current of approximately 0.3 pA, and postacceleration energy of 10 keV were employed throughout the analysis. The primary ion beam had a focused beam size of 1–2 µm, and the primary ion

dose density was maintained at $<1 \times 10^{12}$ ions/cm² throughout to ensure static conditions. Charge compensation of the sample was performed using a low-energy (<20 eV) electron flood gun.

For skin cross section samples, spectra were acquired in high-current bunched mode over $1.5 \text{ mm} \times 3 \text{ mm}$ areas in either positive or negative polarity, at a resolution of 100 pixels/mm. Each $1.5 \text{ mm} \times 3 \text{ mm}$ area was scanned using the macroraster stage function, using a random raster pattern. A total of 18 separate $0.5 \text{ mm} \times 0.5 \text{ mm}$ patches were scanned, with 45 scans acquired per patch.

For tape strip samples, spectra were acquired in high-current bunched mode over $4 \text{ mm} \times 4 \text{ mm}$ areas in negative polarity and positive polarity, at a resolution of 100 pixels/mm. Each $4 \text{ mm} \times 4 \text{ mm}$ area was scanned using the microraster stage function, using a random raster pattern. A total of 64 separate $0.5 \text{ mm} \times 0.5 \text{ mm}$ patches were scanned, with 15 scans acquired per patch. ToF-SIMS data was acquired and analyzed using SurfaceLab 7 software (IONToF, GmbH). Ion intensities were normalized to the total ion count of the spectra. Note that intensities in different ion images do not reflect the relative abundances of the corresponding analytes.

2.3.9 CRM analysis

CRM analysis of skin cross section was performed under ambient conditions using a Horiba Jobin Yvon LabRAM HR confocal Raman microscope (Horiba, Ltd., Kyoto, Japan). Spectra were acquired using a 660 nm red laser source (at a power of 8.6 mW), a 50 \times objective lens and a 300 μm confocal pinhole. Single point measurements were acquired over the range 100 - 4000 cm^{-1} with an acquisition time of 30 s and spectral resolution of 300 gr/mm .

2.3.10 Protein quantification of tape strip samples

2.3.10.1 Dye binding protein assay

Skin tape strips were extracted in individual Eppendorf® tubes, as previously described (Section 2.3.7) using either 75:25 (w/w) 25 mM MPA: MeOH or 0.1M NaOH as the extraction solvent. 10 μL of extraction sample was placed

in the microplate with 150 μL protein assay reagent. Where mentioned, extraction samples were concentrated by evaporating to dryness using a centrifugal evaporator (Jouan RC1010, Jouan SA, France) and reconstituted in water. BSA protein standard was used to prepare calibration curve samples from 25-1500 $\mu\text{g}/\text{mL}$. The microplate protocol from the Pierce™ 660nm Protein Assay Kit (Thermo Scientific™, MA, USA) was followed. Blank wells containing corresponding solvent were used to zero the plate-reader (Tecan microplate reader, Tecan Trading AG, Switzerland) absorbance.

2.3.10.2 Infrared densitometry

Protein content (C_{protein}) was measured directly from the tape strips. Firstly, protein absorption was determined at 850 nm using an infrared densitometer, SquameScan™ 850A (Heiland Electronic GmbH, Wetzlar, Germany), using an empty tape strip as a reference. A reference glass sample provided by the manufacturer was used to confirm instrument calibration prior to each use.

The absorbance value from human tape strips was then converted to protein content as follows:

$$C_{\text{protein}} (\mu\text{g cm}^{-2}) = \frac{\text{absorbance} - 2.703}{0.623} \quad (\text{Equation 2.1})$$

For porcine tape strips, the following equation was used:

$$C_{\text{protein}} (\mu\text{g cm}^{-2}) = \frac{\text{absorbance}}{0.41} \quad (\text{Equation 2.2})$$

Both equations 2.1 and 2.2 originate from previously validated calibration curves.^{60,195} The density of human *stratum corneum* has been previously determined as $\sim 1\text{g}/\text{cm}^3$.¹⁹⁶ The cumulative amount of removed *stratum corneum* proteins can therefore be used to calculate *stratum corneum* depth with the following equation:

$$\text{Depth} (\mu\text{m}) = \frac{\sum C_{\text{protein}} (\mu\text{g cm}^{-2})}{1 \times 10^6 \mu\text{g cm}^{-3}} \times 10^4 \quad (\text{Equation 2.3})$$

2.3.11 Statistics

Graphpad Prism Software vs. 7.03 (GraphPad Software Inc., La Jolla, CA, USA) was used to perform statistical analysis. Shapiro-Wilks Normality Test was used to test for Gaussian distribution of data. An unpaired t test with Welch's correction was used for data which showed Gaussian distribution and an unpaired Mann-Whitney test (nonparametric test) was used for data which did not show Gaussian distribution. When all data to be compared showed a Gaussian distribution, differences between groups were compared using one-way analysis of variance (ANOVA) with Tukey post hoc test. Differences were considered significant at * $p < 0.05$, ** $p < 0.01$, *** $p < 0.001$, **** $p < 0.0001$.

2.4 Results and discussion

2.4.1 Analysis of skin cross sections without embedding material

When obtaining cross sections by cryo-ultramicrotome, it is common to use an embedding medium, such as OCT compound, for fragile and /or small tissue specimens. OCT compound is a water-soluble blend of polyvinyl alcohol (PVA) and PEG and other ingredients. OCT acts as an inclusion medium during the freezing process and does not penetrate inside the cells as embedding with paraffin does.¹⁹⁷ Despite this, there was still a concern that OCT embedding could introduce secondary ions in the ToF-SIMS spectra and/or influence permeant distribution.

A new method has been proposed whereby only a very small amount of OCT is used on one side (not skin surface) of the skin tissue, to be able to mount the tissue on the sample holder of the cryo-ultramicrotome, but to obtain cross sections where the skin surface has not been exposed to OCT compound (Section 2.3.4). This method does not work for dermatomed skin tissue because it is fragile and difficult to mount in the cryo-ultramicrotome without embedding, hence full thickness skin was used.

Fragment ions diagnostic of OCT compound were found in the ToF-SIMS spectra of reference OCT compound, the fragment ion $C_2H_3O^+$ at m/z 44 for instance can be deduced from the PVA monomer C_2H_4O . When analysing the epidermis region of the skin, avoiding the area of the glass slide as shown in Figure 2-2, it was found that skin cross sections embedded in OCT contained higher intensities for fragment ions diagnostic of OCT compound in comparison with the epidermis of the skin cross sections not embedded in OCT.

The presence of OCT in the epidermis spectra suggests a possible permeation into the tissue or spaces within the tissue. The co-localisation of epidermis and OCT compound indicates that embedding in OCT is likely to influence the distribution of topically applied ingredients and should therefore be avoided. OCT compound may also result in matrix effects, for instance D'Alvise *et al.*⁴⁶

analysed skin cross sections using DESI-MS and found that using embedding material, such as OCT compound, led to ion suppression.

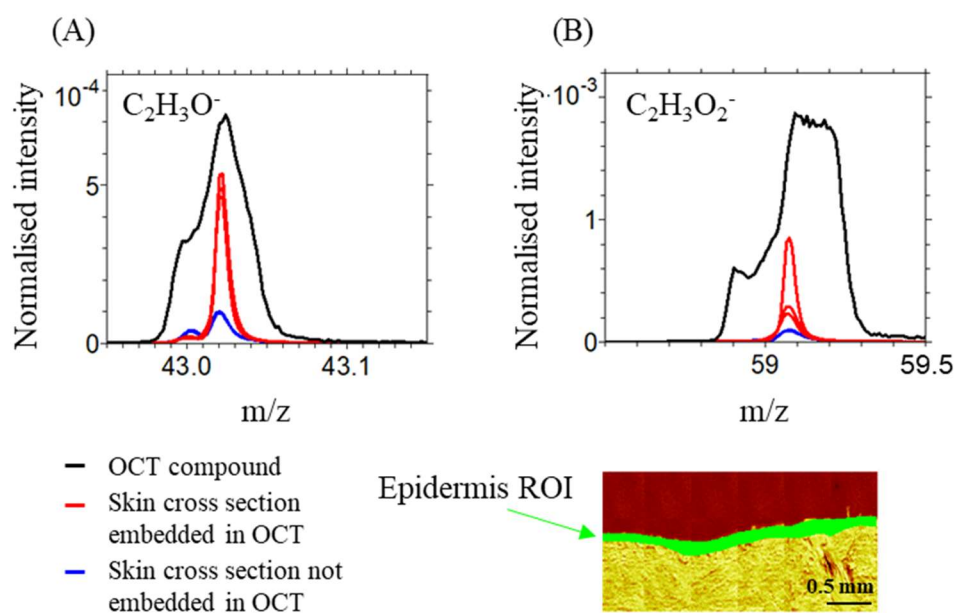


Figure 2-2 Normalised ToF-SIMS intensity of (A) $C_2H_3O^-$ ($m/z = 43$) and (B) $C_2H_3O_2^-$ ($m/z = 59$), which are OCT compound associated fragment ions, from the epidermis region of interest (ROI) of porcine skin cross sections with and without OCT embedding ($n=3$).

Observation of the skin cross sections by optical profilometer microscope found that all layers of the skin, including the *stratum corneum*, were collected onto the glass slide, even without OCT embedding (Figure 2-3). Embedded skin cross sections showed smearing of the OCT close to the skin surface whilst non-embedded skin cross sections showed movement of loose corneocytes away from the skin surface. The former is less preferable as it could disturb the distribution of ingredients at the skin surface, as both ascorbic acid and caffeine are hydrophilic. As such, all skin cross sections were obtained without OCT embedding so that the epidermis containing topically applied drug could be analysed with minimal interference. This is thought to be the first instance of skin tissue sections being produced without an embedding media for analysis by ToF-SIMS (Section 1.3.3.3).

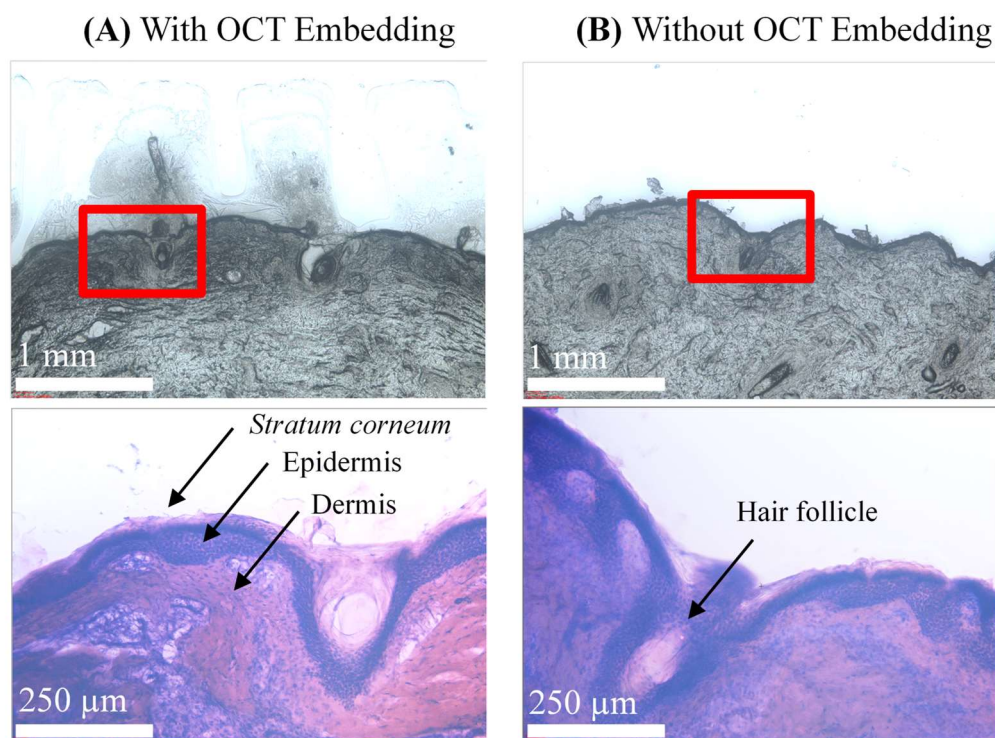


Figure 2-3 Optical profilometer image of porcine skin cross sections with (A) and without (B) OCT embedding. Inset window is location of H&E stained cross section view below.

2.4.2 Investigating the permeation of ascorbic acid and caffeine by imaging techniques

The ToF-SIMS analysis of skin cross sections and tape strip samples has been demonstrated in previous studies to be able to show the spatial distribution of both endogenous and exogenous compounds within the skin barrier (Section 1.3.3.3). Whilst ascorbic acid skin permeation has previously been studied by ToF-SIMS¹¹², caffeine has not been reported.

Ascorbic acid produces a higher intensity molecular ion in the negative ionisation mode than positive ionisation mode, specifically $C_6H_7O_6^-$ at m/z 175, in the ToF-SIMS (Figure 2-4). The ion fragment, with m/z 175, is likely to be from a mixture of ascorbic acid (MW 176 g mol^{-1}) and the oxidised form of ascorbic acid (MW 174 g mol^{-1}) due to the large variation in ionisation probabilities (Section 1.3.3.2).

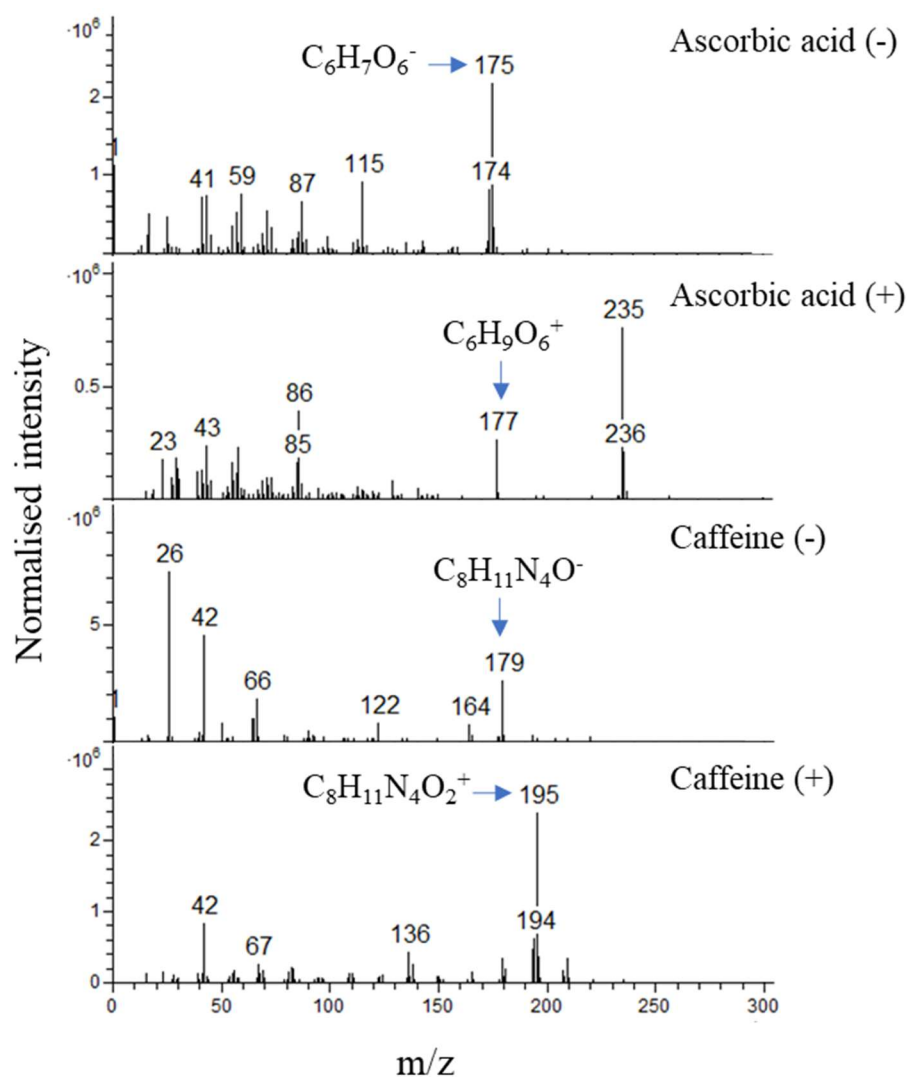


Figure 2-4 Ascorbic acid and caffeine ToF-SIMS reference spectra in negative and positive ionisation mode.

In contrast caffeine produces a higher intensity molecular ion in the positive ionisation mode than negative ionisation mode, specifically $C_8H_{11}N_4O_2^+$ at m/z of 195, and has a similar intensity to the negative molecular ion of ascorbic acid. This is important because the ToF-SIMS can then be assumed to have the same sensitivity in monitoring the permeation of ascorbic acid and caffeine, providing these molecular ions are distinct from those found in untreated skin tissue.

To identify the location of the epidermis and dermis layers of the skin, secondary ions from native skin cross sections (untreated) were examined for their distribution. Various ions associated with skin phospholipids,

sphingolipids, cholesterol, cholesterol sulfate, fatty acids and triglycerides have been previously identified.^{106,111} In negative polarity, cholesterol sulphate $[M-H]^-$ ion, $C_{27}H_{45}O_4S^-$ at m/z 465, was found localised to the *stratum corneum* and epidermis regions of the cross section (Figure 2-5 B). A generic tissue marker ion, CN^- at m/z 26, was found to be homogeneously distributed across both epidermis and dermis (Figure 2-5 C). The ToF-SIMS spectra of the epidermis region of native skin, dermis region of native skin and ascorbic acid reference material was compared to check that the ions $C_{27}H_{45}O_4S^-$, CN^- and $C_6H_7O_6^-$ were diagnostic of epidermis, dermis and ascorbic acid respectively (Figure 2-5 F). There was minimal overlap between the spectra, therefore $C_6H_7O_6^-$ ion at m/z of 175 was established as being specific to ascorbic acid and could be used to monitor skin permeation.

In positive polarity, a ceramide fragment ion, $C_{17}H_{32}N^+$ at m/z 250, was found strongly localised to the *stratum corneum* and epidermis regions (Figure 2-6 B), whilst a phosphatidylcholine fragment ion, $C_5H_{15}PNO_4^+$ at m/z 184 was found strongly localised to the dermis regions (Figure 2-6 C). The *stratum corneum* is known to contain negligible phospholipids.¹⁹⁸ The $C_8H_{11}N_4O_2^+$ ion at m/z of 195 was specific to caffeine and was selected to monitor skin permeation.

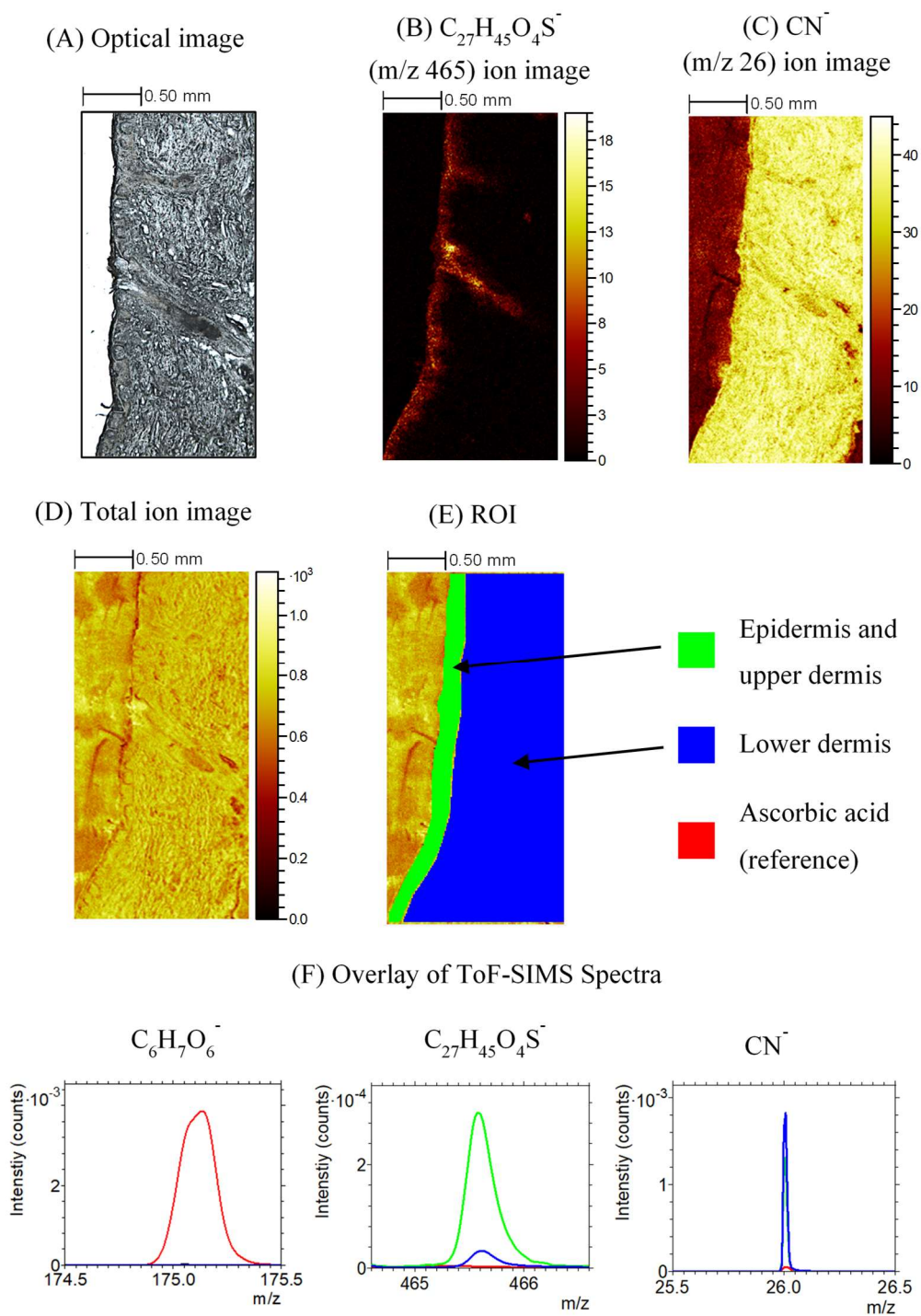


Figure 2-5 Negative-ion ToF-SIMS images (B-D) of an untreated porcine ear skin cross section. (E) Regions of interest (ROI) were defined on the ToF-SIMS ion image. (F) Overlay ToF-SIMS spectra showing the normalised intensity of ions in the epidermis and upper dermis (green), lower dermis (blue) and caffeine reference spectra (red).

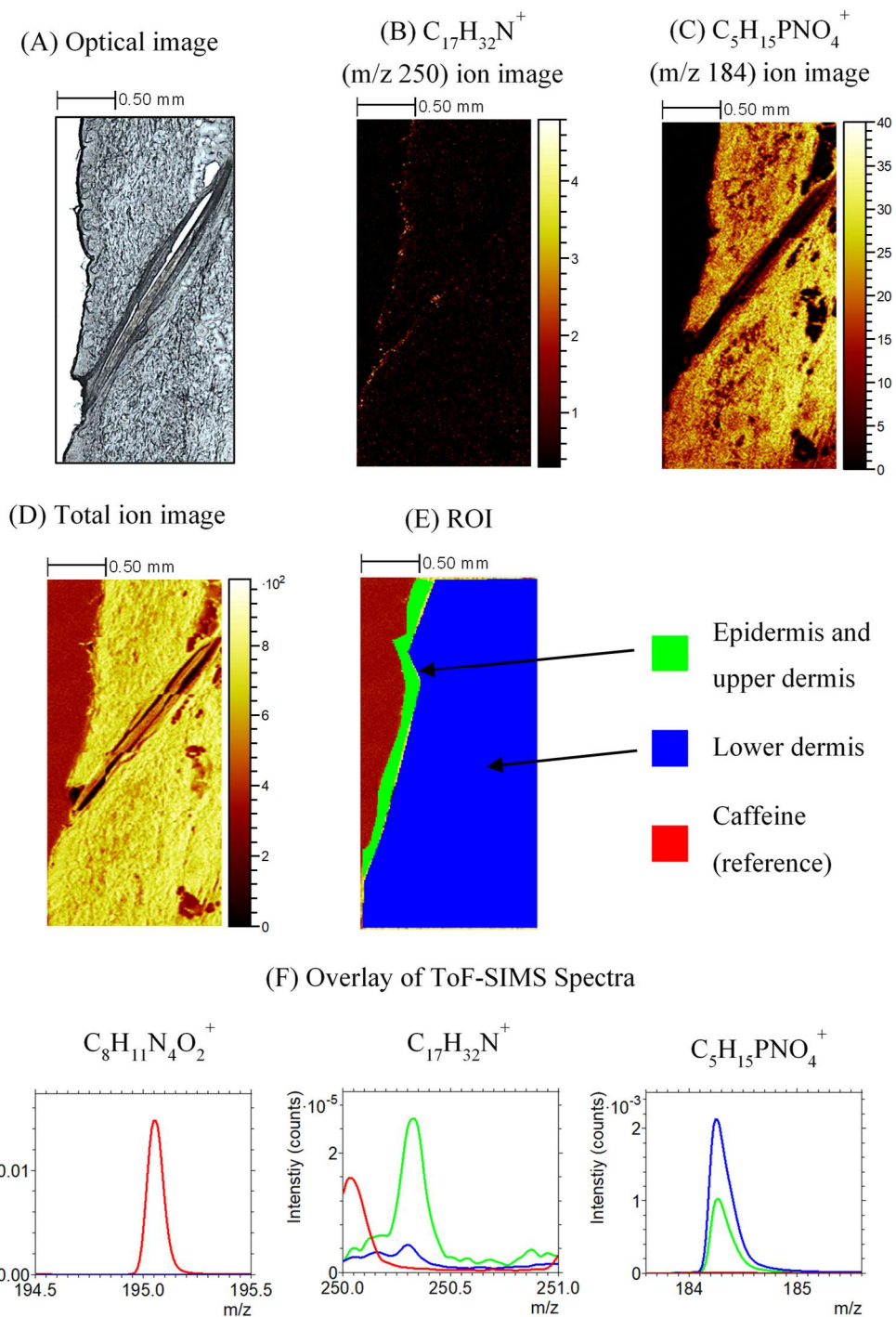


Figure 2-6 Positive-ion ToF-SIMS images (B-D) of an untreated porcine ear skin cross section. (E) Regions of interest (ROI) were defined on the ToF-SIMS ion image. (F) Overlay ToF-SIMS spectra showing the normalised intensity of ions in the epidermis and upper dermis (green), lower dermis (blue) and caffeine reference spectra (red).

An analysis of the permeation of ascorbic acid in porcine skin tissue, using ToF-SIMS, has been carried out before by Starr *et al.*¹¹² using a large infinite dose of formulation ($\sim 1 \text{ g/cm}^2$, 5% w/w ascorbic acid). To check the ToF-SIMS instrument was sensitive with a smaller more clinically relevant applied dose of formulation, preliminary skin permeation experiments were performed, as specified in Section 2.3.3., with $\sim 20 \text{ mg/cm}^2$ of formulation applied. It was possible to detect ascorbic acid, although mainly localised to the *stratum corneum* and epidermis, of the skin cross section ToF-SIMS ion image shown in Figure 2-7. ToF-SIMS instrument therefore had acceptable sensitivity to detect ascorbic acid from clinically relevant topically applied dose to the skin.

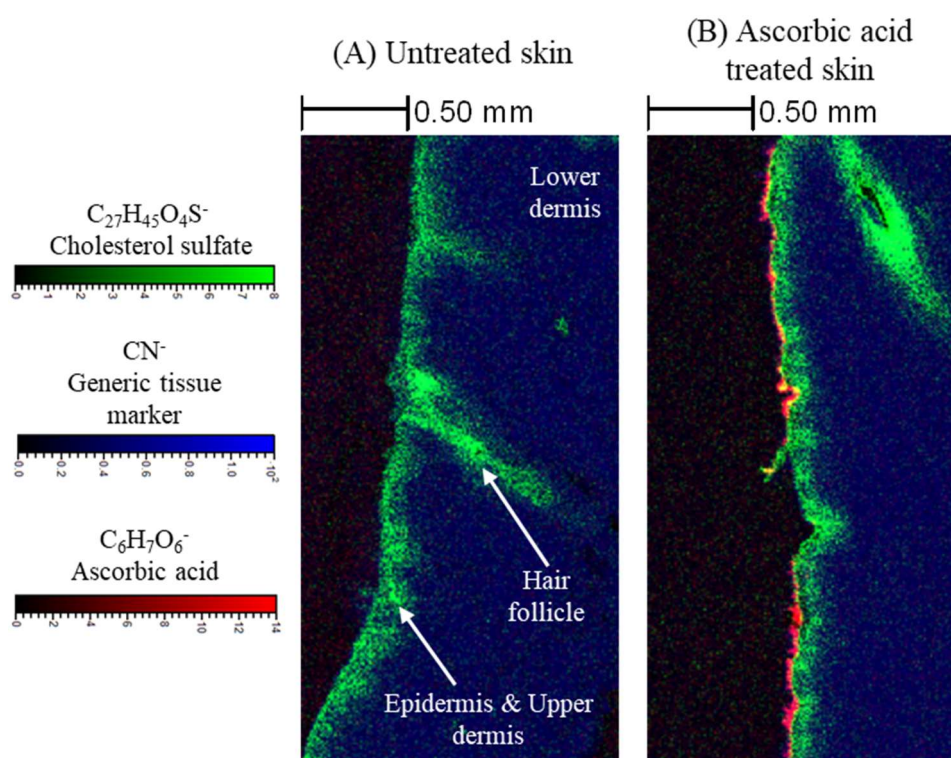


Figure 2-7 ToF-SIMS ion images of (A) untreated porcine skin and (B) ascorbic acid treated skin showing the distribution of ascorbic acid (red).

CRM is another imaging technique that could be used to study skin permeation distribution and unlike ToF-SIMS it can be used on human skin *in vivo* (Section 1.3.2). Whilst caffeine skin permeation has previously been studied by CRM¹⁹⁹, ascorbic acid is unreported so a skin cross section, with known ascorbic acid permeation into the epidermis (Figure 2-7 B) was analysed by CRM. Specific vibrational modes of reference ascorbic acid were first

determined by CRM. Analysis of untreated *stratum corneum* region resulted in a Raman spectrum with a broad background as shown in Figure 2-8. This was expected due to fluorescence interference from biological tissue. This background can be subtracted by the use of an accepted method for automated background subtraction from Raman spectra.²⁰⁰

Analysis of ascorbic acid treated *stratum corneum*, however, resulted in a significant decrease in fluorescence interference. It is believed that this is a result of a light-induced chemical change referred to as photobleaching. Ascorbic acid contains loosely held electrons, which are essential to its function as a reducing agent. Transfer of these electrons to skin fluorophores could quench their fluorescence.²⁰¹

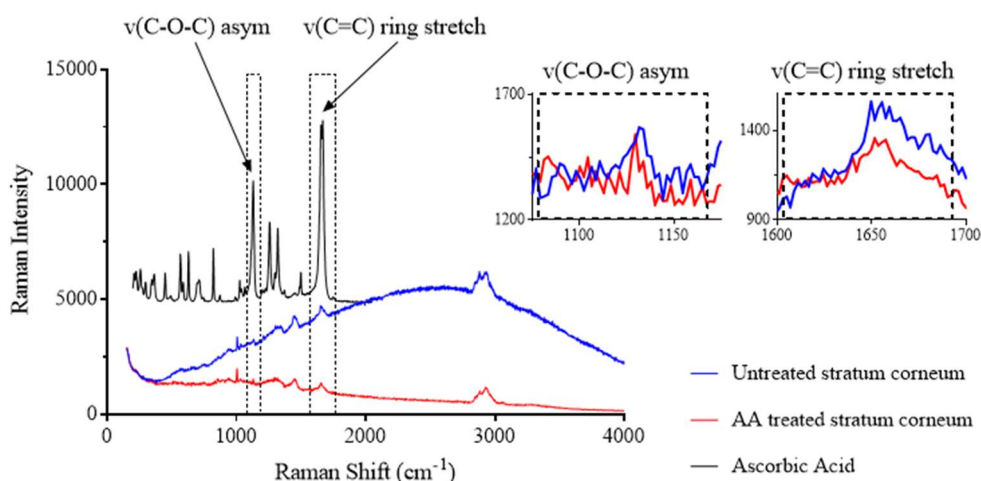


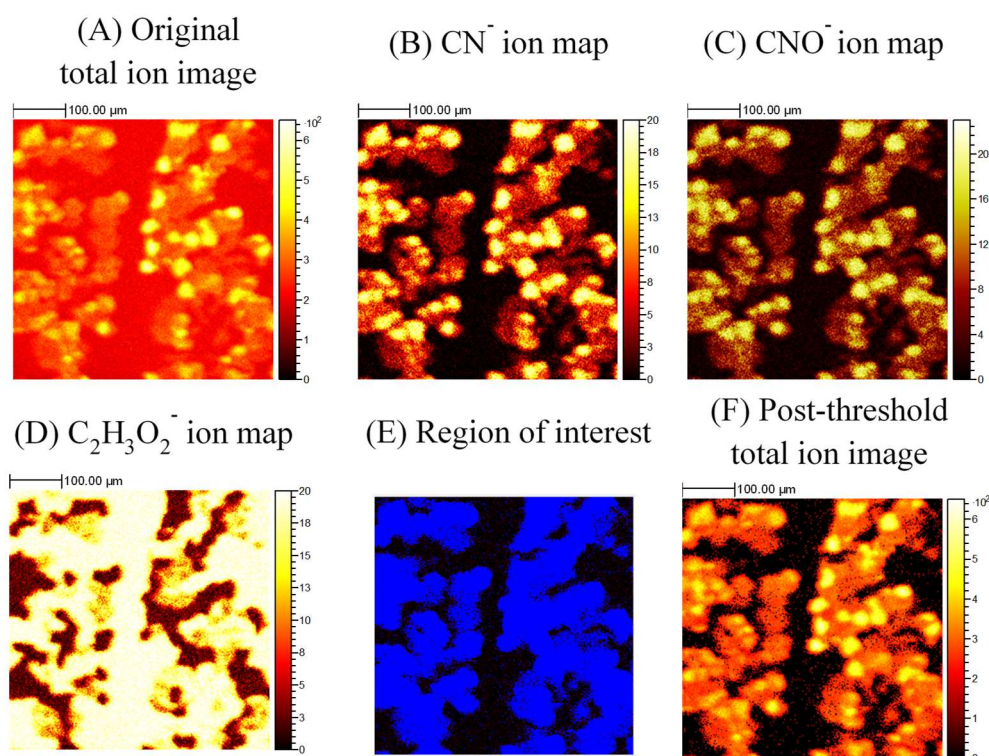
Figure 2-8 Confocal Raman spectra of ascorbic acid (AA), untreated stratum corneum and AA treated stratum corneum of porcine skin cross section. Spectra are unprocessed.

Photobleaching by native level of ascorbic acid in human tissue was investigated by Wright (2010).²⁰¹ The author concluded ascorbic acid was not a significant contributor of photobleaching in human tissue, however, the concentrations investigated (0.06 – 7.5 mM) were much smaller than the topically applied concentration (0.3 M) here. Photobleaching by ascorbic acid makes background subtraction of native tissue photoluminescence unreliable, so it would be difficult to assess ascorbic acid skin permeation. CRM analysis of

skin cross sections was therefore considered unsuitable for the study of ascorbic acid permeation.

Tape stripped *stratum corneum* samples are relatively topographically flat and can also be analysed by imaging mass spectrometry techniques such as ToF-SIMS (Section 1.3.3). Tape stripping does not remove a confluent layer of corneocyte cells due to the furrows in the skin surface and strong corneocyte adhesion (Section 1.2.4.1). Ions associated with the tape adhesive and corneocytes have been previously identified in the ToF-SIMS.^{103,107} In negative polarity, generic tissue marker ions, CN^- at m/z of 26 and CNO^- at m/z of 42, are diagnostic of corneocyte material (Figure 2-9 B and C). The acetate ion, $\text{C}_2\text{H}_3\text{O}_2^-$ at m/z of 59, is diagnostic of the adhesive on the tape (Figure 2-9 D).

Judd *et al.* (2013)¹⁰³ was the first to demonstrate that ToF-SIMS data of tape stripped *stratum corneum* could be retrospectively thresholded using an ion representing the corneocyte material. Generic tissue marker ions, CN^- and CNO^- , were used to threshold the data sets. Data was reconstructed using ROI (shown in blue, Figure 2-9 E) to remove the data from the adhesive tape material found between the furrows in the stripped skin and hence the data can be selectively analysed from the corneocyte material only (Figure 2-9 F). The thresholding process results in a decrease in ion intensities relating to adhesive material and an increase in skin tissue related ions in the spectra (Figure 2-9 G). The thresholding process is therefore useful for determining the amount of ascorbic acid colocalised with the corneocyte material and not localised in the skin furrows.



(G) Original and post-thresholded ToF-SIMS spectra

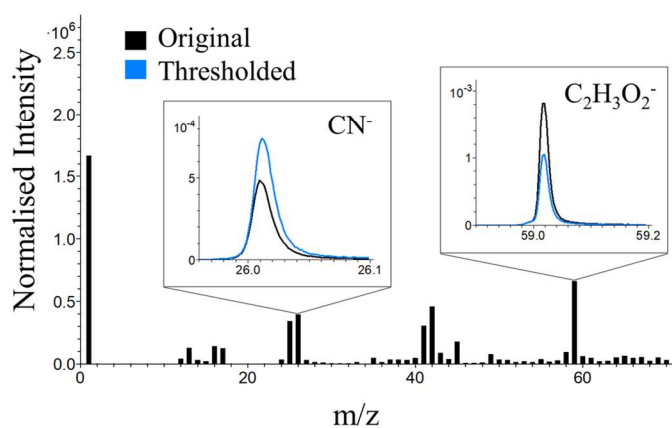


Figure 2-9 ToF-SIMS data for an example skin tape strip sample showing the thresholding process from original (A) to post-threshold (F). Thresholding results in an intensity increase of corneocyte related ions (B and C) and reduction in adhesive related ions (D) in the spectra (G).

2.4.3 Assessing stability of ascorbic acid in aqueous solution

Established analytical methods such as UV-Vis spectroscopy and HPLC require the analyte to be in solution. Therefore, to avoid underestimation of skin permeation, ascorbic acid should be stabilised for the duration of the

Franz cell experiment and/ or tape strip extraction protocol and its subsequent analysis.

The UV-Vis absorbance spectra of ascorbic acid and caffeine was recorded in 25 mM MPA solution (pH 2.4). Ascorbic acid and caffeine were found to have maximum absorbance at 240 nm and 275 nm respectively (Figure 2-10 A and B). In its role as an antioxidant, ascorbic acid oxidizes to dehydroascorbic acid²⁰². Dehydroascorbic acid was found to have a maximum absorbance below 210 nm and negligible absorbance above 250 nm. Therefore, the absorbance of ascorbic acid was measured at 254 nm to avoid the detection of dehydroascorbic acid. Whilst dehydroascorbic acid can be reduced to ascorbic acid, by glutathione and other thiols, it is not an antioxidant ingredient in itself.

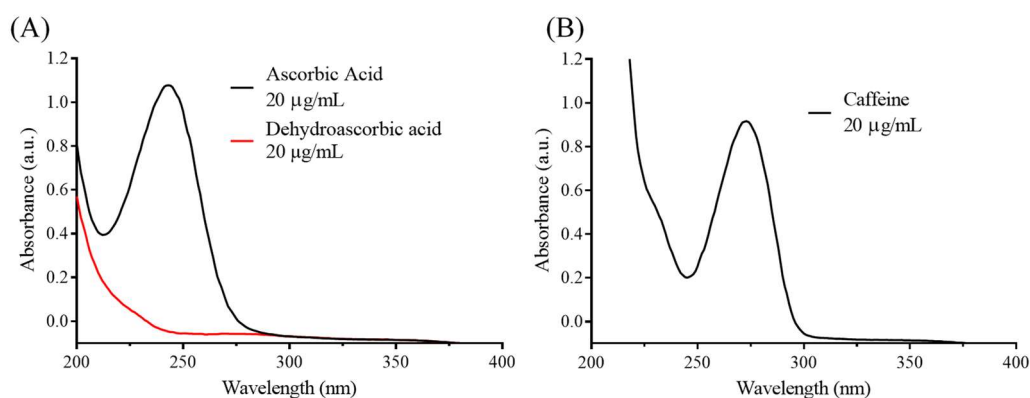


Figure 2-10 UV-Vis absorbance spectra of (A) ascorbic acid, dehydroascorbic acid and (B) caffeine in 25 mM MPA solution.

For quantification, calibration curves of ascorbic acid and caffeine were determined by UV-Vis absorbance (Appendix A1). The stability of ascorbic acid and caffeine in MPA solution (pH 2.4) and PBS buffer (pH 7.4) was compared at a concentration of 20 µg/mL. Based on the exposed surface area of the Franz cells (Section 2.3.3) and application of a finite dose (10 mg/cm²) of ascorbic acid formulation (5% w/w), a concentration of 20 µg/mL in the Franz cell acceptor compartment represents transdermal permeation of ~1.25%. A low percentage of transdermal permeation was estimated due to the hydrophilicity of ascorbic acid (logP -1.85). Furthermore the stability of ascorbic acid in aqueous solution is reported to be concentration dependent²⁰³,

with improved stability at higher concentrations and so a relatively low concentration was selected for evaluating stability.

Ascorbic acid (20 µg/mL) was found to be stable in MPA solution, at 36.5 °C, with no significant difference in concentration in the first 24 hours (Figure 2-11 A). In contrast, ascorbic acid was found not to be stable in PBS buffer with a significant drop in concentration in less than 12 hours. Caffeine (20 µg/mL) was stable in both MPA solution and PBS buffer (Figure 2-11 B).

MPA is reported to stabilise ascorbic acid in solution by inhibiting the copper-catalysed oxidation to dehydroascorbic acid. MPA decreases the amount of copper effective in the catalysis by formation of undissociated copper complex²⁰⁴ and is more effective than citric, perchloric, acetic and orthophosphoric acids.²⁰⁵ At low pH (1-4), oxidation of ascorbic acid occurs via elimination of two protons whereas higher pH (> 5) involves elimination of only one proton. Whilst PBS buffer (pH 7.4) is more physiologically relevant for use in the Franz diffusion cells, it does not stabilise ascorbic acid in solution. It would be inappropriate to use PBS buffer as it could lead to an underestimation of transdermal permeation.

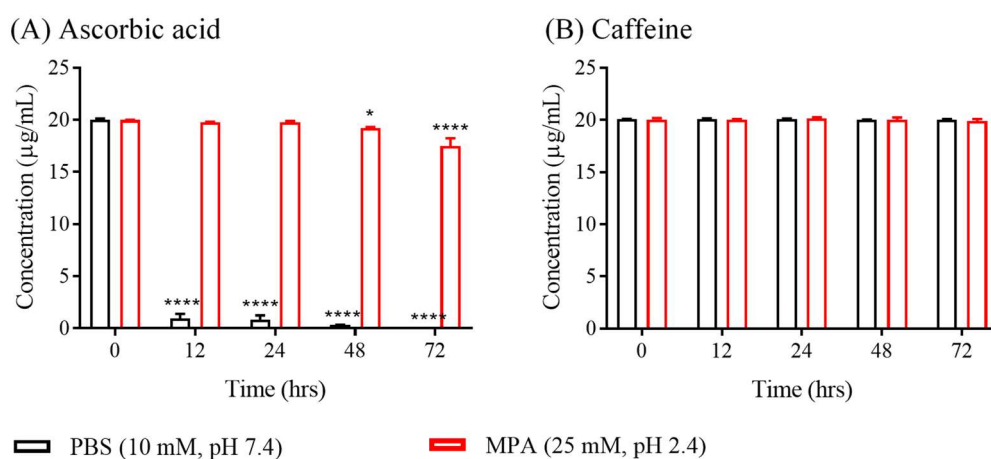


Figure 2-11 Stability of ascorbic acid and caffeine in PBS buffer and MPA solution at 36.5 °C. Data shown as mean ± SD, n=3, statistical differences compared to 0 hr.

UV-Vis analysis of Franz receptor solution requires background absorption subtraction (using receptor fluid of untreated skin permeation experiment).

Differences in background absorption can lead to some variability when quantifying ascorbic acid concentration so chromatographic separation of the ascorbic acid from the background sample matrix is preferable. As such, a HPLC method for quantifying ascorbic acid was therefore investigated.

The Association of Official Analytical Chemists (AOAC) recommend the use of 3% w/v (375 mM) MPA (dissolved in 92:8 water: acetic acid) for the extraction and stability of ascorbic acid in AOAC Official Method 967.21.²⁰⁶ However, this is a relatively high concentration that would not be suitable for injection into a HPLC system due to chemical reaction with bonded C18 and NH₂ bonded phases, precipitation and line blockage.²⁰⁵ Maia *et al.* (2007)¹⁹⁴ therefore investigated a HPLC mobile phase containing 0.2% w/v (25 mM) MPA solution (90/8/2 v/v/v MPA solution: methanol: acetonitrile). The HPLC method was fully validated for its reliability, precision, accuracy and specificity and was therefore adapted for use in this work.

The signal: noise (S: N) ratio was determined to evaluate the sensitivity of the HPLC method for quantifying ascorbic acid in Franz receptor solutions. A minimum S: N ratio of 10:1 is desired for quantification.²⁰⁷ Chromatographic separation of the ascorbic acid peak from the sample matrix peaks (Franz receptor solution) was not optimum meaning the limit of quantification (LOQ) was 100 µg/mL (Figure 2-12 A). One reason the LOQ is suboptimal, is because the receptor solution was obtained after exposure to full thickness skin sections (~ 2 mm depth) hence a chromatogram with high S: N was observed. In contrast Maione-Silva *et al.* (2019)¹⁷⁸ report a LOQ of 10 µg/mL for ascorbic acid. The authors used dermatomed (750 µm) porcine ear skin thereby achieving a “cleaner” chromatogram with less interfering sample matrix peaks. However, this LOQ was only adequate for *in vitro* skin permeation experiment involving a large infinite dose of formulation (>100 µg/mL) which does not mimic real life application conditions.⁶² Furthermore, the method of obtaining split-thickness skin with porcine tissue by dermatome is recognised to have difficulties so the use of full thickness skin can be justified³⁵, in particular if skin with minimal handling is required for experiment. In contrast, caffeine LOQ is estimated to be 10 µg/mL (Figure 2-12 B).

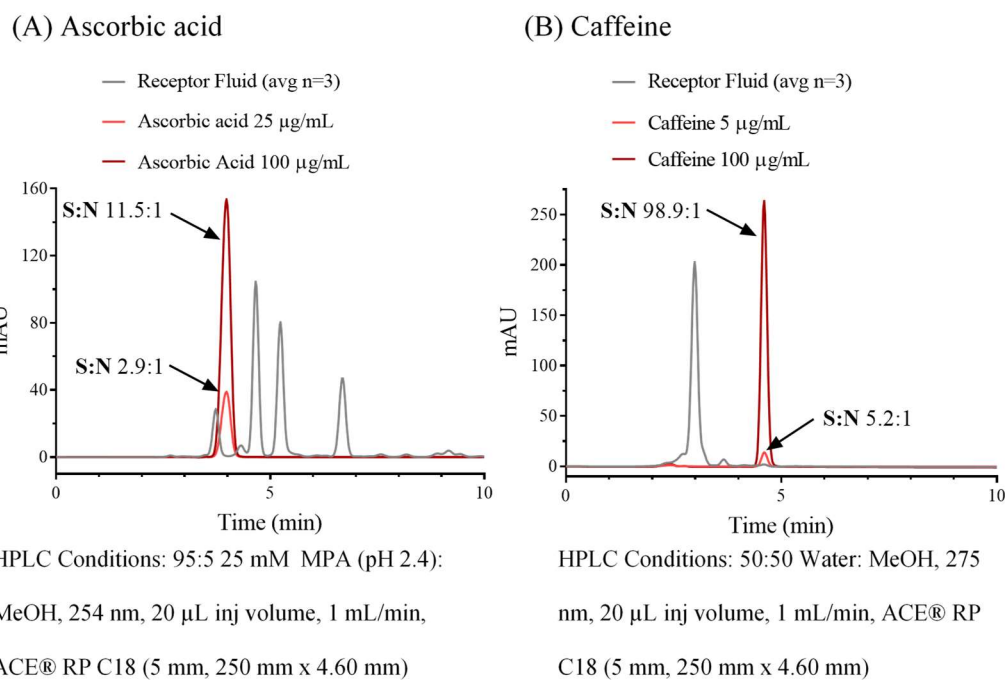


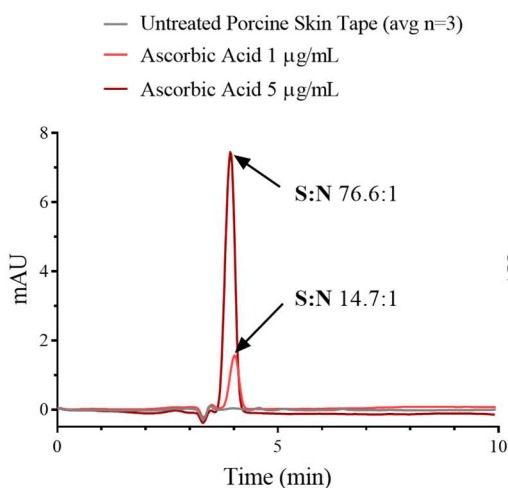
Figure 2-12 HPLC chromatogram of ascorbic acid (A), caffeine (B) and untreated porcine skin Franz cell receptor fluid (A and B). Signal:noise (S:N) ratios were determined from n=3 biological repeats.

It was therefore considered that HPLC analysis of the Franz receptor fluid was not feasible when applying a relatively small dose of ascorbic acid to the skin, using full thickness porcine ear skin and using MPA solution to stabilise ascorbic acid in solution. Analysis of the Franz receptor fluid could be achievable if using carbon isotope labelled ascorbic acid, however, this is expensive considering the formulations prepared have high ascorbic acid concentration (5% w/w). The Franz receptor fluid could be analysed by using fluorescent tagged ascorbic acid however this would change the physiochemical properties and influence skin permeation.

The S: N ratio was next determined to evaluate the sensitivity of the HPLC method for quantifying ascorbic acid in tape strip samples extracted into solution. Unlike the Franz receptor solutions, extractions of untreated skin tape strips yielded chromatograms with minimal matrix peaks and good separation of the ascorbic acid peak (Figure 2-13). A LOQ of 1 µg/mL and 0.5 µg/mL was determined for ascorbic acid in porcine and human skin tape strip extractions respectively. Based on a finite dose of formulation (10 mg/cm², 5%

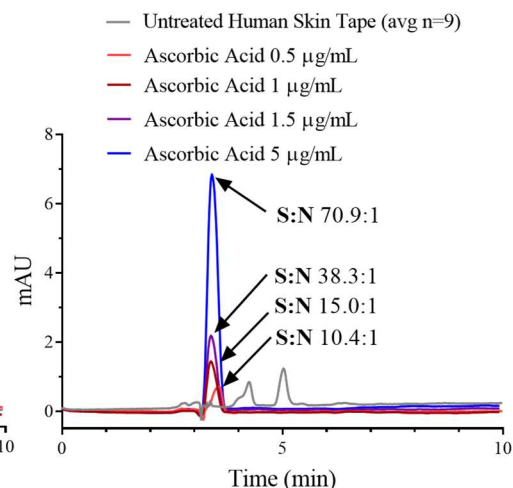
w/w ascorbic acid) to the skin, the LOQ is sensitive enough to detect 0.025 - 0.05% of the applied ascorbic acid per tape strip layer. The HPLC method therefore had suitable sensitivity for ascorbic acid quantification from individual skin tape strip samples. A linear range between 1 – 200 $\mu\text{g/mL}$ was determined for the ascorbic acid HPLC method (Appendix A2).

(A) Porcine skin tape strips



HPLC Conditions: 95:5 25 mM MPA (pH 2.4):
MeOH, 254 nm, 20 μL inj volume, 1 mL/min,
ACE® RP C18 (5 mm, 250 mm x 4.60 mm)

(B) Human skin tape strips



HPLC Conditions: 95:5 25 mM MPA (pH 2.4):
MeOH, 254 nm, 20 μL inj volume, 1 mL/min,
GraceSmart™ RP C18 (5 mm, 250 mm x 4.60 mm)

Figure 2-13 HPLC chromatogram of untreated porcine skin tape strip (A), untreated human skin tape strip (B), and ascorbic acid (A and B). S: N ratios were determined from $n \geq 3$ biological repeats.

An analytical method is considered to be precise and accurate if the values of relative standard deviation (RSD) and relative error (RE) are within the acceptable limits of the FDA Guidance for Bioanalytical Method Validation ($\text{RSD} \leq 15\%$ and RE within $\pm 15\%$)²⁰⁸. Intra-day and inter-day accuracy and precision was found to be within the acceptable guidelines (Table 2-1).

Table 2-1 Intra-day (n=6) and inter-day (n=11) precision and accuracy of ascorbic acid HPLC method.

Ascorbic acid ($\mu\text{g/mL}$)	Accuracy (%RE)		Precision (%RSD)	
	Intra-day	Inter-day	Intra-day	Inter-day
1.5	8.24	0.57	7.68	6.49
40	0.95	1.30	2.90	9.10
160	0.01	0.62	2.78	9.18

The stability of ascorbic acid in MPA solution was evaluated at ambient temperature and was found to be concentration dependent as shown in Figure 2-14. No significant change in ascorbic acid concentration was found within the first 48 hours. Therefore, all tape strip samples were extracted into solution and injected into the HPLC system within 48 hours. This ensures that at the smaller concentrations of the linear range, ascorbic acid had not significantly oxidised.

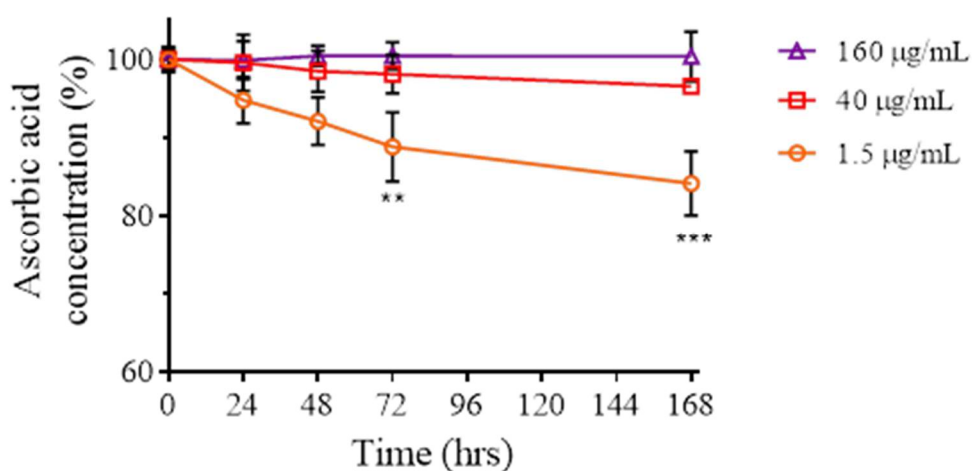


Figure 2-14 Stability of ascorbic acid in MPA solution (25 mM, pH 2.4) at ambient temperature (18-22 °C). Data shown as mean \pm SD, n=3. Statistical differences compared to 0 hrs.

To determine if there was a matrix effect when quantifying ascorbic acid, untreated skin tape strips (2 tape strips each from 3 human subjects) were extracted according to the extraction procedure (Section 2.3.7.1). Each skin tape extraction solvent was individually spiked with ascorbic acid maintaining

at least 90% of the skin matrix. No significant matrix effect was found (Table 2-2) therefore the HPLC method is thought to be suitable for the accurate quantification of ascorbic acid. The HPLC method was fully validated for its accuracy, precision and specificity in quantifying ascorbic acid from skin tape strip samples.

Table 2-2 HPLC method matrix effect of ascorbic acid in skin tape extraction matrix. Data shown as mean \pm SD, n=6.

Ascorbic acid concentration ($\mu\text{g/mL}$)	Matrix effect (%)		P value
	Solvent	Skin tape extraction matrix	
5	97.43 \pm 0.53	96.21 \pm 1.39	0.0725
50	100.32 \pm 1.12	99.86 \pm 1.18	0.5035
150	99.61 \pm 1.03	98.71 \pm 0.83	0.1282

2.4.4 Method development for extraction of ascorbic acid from tape strip samples

There is no standardised protocol for the extraction of tape stripped *stratum corneum* samples, however a complete extraction recovery is necessary to avoid underestimation of skin permeation. Extraction of tape strip samples pooled in a stack in a Falcon™ tube was compared to extraction of tape strips individually in Eppendorf® tubes. Pooling tape strips is preferred with large numbers of tapes in order to decrease sample processing time, however, there is an associated loss in depth information. Pooling tape strips may also be necessary if analyte concentration is low.

Extraction recovery of ascorbic acid from pooled tape strips was 99% when the spiked tape strip was at the top of the pooled stack (Figure 2-15 A). In contrast the recovery was 71% when the spiked tape strip was placed in the middle of the pooled stack (Figure 2-15 B). A low extraction recovery would lead to an underestimation of ascorbic acid content so pooling tape strips was not considered appropriate. Extraction recovery from individual tape strips was

98% (Figure 2-15 C). More importantly the extraction recovery was more repeatable (smaller SD) than pooled tape strip extraction. All tape strip samples were therefore individually extracted, despite the increased sample processing time involved in a study with a large number of tape strips. Furthermore, individual tape strip analysis retains the depth information in comparison to pooled strip analysis.

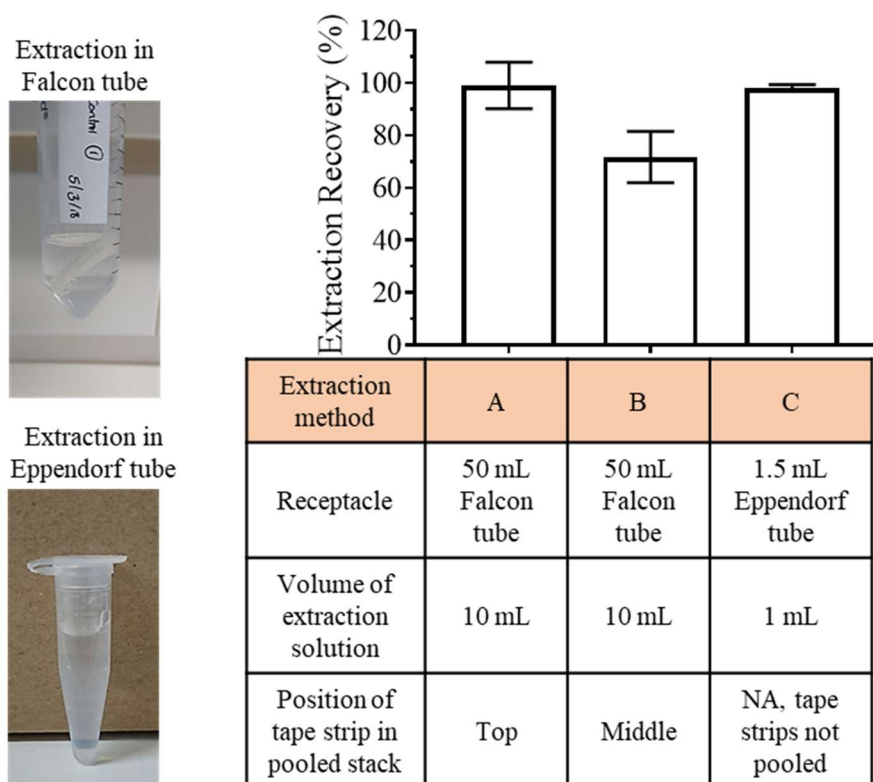


Figure 2-15 Percent recovery of ascorbic from spiked tape strips by extraction methods A-C. Data shown as mean \pm SD, $n=6$.

Extraction recovery of ascorbic acid from individual tape strip samples and sponge was then assessed at different concentrations that could be expected on the tape strip after skin permeation experiment. Ascorbic acid recovery was found not to be concentration-dependent (Table 2-3). Storage of tape strips at -20 °C, for up to 70 days, showed no statistical difference in the extraction recovery of ascorbic acid compared to tapes that were not stored. Therefore, collected skin tape strip samples were immediately stored at -20 °C and analysed within 70 days to ensure no effect on the amount of ascorbic acid recovered.

Table 2-3 Extraction recovery of ascorbic acid, from tape strip samples and sponge, based on a formulation application of 10 mg/cm² containing 5% w/w ascorbic acid. Data shown as mean \pm SD, n=6.

Ascorbic acid concentration on substrate (%)	Storage time before extraction (days)	Substrate	Ascorbic acid extraction recovery (%)
0.1	0	Corneofix® tape	97.86 \pm 4.20
1	0	Corneofix® tape	99.07 \pm 3.86
1	28 (at -20 °C)	Corneofix® tape	102.96 \pm 4.04
1	70 (at -20 °C)	Corneofix® tape	97.97 \pm 4.10
10	0	Corneofix® tape	101.23 \pm 4.34
100	0	Polyurethane sponge	100.44 \pm 0.54

2.4.5 Quantification of protein on tape strip samples collected after ascorbic acid skin permeation

A dye-binding assay, specifically Pierce™ 660 nm, was investigated in order to quantify *stratum corneum* proteins. A calibration curve of bovine serum albumin (BSA) protein was established in water, from 25 to 1500 μ g/mL, with acceptable sensitivity (Figure 2-16 A). When the calibration curve was repeated in the extraction solvent containing MPA, which is capable of stabilising ascorbic acid in solution (Figure 2-11), the gradient of the calibration curve decreases to almost zero. This suggest that MPA interferes with the assay and is not compatible.

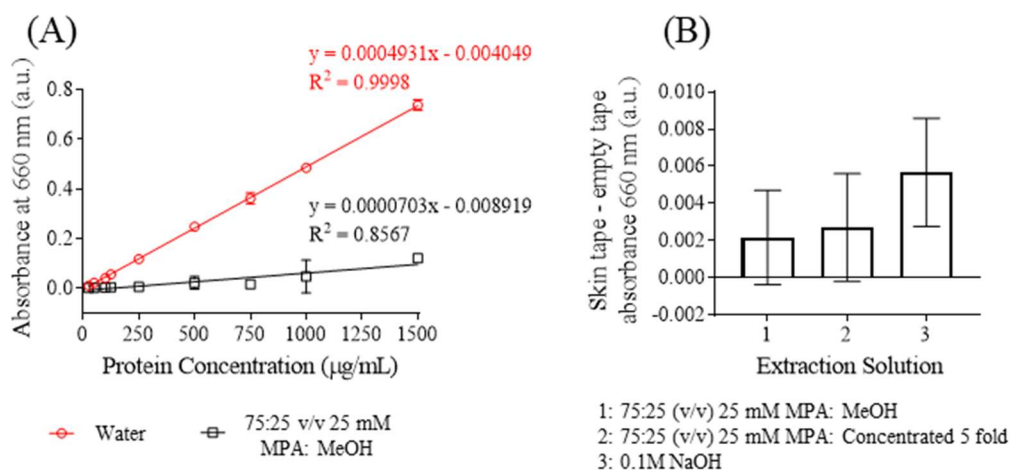


Figure 2-16 Evaluation of Pierce™ 660 nm Protein Assay Kit for determining protein content of tape strips. (A) BSA protein calibration curve. (B) Absorbance of skin tape extraction, with blank tape subtracted, in various extraction solutions. Data shown as mean \pm SD, $n=3$.

The absorbance value at 660 nm of a skin tape strip extraction, with blank tape strip extraction (background) subtracted was found to be negligible (Figure 2-16 B). This could be due to interference from MPA or the amount of protein extracted could be below the assay's linear range. A 0.1 M NaOH solution (pH 13) was then tested as an extraction solvent and was noted to be compatible with the assay kit. Alkali pH (hydroxide ions) can break-down disulphide bridges in keratin protein and can therefore extract more protein into solution as previously reported by Kezic *et al.* (2013).⁷² Alkali extraction solution increased the absorbance of skin tape extraction at 660 nm, indicating perhaps increased extraction of protein into solution ($\sim 20 \mu\text{g/mL}$), but this difference was very small with large variability.

The amount of protein extracted with 0.1M NaOH is in agreement with the findings of tape strip extractions by Clausen *et al.* (2016),¹⁹³ who used a BCA protein assay kit which has a lower LOQ. In addition, ascorbic acid is not stable in alkali pH so protein quantification would require a second extraction once ascorbic acid had been removed from the tape strips. Therefore, protein dye-binding assay was not a practical option.

Infrared densitometry, which does not require extraction of tape strip protein, was therefore investigated as a method for determining protein content. The

absorbance, at 850 nm, of porcine and human tape strips was measured with the SquameScan™ 850A. This was converted to protein content using previously validated calibrations (Figure 2-17).^{60,195} All 15 sequential tape strips, porcine and human, had a protein content within the linear working range of the instrument. Infrared densitometry is non-destructive and so the infrared densitometer was therefore considered the most suitable method for protein quantification of tape strip samples.

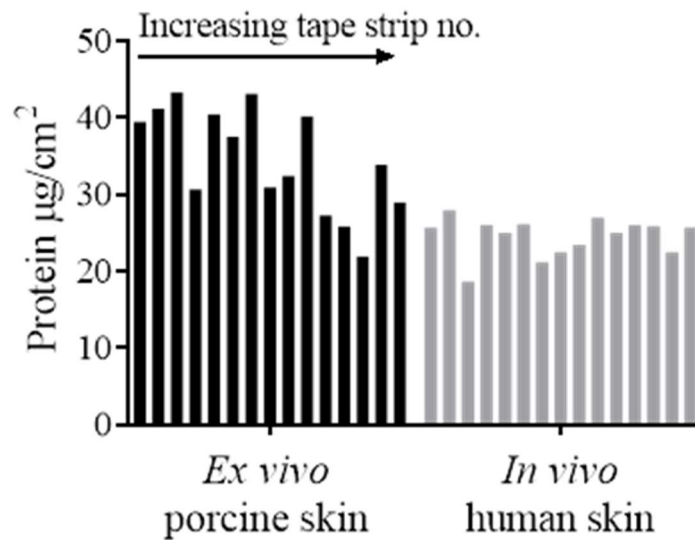


Figure 2-17 Protein content of tape strip samples, with increasing tape strip number, determined by infrared densitometry.

Whilst protein content of porcine tape strips decreased with tape strip number, human tape strips generally picked up an equivalent amount of corneocytes for the first 15 tape strip layers. This finding is in agreement with Klang *et al.* (2011)⁶⁰ who found that the pattern of protein removal with porcine skin differs from that of human skin due to more pronounced corneocyte clustering so more corneocyte clusters adhere to the initial tape strips of porcine skin. Secondly porcine skin has deep ‘canyons’ compared to human skin furrow size so less corneocytes are picked up in these regions. This finding was verified when tape strip samples were observed under an optical profilometer microscope (Figure 2-18).

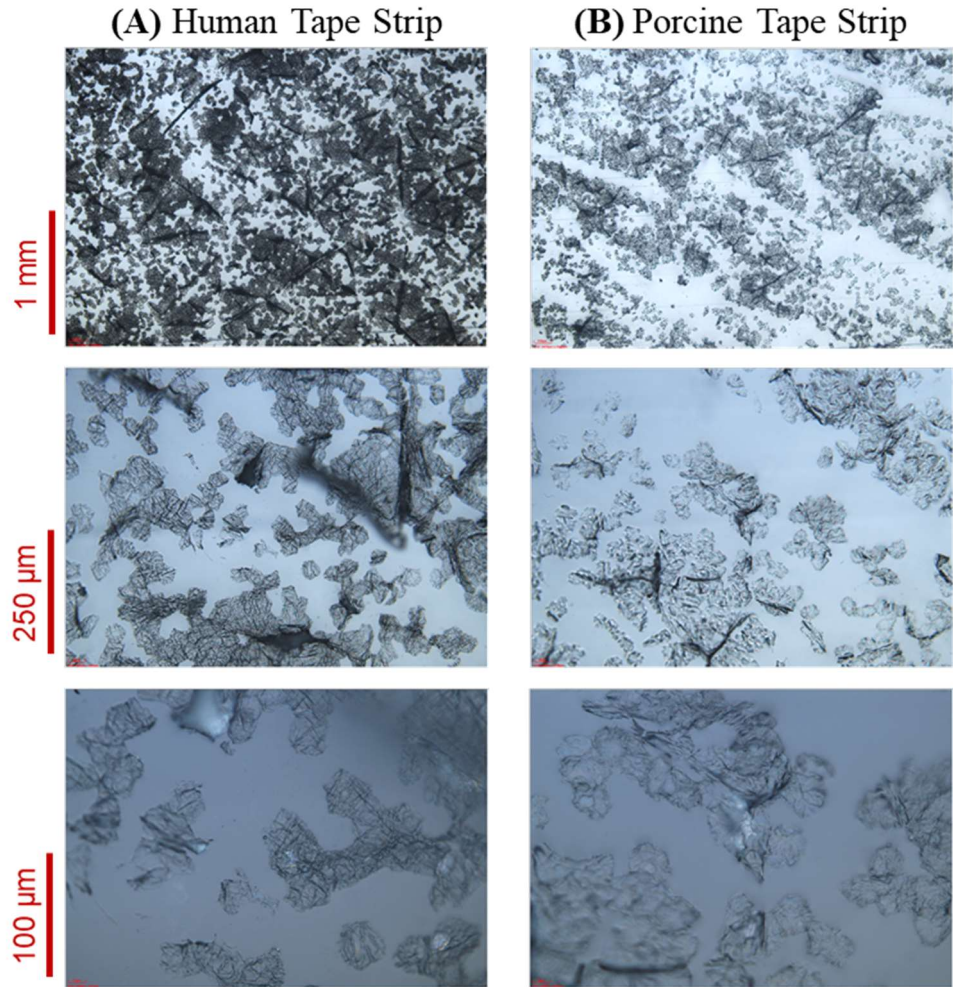


Figure 2-18 Optical profilometer image of human and porcine corneocytes on Corneofix® tape.

2.5 Conclusions

This work has demonstrated that complete intact skin cross sections can be obtained without the use of embedding agents. This method can be applied to studying permeant distribution in the skin, by ToF-SIMS, without interference from the embedding agent and its associated secondary ions. In addition, the ToF-SIMS instrument was found to have acceptable sensitivity in detecting ascorbic acid after application of a clinically relevant topically applied dose. However, CRM analysis of skin cross sections was found not to be suitable for analysis of ascorbic acid due to unexpected photobleaching effect on the Raman spectrum.

MPA solution (25 mM, pH 2.4) could stabilise ascorbic acid in solution and was therefore found to be the most appropriate to use as the Franz cell acceptor solution and for extraction of tape strip samples. HPLC analysis of Franz cell acceptor solution, following permeation experiment with clinically relevant dose and full thickness skin, was not suitable because full chromatographic separation could not be achieved. However, full chromatographic separation was achieved for tape stripped *stratum corneum* extraction solutions and the HPLC method was fully validated for accurate quantification of ascorbic acid.

Extraction of tape strip samples individually, rather than pooling, was required to obtain reproducible and complete recovery of ascorbic acid. This extraction method retains the layer by layer depth information of ascorbic acid *stratum corneum* permeation and enables a direct comparison with ToF-SIMS analysis of individual tape strips.

In summary, *ex vivo* skin permeation experiment, yielding skin cross sections and Franz receptor solution, could be assessed by a combination of ToF-SIMS and UV-Vis analytical methods. *In vivo* and *ex vivo* skin permeation experiments, yielding tape strip samples, could be assessed by a combination of ToF-SIMS and HPLC analytical methods. The use of two complimentary analytical techniques, one with imaging capability and the other for absolute quantification, has the potential to discover previously unreported insights into ascorbic acid and caffeine skin permeation when used together.

Chapter 3: Comparative study of ascorbic acid and caffeine permeation into *ex vivo* porcine skin

3.1 Introduction

Ascorbic acid formulations typically contain a high ascorbic acid concentration ($\geq 5\%$ w/w) in order to observe beneficial therapeutic effects in the skin (Section 1.5.2). Currently there is a limited number of ascorbic acid *ex vivo* skin permeation studies, furthermore, *in vivo* human skin permeation of ascorbic acid is presently unreported. As such there is a limited understanding regarding its extent and route of skin permeation (Section 1.5.3).

In contrast, caffeine *in vivo* and *ex vivo* permeation has been widely reported in the literature¹⁸⁶. Moreover, despite the hydrophilicity of caffeine, it has been demonstrated that the transfollicular route of permeation contributes to approximately 50% of the total penetration of caffeine into human skin (Section 1.6.2). The transfollicular route of permeation would offer several advantages in the dermal delivery of ascorbic acid including enhanced permeation depth and prolonged residence duration.

In this chapter the permeation of ascorbic acid via the transepidermal and transfollicular route was monitored using ToF-SIMS. The ToF-SIMS analysis of ascorbic acid permeation into porcine skin has previously been reported by Starr *et al.*¹¹², however, the authors applied an infinite dose to the skin which does not mimic clinical in use conditions. It has been demonstrated in Chapter 2 that ToF-SIMS does have the sensitivity to analyse ascorbic acid permeation after topical application of a small clinically relevant dose whilst CRM does not.

It is common practise to rub or massage a topical product into the skin. The effect of rubbing a topical formulation, with a gloved finger, has been demonstrated *in vitro* to deliver significantly higher quantities of drug into the skin.⁷⁰ Disappointingly though, many *in vitro* permeation studies do not rub, or specify rubbing in the method, the formulation into the skin. In this study the developed formulations will be rubbed into the skin despite it not being

mentioned in recent SCCS and OECD guidance on conducting *in vitro* permeation experiments.^{32,33,35,36}

SCCS and OECD guidance on conducting *in vitro* dermal absorption experiment specifies the use of Franz diffusion cells.^{32,33,35,36} A limitation of Franz cells is the overhydration of the skin tissue caused by contact with a liquid acceptor medium and contraction of the hair follicles caused by mounting excised skin. This has been reported to effect skin permeation compared to the *in vivo* situation (Section 1.2.3.2). In this chapter, skin permeation experiments were performed with excised skin and intact skin to establish if that has an effect on skin permeation.

3.2 Chapter aims

The aim of this chapter is to examine the *ex vivo* porcine skin permeation, transepidermal and transfollicular, of ascorbic acid compared to caffeine. Firstly, suitable topical formulations containing 5% of the active ingredient will be prepared. Skin permeation experiments will then be performed in parallel with excised skin and intact skin. Skin cross sections will be analysed by ToF-SIMS to obtain information about the permeation distribution of ascorbic acid and caffeine in the epidermis and hair follicles of the skin. This knowledge would help understand the principal routes of permeation into the skin and inform formulation development. Finally, UV-vis spectroscopy analysis of Franz receptor fluid will be used as a supporting technique to cross-validate any findings from ToF-SIMS.

3.3 Materials and methods

3.3.1 Materials

Ethanol, propylene glycol (PG), glycerol and xanthan gum were purchased from Sigma-Aldrich.

3.3.2 Preparation of ascorbic acid and caffeine formulations

3.3.2.1 *Cosolvent formulation*

Cosolvent formulations containing 5% w/w active ingredient were prepared. Caffeine was dissolved in ultrapure water (55% w/w, 70 °C) in a scintillation vial (20 mL, glass, Sigma-Aldrich) using a hotplate with stirrer bar (1000 rpm). When caffeine had dissolved in the water, ethanol (40% w/w, room temp.) was immediately added with continuous stirring (~1 minute). The solution was left to cool to room temperature before further use. Cosolvent formulations were made with varying concentration of ethanol (0%, 10%, 20%, 30%, and 40%) and water *quantum satis* (q.s.). Ascorbic acid cosolvent formulations were made in the same way but ascorbic acid was added after water and ethanol mixture had cooled to room temperature (<25 °C) with vortex mixing until a clear solution was obtained. The pH values of ascorbic acid formulations were measured using Jenway 3505 pH meter (Jenway, UK), to an accuracy of ± 0.2 .

3.3.2.2 *Gel formulation*

Gel formulations were also made with 5% w/w active ingredient. Caffeine (5% w/w), PG (10% w/w), glycerol (2.5% w/w) and ultrapure water (82% w/w, 50 °C) were added to a scintillation vial (20 mL, glass, Sigma-Aldrich) using a hotplate with stirrer bar (1500 rpm). Once a clear solution was obtained, xanthan gum (0.5% w/w) was added and the mixture continuously stirred (1500 rpm) until a clear gel was formed. Gel formulations were made with varying concentrations of PG (0%, 10%, 30%, and 50%) and water q.s. Ascorbic acid gel formulations were made in the same way, but ascorbic acid was added after PG, glycerol and water solution cooled to room temperature (<25 °C) with vortex mixing until a clear solution was obtained.

3.3.3 Formulation stability

Formulation stability of cosolvent and gel formulations was observed at ambient temperature (18-22 °C) up to 14 days. The vials were stored in the dark to remove exposure to light.

3.3.4 *Ex vivo* skin permeation experiment

Porcine ear skin, prepared as stated in Section 2.3.2., was used for *ex vivo* skin permeation experiment. A pair of ears was used for each experiment (n=6) with one excised into smaller pieces so it could be used in the Franz cells and the other used intact with no separation, as shown schematically in Figure 3-1. The skin test site areas were delineated with a plastic adhesive template (Sadipal adhesive film, Girona, Spain) with an inner window of 1.5 cm × 1.5 cm where the formulation could be applied. Paper based adhesive was not used since it was found to absorb adjacent formulation. Adjacent skin test sites on the intact ear were separated by at least 1 cm and labelled with the formulation applied.

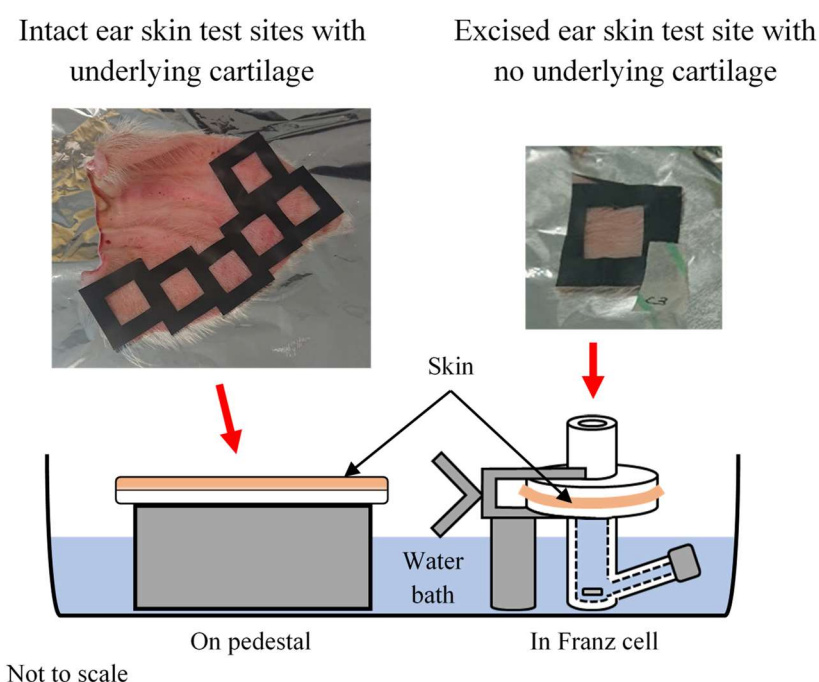


Figure 3-1 Schematic diagram of ex vivo porcine ear skin permeation experiment with intact and excised skin.

An infinite dose (50 mg) of the formulation was applied by gloved finger, moving gently in a circular clockwise motion 20 times, to homogeneously

spread the formulation across the skin test site. The formulation weight applied was determined by difference. It was important the formulation was rubbed into the skin as firstly to homogenously spread the formulation across the skin test site area and secondly it has been reported to improve permeation and also closely mimic real life application⁷⁰. The dose applied to the skin was 22.22 mg/cm².

Franz cell experiments were performed for 24 hours as specified in Section 2.3.3. For each experiment, the pair of ears was obtained from the same animal donor so it can be assumed there are no differences in the skin barrier properties.

Skin integrity of intact ear skin was assessed visually because TEER cannot be measured due to the underlying cartilage. Skin integrity of excised skin, mounted in Franz cell, was performed on one test skin piece that was considered to be representative of the ear tissue used. The other skin test sites used for permeation experiment did not have TEER measured before or after permeation experiment. TEER measurement before permeation experiment would hydrate the skin, affecting the comparison between excised and intact skin, so was avoided (Section 1.2.3.3). TEER measurement could not be performed after permeation experiment as skin was cross sectioned. Full thickness porcine skin tissue was used, rather than dermatomed skin, so impairment of skin barrier was not expected.

3.3.5 UV-Vis spectroscopy and ToF-SIMS Analysis

Following skin permeation experiment, skin samples were frozen and cross sections obtained as detailed in Section 2.3.4. The skin surface was not cleaned of any remaining formulation prior to freezing. Cross sections were analyzed by ToF-SIMS as detailed in Section 2.3.8. When skin permeation was conducted with excised skin mounted in Franz cells, the receptor fluid was collected and analysed by UV-Vis spectrophotometry as detailed in Section 2.3.6.

3.3.6 Statistics

Statistical analysis was performed as stated in Section 2.3.11.

3.4 Results and discussion

3.4.1 Stability of cosolvent and gel formulations

Investigating formulation stability is an important step when developing topical products. Changes in product composition and consistency can affect the performance of the product in providing its intended benefit or efficacy.²⁰⁹ It was important that the formulation was at least stable for the duration of the skin permeation experiment (24 hrs).

It was important to assess a formulation of ascorbic acid that contained an efficacious concentration hence a 5% w/w formulation was prepared. In order to make a direct comparison, a caffeine formulation with the same dose was also prepared. Whilst a 5% w/w solution of caffeine in water can be achieved at high temperature, at ambient temperature (25 °C) caffeine has a solubility of 2.2% w/w²¹⁰, therefore water alone could not be used as a control in the permeation study. A cosolvent solution was therefore prepared. Cosolvents can increase the solubility of nonpolar molecules, by reducing the interfacial tension between the aqueous solution and hydrophobic solute²¹¹.

Ethanol was selected to prepare cosolvent formulations as it is widely used in a variety of cosmetic products and when applied on undamaged skin it is considered not to cause acute or systemic toxic effects.²¹² Ascorbic acid, in cosolvent solution with 0% to 40% ethanol, was stable for two weeks as shown in Figure 3-2. In contrast there was only one stable caffeine cosolvent formulation after two weeks and that was the one with 40% ethanol. Cosolvent solutions prepared with less ethanol showed caffeine precipitation so the formulation with 40% ethanol was selected for the skin permeation experiments. Whilst ethanol, at a concentration ranging between 60% and 95% is classified to be safe for skin preparation products and topical use according to the assessment of FDA and WHO^{213,214}, high concentrations of topically applied ethanol may result in adverse effects such as skin irritations or allergic contact dermatitis so smaller ethanol concentration is preferable.

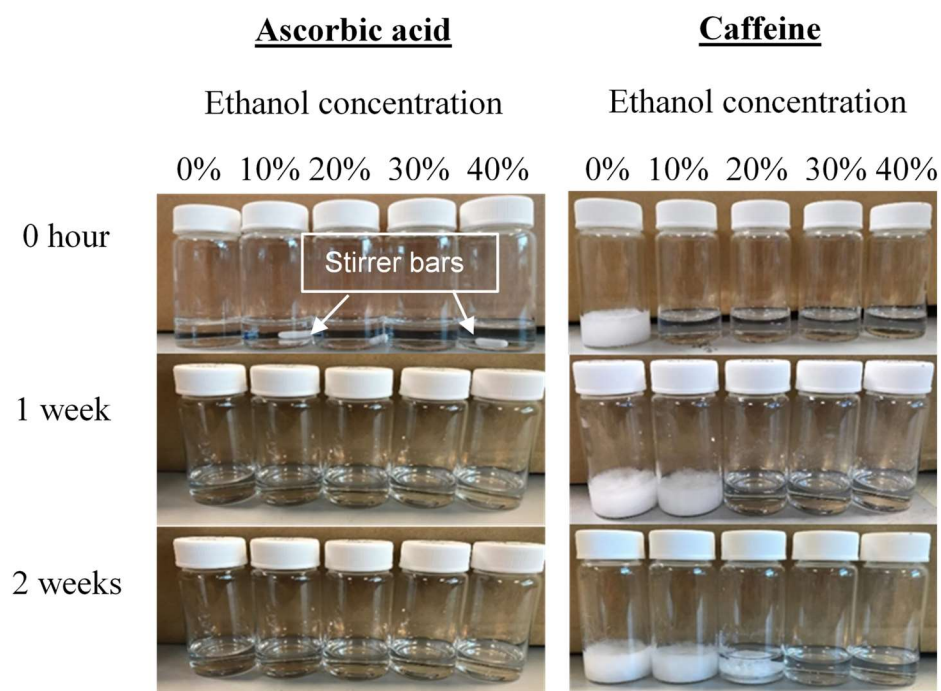


Figure 3-2 Stability of ascorbic acid and caffeine cosolvent formulations made with varying ethanol concentrations.

A comparator gel formulation was made with PG, glycerol and xanthan gum. There are a number of previous studies which use PG as a penetration enhancer for caffeine hence it was incorporated into the gel formulation. Pires-de-Campos *et al.* (2008)²¹⁵ reported gel formulations containing 10% w/w PG resulted in increased cutaneous permeation, in combination with ultrasound treatment, for *in vivo* porcine skin experiments. Duracher *et al.* (2009)²¹⁶ found formulations containing 5% w/w PG increased the permeation of caffeine for *in vitro* porcine skin permeation experiments. Trauer *et al.* (2009)²⁴ reported that a formulation containing 67.5% w/w PG, resulted in up to 50% of the applied caffeine permeating via the hair follicle route from *in vivo* and *in vitro* human skin experiments. The CIR panel have concluded that PG is safe for use in topical products at a concentration up to 50% as > 50% of PG induces skin irritation.²¹⁷ Therefore, gel formulations with PG concentrations from 0% to 50% w/w were prepared.

Ascorbic acid in gel formulations with 0% to 40% PG were stable for two weeks, however, caffeine gel formulation with 10% PG was the only formulation stable for one week (Figure 3-3). After two weeks, the caffeine had partially precipitated. As a result, gel formulation prepared with 10% PG was selected for skin permeation experiment.

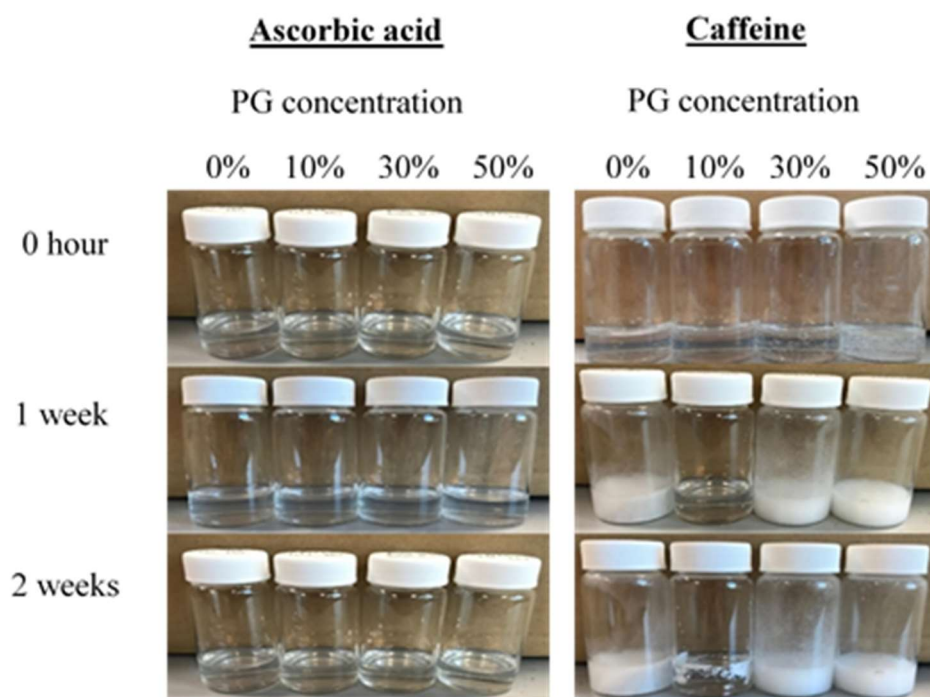


Figure 3-3 Stability of ascorbic acid and caffeine gel formulations made with varying PG concentrations.

10% PG concentration appears to be within the optimum range for caffeine solubility. Typically, a semi-logarithmic relationship between solubility and fraction co-solvent is expected however PG shows a parabolic relationship. This has been observed previously by Gould *et al.* (1984)²¹⁸ who found 40-80% PG v/v showed highest caffeine solubility with lower and higher PG concentrations having less caffeine solubility. This behaviour is believed to be the result of self-complexation of caffeine from monomeric to tetrameric state as the polarity of the system increases. The optimum caffeine solubility at a lower PG concentration, than that of Gould *et al.*²¹⁸, could be due to the presence of additional polar excipients (glycerol and xanthan gum) in the formulation. Gould *et al.*²¹⁸ also observed a parabolic relationship between ethanol fraction and caffeine solubility with the optimum range 40-60%

ethanol v/v. As 40% ethanol formulation showed the best stability (Figure 3-2), this would agree with previous findings.

Discoloration of the formulations is indicative of oxidation of the ascorbic acid and is considered unacceptable to consumers.¹⁵⁵ The ascorbic acid formulations did not discolour (turn yellow) over the two week period. Ascorbic acid cosolvent formulation (40% ethanol) had a pH of 2.9 and gel formulation (10% PG) had a pH of 2.6. At these low pH, the rate of oxidation of ascorbic acid is at a minimum.²¹⁹ It is known that low pH (< 3.5) of formulation increases skin permeation of ascorbic acid, however, Pinnell *et al.* (2001)¹⁷¹ found no significant difference in *in vivo* porcine skin permeation between pH 2.5 and pH 3.0.

The ascorbic acid and gel formulations, presented in Figures 3-2 and 3-3, were only assessed by their physical stability and not chemical stability (i.e. composition). Knowing that ascorbic acid oxidises in aqueous solution, the formulations were made immediately prior to dosing the skin to minimise differences in ascorbic acid concentration between experiments.

3.4.2 Effect of receptor fluid pH on skin permeation

MPA solution (pH 2.4) was found to stabilise ascorbic acid in aqueous solution and was thought to be the most appropriate Franz cell receptor fluid as observed in Section 2.4.3. To ensure that using MPA solution in the receptor compartment did not influence skin permeation, for example by affecting skin integrity or skin viability, a caffeine cosolvent formulation was applied to Franz cells with MPA solution or PBS buffer (pH 7.4) as the receptor fluid.

The weight of formulation applied and rubbed into the skin was not significantly different when using MPA or PBS as the receptor fluid (Figure 3-4 A), therefore, any differences in skin permeation are believed to be as a result of the receptor fluid used. After a 24 hour skin permeation experiment there was no significant difference in caffeine that had reached the receptor compartment after using MPA solution rather than PBS as the receptor fluid as shown in Figure 3-4 B.

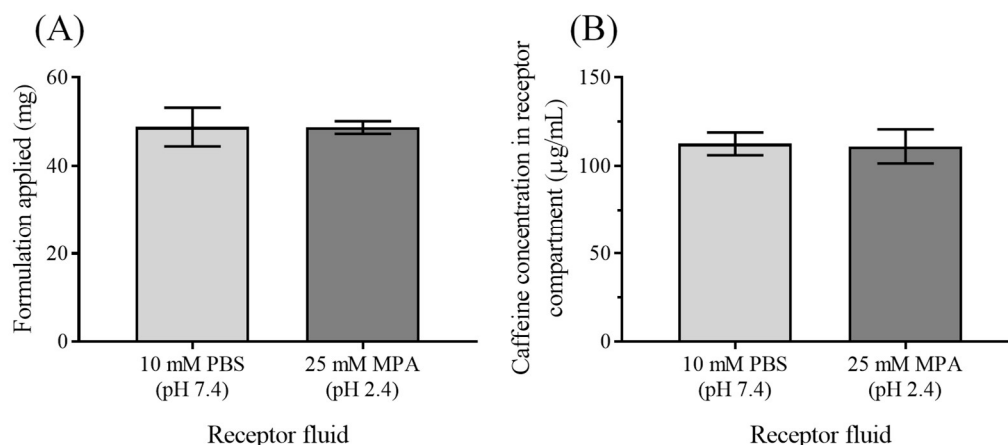


Figure 3-4 Skin permeation of caffeine, from cosolvent formulation, with different Franz cell receptor fluid. (A) Weight of formulation applied, mean \pm SD. (B) Caffeine concentration in receptor compartment, mean \pm SEM. ($n=6$)

In order to maintain sink conditions, and minimise back diffusion, it is generally accepted that the test compound concentration in the receptor solution reached under experimental conditions should be at least 10 times smaller than the solubility limit of the test compound.³³ Caffeine has a solubility limit of 16 mg/mL²²⁰ so the concentration in the Franz cell receptor fluid was \sim 130 times smaller than the solubility limit. Caffeine *ex vivo* skin permeation is not enhanced or limited by using MPA in the Franz cell receptor. Ascorbic acid has a solubility limit of 330 mg/mL²²¹ so it is unlikely sink conditions would not be maintained.

3.4.3 Transdermal permeation of ascorbic acid and caffeine

Ex vivo skin permeation experiments were performed with full thickness porcine ear skin. To check that the thickness of the skin did not contribute to differences in skin permeation between the different formulations, the skin depth of cross sections was measured with an optical profilometer. As shown in Figure 3-5 A no significant difference was found in skin thickness between the different experiments. Additionally, the weight of formulation applied and rubbed into the skin was not significantly different (Figure 3-5 B) therefore any differences in skin permeation are thought to be attributable to the effect of the formulations.

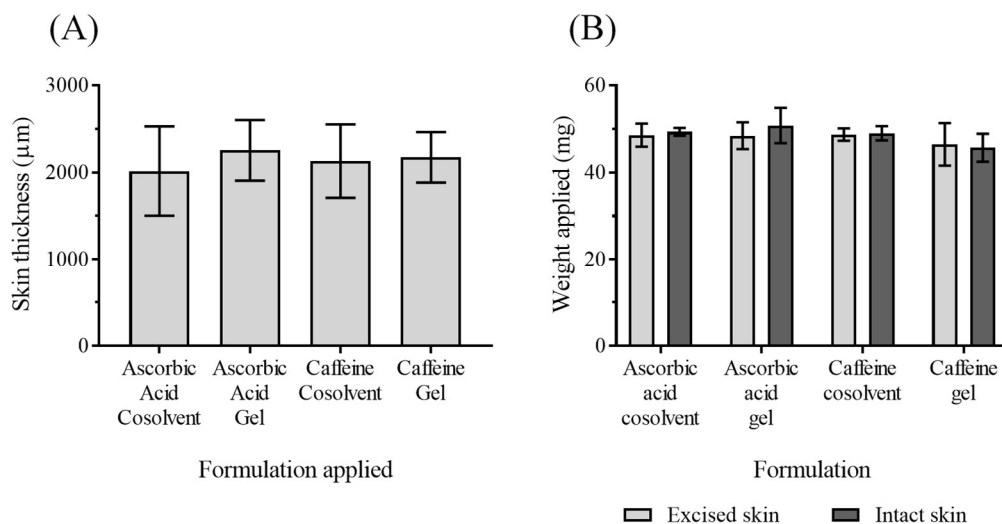


Figure 3-5 (A) Thickness of skin used and (B) weight of formulation applied in ex vivo permeation experiment. Data shown as mean \pm SD, (A) $n=12$ and (B) $n=6$.

It was observed that more caffeine (13.7% of the applied dose) reached the receptor compartment than ascorbic acid (6.4% of the applied dose) when formulated as a cosolvent, as shown in Figure 3-6. This can be explained by their physiochemical properties. Specifically, caffeine, has a log P value of -0.07²²², which is closer to the suggested ideal range of log P value between 1 and 3 for skin permeation²²³ in comparison to ascorbic acid which has a log P value of -1.85.²²⁴

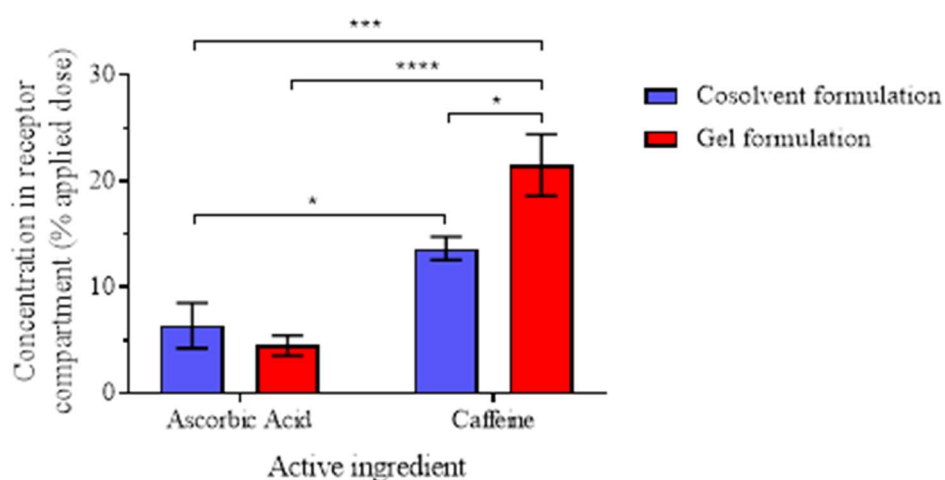


Figure 3-6 Concentration of ascorbic acid and caffeine in Franz cell receptor compartment after application of cosolvent and gel formulations. Data shown as mean \pm SEM, $n=6$.

The closest comparable study is that of Davies *et al.* (2017)²²⁵ who found that around 5% of the applied dose of caffeine reached the Franz cell receptor in an *in vitro* porcine skin permeation experiment with finite dose of an emulsion (~ 10 mg/cm²). The amount of caffeine permeated here was 2.7× more than in Davies's study²²⁵. There could be a variety of reasons that can explain this difference such as formulation composition, biological variability, and rubbing the formulation into the skin. For example Iswandana *et al.* (2018)²²⁶ reported that emulsions can more than double skin permeation of caffeine compared to aqueous control, however, the experiments were conducted on rat skin which is more permeable than human and porcine skin.²²⁷ Nguyen *et al.* (2017)⁷⁰ found the amount of salicylic acid permeated into *in vitro* porcine skin was significantly higher when the formulation was rubbed into the skin by gloved finger, which Davies's study did not do, but is relevant to the application of cosmetic formulations.

Maione-silva *et al.* (2019)¹⁷⁸ found that around 0.8% of the applied dose of ascorbic acid reached the Franz cell receptor in an *in vitro* porcine ear skin permeation experiment with infinite dose (~ 100 mg/cm²). The amount of ascorbic acid permeated here was 8× more than in Maione-Silva's study¹⁷⁸. The use of a large infinite dose is not representative of finite in use dosage since it could affect the hydration of the skin tissue and this may influence partitioning of the ascorbic acid into and out of the skin barrier.

More caffeine from the gel formulation (21.5% of the applied dose) was observed to reach the receptor compartment than caffeine cosolvent formulation (13.7% of the applied dose). PG is a skin penetration enhancer, however, its mechanism of action has not presently been elucidated.

Brinkmann and Müller-Goymann (2005)²²⁸ studied the effects of PG on human *stratum corneum* using x-ray diffraction and they proposed that PG integrates into hydrophilic regions of hexagonally ordered lipids, thereby increasing the distance of the lipids and resulting in higher skin permeation. Glycine is used in topical products as a humectant and skin conditioning agent. Bettinger *et al.* (1998)²²⁹ attributed the penetration enhancer effect of glycine due to its interaction with *stratum corneum* lipids, enhanced desmosomal degradation, and the hydrating effect of glycerol. More recently Brinkmann and Müller-Goymann (2005)²²⁸ proposed glycine intercalates between the hydrophilic

heads of the orthorhombically packed lipids of the *stratum corneum*, increasing the gaps in the lipid bilayers and increasing skin permeation. These penetration enhancer effects could explain why more caffeine permeated through the skin from the gel formulation.

In contrast to caffeine, the gel formulation did not significantly enhance the amount of ascorbic acid that reached the receptor compartment compared to cosolvent formulation (4.5% vs 6.4% of the applied dose). This could be due to xanthan gum, which has a large average molecular weight of ~ 2000 kDa, used in topical products as a viscosity thickening agent. Xanthan gum is a hydrophilic polymer, containing many hydroxyl groups, so forms hydrogen bonds with water molecules. Xanthan gum is also anionic, however, ascorbic acid at pH 2.6 is neutral so electrostatic interactions are not expected. Since ascorbic acid is more hydrophilic (polar) than caffeine, xanthan gum would have a higher binding capacity, via hydrogen bonding, to ascorbic acid and therefore could retard its skin penetration.

A study by Cross *et al.* (2001)⁶³ found that a thickening agent (Carbomer 940) could retard benzophenone-3 (a sunscreen) penetration through the skin in infinite dose studies but the opposite effect was observed in finite dose (in use) studies. In this study 22.22 mg/cm² of formulation was applied to the skin which is more than a typical finite dose (< 10 mg/cm²). However, evaporation of solvent from the formulation was observed during the permeation study (by way of precipitation of the active ingredients on the skin surface) and therefore the dose applied cannot be considered an infinite dose but more like a finite dose application. This would mean the finding that ascorbic acid permeation was retarded by the thickening agent is contrary to the observations of Cross *et al.*⁶³.

More recently Cai *et al.* (2016)²³⁰ found xanthan gum gel to retard skin permeation of tetracaine (logP 3.54) in finite dose studies more than a gel made with hydroxyl methylcellulose (HPMC). The authors explained their findings by stating that in finite dose studies, solvent evaporation, i.e., an increase in gel dehydration, intermolecular interactions in xanthan gum gel are strengthened and impart a greater diffusional restriction on the drug. The

xanthan gum gel was reported to have a smaller pore size than the HPMC gel and to form electrostatic interactions with tetracane. A similar effect would be applicable to ascorbic acid here by way of hydrogen bond interactions.

3.4.4 Amount of permeant detected in epidermis and dermis of excised skin and intact skin permeation experiments.

A limitation of Franz diffusion cells is an overhydration of the skin tissue, by the liquid acceptor medium, more than would occur physiologically under *in vivo* conditions (Section 1.2.3.2). This has been previously found to increase permeation of flufenamic acid (logP 5.25) into the skin layers.⁴⁴ To establish if this effect was applicable to ascorbic acid and caffeine, skin permeation experiments were performed with skin in Franz cells (excised skin) and without an acceptor medium (intact skin).

The ToF-SIMS intensity of ascorbic acid and caffeine molecular ion, in the epidermis and dermis ROIs of the skin cross sections, from excised skin and intact skin permeation experiments were compared as shown in Figure 3-7 A and B respectively. No significant difference ($P < 0.05$) was found between excised skin and intact skin permeation experiments.

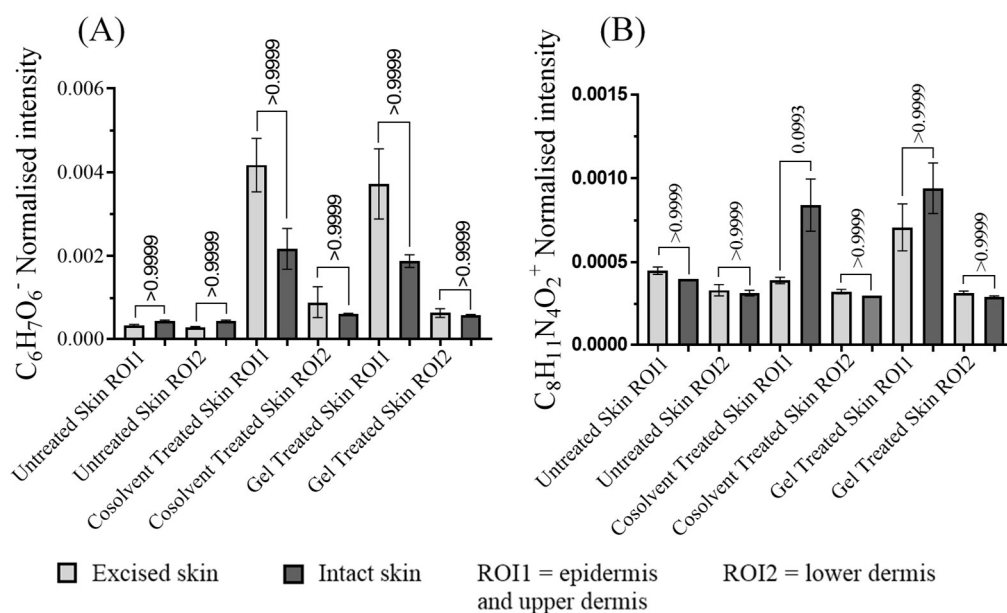


Figure 3-7 Comparing ToF-SIMS ion intensity from excised skin and intact skin cross section regions of interest (ROI) after ex vivo permeation experiment with (A) ascorbic acid and (B) caffeine formulations. Data is shown as mean \pm SD, $n=12$.

A potential explanation for why no difference was observed, between excised skin and intact skin experiments, could be due to the large variability in secondary ion intensities between cross sections. Whilst untreated skin showed relatively small standard deviation ($\sim 5 \times 10^{-5}$ for $C_6H_7O_6^-$ normalised intensity), treated skin showed much larger values (1×10^{-3} for $C_6H_7O_6^-$ normalised intensity). This would indicate that mapping the distribution of exogenous molecules is inherently more variable than mapping the distribution of endogenous molecules.

Furthermore, ascorbic acid and caffeine are both hydrophilic and would disperse freely within the deeper skin layers without reaching saturation. For example, Pinnell *et al.*¹⁷¹ determined porcine skin to only reach saturation after 72 hours with an infinite dose of 20% w/w ascorbic acid formulation. The quantity of ascorbic acid applied by Pinnell *et al.*¹⁷¹ was much greater than the quantity applied here so it is unlikely the dermis reached saturation in the excised and intact skin experiments in this work.

Bronaugh *et al.* (1984)²³¹ found that the amount of lipophilic test substance retained by the skin will vary with the receptor fluid used to solubilise the compounds. Since ascorbic acid and caffeine have high solubility limits, the saturation limit was not approached in the receptor compartment so did not influence retention in the skin layers. Since no significant difference was determined, the ToF-SIMS data from excised skin and intact skin cross sections were combined for statistical analysis.

3.4.5 Permeation distribution of ascorbic acid and caffeine in porcine skin *ex vivo*

ToF-SIMS images of porcine skin cross sections, in Figure 3-8, show ascorbic acid, in red, to have permeated into the epidermis of the porcine skin. Where it is co-localised with cholesterol sulfate, a marker ion for the epidermis (Figure 2-5), ascorbic acid distribution appears yellow. Despite the formulation being rubbed homogeneously into the skin by gloved finger, the observed ascorbic acid distribution is non-uniform. There does appear to be some localisation of ascorbic acid in skin furrows and around the orifices of the hair follicle to a depth of 0.1 mm as seen in Figure 3-8 images 5 and 6 (left to right).

ToF-SIMS images of porcine skin cross sections, in Figure 3-9, show caffeine to also have permeated into the epidermis of the porcine skin. Caffeine distribution is also non-uniform and there does appear to be some localisation around hair follicle orifices as seen in Figure 3-9 images 10 and 11 (left to right). Acquiring skin cross sections showing the full length of the hair follicle is challenging since hair grows at an angle and not perpendicular to the skin surface.

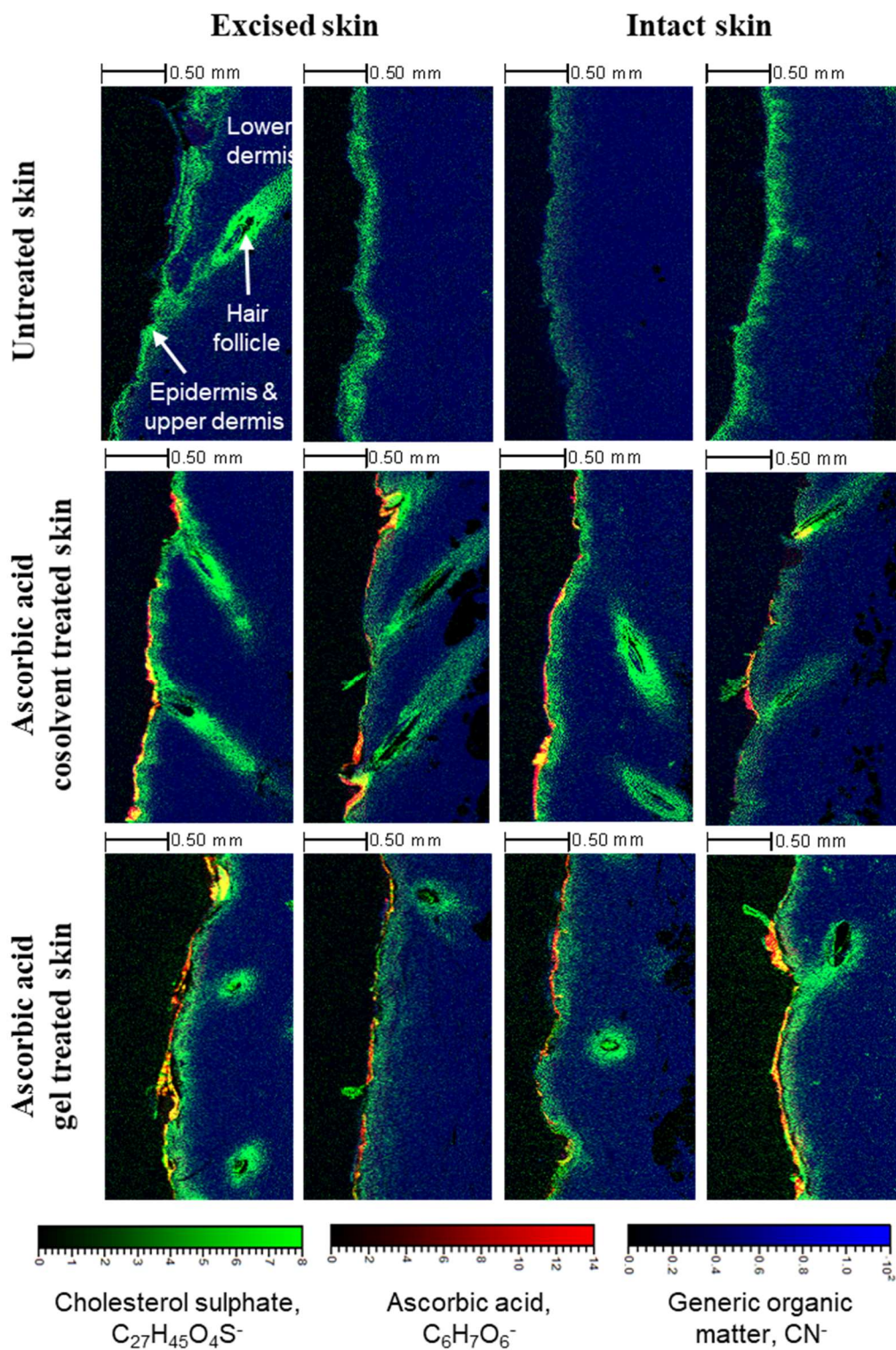


Figure 3-8 Representative ToF-SIMS secondary ion images of excised skin and intact skin cross sections, highlighting the spatial distribution of ascorbic acid ion $C_6H_7O_6^-$ (red) after treatment with cosolvent and gel formulation.

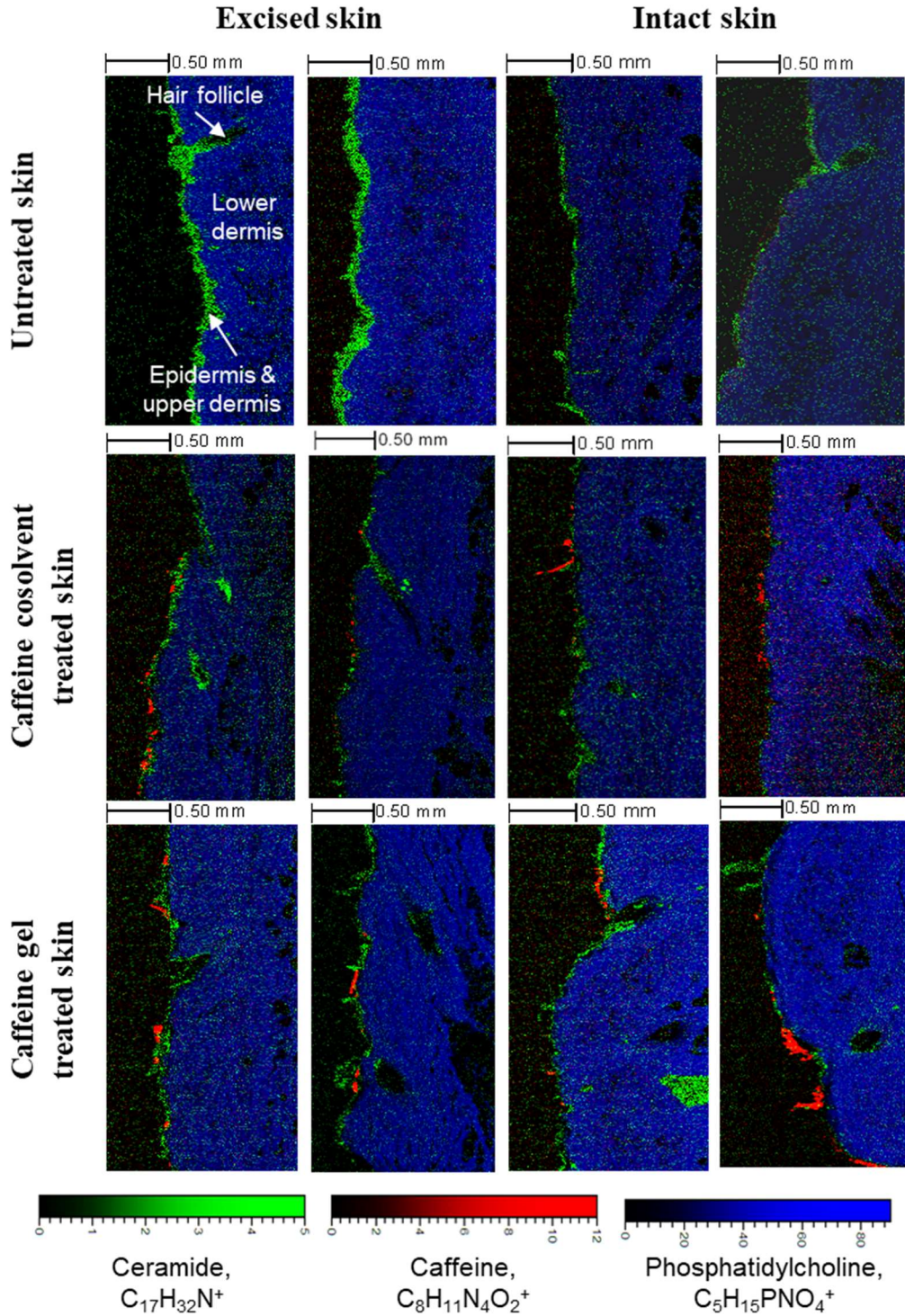


Figure 3-9 Representative ToF-SIMS secondary ion images of excised skin and intact skin cross sections, highlighting the spatial distribution of caffeine ion $C_8H_{11}N_4O_2^+$ (red) after treatment with cosolvent and gel formulation.

Whilst caffeine and ascorbic acid in the hair follicle orifice can act as a reservoir for delayed permeation, it cannot be considered to have penetrated the skin by the hair follicle pathway. The hair follicles are an invagination of

the epidermis extending deep into the dermis²³², hence cholesterol sulfate ion ($C_{27}H_{45}O_4S^-$) and ceramide fragment ($C_{17}H_{32}N^+$) diagnostic of corneocytes show the location of hair follicles in the ToF-SIMS images. Ascorbic acid and caffeine could not be detected in the corneocytes surrounding the hair follicle at a depth > 0.1 mm, despite being detected in the epidermis which would have the same matrix effect as the corneocytes surrounding the hair follicle. This would suggest the concentration of ascorbic acid and caffeine in the hair follicle to be less than the sensitivity of the ToF-SIMS.

D'Alvise *et al.* (2014)⁴⁶ demonstrated lidocaine to permeate via the follicular route for the first time using porcine ear skin that was left attached to the underlying cartilage via DESI mass spectrometry imaging. The authors commented that the elastic fibres surrounding the hair follicles did not contract, as would occur in excised skin, and therefore follicular transport was observed. However, the number of cross sections, and by extension hair follicles, analysed was small and they may not be representative of all hair follicles. In this study a much larger number of cross sections were analysed, from different biological donors, yet follicular transport was not observed. All the ToF-SIMS cross sectional images are available in the Appendix (Figures A-3 to A-6).

Otberg *et al.*¹⁸⁷, Trauer *et al.*²⁴ and Liu *et al.*²³ previously demonstrated hair follicles to significantly contribute to skin permeation of caffeine (Section 1.6.2). However, in this study, caffeine was not visualised in the hair follicles despite using the same penetration enhancers as these previous studies. Porcine hair follicles show a diameter of approximately 200 μm , two to three times higher than those on human skin (78 μm)^{37,38} should also have facilitated transfollicular permeation. It must be noted that Otberg *et al.*¹⁸⁷, Trauer *et al.*²⁴ and Liu *et al.*²³ assumed permeation of caffeine into hair follicles via experiments involving unblocked and blocked hair follicles.

A possible explanation for the discrepancy could be to do with the wax that was applied to the skin by Otberg *et al.*,¹⁸⁷ when conducting experiments with unblocked hair follicles. The wax on the skin could lead to occlusion of the skin surface which may increase skin permeation of caffeine and thus an

overestimation of follicular transport. Some of the ethanol from the formulation may also interact with the wax, hindering its evaporation from the skin and so is available for skin permeation enhancement. Being able to see the spatial distribution of the active ingredient is important in being able to understand the mechanism of permeation.

Recently Christmann *et al.* (2019) showed that the permeation of fluorescently labelled nanoparticles into hair follicles was independent of hair follicle type (e.g. absence of hair shaft, vellus hair and terminal hair) despite their fundamental morphometric differences. The deposition of the nanoparticles per hair follicle did not differ and was demonstrated by differential tape stripping and CLSM analysis. Therefore, in this study, hair follicle type differences are not expected to contribute to the amounts permeated via the follicular route.

The miscibility of an ingredient with sebum is a good predictor of follicular route permeation. Abd *et al.* (2016)²³³ showed this when they developed lipophilic caffeine formulations and observed increased follicular transport by differential tape stripping. Ascorbic acid, caffeine, PG and ethanol are all water miscible so would not be predicted to permeate via the hair follicles. Ethanol is reported to increase skin permeation of active ingredients by lipid fluidisation, lipid extraction and effects on lipid ordering.¹⁴ These effects would be applicable to sebum as well as corneocytes, however, the cosolvent formulation herein did not lead to detection of caffeine deeper in the hair follicles. However, in finite dose studies the evaporation of ethanol is thought to limit the contribution of ethanol to drug permeation enhancement.

3.4.6 Statistical analysis of ascorbic acid and caffeine permeation into epidermis and dermis by ToF-SIMS.

Comparison of the normalised ion intensities of ascorbic acid molecular ion obtained from the epidermis and upper dermis ROI and lower dermis ROI is shown in Figure 3-10 A and B respectively. Both cosolvent and gel treated skin showed significantly higher ascorbic acid ion intensity than untreated skin, with no significant difference between the formulations. This agrees with

the UV-Vis data, in Figure 3-6, where gel formulation did not significantly increase ascorbic acid permeation compared to cosolvent formulation.

Data of normalised ion intensity of caffeine molecular ion showed the gel formulation to have higher intensity than the cosolvent formulation in the epidermis and upper dermis ROI, shown in Figure 3-10 C. This is also in agreement with the UV-Vis data, in Figure 3-6, where the gel formulation significantly enhanced the permeation of caffeine compared to cosolvent formulation. Whilst the ion intensities in ToF-SIMS do not reflect the relative abundance of ascorbic acid and caffeine, the same conclusions regarding skin permeation from the formulation was reached as with UV-Vis spectroscopy data (Section 3.4.3).

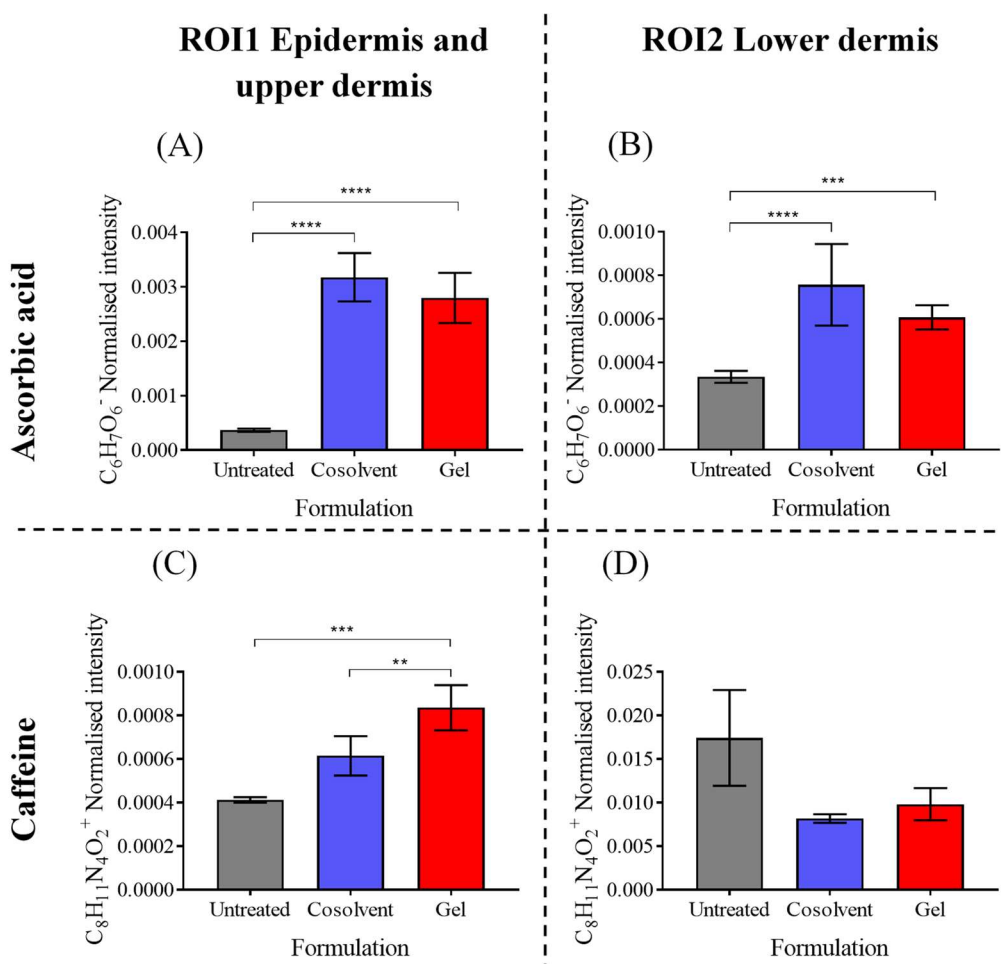


Figure 3-10 Exported ToF-SIMS data showing average secondary ion intensities for ascorbic acid and caffeine in epidermis and upper dermis ROI (A and C) and lower dermis ROI (B and D). Data shown as mean \pm SEM,

$n=24$.

The UV-Vis spectroscopy data showed more caffeine to permeate through the skin than ascorbic acid, however, the caffeine molecular ion intensity in the epidermis of untreated skin and cosolvent treated skin was not significantly different as shown in Figure 3-10 C. This could be due to caffeine ionising less well when surrounded by other analytes in biological tissue matrix (matrix effects) despite it having a normalised ion intensity similar to ascorbic acid when analysed on silicon wafer alone (Figure 2-4). In addition, no significant differences in caffeine molecular ion intensity were observed in the dermis, Figure 3-10 D, despite UV-Vis data showing a significant flux of caffeine into the Franz cell acceptor compartment. In positive ionisation mode, several compounds such as amino acids and salts are able to produce positively charged ions which contribute to a higher degree of ion suppression, thereby resulting in a higher matrix effect.^{234,235} Due to ion suppression, caffeine is detected with less sensitivity in the ToF-SIMS.

3.4.7 Variability in ascorbic acid and caffeine ion intensity in epidermis of skin cross sections.

The most recent (2016) guidance by the SCCS³⁶ considers that for a reliable dermal absorption study, 8 skin samples from at least 4 donors should be used to be able to report on the variability, validity and reproducibility of the method. This guidance is specifically for mass balance experiments with conventional chromatographic analysis. To the best of the author's knowledge, no such guidelines exist for analysis of skin cross sections by imaging techniques and at present is a subjective judgement. In this study, each formulation was applied to 12 skin test sites from 6 biological donors meeting the criteria of the SCCS.

The skin cross sections were put into an order using a random number generator to see how the mean average ion intensity and SEM of the test compound changed with the number of skin cross sections analysed. The mean average ion intensity of ascorbic acid molecular ion (Figure 3-11 A), from untreated skin cross sections remained relatively unchanged with the number of cross sections analysed. In contrast with cosolvent and gel treated skin cross sections, the average changed significantly with the number of cross sections

analysed. Only after 15 cross sections were analysed, did the average stay relatively unchanged and the SEM begin to decrease. The same trends were observed for caffeine molecular ion also (Figure 3-11 B). This illustrates that when monitoring permeation of an exogenously applied compound, many skin cross sections should be analysed to get a reproducible result. It would appear that an adequate number of cross sections have been analysed in this study.

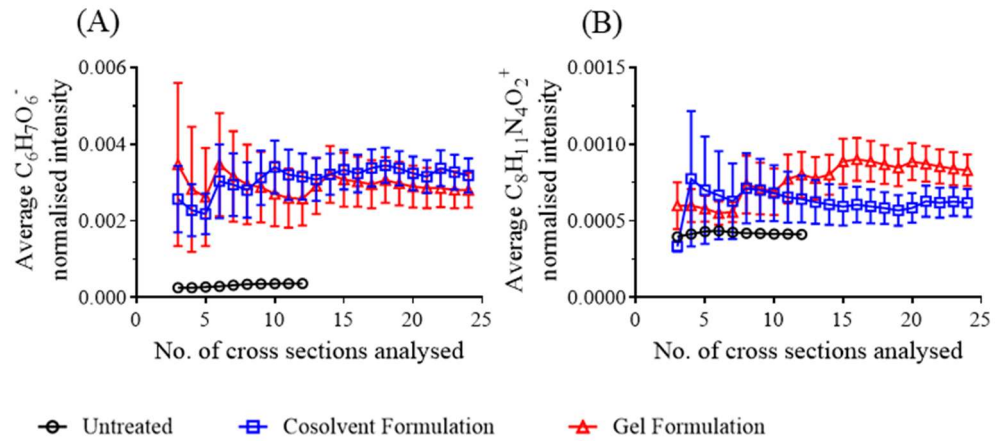


Figure 3-11 Change in average secondary ion intensity, of (A) ascorbic acid and (B) caffeine, with number of cross sections analysed. Data originates from epidermis and upper dermis ROI. Data shown as mean \pm SEM.

3.5 Conclusions

This chapter shows a comprehensive analysis of the permeation distribution of ascorbic acid and caffeine into *ex vivo* porcine skin tissue. In this study ascorbic acid was found to have limited skin permeation compared to caffeine. Whilst a gel formulation significantly enhanced the delivery of caffeine into the skin compared to a cosolvent control, the gel formulation did not enhance ascorbic acid delivery. It is thought that the use of a thickening agent, which is widely used in topical products, retarded the skin permeation of ascorbic acid. Future formulation development could look to avoid or employ an alternative thickening agent.

The principal route of permeation was demonstrated to be transepidermal for both ascorbic acid and caffeine by ToF-SIMS. Some of the ascorbic acid and caffeine was found localised in the orifices of the hair follicle (max depth 0.11 mm), but not found deeper in the hair follicle structures. Thus, transfollicular route of permeation was not detected for ascorbic acid and caffeine, despite wide reporting of follicular permeation for the latter which contradicts the present understanding of caffeine route of permeation.

Previous work in this area was not able to visualise the distribution of caffeine into the hair follicle but hair follicle permeation was assumed to occur by experiments involving blocked and unblocked hair follicles. A possible explanation for the discrepancy could be the wax applied to the skin of unblocked hair follicle experiment which could occlude the skin surface and lead to overestimation of follicular transport.

No difference in permeation was observed when skin was excised (and mounted in Franz cells) or used intact. It is thought this was due to application of a finite dose of hydrophilic drug which did not reach saturation limit in the skin tissue. Either approach can therefore be used in future depending on experimental requirements.

Since most of the ascorbic acid and caffeine was delivered and detected in the *stratum corneum* and epidermis of the skin, subsequent permeation investigation should focus on this layer of the skin, for example by tape

stripping. Of particular interest is the non-uniform distribution of the test compounds in the epidermis, despite being rubbed homogenously into the skin. The permeation of ascorbic acid and caffeine through and into the skin was analysed by two independent analytical techniques which both agreed with each other.

Chapter 4: Preparation and characterisation of ascorbic acid lipid nanoparticle formulations

4.1 Introduction

The permeation study, in chapter 3, has shown ascorbic acid to have limited skin permeation compared to another hydrophilic molecule – caffeine. Here an ascorbic acid gel formulation appeared to not significantly enhance the permeation of ascorbic acid compared to a solvent based control. In order to further improve permeation of ascorbic acid, lipid nanoparticle formulation, specifically NLCs, were chosen for investigation.

NLCs have been intensively studied as carriers for a wide range of dermatological applications such as treatment of hyperpigmentation, acne, dermatitis, herpes labialis and aesthetic (cosmetic) medicine (Section 1.4.2.3). NLCs are a nanoemulsion colloidal dispersion with mean size between 40 and 1000 nm and containing a combination of solid and liquid lipids in ratios from 70:30 up to 99.9:0.1. NLCs have many features that are advantageous for cutaneous applications, such as increased chemical stability of their active cargo, high tolerability and their smaller size ensures close contact with the *stratum corneum* with subsequent enhanced permeation of active ingredient.¹²⁸

4.2 Chapter aims

The aim of this chapter is to develop an NLC formulation for ascorbic acid that is suitable for topical application. A comparator cream formulation will also be developed with both formulation types characterised to determine their suitability. Enhanced skin permeation of ascorbic acid, by means of an appropriate carrier formulation, may increase the efficacy of ascorbic acid formulations, for example, to provide antioxidant protection against UV-induced photodamage.

4.3 Materials and methods

4.3.1 Materials

Ascorbic acid (>99.5% purity), polysorbate 80, xanthan gum and Euxyl® PE 9010 were purchased from Guinama (Valencia, Spain). Poly(vinyl alcohol) (PVA) (87-90% hydrolysed, avg. molecular wt. 30000-70000), oleic acid and dichloromethane were obtained from Sigma-Aldrich (St. Louis, USA). Witepsol® E85 (hydrogenated coco-glycerides, m.p. 42-44 °C) was kindly supplied by Sasol (Witten, Germany). Sodium hydroxide was purchased from Panreac Quimica SLU (Barcelona, Spain). Type II water was produced in house using a water purification system (Evoqua Labostar® RO DI) from Evoqua Water Technologies LLC (Pittsburgh, USA). All reagents used were of analytical grade and used without further purification.

4.3.2 Preparation of NLC formulation

NLC dispersion was prepared by a modified solvent emulsification-evaporation method based on a (W/O/W) double emulsion technique as shown in Figure 4-1. Briefly Witepsol® E85 (500 ± 4 mg, 10% w/w) and oleic acid (125 ± 3 mg, 2.5% w/w) was dissolved in 1 mL of dichloromethane in a glass tube (diameter 24 mm). Then 250 mg (5% w/w) ascorbic acid dissolved in 850 μ L type II water (17% w/w) was added to the lipid mixture. The mixture was homogenised using a sonicator (Vibra-Cell™ ultrasonic processor, Sonics & Materials Inc., Newtown USA) equipped with a 6 mm sonication probe during 3 minutes with 70% of amplitude. The formed W/O primary emulsion was then quickly dispersed in PVA (30 ± 0.5 mg, 0.6% w/w) and polysorbate 80 (270 ± 5 mg, 5.4% w/w) dissolved in 2925 μ L type II water (58.5% w/w) in a glass tube (diameter 24 mm) with sonication during 3 minutes with 70% of amplitude. Ultrasonication was always performed by placing the glass tubes in an ice-water bath to maintain temperature <20 °C.

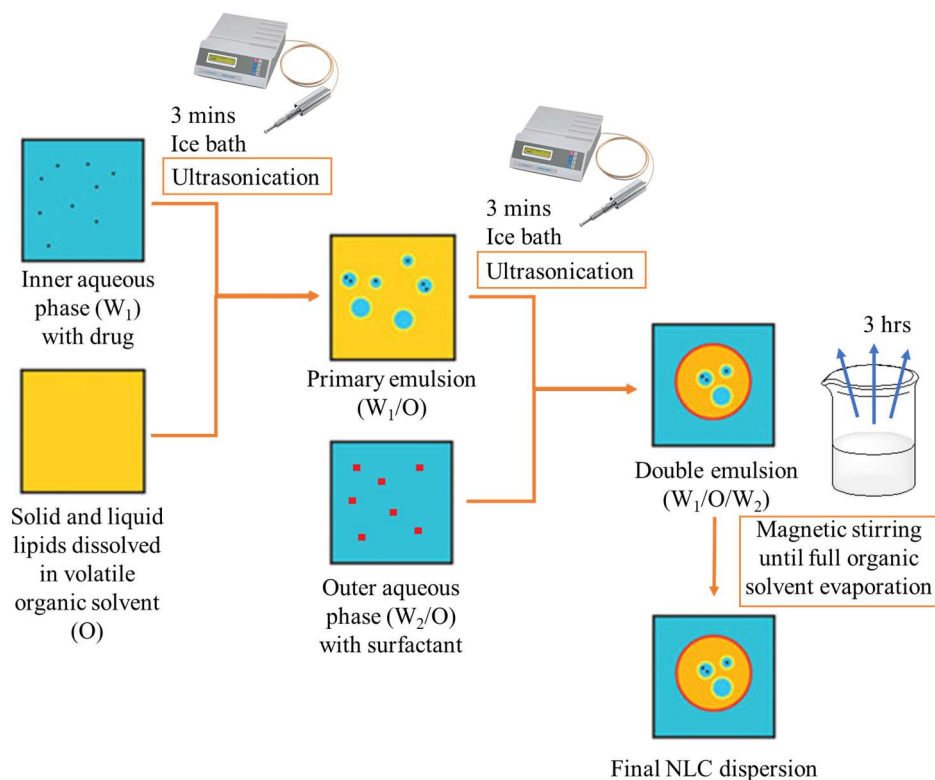


Figure 4-1 Schematic of double-emulsion NLC preparation by solvent emulsification-evaporation method. Adapted from Soares et al. (2013)²³⁶

The W/O/W double emulsion formed was poured into an empty beaker and left under magnetic stirring (300 rpm, IKA® RO 15 magnetic stirrer, IKA-Werke GmbH & Co (Staufen, Germany)) for full organic solvent evaporation (3 hours). During this time, the sides of the beaker were wrapped in aluminium foil and magnetic stirring performed in an unlit fume hood. The NLC dispersion was weighed before and after magnetic stirring to calculate total evaporated losses. The weight of any water evaporation was determined and subsequently added to the NLC dispersion with calibrated micropipette. NLC dispersion was then transferred to a clean glass vial and 1% w/w of Euxyl® PE 9010 added and mixed through. The pH of the formulation was measured and 2.0M NaOH added to raise the pH to 3.0 – 3.2. The pH was raised to above 3.0 because the preservative is effective in the pH range 3 – 12²³⁷, it is closer to the normal skin pH of 5.5 to maintain skin homeostasis and is more suitable for individuals with sensitive skin.²³⁸ Formulations were stored at 4 °C (in the dark) until further use.

4.3.3 Preparation of cream formulation

Ascorbic acid O/W emulsion (cream) was prepared using the same lipid and surfactant composition as used for the NLCs (Section 4.3.2). Xanthan gum was also included in the formulation. Both the oil phase (Witepsol® E85, 10% w/w and oleic acid, 2.5% w/w) and water phases (Type II water, 75% w/w; polysorbate 80, 5.4% w/w; poly(vinyl alcohol), 0.6% w/w and xanthan gum, 0.5% w/w) of the cream were heated separately to 75 °C. The oil phase was then added slowly to the aqueous phase using a glass rod and continuous magnetic stirring. The hot O/W emulsion was then homogenised at 6000 rpm for 10 min (IKA® T25 digital ULTRA TURRAX® disperser, IKA-Werke GmbH & Co (Staufen, Germany)). The resulting O/W emulsion was then cooled to ambient temperature. When the temperature was < 25 °C, ascorbic acid (5% w/w) was added and mixed thoroughly using a glass stirring rod. The formulation was weighed before and after heating so that the water lost by evaporation could be replaced. Then 1% w/w of preservative, Euxyl® PE 9010, was added and mixed through. The pH of the formulation was measured and 2.0M NaOH added to raise the pH to 3.0 – 3.2. Note that the same volume of NaOH solution was added per weight of cream and NLC for consistency. Formulations were stored at 4 °C (in the dark) until further use.

4.3.4 Dynamic light scattering

The particle size and polydispersity index (PDI) of NLCs was determined by dynamic light scattering (DLS) using a Malvern Zetasizer Nano NS (Malvern Instruments Ltd, Malvern, UK) at a temperature of 25 °C and measurement angle of 175°. Zeta potential of the NLC dispersion was also determined by laser Doppler micro-electrophoresis using the equipment previously described. Samples were diluted 1:100 in aqueous sodium chloride (10 mM) and vortex mixed prior to analysis. All measurements were carried out in triplicate with 3 independently prepared samples.

4.3.5 Association efficiency

The association efficiency (AE) % defines the amount of ascorbic acid associated with or encapsulated within the NLCs. It was determined indirectly

by quantifying the difference between the total amount of ascorbic acid used to prepare the systems and the total amount of ascorbic acid that remained in the aqueous phase after NLC isolation by centrifugation. AE% was calculated as follows:

$$AE \% = \frac{\text{total amount of AA} - \text{free AA in filtrate}}{\text{total amount of AA}} \times 100 \text{ (Equation 4.1)}$$

Where AA = ascorbic acid

NLC dispersion was diluted 1:625 in 0.2% w/v MPA. Diluted NLC dispersion (2 mL) was centrifuged (Eppendorf Centrifuge 5810R, Hamburg, Germany) through centrifugal filter units (Amicon® Ultra-15 Centrifugal Filters, Ultracel -100 kDa, Merck Milipore, USA) at 4000 rpm at 20 °C (ambient conditions) until separation (30 mins) between the NLCs retained in the filter unit and the aqueous phase corresponding to the filtrate was achieved. The filtrate was used to quantify the amount of non-incorporated ascorbic acid. This method was adapted from Rodrigues *et al.* (2016)²³⁹.

The drug loading (DL) % defines the weight percentage of ascorbic acid to the total dry weight of NLC and was calculated as follows

$$DL \% = \frac{\text{total amount of AA} - \text{free AA in filtrate}}{\text{total dry weight of nanoparticles}} \times 100 \text{ (Equation 4.2)}$$

Where AA = ascorbic acid

For the quantification of free ascorbic acid in the filtrate, a HPLC method was used as described in Section 2.3.7.2. Since the formulations are made in a weight by weight manner, the density of the NLC formulation was determined, to convert concentration of ascorbic acid from w/w to w/v.

4.3.6 Formulation stability testing

The stability of the NLC dispersion, cream formulation and a positive control was carried out at 3 temperature conditions: fridge (4 °C), ambient cupboard (18-22 °C) and oven (40 °C, Heratherm Incubator, Thermo Fisher, Waltham, MA, USA). The positive control was ascorbic acid (5% w/w), Euxyl® PE 9010 (1% w/w) and water (q.s), with the pH adjusted to 3.0-3.2 using the same per weight volume of 2.0M NaOH as put into NLC and cream formulations.

Stability was assessed in terms of their physical appearance and ascorbic acid concentration at 1, 7, 14 and 28 days after preparation of the formulations.

In order to quantify ascorbic acid associated with/within the nanoparticles and cream emulsions, the emulsions had to be broken. An aliquot of the emulsion (100 mg) was first weighed out into a glass scintillation vial. Dichloromethane (3 mL) was added and the vial vortexed until the emulsion was lysed/dispersed. MPA buffer (15 mL) was then added and the vial vortexed (2 mins). The vial was left to stand (1 hour) for phase separation to occur. 10 mL of the middle aqueous phase was removed, via needle and syringe, and placed into a Falcon tube for centrifugation (4000 rpm, 10 mins, Heraeus Multifuge 3S, 18 °C). The supernatant was injected into HPLC to determine ascorbic acid concentration as detailed in Section 2.3.7.2.

4.3.7 Cryo-transmission electron microscopy

Lipid nanoparticle dispersion was diluted 1:100 with ultrapure water and added (3 $\mu\text{L}/\text{grid}$) to glow discharged (10 s at 5 mA using an agar turbo coater aux power unit and dedicated glow discharge head) holey carbon copper transmission electron microscopy (TEM) grids (electron microscopy resolutions). Samples were let to adsorb onto the grids for 1 minute before frozen using a Gatan CP3 plunge freezing unit, blotting for 1 s and freezing in liquid ethane. Samples were then transferred to cryo-TEM storage boxes and then loaded into a Gatan 626 cryo-TEM holder on a JEOL 2100+ TEM. Throughout the examination, the sample temperature was kept below -175 °C. Images were acquired for 2-4 s at a dose of below 10 e/A^2 , using a US1000 CCD camera and Digital Micrograph GMS 3 software. 3 independently prepared samples were analysed.

4.3.8 Laser diffraction particle size analysis

The droplet size distribution of the emulsions was obtained using a Coulter LS 230 laser diffraction particle size analyser (Beckman Coulter GmbH, Krefeld, Germany) using water as working fluid at 15-20°C. The sample was diluted to 10 mg/mL with ultrapure water, and vortex mixed, before adding to the

instrument sample compartment. The Fraunhofer optical model was used. Triplicate measurements were taken from three separate dilutions of the cream.

4.3.9 Rheology

Modular compact rheometer (MCR302, Anton Paar GmbH, Austria) was used to perform dynamic rheology and viscosity measurements. An aluminium parallel plate assembly (top plate diameter 50 mm) was used and measurements were recorded at 1.0 mm height and at 32 °C. Oscillatory amplitude sweeps were performed in the strain range of 0.01% to 100% at a constant frequency of 10 rad s⁻¹. Viscosity measurements were carried out in rotational mode under the same operating conditions.

4.3.10 ToF-SIMS analysis of formulations

ToF-SIMS reference spectrum of NLC, cream and positive control formulation was recorded, in negative polarity, by depositing a drop (~ 20 µL) of the formulation (n=6) onto a clean silicon wafer. ToF-SIMS spectra was acquired as specified in Section 2.3.8, but over a smaller 100 µm × 100 µm area, at a resolution of 256 pixels/ mm and 18 scans acquired per area. The NLC formulation was made with and without ascorbic acid (water q.s.) to identify secondary ions relevant of ascorbic acid and other excipient ingredients.

4.3.11 Statistics

Statistical analysis was performed as detailed in Section 2.3.11.

4.4 Results and discussion

4.4.1 NLCs with composition suitable for topical use

O/W emulsions are appreciated by the consumer for being less greasy than W/O emulsions and are therefore the most common type of cosmetic formulation for skin care.¹²⁴ The NLC dispersion developed herein has a composition of emollient (12.5% w/w) and surfactant (6% w/w) which would be classified as a cream formulation by Cheng *et al.* (2009)¹²⁵. This means that the NLC formulation is suitable for topical application. Nanoparticle and nanosized carrier formulations typically contain a higher percentage of surfactant, more than would be found in a typical skin cream, to give small particle size, however this could result in irritation and damage to the skin.²⁴⁰ For example, Maione-Silva *et al.*¹⁷⁸ developed a liposome formulation, encapsulating ascorbic acid using a high surfactant concentration of ~15% w/w. In contrast, the NLC formulation developed herein does not contain a surfactant concentration more than a typical skin cream product (i.e. > 6% w/w).

The NLC formulations developed contain a concentration of ascorbic acid (5% w/w) that would be considered to show therapeutic benefits based on previous efficacy studies presented in Section 1.5.2; and therefore, would be suitable for cosmetic use. Higher concentrations of ascorbic acid, up to 20% w/w, could have been incorporated into the formulation however was avoided as it may cause skin sensitivity in some individuals.¹⁶⁷

4.4.2 Characterisation of particle/droplet size, and charge, of NLCs and cream

In order to identify NLCs with suitable properties for topical application, a range of NLCs were produced with different ascorbic acid concentration, with or without ascorbic acid encapsulation and with different ultrasonication times (NLCs A-E, Table 4-1). NLC properties characterised include particle size, PDI, zeta potential and AE.

NLCs encapsulating ascorbic acid (NLC B), had mean particle size of 271.3 nm, which was larger than NLCs prepared without ascorbic acid (NLC A) which had mean particle size of 250.7 nm, as shown in Table 4-1. Meanwhile NLCs prepared with non-encapsulated ascorbic acid (NLC C) had mean particle size of 255.6nm, which was not statistically different to particle size of NLC prepared without ascorbic acid (NLC A). This would suggest successful encapsulation of ascorbic acid in the double emulsion NLCs. Encapsulation efficiency is further discussed in Section 4.4.3.

Table 4-1 Hydrodynamic diameter, polydispersity index (PDI) and zeta potential of NLCs A-E and cream. Statistical differences compared with NLC A, data shown as mean \pm SD (n=9; 3 independent samples). AA = ascorbic acid.

	NLC A (no AA)	NLC B (loaded)	NLC C (free AA)	NLC D (1 minute)	NLC E (0.5% AA)	Cream
AA concentration (% w/w)	0	5	5	5	0.5	5
Encapsulated (Yes or No)	N/A	Y	N	Y	Y	N
Ultrasonication time (mins)	3	3	3	1	3	N/A
Particle Size (nm)	250.7 \pm 5.8	271.3 \pm 9.4	255.6 \pm 5.0	319.1 \pm 12.0 ****	297.6 \pm 28.5 **	2017.3 \pm 59.1 ****
PDI	0.224 \pm 0.009	0.242 \pm 0.013	0.247 \pm 0.012	0.378 \pm 0.026 ****	0.299 \pm 0.033 **	0.990 \pm 0.015 ****
Zeta Potential (mV)	-7.7 \pm 1.0	-1.6 \pm 0.2 ****	-1.5 \pm 0.1 ****	-1.6 \pm 0.1 ****	-2.4 \pm 0.2	-4.9 \pm 0.6

NLCs prepared with an ultrasonication time of 3 minutes (NLC B) gave mean particle size of 271.3 nm and PDI of 0.242. In contrast, NLCs prepared with a shorter ultrasonication time of 1 minute (NLC D) gave larger mean particle size of 319 nm and a PDI of 0.378. A comparison of the particle size

distributions, shown in Figure 4-2, demonstrates an ultrasonication time of 3 minutes gave a more reproducible particle size distribution than ultrasonication time of 1 minute. Therefore, an ultrasonication time of 3 minutes was preferred (NLC B). The NLCs all had mean particle size < 500nm, which Souto and Muller¹⁴⁷ discuss as being able to form a dense film layer on the skin with subsequent occlusive effect. The NLCs developed are considered to show suitable particle size for topical application.

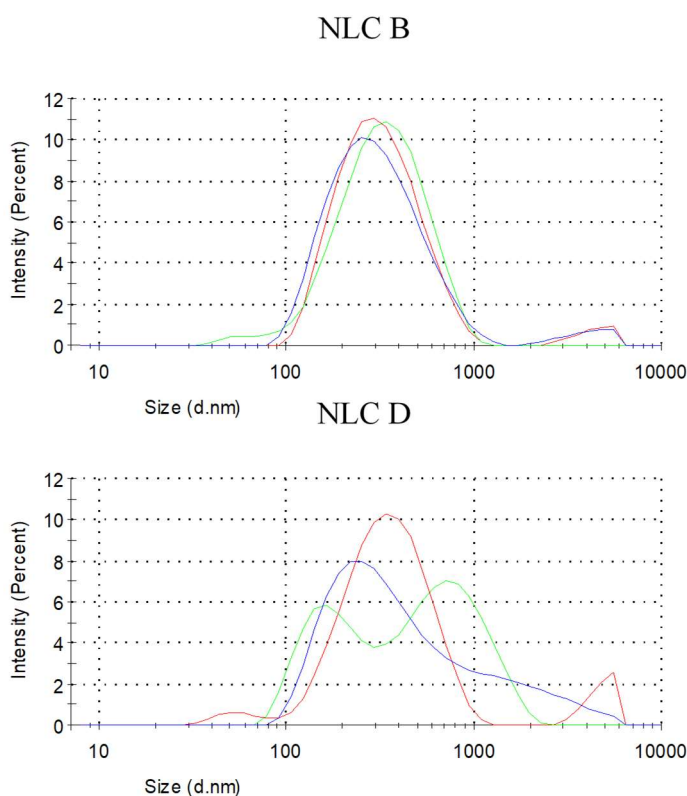


Figure 4-2 Size distribution of ascorbic acid encapsulated NLC with ultrasonication time of 3 minutes (NLC B) and 1 minute (NLC D). The distribution of 3 independent samples is shown.

In drug delivery applications using lipid-based carriers, a PDI of ≤ 0.3 is considered acceptable as it indicates a monodisperse population of nanocarriers.²⁴¹ NLC B, which showed a reproducible particle size distribution, had a PDI of 0.242 (Table 4-1) which would be considered acceptable for topical application.

A 1:100 dilution of the cream formulation was also analysed by DLS where a PDI of 1 was measured indicating a very broad distribution of size and that the

particle size cannot be accurately determined using the model in the DLS instrument. As such the droplet size of the cream was determined using a laser diffraction particle size analyser.

The cream had a mean droplet size of 20.73 μm (Figure 4-3). The lipid nanoparticle formulation was diluted to the same concentration as the cream, however, an acceptable level of obscuration of the laser intensity (8-12%), as specified by the software, could not be obtained. The obscuration of 0-2% achieved by the lipid nanoparticle sample means that the laser diffraction technique is not suitable and would suggest sub-micron particle size distribution, as witnessed in the DLS previously (Figure 4-2). The Fraunhofer model assumes that particles are non-transparent so smaller particles ($< 1 \mu\text{m}$), which scatter light also by refraction, can lead to errors in the retrieved particle size.²⁴²

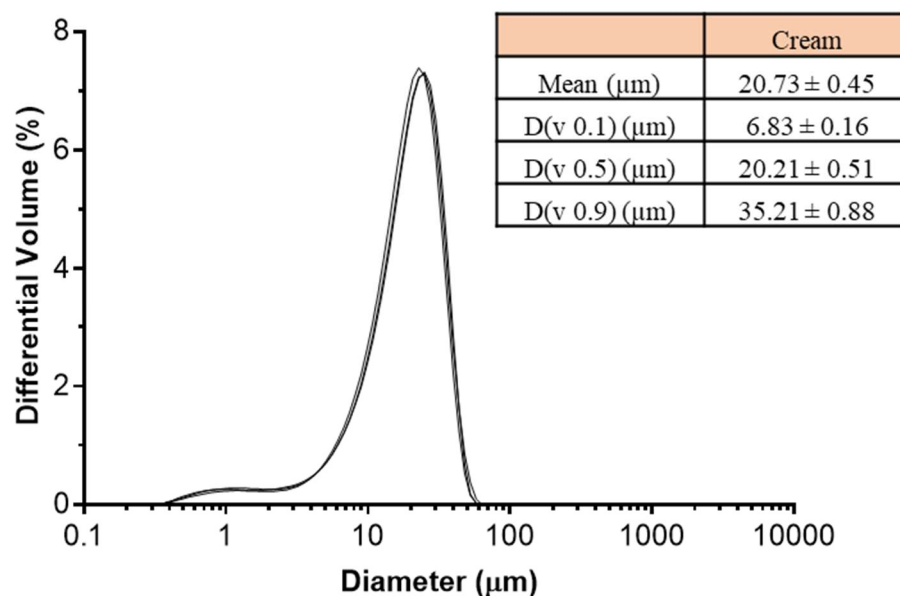


Figure 4-3 Droplet size distribution of cream formulation, measured by laser diffraction. Tabulated data shown as mean \pm SD of 3 independent samples.

There is presently some concern about the use of nanoparticles in skin care formulations. The EC Cosmetics Regulation No. 1223/2009 defines a nanomaterial as “an insoluble or biopersistent and intentionally manufactured material with one or more external dimensions, or an internal structure, on the scale from 1 to 100 nm”. Nanoparticles of this description require additional

safety assessment of the product prior to placing the product on the market for consumer use/trial.²⁴³ The nanoparticles prepared herein have external size dimension > 100 nm and are made from physiological lipids so cannot be described as biopersistent. Additionally, the concentration of the ingredients used in the preparation of NLCs are within any specified restrictions according to EC Cosmetics Regulation 1223/2009 so additional safety assessment is not required prior to application on human skin. In contrast, polymeric nanoparticles or liposomal carriers, which typically contain ingredients not listed in the EC cosmetic ingredient database (CosIng)²⁴⁴, would require additional safety assessment to check for biocompatibility or toxicity as the ingredients are not widely used in existing skin care products.

NLCs prepared without ascorbic acid (NLC A) showed a zeta potential of -7.7 mV. A more neutral zeta potential was measured for nanoparticle systems containing ascorbic acid (NLCs B – E) as presented in Table 4-1. This is because at pH 3.0 – 3.2 ascorbic acid is fully protonated and therefore uncharged in the formulation.

A higher electric charge on the surface (± 30 mV) of nanoparticles is preferable to prevent aggregation because of the strong repellent forces among particles.²⁴⁵ Despite the small negative surface charge, the NLC formulations were stable for at least four-weeks at room temperature with no phase separation and a homogenous appearance (to be discussed in detail in Section 4.4.4). This is because polysorbate 80 (MW 1310 g/mol) also provides a steric stability for maintaining the stability of nanoemulsions. Furthermore, it is known that adsorbed layers of polymers/large molecules shift the plane of shear to a farer distance from the particle surface which leads to a reduction of the measured zeta potential. That means even in case of highly charged particle surfaces, a relatively low zeta potential will be measured²⁴⁶.

4.4.3 Association efficiency of NLCs

NLC B, which contains an efficacious concentration (5% w/w) of ascorbic acid, had an AE of 18.13%, whereas NLC E, made with a smaller concentration (0.5% w/w) of ascorbic acid showed higher AE% of 41.98% (Table 4-2). A low encapsulation was recorded for 5% w/w ascorbic acid

formulation due to ascorbic acid partitioning preferentially out of the lipid phase and into the outer aqueous phase during ultrasonication.

Long ultrasonication times also lead to reduced AE. NLC D, prepared with 1 minute ultrasonication time had AE of 53.84%, higher than NLC B which was prepared with 3 minutes ultrasonication time and had AE of 18.13%. NLC B was found to have reproducible particle size distribution with mean particle size of 271.3 nm and acceptable PDI of 0.242, which was considered more important than the low AE%. Generally for drug delivery applications, high AE% is desirable (70 – 90%)¹⁸⁴ whereas for topical administration it could be argued AE% is less important as the particles do not permeate intact as discussed in Section 1.4.2.4.

Table 4-2 Association efficiency (AE) and drug loading (DL) of NLCs A-E and cream. Statistical differences compared to NLC B, data shown as mean ± SD (n ≥ 3). ND = not determined. AA = ascorbic acid.

	NLC A (no AA)	NLC B (loaded)	NLC C (free AA)	NLC D (1 minute)	NLC E (0.5% AA)	Cream
AE (%)	ND	18.13 ± 4.84	-2.56 ± 4.32 ***	53.84 ± 2.66 ****	41.98 ± 0.70 ****	ND
DL (%)	ND	3.86 ± 1.03	-0.55 ± 0.89 ***	11.45 ± 0.57 ****	1.10 ± 0.02 **	ND

To confirm that lipid nanoparticles were fully separated by centrifugation through filter units, NLC C was prepared with ascorbic acid added after production of the nanoparticles (i.e. not encapsulated), which were found to have an AE% of effectively zero when the error is taken into account (Table 4-2). This would suggest that the centrifugation method used to separate ascorbic acid encapsulated in NLC and not encapsulated in NLC was appropriate.

Previous studies of ascorbic acid nanoparticles report high AE of over 85% (Table 1-4). Although Guney *et al.*¹⁸⁰ and Duarah *et al.*¹⁷⁷ achieved relatively high AE, ascorbic acid was added to the lipid matrix at 80 °C and the

nanoparticle dispersion was formulated with a pH of 4.89, (which is above the pKa of ascorbic acid (4.2)) respectively. In both of these instances ascorbic acid would start to oxidise and degrade. Since the AE was calculated using an indirect method, meaning non-encapsulated ascorbic acid is determined, any degradation of ascorbic acid could be mistaken as being encapsulated. Therefore, the high encapsulation efficiency reported in these previous works could be unrepresentative. The oxidation of ascorbic acid was circumvented in this work by using MPA solution to stabilise ascorbic acid, as detailed in Section 2.4.3.

Whilst Duarah *et al.*¹⁷⁷ reported high AE%, the final ascorbic acid concentration in the formulation was 0.5% w/w which is far below the concentration required to observe antiaging efficacy in the skin (Section 1.5.2). As such they would not be deemed appropriate for cosmetic use. At the present time, it is not understood whether high AE% of the drug is linked to increased skin permeation of the drug, however this is outside the scope of the thesis.

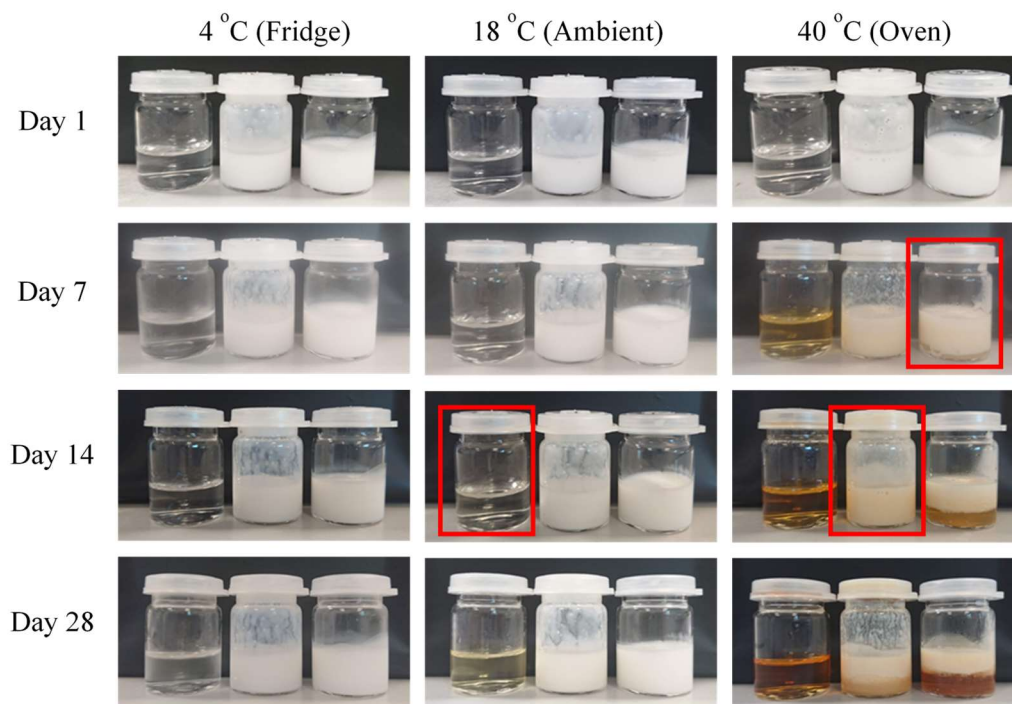
NLC B was considered as the most suitable NLC, for topical application, in terms of particle size and polydispersity index and was selected for further characterisation (Sections 4.4.4 to 4.4.7).

4.4.4 Stability of emulsion and ascorbic acid in the formulations

Encapsulation into lipid nanoparticles has been shown to increase the chemical stability of a number of cosmetic ingredients including coenzyme Q10¹⁴¹, AP²⁴⁷, retinol (vitamin A)¹³⁶ and tocopherol (vitamin E)²⁴⁸ but thus far not been investigated for ascorbic acid. Ascorbic acid is unstable in aqueous solution and becomes oxidised to dehydroascorbic acid, so its encapsulation into NLCs could be a strategy to stabilise ascorbic acid in cosmetic formulations and as such was investigated.

The positive control solution first becomes visibly yellow at 14 days, when kept at ambient temperature, which is a visual indicator that ascorbic acid has become oxidised (Figure 4-4). At this point, the antioxidant potential of the formulation is reduced so less therapeutic effect would be expected if applied

to the skin. In addition, the consumer is unlikely to want to apply a discoloured formulation to their skin.



Order of vials: positive control, NLC, cream

Figure 4-4 Stability photographs of positive control, NLC and cream formulations. Vials marked with a red box show when a formulation first becomes unacceptable to a consumer.

The cream begins to phase separate at day 7 when kept at 40 °C, even with the presence of a thickening agent in the form of xanthan gum. In contrast the NLC formulation begins to phase separate much later at day 28 at 40 °C (Figure 4-4). This shows the NLC formulation is more stable than the cream. Both formulations contain the same surfactant and lipid composition, so the smaller particle size of the nanoparticles must be responsible for the enhanced colloidal stability. The nanoparticles have a large surface area: volume ratio so there is a greater area over which electrostatic and/or steric stabilisation of particles can occur and therefore avoid agglomeration.

The ascorbic acid concentration of the positive control, lipid nanoparticle and cream were measured over time and no significant differences between the formulations at any of the time points were found (Figure 4-5). Previously

Grabnar *et al.*²⁴⁷ and Teeranachaideekul *et al.*²⁴⁹ incorporated AP into lipid nanoparticles. Lipid nanoparticles do not allow oxygen to diffuse into the carrier easily so entrapped AP was protected and enhanced stability reported. It was found that improved entrapment of the active ingredient within the nanoparticle structure could be responsible for the enhanced stability of AP. In contrast, ~80% of the ascorbic acid in the NLC formulation herein was not encapsulated so any differences in stability may have been masked by unencapsulated ascorbic acid.

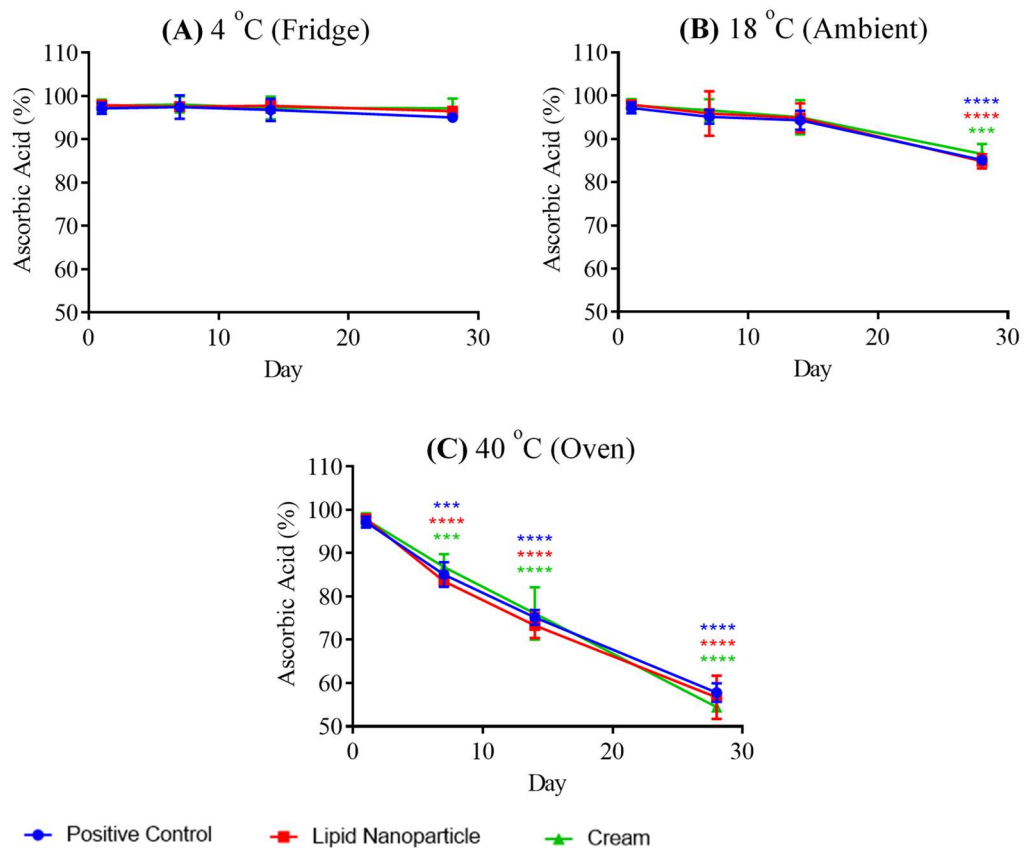


Figure 4-5 Ascorbic acid concentration of positive control, lipid nanoparticle and cream formulation over time at (A) 4 °C, (B) 18 °C and (C) 40 °C. Data shown as mean \pm SD, $n=3$. Statistical differences compared to day 1.

The cream formulation, which had 0.5% thickening agent, also did not show improved stability of ascorbic acid compared to the positive control despite the thickening agent which entraps water molecules in its network structure. This would suggest that the differences in ascorbic acid stability, between the different formulations, is much smaller than the variability observed with the

extraction method used to break the emulsions. In future, extraction variability could be reduced further by using an internal standard.

When the formulations were stored at 4 °C, no significant difference in ascorbic acid concentration was found after 28 days storage. When stored at ambient conditions, no significant difference in ascorbic acid concentration was found at 14 days storage, which correlates with the performance of existing commercial products. For example, Boots No7 Youthful Vitamin C Fresh Radiance Essence is to be used within 10 days.²⁵⁰

The stability of ascorbic acid could be enhanced with the addition of antioxidants to the formulation (e.g. Ferulic acid, Alpha Tocopherol) as done by SkinCeuticals C E Ferulic formulation.¹⁷⁹ As the formulations developed herein are biphasic emulsion systems, the addition of ferulic acid would not infringe the patent of SkinCeuticals.¹⁷⁹ These antioxidants were not included in the NLC formulation to see if the NLCs alone could stabilise ascorbic acid.

In this work, owing to the stability of the systems applied, a large batch of the formulation can be made on one day and used subsequently to test *in vivo/ex vivo* skin permeation. All skin permeation experiments, in the next chapter (Chapter 5) were thus conducted within 7 days, with the formulations stored in the fridge at 4 °C, to avoid any large decrease in ascorbic acid concentration.

4.4.5 Imaging of NLC nanoparticles using Cryo-TEM

Cryo-TEM avoids dehydration, as occurs under vacuum in conventional TEM, so was suitable for the analysis of double emulsion lipid nanoparticles with minimal damage. Cryo-TEM images confirmed the presence of polydispersed lipid nanoparticles with a size range between 80 to 140 nm in size, as indicated by red arrows in Figure 4-6. images A-D. It is difficult to make definite conclusions about particle size because only few particles were observed adsorbed in the holes of the carbon copper grids (3 independent samples, > 10 TEM images per sample).

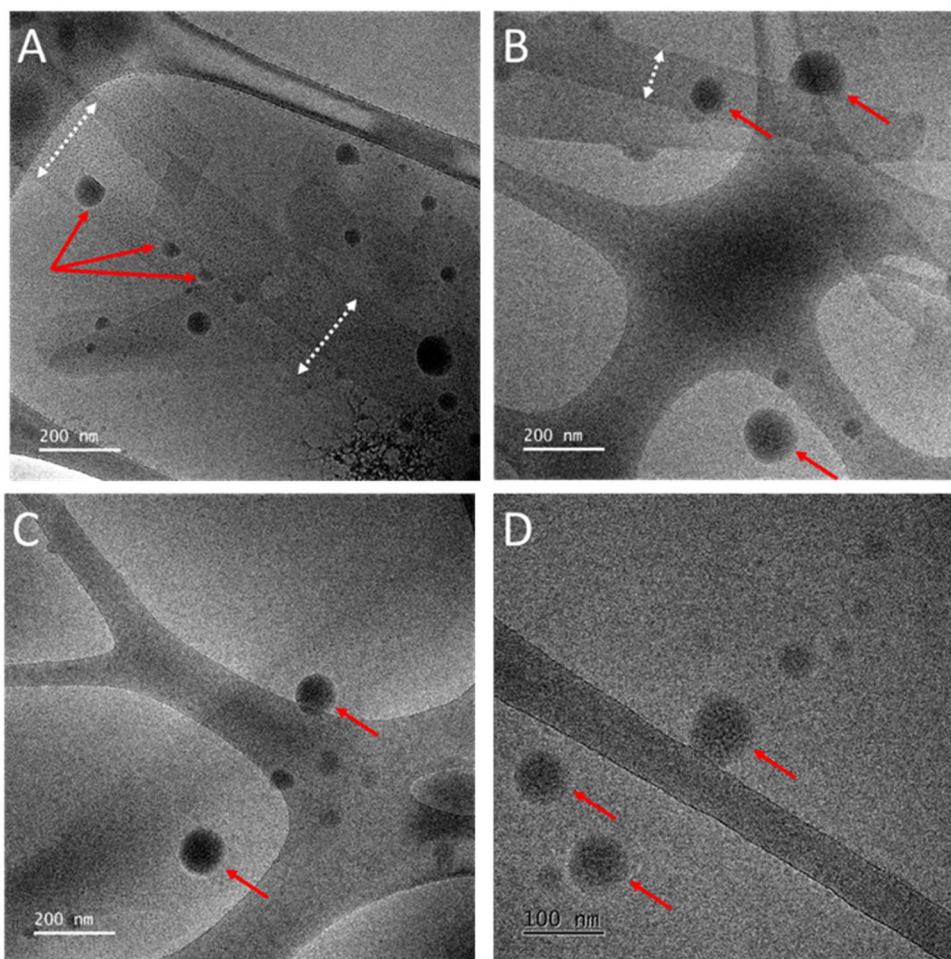


Figure 4-6 Representative cryo-TEM images of ascorbic acid loaded lipid nanoparticle formulation (images A-D). Scale bars are defined in each image.

DLS technique measured NLCs with mean particle size of 271.3 nm (Section 4.4.2), however, cryo-TEM did not show particles larger than 300 nm. Some deviation in particle size between these techniques is expected because DLS measures the hydrodynamic radius of the particles which generally gives larger particle sizes than TEM images.²⁵¹ The cream formulation, with the same dilution as NLC dispersion, was too thick to be analysed by cryo-TEM.

The identified NLCs showed internal structures (dark shaded spots) by the contrast in electron density within the particles, which is more clearly seen in Figure 4-6 image C. The use of blends of lipids in solid (i.e. hydrogenated coco glycerides) and liquid state (i.e. oleic acid) is reported to lead to the formation of one imperfect lipid matrix structure.^{252,253} However, the electron

density contrast observed within the particle would indicate a multiple type lipid matrix structure.

Vitrified water gives a light background in cryo-TEM. Hanson *et al.*²⁵⁴ reported a stabilised W/O/W emulsion to show a vitrified water region that was ~ 40% of the total nanoparticle area by cryo-TEM imaging. Herein, a vitrified water compartment within the particle, consistent with a double emulsion, was not observed within the nanoparticles. This could be because the inner aqueous phase is not a continuous region but made of multiple small regions²⁵⁵ (as illustrated in Figure 4-1) that could not be resolved in the cryo-TEM set-up used. Additionally, it was expected that some of the inner aqueous phase would partition out, with the dissolved ascorbic acid, to the outer aqueous phase during ultrasonication. The ascorbic acid DL was 3.86% (Table 4-2), so the inner aqueous compartment would make up only a small fraction of the nanoparticle. Negative staining techniques could be used to improve contrast between the lipid and aqueous phases of the emulsions.²⁵⁶

Unexpectedly thin sheet structures, of approximate width 100 nm, indicated by the white arrows in Figure 4-6 images A and B, and > 1 μm in length, were also identified in the cryo-TEM images. These structures are likely to contain surfactant because they have an electron density higher than vitrified water. Their presence is interesting due to the observation of aligned nanoparticles, as shown by the red arrows in Figure 4-6 A, in these sheet structures. It is not known if the structures could be an artefact of the blotting and freezing process.²⁵⁷ It is thought that high-pressure freezing could be used to avoid such artefacts, but that is outside the scope of this work.²⁵⁸

4.4.6 Rheological properties of lipid nanoparticle and cream formulations

The rheological properties of the NLC and cream formulation were measured at 32 °C to simulate their behaviour on skin. The cream formulation was found to have a higher structural strength than the lipid nanoparticle formulation as shown by the higher yield point, τ , in Figure 4-7. The measurement values also show that the storage and loss modulus of the cream are higher than the values

for the lipid nanoparticle formulation. The cream formulation thus requires more external force to flow on the skin than the lipid nanoparticle.

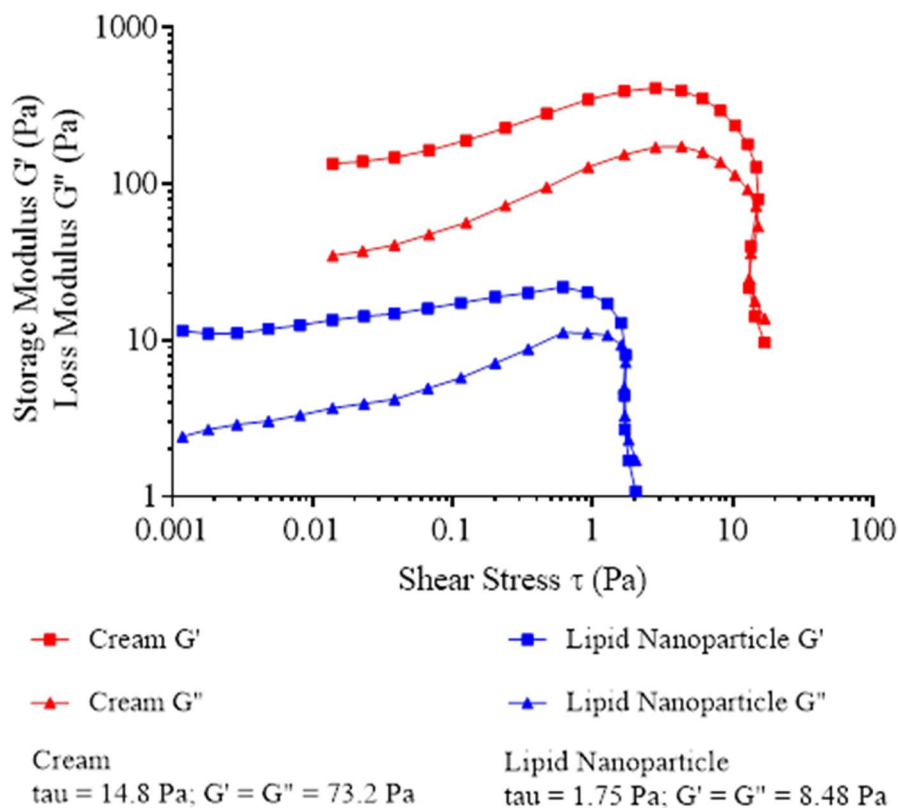


Figure 4-7 Oscillatory amplitude sweep versus the shear stress τ , of cream and lipid nanoparticle formulation performed at $\omega = 10 \text{ rad/s}$ and at $32 \text{ }^\circ\text{C}$.

Topical lotions/ creams show typical elastic behaviour such that they do not drip off but can still be rubbed into the skin.²⁵⁹ A cream is the most common skin formulation type due to its high consumer acceptability in terms of its skin feel, and also its texture when rubbed into the skin.¹²⁴ The lipid nanoparticle formulation, however, shows lower elastic behaviour meaning the product requires less external force to be rubbed into the skin but is more likely to drip compared to conventional skin creams/lotions; which may be considered less acceptable to the consumer.

Both the cream and lipid nanoparticle formulation showed shear-thinning behaviour, as shown in Figure 4-8. It is assumed that the formulation can be spread easier at a low viscosity value. The lipid nanoparticle formulation viscosity values were less than the cream during the whole measuring process. The difference in spreadability of the cream and lipid nanoparticle did not

converge or diverge with increasing shear stress. Therefore, for a given shear rate, the lipid nanoparticle is more spreadable and likely to achieve homogenous skin distribution quicker than the more viscous cream.

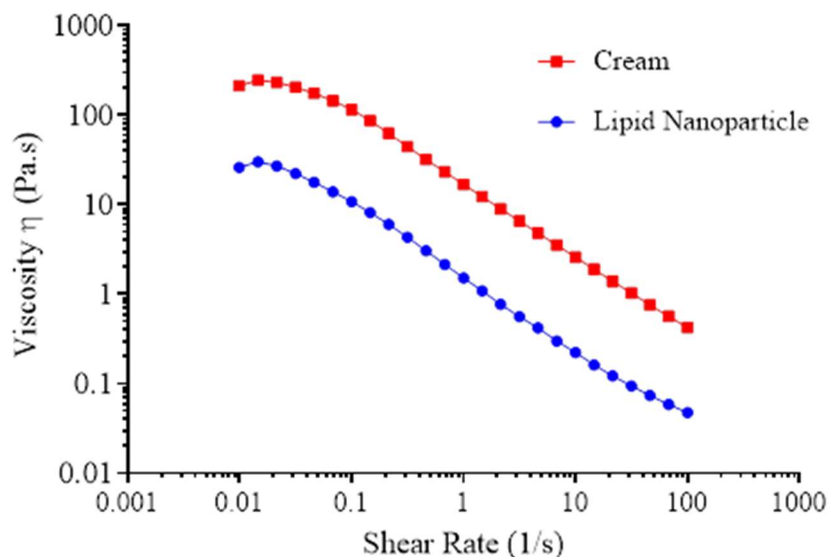


Figure 4-8 Shear-rate dependent viscosity curves of cream and lipid nanoparticle formulation at 32 °C.

It is expected that at low shear rates, a formulation with a small narrow particle size distribution would have a higher viscosity than a larger broad particle size distribution due to an increase in the number of interactions between particles. However, this could not be observed for the lipid nanoparticle vs cream formulation because particle-particle interaction is a relatively weak force. Moreover, the cream contained xanthan gum (0.5% w/w), an effective thickening agent, and explains why the cream had a higher viscosity. Strong xanthan gum-water interactions have been demonstrated to resist flow/spreading.²⁶⁰

4.4.7 Identifying secondary ions in ToF-SIMS spectra of the formulation that could be used to monitor skin permeation

The final characterisation step, for the NLC and cream formulations, was to assess if ascorbic acid could be detected by ToF-SIMS, with good sensitivity, in the formulations so that skin permeation could be monitored by ToF-SIMS. To aid identification of secondary ions which could be used to monitor the

permeation of ascorbic acid, as well as other excipient ingredients, the mass spectrum of the NLC formulation was made with and without ascorbic acid (water q.s.).

Ascorbic acid relevant secondary ions were determined by subtracting the ToF-SIMS spectrum of the NLC formulation made without ascorbic acid from the ToF-SIMS spectrum of the NLC formulation made with ascorbic acid. Excipient relevant secondary ions were identified by performing the subtraction in reverse. The top 10 secondary ion intensities, after performing the subtraction, are shown in Figure 4-9.

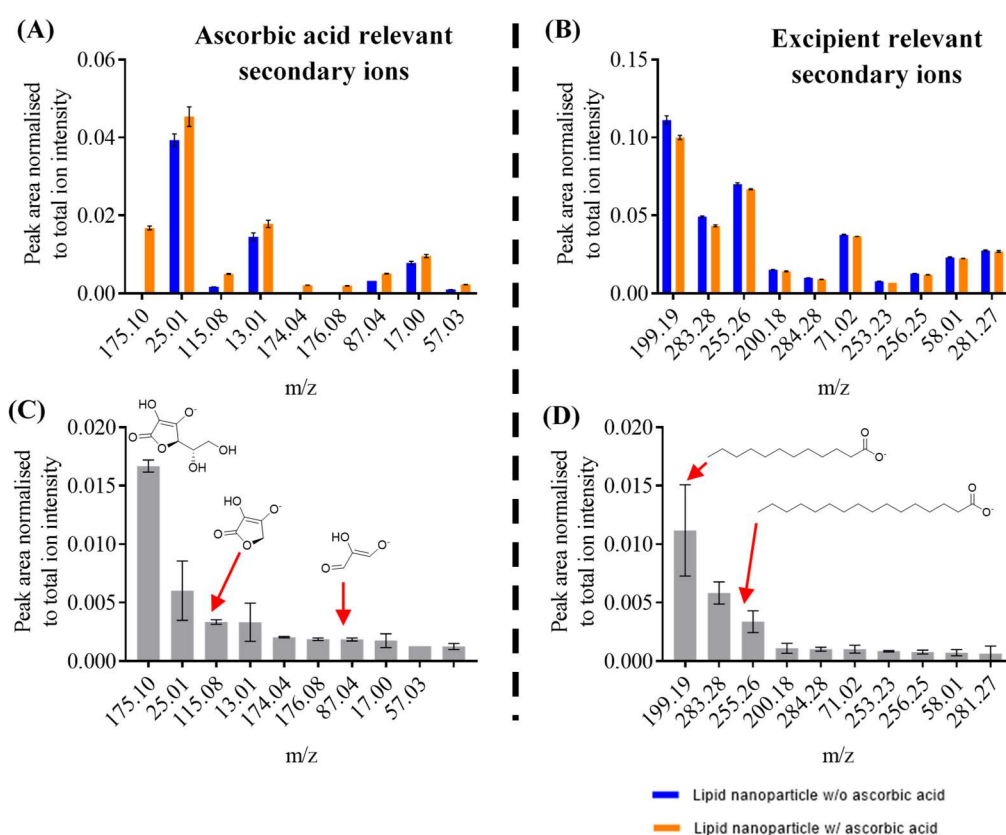


Figure 4-9 ToF-SIMS normalised ion intensities of lipid nanoparticle formulation made with and without ascorbic acid in negative polarity. Top 10 secondary ions diagnostic of ascorbic acid (A) and excipients (B). Diagnostic secondary ions are shown as a difference between the two spectra (C and D respectively). Data shown as mean \pm SD, n=6.

A series of secondary ions associated with ascorbic acid (m/z 175, 115 and 87) were found to be related to the fragmentation and ring-opening of that

molecule (Figure 4-9 C). Secondary ions least associated with ascorbic acid, and therefore diagnostic of other excipient ingredients were also identified (Figure 4-9 D). To confirm that these secondary ions were relevant to ascorbic acid, or excipient ingredients, the ToF-SIMS reference spectra of individual ingredients was recorded and overlaid, the spectra for which is shown in Figure 4-10.

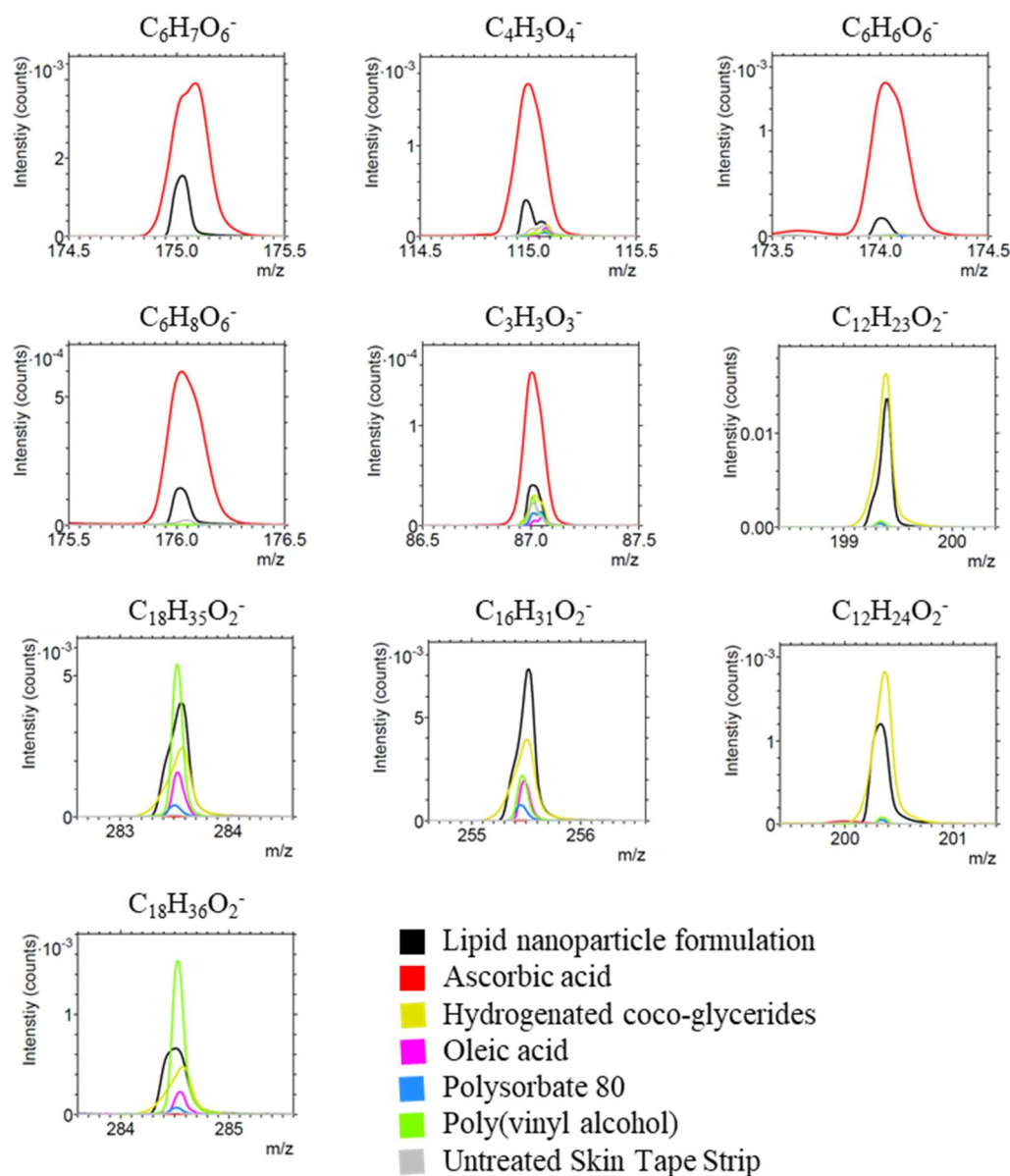


Figure 4-10 Overlay of ingredient ToF-SIMS spectra in negative polarity, normalised to total ion intensity.

In Figure 4-10, the secondary ion with an m/z of 175 ($C_6H_7O_6^-$) was most specific to ascorbic acid: it is the $[M-H]^-$ ascorbic acid molecular ion.

Other secondary ions with an m/z of 115, 174, 176 and 87 are also diagnostic of ascorbic acid, and could also be used to monitor ascorbic acid skin permeation, however, these peaks have reduced sensitivity (ion intensity) and reduced specificity (overlap with excipient ingredients).

In Figure 4-10, the secondary ion with an m/z of 199 ($C_{12}H_{23}O_2^-$) was most specific to the excipients in the lipid nanoparticle formulation. The lipid nanoparticle formulation (black line) shows good overlap with hydrogenated coco-glycerides (yellow line) which is the main excipient in the formulation. The ingredient, hydrogenated coco-glycerides, contains a mixture of saturated (C10-C18) fatty acids. Therefore, ion at m/z of 199, and also the ion at m/z of 255, can be presumed to be the $[M-H]^-$ of lauric acid (C12) and palmitic acid (C16) respectively. Other secondary ions with an m/z of 283, 255, 200 and 284 are also diagnostic of excipient ingredients, however, as before these ions will have a reduced sensitivity and specificity for monitoring excipient permeation.

A problem associated with ToF-SIMS is matrix-related effects which could suppress or enhance the signal of an analyte.²³⁴ Formulations with different compositions have different matrix ions and therefore can introduce matrix-related effects. Therefore, the matrix effect was evaluated by comparing the normalised ion intensities of m/z 175 (ascorbic acid diagnostic ion) and m/z 199 (excipient diagnostic ion), from the formulations as shown in Figure 4-11.

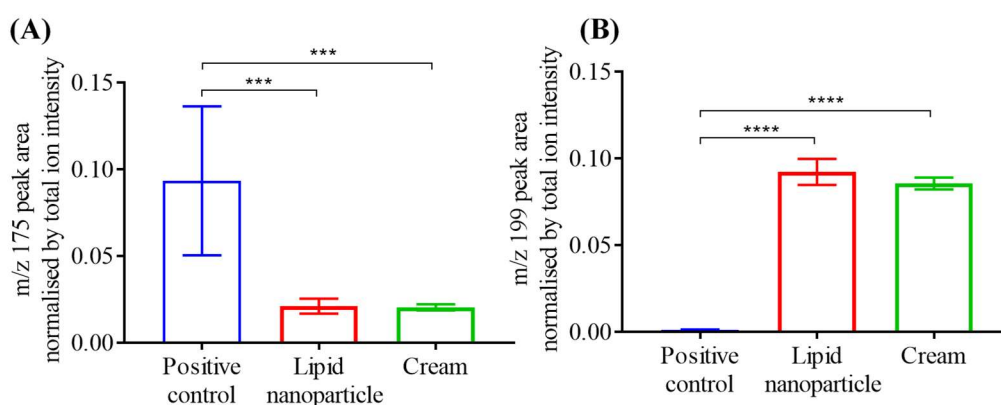


Figure 4-11 Normalised ion intensities of positive control, lipid nanoparticle and cream formulation measured on silicon wafer in negative polarity. Data shown as mean \pm SD, $n=6$.

The positive control was found to have a significantly larger ion intensity, for m/z 175, than the lipid nanoparticle and cream formulations (Figure 4-11 A). This is due to loss of water in the ToF-SIMS vacuum and the positive control does not contain any excipients, except preservatives, so a higher m/z 175 ion intensity was measured for the positive control. On the other hand, the positive control had a significantly smaller ion intensity, for m/z 199, than the lipid nanoparticle and cream formulations (Figure 4-11 B) since it does not contain hydrogenated coco-glycerides.

No significant difference between lipid nanoparticle and cream formulation, for m/z 175 ion intensity (Figure 4-11 A) and m/z 199 ion intensity (Figure 4-11 B) was found. This is because the composition of the nanoparticle and cream formulations are the same except for the xanthan gum (0.5% w/w) in the cream (Section 4.3.3). Therefore, no formulation associated matrix related effects are expected in the ToF-SIMS when comparing lipid nanoparticles with cream. A limitation associated with ToF-SIMS analysis was therefore minimised so direct comparison could be made between the nanoparticle and cream formulation.

4.5 Conclusions

A novel lipid nanoparticle containing formulation, not reported in previous studies, has been developed for ascorbic acid. The nanoparticle formulation does not contain excessive amounts of surfactant which could lead to skin irritation. The formulation had an appropriate particle size distribution which could lead to dense film formation on the skin surface according to the opinion of other scientists. In comparison with previous reported nanosized formulations, the nanoparticle formulation developed contains a high ascorbic acid content that would be considered to show anti-aging efficacy according to previous efficacy studies. The nanoparticle formulation was found to be more spreadable than a conventional cream formulation which is desirable for homogenous skin permeation.

The nanoparticle formulation has a composition and particle size that would not require additional safety assessment according to EC Regulation 1223/2009 on cosmetic products and therefore can be used readily in a clinical trial to assess *in vivo* human skin permeation. A comparator cream formulation was also developed that could be used to compare skin permeation against the nanoparticle formulation. In comparison to previous studies, the cream and nanoparticle formulation contain the exact same composition of lipids and surfactants therefore any differences in skin permeation would be a result of the physical properties of the formulation rather than additional chemical penetration enhancer effect. The nanoparticle formulation and cream formulation developed herein were extensively characterised and deemed suitable for topical use and could be applied to other hydrophilic cosmetic and topical pharmaceutical agents.

Chapter 5: *In vivo* and *ex vivo* assessment of ascorbic acid permeation amount and distribution in the *stratum corneum* from lipid nanoparticle formulation

5.1 Introduction

NLC formulations have been intensively investigated as topical formulation vehicles, since their small size achieves a close contact with the *stratum corneum*, forming a dense film on the skin surface, which increases both skin hydration and drug permeation, as described in Section 1.4.2.3. The majority of studies comparing lipid nanoparticle and cream formulations on *ex vivo*¹³³ and *in vivo*^{135,141} human skin, report improved permeation with lipid nanoparticle formulations whilst using more surfactant concentration than the cream formulation. In these studies, permeation enhancement is achieved via the physical properties of the formulation as well as the chemical penetration enhancer effect of the lipids and surfactants used in the formulation. To deconvolute between these effects, an ascorbic acid NLC formulation was developed alongside an ascorbic acid cream formulation, in Chapter 4, that contained the exact same composition of lipids and surfactants.

These formulations are intended for human use, so it is most appropriate and relevant to assess skin permeation on human skin *in vivo*. Tape stripping of the *stratum corneum* can be used to study skin permeation from topically applied formulations, and as it is minimally non-invasive can be performed on human volunteers (Section 1.2.4.1). Monitoring ascorbic acid skin permeation on human skin *in vivo* has not been previously reported (Section 1.5.3), despite its clinical relevance.

However, tape strip data should be analysed with caution since corneocytes on one tape strip may be derived from different *stratum corneum* depths because corneocytes are less well lifted in the furrows of the skin (Figure 1-7). Consequently, analysis of tape strips by extraction and chromatography method may overestimate the depth of permeation in instances where a compound is localised in the skin furrows but not penetrated the *stratum*

corneum barrier (Section 1.2.4.1). On the other hand, analysis of tape strip samples by ToF-SIMS allows the permeant distribution on the tape strips to be visualised (Section 1.3.3.3). So if the permeant is found localised within the furrows of the skin, the ions from these regions can be removed from the analysis retrospectively, as detailed in Figure 2-9, to obtain a more accurate permeation profile.

5.2 Chapter aims

The aim of this chapter is to compare the skin permeation of ascorbic acid from an NLC formulation and an O/W cream, into human skin *in vivo* and porcine skin *ex vivo*. This will be achieved using tape stripping. To allow a complete understanding of skin permeation, tape strip samples will be analysed both by ToF-SIMS, to visualise ascorbic acid distribution, and by extraction and HPLC analysis, to determine absolute ascorbic acid concentrations. This work therefore demonstrates the first reported correlation between HPLC and ToF-SIMS for tape strip *stratum corneum* samples. The TEWL, after application of the formulations to the skin, will also be evaluated to determine effects on skin hydration.

5.3 Materials and Methods

5.3.1 *Ex vivo* tape stripping test

Ex vivo skin permeation study was performed on intact porcine ear skin as described in Section 3.3.4, however the delineated skin test site area was increased to 2 cm × 2 cm, which is the same area as the Corneofix® tape strips. Porcine ear skin which remains on the underlying cartilage does not contract, its dehydration is decelerated, and its skin barrier is not interrupted, and therefore would be considered more suitable tape stripping than excised porcine skin.²⁶¹ In chapter 3, no significant difference was found between intact porcine skin and excised porcine skin mounted in Franz cell, which suggests the dermis is sufficient to provide sink conditions for ascorbic acid.

The test formulations (Table 5-1), prepared as detailed in Sections 4.3.2 and 4.3.3, were accurately applied to each skin test area by weight. The formulations were spread uniformly across the test site by means of a gloved finger resulting in an applied dose equivalent to 10-12.5 mg/cm².

Table 5-1 Composition of test formulations (% w/w). The positive control, lipid nanoparticle and cream formulations had their pH adjusted to 3.0-3.2.

		Negative Control	Positive Control	Lipid nanoparticle	Cream
	Ascorbic acid	0	5	5	5
Oil Phase	Witepsol® E85	0	0	10	10
	Oleic acid	0	0	2.5	2.5
Water Phase	Polysorbate 80	0	0	5.4	5.4
	Poly(vinyl alcohol)	0	0	0.6	0.6
	Xanthan gum	0	0	0	0.5
	Euxyl® PE 9010	0	1	1	1
	Type II Water	100	94	75.5	75

The skin was left undisturbed for 4h. The application of the formulation to the skin test sites was staggered so that tape stripping could commence immediately after the 4 hr permeation time. After this period, the skin test site was wiped using a sponge (polyurethane, $\sim 1 \text{ cm}^3$) to remove excess formulation remaining on the skin. Tape stripping was performed exactly as described in Section 2.3.5, taking up to 30 consecutive tape strip layers.

5.3.2 *In vivo* tape stripping test

In vivo skin permeation study was performed on human volunteers with healthy skin. All subjects gave their informed written consent for inclusion (Appendix II) before they participated in the study. The clinical trial was conducted according to the guidelines for Good Clinical Practice and the Declaration of Helsinki.⁵² The clinical trial was approved by the Inovapotek's Ethics Committee for Health (PPF7A17, November 2017) and registered with the Portuguese registry for clinical studies - Registo Nacional Estudos Clínicos (RNEC No. 8621, INFARMED, I.P.). Data collection from the clinical trial was also authorised by the Portuguese data protection authority (CNPD Authorisation No, 8686/2017).

11 female subjects (Fitzpatrick type I-IV, age 27.0 ± 5.4 (Mean \pm SD)) completed the study as per the approved protocol. The main inclusion criteria for the study was that participants should not have applied any product in the prior 24 hours and that the test regions were free from cutaneous alterations. Only female subjects were recruited for the study to minimise variability and easier recruitment from a female majority database.

Participants were rested (20 min) for acclimatization ($23.0 \pm 1.0 \text{ }^\circ\text{C}$; $50 \pm 10\%$ RH), with their forearms uncovered, prior to the experiments. Four test sites ($2 \text{ cm} \times 2 \text{ cm}$) were defined across the volar forearms using a plastic template/adhesive. The formulation was applied and rubbed into the skin exactly as specified for the *ex vivo* test (Section 5.3.1), and the skin left undisturbed for 1 hr. After this time, excess formulation was removed with a sponge and 15 sequential tape strip layers taken. The whole *stratum corneum* was not removed by tape stripping, as previous studies suggest 30 – 70 tape

strip layers need to be taken. This can be an additional strain on the volunteers and the process may require supervision from a medical practitioner.²⁶²

The study was single blinded with randomisation of the order and site of formulation application on the forearms. The application of the formulation to the skin test sites was staggered so that tape stripping could commence immediately after the 1 hr permeation time. Study participants were held in a room with controlled temperature and humidity (23.0 ± 1.0 °C; $50 \pm 10\%$ RH) for the duration of the study and instructed not to touch the skin test sites. Longer study durations, for example 4 hours as performed with porcine skin *ex vivo*, would have required the skin to be covered to avoid contact with the skin test site, however, this could affect the dehydration of the formulation.

TEWL measurements were taken from the skin sites before application of formulation (baseline), 1h after formulation application and after removal of 15 tape strip layers using a Tewameter® (TM 300, Courage-Khazaka, Germany). The Tewameter® is an open chamber device so it is essential to maintain a controlled temperature and humidity environment to accurately determine TEWL. All subjects had baseline TEWL < 10 g/h/m² indicating healthy skin barrier function.⁵⁰

No adverse effects to the formulations were observed after single application to the skin of the volunteers.

5.3.3 Analysis of tape strip samples

Tape strip samples were analysed for their protein content by infrared densitometry, their ascorbic acid distribution by ToF-SIMS, and their ascorbic acid content by extraction and quantification by HPLC as detailed in Sections 2.3.10.2, 2.3.8 and 2.3.7 respectively. Determination of protein content on tape strips was performed on the same day as the permeation study and tapes stored at -20 °C before subsequent ToF-SIMS and HPLC analysis. Tape strips from 4 subjects were selected for ToF-SIMS analysis, prior to HPLC analysis, at random. Tape strips analysed by ToF-SIMS were kept in high vacuum conditions for a maximum of 4 hours before being extracted for HPLC. Each tape strip sample was extracted into solution in individual Eppendorf tubes.

For HPLC, human tape strip extractions were injected individually but porcine tape strip extractions were pooled (tape strip numbers 1-2, 3-5, 6-10, 11-15, 16-20, 21-25, 26-30) to minimise instrument run-times.

5.3.4 Statistics

Statistical analysis was performed as detailed in Section 2.3.11.

5.4 Results and Discussion

5.4.1 Depth of *stratum corneum* removed by tape stripping

Tape stripping of the *stratum corneum* removes variable amounts of corneocytes so it is important to normalise to protein content of corneocytes lifted on each tape strip (Section 2.4.5). Residual formulation on the skin surface, particularly lipophilic excipients, can impair the tackiness of the tapes and affect the removal of *stratum corneum* corneocytes.²⁶³ In this work, the skin was wiped with sponge to remove excess formulation, and so a repeatable amount of corneocytes could be removed across the skin test sites. The skin was not cleaned with detergent or solvents as that may influence the drug concentration obtained with the first adhesive tapes.²⁶⁴

On *ex vivo* porcine skin, the positive control formulation was found to significantly reduce the amount of corneocytes picked up by the tape strips (Figure 5-1 A). This is because ascorbic acid had crystallised on the skin surface and could not be easily wiped off the porcine skin by sponge. Crystallised ascorbic acid decreased the tackiness of the tapes and their ability to lift corneocytes.

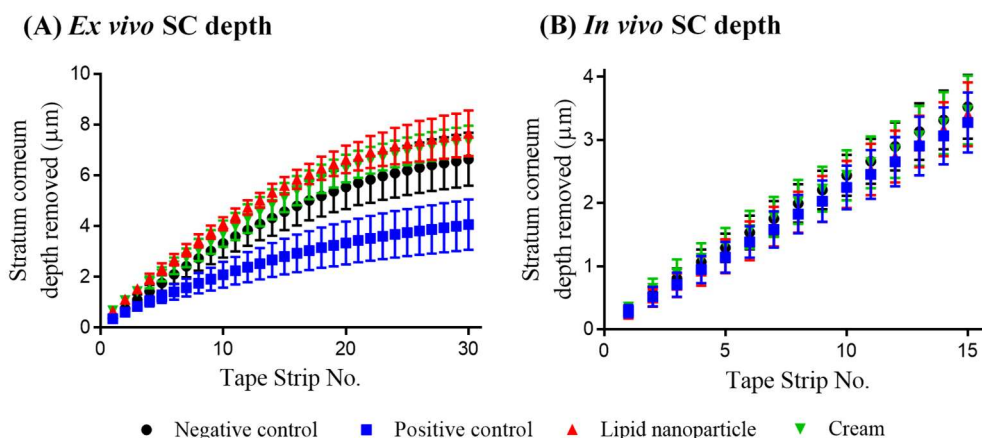


Figure 5-1 Depth of the stratum corneum (SC) reached after removal of 30 sequential tape strips on *ex vivo* porcine skin (A) and after removal of 15 sequential tape strips on *in vivo* human skin (B). Mean \pm SD, *ex vivo* $n=6$ and *in vivo* $n=11$.

In contrast on *in vivo* human skin, the formulation was found not to influence corneocyte removal (Figure 5-1 B). Human skin is known to have less deep and wide skin furrows than porcine skin which aided the removal of excess formulation.⁶⁰

Well-established reference values for *stratum corneum* thickness are 8.2 μm for porcine ear skin and 11.0 μm for human volar forearm.²⁶⁴ Thus $\sim 90\%$ and $\sim 35\%$ of the *stratum corneum* was removed in *ex vivo* porcine skin and *in vivo* human skin respectively.

5.4.2 Amount of formulation topically applied

Rubbing the formulation into the skin with a gloved finger is reported to deliver significantly higher amount of drug into the skin compared to not rubbing.⁷⁰ The products were therefore rubbed into the skin test sites, in a controlled manner, by gloved finger to closely mimic real-life application conditions. It was more difficult to apply a consistent amount of cream to the skin test site area (Figure 5-2 A and B) compared to the other formulations. The large variability in amount applied is due to the high viscosity of the cream (Section 4.4.6). This high variability is not ideal for the delivery of a consistent amount of active ingredient day to day. There was no significant difference in the amount of product applied either *ex vivo* (Figure 5-2 A) or *in vivo* (Figure 5-2 B) so the amount applied can be assumed to have no effect on permeation behaviour.

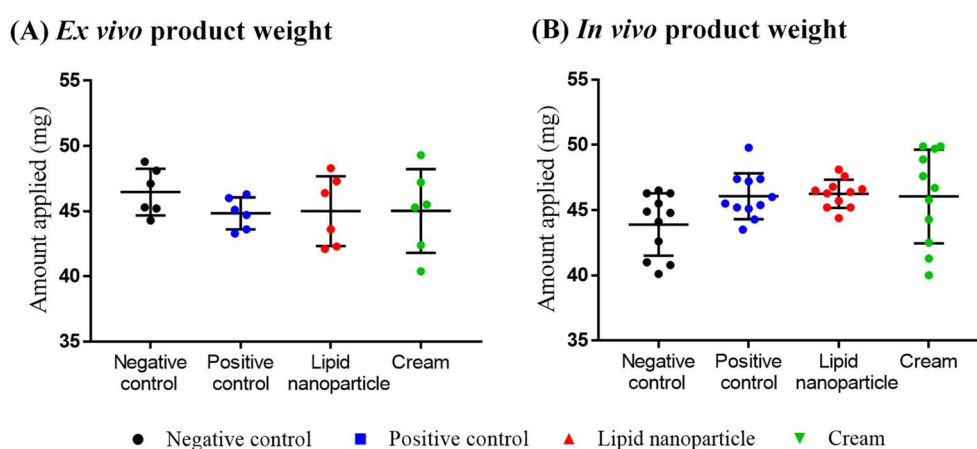


Figure 5-2 Weight of formulation applied to skin test sites *ex vivo* (C) and *in vivo* (D). Mean \pm SD, *ex vivo* $n=6$ and *in vivo* $n=11$.

The amount of formulation applied was 10-12.5 mg/cm². This was considered a finite dose because the formulation had evaporated and dried on the skin surface therefore mimicking in-use conditions. The dose applied is more than typical cosmetic usage (1-5 mg/cm²)^{35,36} but less than what consumers apply, when undirected, for sunscreen (20 mg/cm²).⁶⁷ The amount applied can therefore be considered representative of in-use conditions. Application of a large finite dose can also be justified, by OECD Guidance Notes on Dermal Absorption No. 156³², if there are limitations regarding the sensitivity of the analytical method employed. In the end, only a small percentage (1.8%) of all the tape strips that were collected from positive control treated skin were below the HPLC LOQ. None of the tape strips from NLC and cream treated skin were below HPLC LOQ.

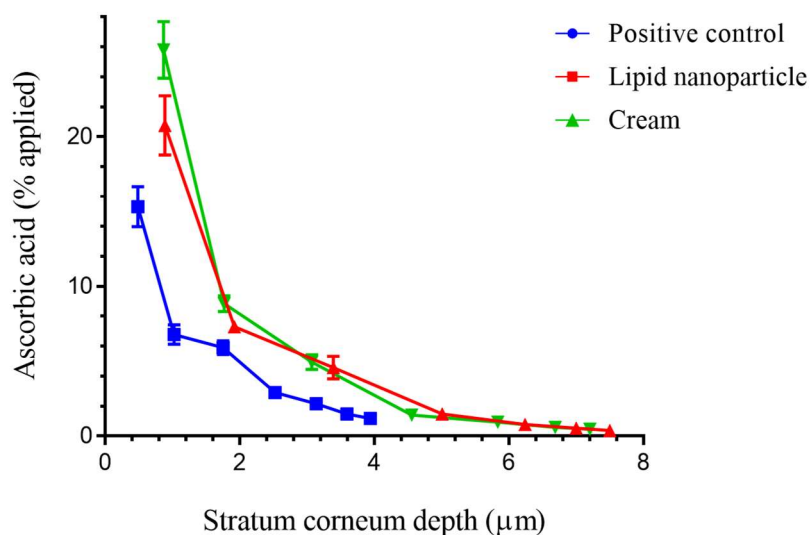
5.4.3 Amount of ascorbic acid skin permeation

Ascorbic acid *stratum corneum* permeation profile was determined by extraction of tape strips in solution and absolute quantification by HPLC. It was found that both the lipid nanoparticle and cream significantly enhanced the permeation of ascorbic acid into porcine *stratum corneum ex vivo* (Figure 5-3 A) and human *stratum corneum in vivo* (Figure 5-3 B) compared to positive control. This could be attributed to the chemical penetration enhancer effect of the lipids and surfactants in the nanoparticle and cream formulations.

The cream formulation was found to deliver the most ascorbic acid into human skin, however, in porcine skin the cream did not deliver more ascorbic acid compared to the lipid nanoparticle formulation. There are a few reasons why the *ex vivo* porcine permeation data does not fully agree with the *in vivo* human permeation data. Firstly, the *ex vivo* permeation experiment was 4 hrs, longer than the *in vivo* experiment. Secondly, *ex vivo* porcine skin is found to have a lower skin barrier function compared to *in vivo* human skin,²⁶⁵ despite previous studies which have shown *ex vivo* porcine ear skin to be a suitable substitute for human skin.^{264,266,267} Thirdly, porcine skin is reported to have larger skin furrows than human skin which can affect how the formulation interacts with the *stratum corneum* barrier.⁶⁰ Fourthly, the porcine permeation profile

contains less data points, as tape strip extractions were pooled for HPLC injection, so the permeation profile is less precise than the human data.

(A) *Ex vivo*, Porcine, 4 hrs



(B) *In vivo*, Human, 1 hr

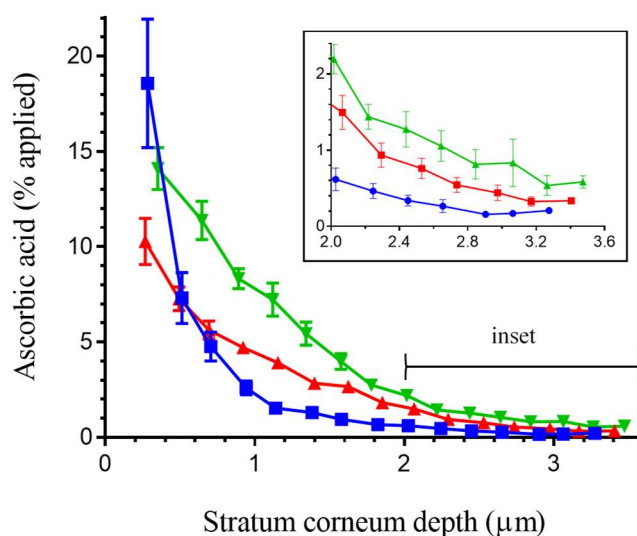


Figure 5-3 Ascorbic acid stratum corneum permeation profile in *ex vivo* porcine skin (A) and *in vivo* human skin (B). Mean \pm SD, *ex vivo* $n=6$ and *in vivo* $n=11$.

It is thought that the longer permeation time is not responsible for different permeation profiles *ex vivo* and *in vivo*, as within 1 hour the formulations were observed to dry on the skin surface. Klang *et al.*²⁶⁴ performed *ex vivo* porcine skin permeation experiments for 1 hour and 4 hours, and reported no significant differences in penetration depth and amount with increased

permeation time. This was explained by the further dehydration of the formulation, and crystallisation of the drug on the skin surface at 4 hrs, so it is no longer available for penetration. The larger skin furrows in porcine skin could be responsible for the different permeation observed however because tape strip samples were extracted there is a loss of spatial information.

When analysing tape strip data, often the first two tape strips are discarded/ not included in the analysis because they remove superficial/loose corneocytes therefore the active ingredient is not considered to have properly entered the *stratum corneum*.^{268,269}

The human skin *in vivo* tape strip data can be analysed either by taking the area under the curve or the sum of tape strips 3 through to 15 (Figure 5-4). The area under the curve method considers different *stratum corneum* depths between subjects and between skin test sites due to the variability in tape stripping however the units obtained ($\mu\text{m}\cdot\%$ applied) are difficult to understand.²⁷⁰⁻²⁷² In contrast the sum of tape strips method results in easier to understand units ($\%$ applied) and because no significant difference in corneocyte removal was found, its use can be justified however it does not consider the different *stratum corneum* depths.^{264,273,274} The concentration of ascorbic acid is reported as $\%$ applied to take account of the variability in product weight applied (Section 5.4.2).

When the statistical analysis was performed, there was no large difference between the methods (Figure 5-4). The cream formulation delivered significantly more ascorbic acid into the human *stratum corneum* than the lipid nanoparticle formulation, which in turn delivered significantly more than the positive control. The area under the curve method (method 2) is the preferred approach since it takes into account differences in *stratum corneum* depth.

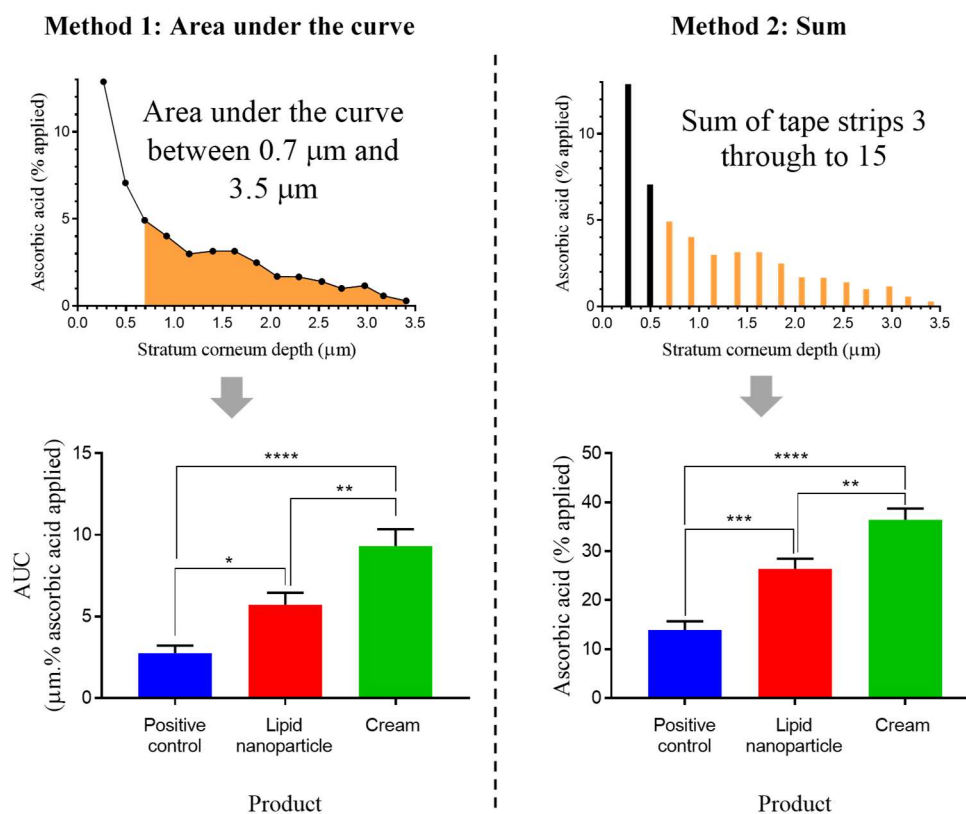


Figure 5-4 Statistical analysis of *in vivo* human stratum corneum ascorbic acid permeation by taking the area under the curve (method 1) or the sum of tape strips 3 through to 15 (method 2). Mean \pm SD, $n=11$.

Each subject had all four formulations applied to their skin, so permeation differences within individuals should be taken into consideration. In 82% of subjects, the cream delivered more ascorbic acid than the lipid nanoparticle (Table 5-2). The cream delivered on average 120% more ascorbic acid into the *stratum corneum* than lipid nanoparticle formulation, with the maximum increase of 477% observed in one subject.

It is difficult to make comparisons with previous ascorbic acid skin permeation studies as they have applied large infinite dose of formulation to the skin (Section 1.5.3). Large volumes of formulation could have an occlusive effect on the skin that would not be representative of the *in vivo* situation.⁶² However, Darr *et al.*¹⁵⁸ found 8.2% of the applied ascorbic acid in porcine skin 48 hrs after finite dose application of a gel formulation. This would appear to be comparable with the positive control solution in this work. Hakozaiki *et al.*²⁷⁵ studied AG permeation from a hydrogel formulation and after 10 minutes, ~

4% of the applied AG was present in the tape strip samples from human skin *in vivo*. AG is a more hydrophilic derivative of ascorbic acid and could explain why its permeation was less than the amount of ascorbic acid permeated from positive control in this work. Both lipid nanoparticle and cream formulation have enhanced permeation of ascorbic acid compared to the aforementioned studies.

Table 5-2 Comparison of test formulations for their delivery of ascorbic acid into human stratum corneum by taking the area under the curve from 0.7 to 3.5 μm (units of $\mu\text{m}\cdot\%$ ascorbic acid applied). ^aComparison with positive control and ^bcomparison with lipid nanoparticle. AA = ascorbic acid.

	Positive control	Lipid nanoparticle ^a	Cream ^a	Cream ^b
Mean values ($\mu\text{m}\cdot\%$ applied)	2.76	5.72	9.32	9.32
SEM	0.46	0.74	1.04	1.04
Mean differences ($\mu\text{m}\cdot\%$ applied)		2.96	6.56	3.60
SEM		0.97	1.01	1.61
Mean differences (%)		205.45	313.73	119.82
SEM		89.01	68.91	53.93
Number of subjects with AA permeation increase		9	11	9
Number of subjects with AA permeation increase (%)		81.82	100	81.82
Maximum increase (%)		823.18	781.83	476.64
Mean increase of the subjects who presented positive effects (%)		205.45	313.73	157.69
p value		0.0319	<0.0001	0.0078

Differences in ascorbic acid permeation from cream and lipid nanoparticle formulation can be attributed to physical properties of the formulation since they are expected to have the same chemical penetration enhancer effects. Similarly Klang *et al.*²⁶⁴ compared permeation of a nanoemulsion with a macroemulsion, with the exact same composition of ingredients and reported no statistically significant differences in the human skin *in vivo* permeation profile, despite the marked difference in particle size and rheological properties. This contradicts the findings here where a significant difference was observed. A key difference is in Klang's study,²⁶⁴ the drug investigated was curcumin (logP ~ 3.0) which is hydrophobic. Although the encapsulation efficiency of curcumin was not reported, it is predicted that a large percentage of the curcumin in the formulation would be in the inner oil phase of the emulsions; in contrast to the ascorbic acid formulation here which had low encapsulation efficiency (Section 4.4.3). Therefore, skin permeation of curcumin is limited by its partitioning from the inner oil phase to the outer water phase before it can enter the *stratum corneum*.

The amount of ascorbic acid removed from the initial sponge wipe and two tapes was also determined (Figure 5-5 A). There was no significant difference in the amount of ascorbic acid removed from these samples so it can be assumed not to have an effect on the permeation profiles. The unrecovered amount of ascorbic acid was back-calculated (Figure 5-5 B). It can be seen that a significantly less amount of the ascorbic acid was recovered from the positive control. This could be due to spreading of the positive control solution into the surrounding skin area despite the skin test site being delineated with a non-absorbent adhesive template.

Jacobi *et al.*²⁷⁶ and Pelchrzim *et al.*²⁷⁷ both reported lateral diffusion of topically applied drugs, from (viscous) cream formulations, beyond the delineated skin test site by tape strip sampling of adjacent skin. The distribution of the drug was measured on the skin surface and by tape stripping which confirmed that spreading of the drug takes place predominantly along the skin surface. Lateral permeation is an important consideration for cosmetic formulations. For example, when ascorbic acid is used to treat

hyperpigmentation, lateral permeation beyond the treated site would be undesirable.

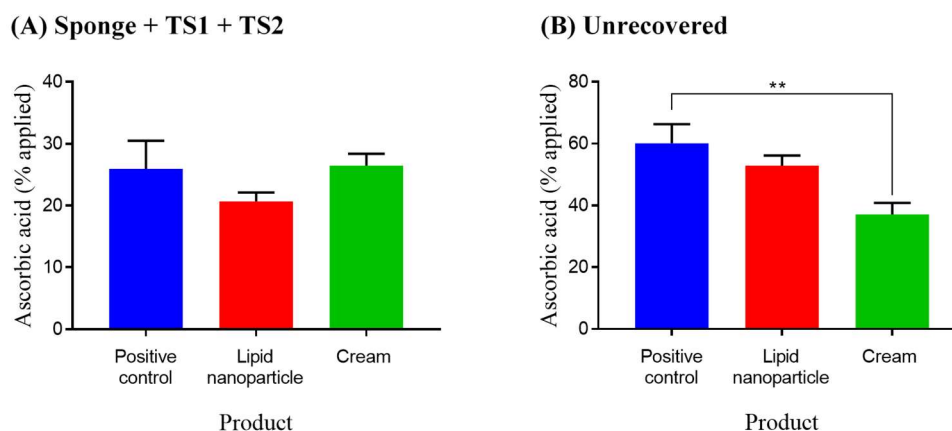


Figure 5-5 Ascorbic acid recovered in sponge wipe and superficial tapes (A) and unrecovered ascorbic acid (B). Mean \pm SD, $n=11$.

It is likely a fraction of the ascorbic acid will have permeated beyond the 15th tape strip layer. Indeed the OECD guidelines on dermal absorption tests recommend mass balance (full recovery) experiments for *in vitro*³⁴ and *in vivo*⁶⁸ experiments however this would require collection of a skin biopsy (Section 1.2.4.3) which volunteers are less willing to agree to.

5.4.4 Distribution and localisation of ascorbic acid in the *stratum corneum*

In Section 4.4.7, secondary ions diagnostic of ascorbic acid and excipients were identified that could be used to track their permeation by ToF-SIMS. Ascorbic acid permeation profile was ascertained by monitoring the ascorbic acid molecular ion (Figure 5-6 A) and the sum of four ascorbic acid associated secondary ions (Figure 5-6 B). In agreement with HPLC, ToF-SIMS showed both the lipid nanoparticle and cream permeation profiles were higher than the positive control in the human *stratum corneum*. However, contrary to HPLC method, the cream permeation profile was no longer higher than the lipid nanoparticle permeation profile. This observation cannot be due to matrix related effects, since no significant difference was observed in secondary ion

(m/z 175) intensity between the lipid nanoparticle and cream formulation (Figure 4-11).

Meanwhile excipient permeation profile was ascertained by monitoring the lauric acid molecular ion (Figure 5-6 C) and the sum of five excipient associated secondary ions (Figure 5-6 D). The positive control did not show increased ion intensity compared to negative control, confirming that these secondary ions are not diagnostic of ascorbic acid but excipients only. The lipid nanoparticle showed higher excipient permeation profile than the cream in the human *stratum corneum*, suggesting improved excipient permeation.

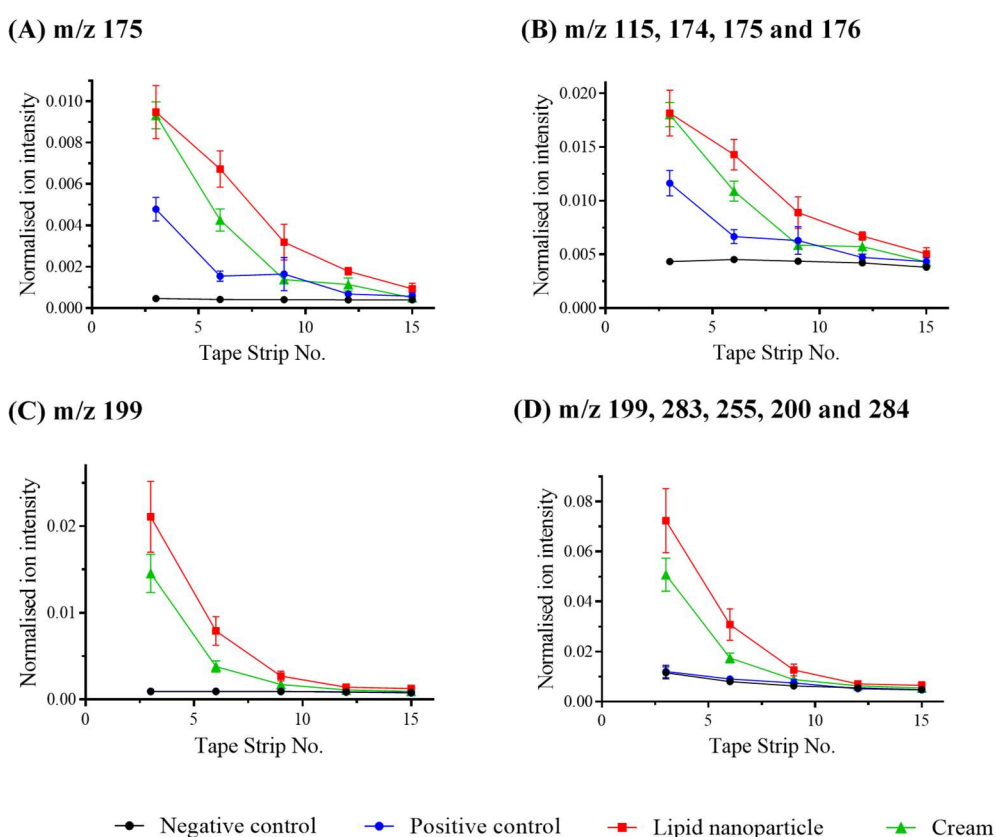


Figure 5-6 Normalised intensity of ascorbic acid $[M-H]^-$ ion (A), sum of ascorbic acid associated ions (B), lauric acid $[M-H]^-$ ion (C) and sum of excipient associated ions (D) with increasing tape strip depth. Mean \pm SEM, $n=4$.

It was noticed that monitoring permeation with a sum of ascorbic acid related ions did not improve measurement sensitivity compared to following ascorbic acid molecular ion alone. Despite the higher ion intensity when taking the sum

of several peaks, the negative control tape strips also showed elevated ion intensity, which suggests that these other ions (m/z 115, 174 and 176) are not as specific to ascorbic acid. Consequently, the permeation of ascorbic acid was monitored using the molecular ion at m/z 175 only. A similar observation was also made for the excipient ions, so the permeation of excipient was monitored using the molecular ion at m/z 199 only.

The main advantage of ToF-SIMS analysis is that the spatial distribution of ascorbic acid, and excipient, in the tape strip samples can be identified. ToF-SIMS analysis of porcine skin tape strips reveal ascorbic acid and excipient distribution to be non-uniform and mainly located in the skin furrows as shown in Figure 5-7. The skin furrows are the black intersecting lines which appear in the field of view, indicating an absence of corneocyte material. The complete set of 24 porcine tape strip ToF-SIMS ion images can be found in the Appendix I Figure A-7. The positive control treated skin tape strips show a strong ascorbic acid signal compared to the lipid nanoparticle and cream tape strips which could be due to improved ionisation of ascorbic acid in the absence of excipient molecules (Figure 4-11).

Ascorbic acid localised in the skin furrows would not be considered to have penetrated the *stratum corneum*, more so if it has crystallised on the skin surface. Previous ToF-SIMS studies on tape strip samples have not shown furrow localisation of active ingredients. Judd *et al.*¹⁰³ and Holmes *et al.*¹¹⁰ both report a non-uniform permeation distribution of chlorhexidine but generally co-localised with corneocyte material on porcine tape strip samples. The authors conducted their experiments for 24 hrs with large infinite dose ($\sim 390 \mu\text{L}/\text{cm}^2$) of formulation which increases skin hydration and skin permeability.^{64,65} Hydration of the *stratum corneum* is also associated with a decrease in the mean depth and spacing of furrows.²⁷⁸ This may explain why Judd *et al.*¹⁰³ and Holmes *et al.*¹¹⁰ did not observe drug localisation in the furrows of the skin.

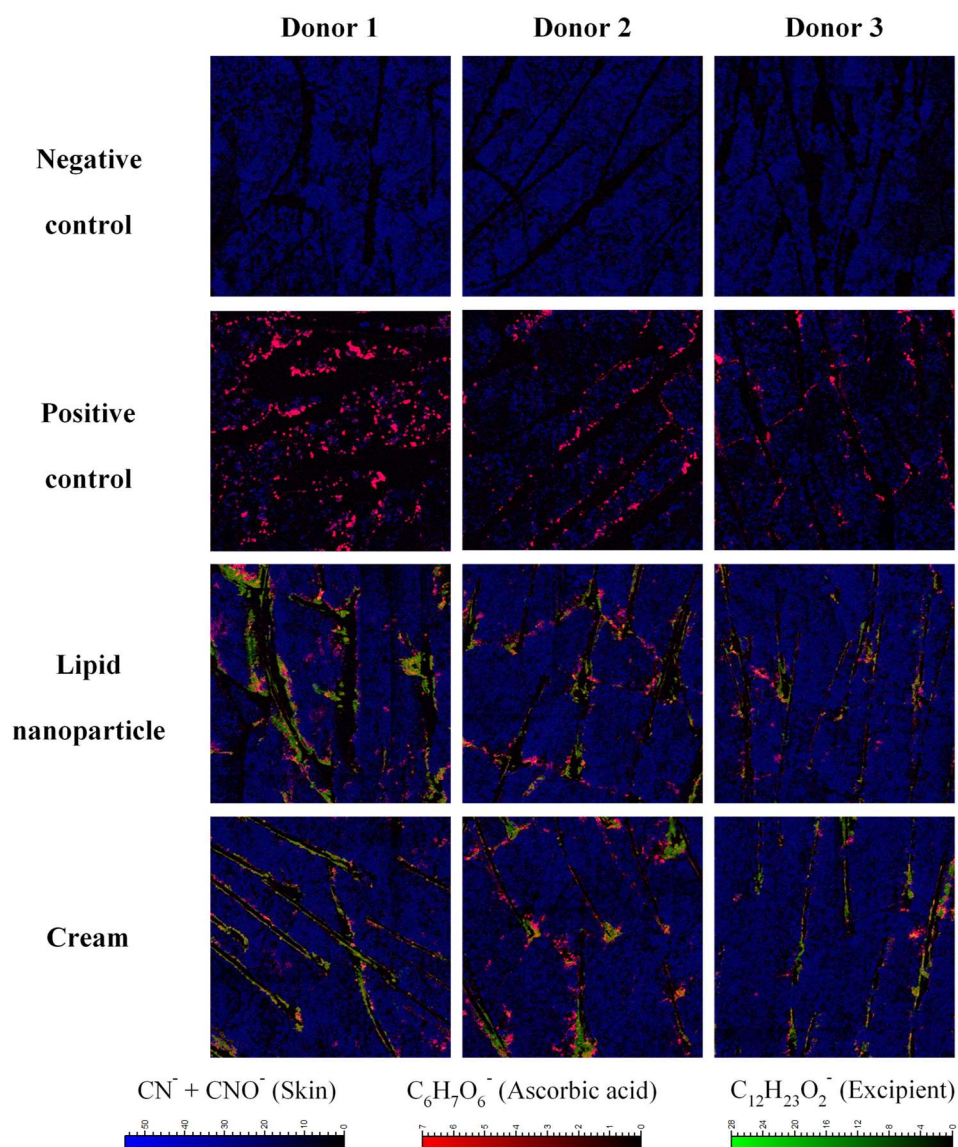


Figure 5-7 ToF-SIMS ion images of porcine tape strips collected at a SC depth of approximately 3.2 μm highlighting the distribution of corneocyte material ($CN^+ + CNO^-$, blue), ascorbic acid ($C_6H_7O_6^-$, red) and excipient ($C_{12}H_{23}O_2^-$, green) from test formulations. Field of view = $4 \times 4\text{mm}$.

ToF-SIMS analysis of human skin tape strips, presented in Figure 5-8, also show non-uniform ascorbic acid and excipient distribution with localisation in the skin furrows, as observed with porcine skin tape strips. Tape strips from positive control treated skin show ascorbic acid (red) to be mainly located in the skin furrows except for subject 1, where the distribution is all over the tape strip. This may be because subject 1's skin is more permeable than the others. Tape strips from lipid nanoparticle treated skin again show localisation of

ascorbic acid in the skin furrows but it can also now be observed the lateral movement of ascorbic acid into surrounding corneocyte cells (subjects 1 and 2) which was not observed in the positive control treated skin. Shown in green is the distribution of the excipients and where it is co-localised with ascorbic acid it appears yellow. The tape strips from cream treated skin show localisation of ascorbic acid in the furrows of the skin also, but less lateral spreading into surrounding corneocytes compared to the nanoparticle formulation.

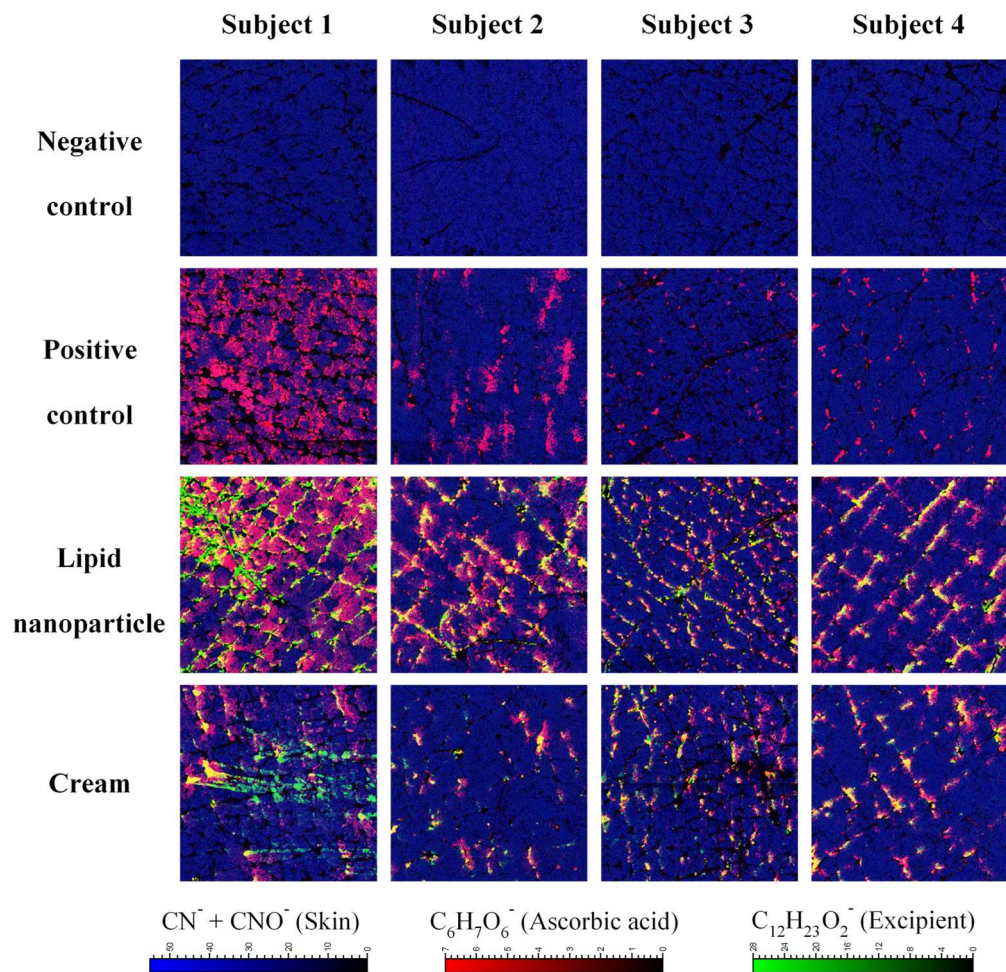


Figure 5-8 ToF-SIMS ion images of human tape strips collected at a SC depth of approximately 2.1 μm highlighting the distribution of corneocyte material ($\text{CN}^- + \text{CNO}^-$, blue), ascorbic acid ($\text{C}_6\text{H}_7\text{O}_6^-$, red) and excipient ($\text{C}_{12}\text{H}_{23}\text{O}_2^-$, green) from test formulations. Field of view = $4 \times 4 \text{ mm}^2$.

Inclusion of ascorbic acid in the skin furrows could lead to an overestimation of its permeation profile. Therefore, the ToF-SIMS data was retrospectively

thresholded to remove ions that were not co-localised with corneocyte material (i.e. in furrows), as explained in Figure 2-9, and shown in Figure 5-9.

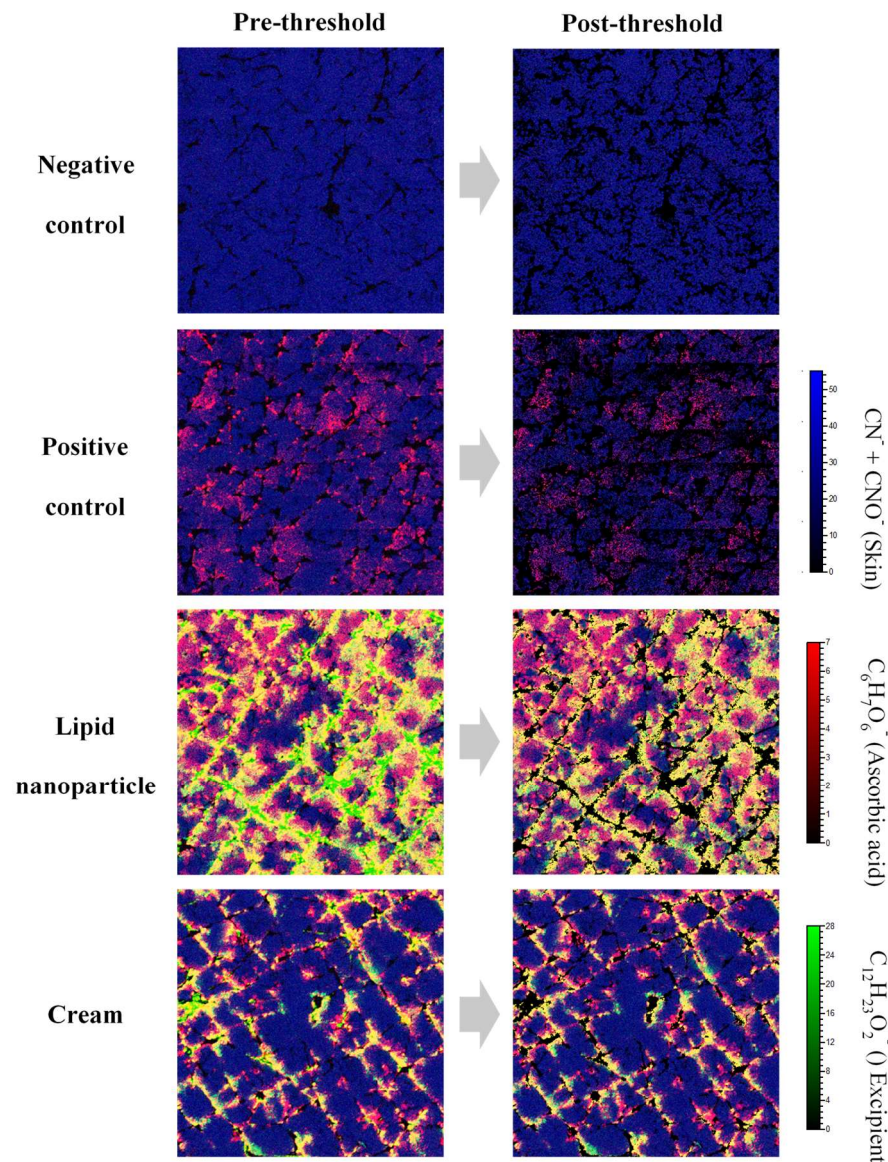


Figure 5-9 ToF-SIMS ion images pre and post thresholding to select corneocyte containing areas on tape strips collected at a SC depth of approximately 1.5 μm from one human subject. Distribution of corneocyte material ($\text{CN}^- + \text{CNO}^-$, blue), ascorbic acid ($\text{C}_6\text{H}_7\text{O}_6^-$, red) and excipient ($\text{C}_{12}\text{H}_{23}\text{O}_2^-$, green). Field of view = $4 \times 4 \text{ mm}^2$.

Thresholding could not be achieved objectively due to the different coverage of corneocytes from one tape strip sample to another so the same threshold limit (CN^- and CNO^- ion intensity) across the tape strips would not be

appropriate. Therefore, thresholding was achieved subjectively aiming for a similar post-threshold ion image where clusters of corneocyte cells remain visually intact. This can be illustrated by comparing the appearance of a post-threshold ion image (Figure 2-9 F) with an optical image of a tape strip (Figure 2-18). An alternative approach to analysing the ToF-SIMS data would be normalising the permeant signal to the signal of the skin marker directly however the resulting signal would be dependent on corneocyte coverage on the tape strip and independent of corneocyte co-localisation so was avoided.

What is particularly interesting is that whilst the HPLC data showed the cream to deliver more ascorbic acid into the human *stratum corneum*, the uniformity and intensity of the ascorbic acid molecular ion is less than the equivalent nanoparticle tape strip. This would suggest a strong localisation of the ascorbic acid in the skin furrows with the cream formulation. The complete set of 80 human tape strip ToF-SIMS images can be found in the Appendix I Figures A-8 to A-12, where this permeation behaviour was observed consistently at different *stratum corneum* depths (Tape strip numbers 3,6,9,12 and 15).

Skin furrow deposition of formulation could be exploited as a reservoir for enhanced retention and delayed release and *stratum corneum* penetration.¹⁴⁴ Previous studies have reported inorganic TiO₂ and ZnO microparticles to localise within skin furrows using scanning electron microscopy in combination with energy dispersive x-ray spectroscopy (EDXS) or x-ray fluorescence (XRF).²⁷⁹⁻²⁸¹ Adlhart *et al.*²⁸² found micronized (< 200 nm) methylene bis-benzotriazolyl tetramethylbutylphenol, a particulate UV absorber commonly found in sunscreens, to be localised within skin furrows by CRM. Lademann *et al.*⁷⁶ reported a fluorescent labelled formulation to localise within human skin furrows by CLSM analysis of tape strip samples. The authors applied the emulsion for one hour on the skin, the same as performed in this study, and found furrow localisation of the fluorescent compound, which is consistent with the findings here for the cream. Alvarez-Roman *et al.*²⁸³ observed fluorescently labelled nanoparticles to localise within porcine skin furrows by CLSM which is also consistent with the findings here.

Formulation deposition in skin furrows is therefore of important consideration when evaluating tape strip data, particularly as the depth and density of skin furrows differs interindividually with age, lifestyle and genetic factors.¹⁸⁷ Previous studies with EDXS, XRF, CRM and CLSM cannot be replicated with many cosmetic and pharmaceutical ingredients as they are typically organic, may not have unique Raman bands or be fluorophores. On the other hand, ToF-SIMS was shown to visualise the spatial distribution of ascorbic acid and excipient ingredients label-free; and could be further applied to study a wide range of active ingredients.

The deep and wide furrows found on porcine skin⁶⁰, as seen in the ToF-SIMS images in Figure 5-7, could explain why nanoparticle formulation, despite its significantly different rheological properties from cream, accumulated in the furrows. Therefore, the interaction of the formulation with the furrow structures may explain why permeation differences were observed between *ex vivo* porcine skin and *in vivo* human skin. It would not be possible to determine this with HPLC method which has no spatial resolution of the permeant in the tape strips.

5.4.5 HPLC and ToF-SIMS analytical method correlation

80 human skin tape strip samples (~ 12% of the total collected) were analysed by ToF-SIMS, prior to extraction and HPLC analysis. These 80 tape strips were representative of the full HPLC data set (Figure 5-3 B) as they show the cream to have a significantly higher permeation profile than the lipid nanoparticle, which was significantly higher than the positive control (Figure 5-10 A).

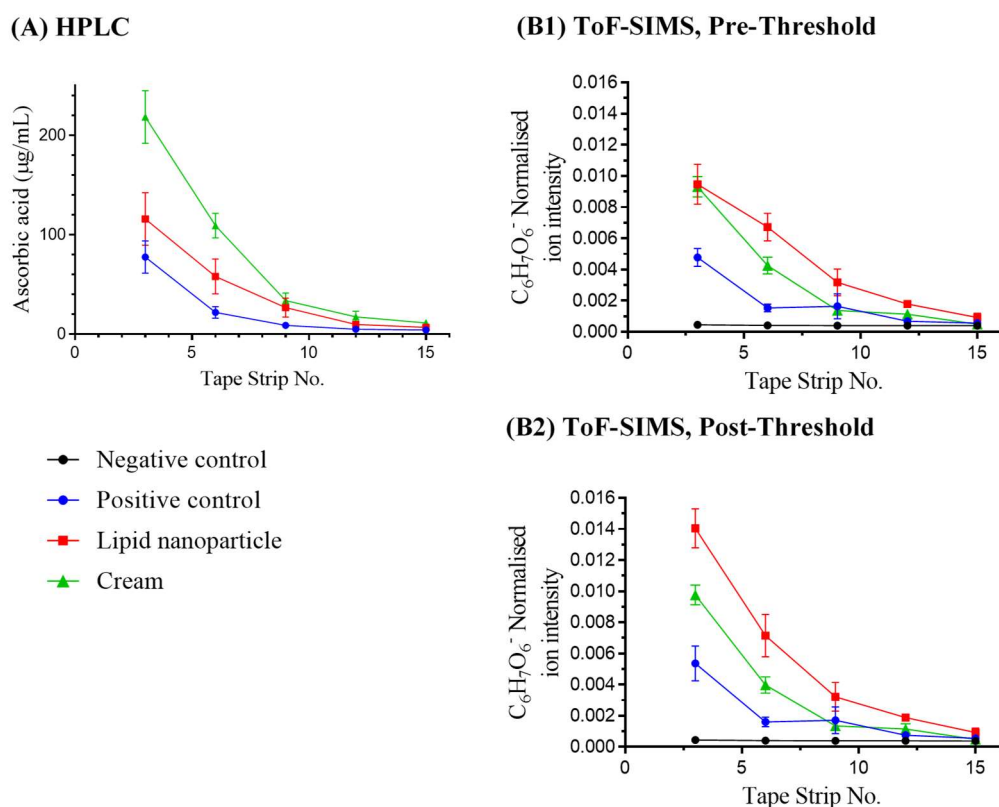


Figure 5-10 Ascorbic acid human stratum corneum penetration profile determined by HPLC analysis (A) and ToF-SIMS analysis (B) of tape strip samples. The ToF-SIMS ascorbic acid $[M-H]^-$ ion intensity is shown pre (B1) and post thresholding (B2). Mean \pm SEM, $n=4$.

The ToF-SIMS, pre-thresholding, shows the cream and nanoparticle formulations to have similar permeation profiles but with the lipid nanoparticle profile higher than the cream. Post-thresholding, the ToF-SIMS shows the nanoparticle formulation to have a significantly higher permeation profile than the cream. This suggests more ascorbic acid from the nanoparticle formulation is co-localised with corneocyte cells, and not furrows, on the tape strips. The difference is most pronounced for the first 10 tape strips (approximate *stratum corneum* depth 10 μm) where the size of the furrows will be largest.

The analytical methods, HPLC and ToF-SIMS, evidently differ from each other. In HPLC, the full contents of the tape strip are extracted into solution so it can be considered a complete 3D extraction and analysis. On the other hand, ToF-SIMS only analyses the top 2 nm of the tape strip sample so it can be described as a 2D surface analysis. In HPLC, interfering analytes are separated

so the ascorbic acid can be quantified free of the sample matrix, whereas in ToF-SIMS, the ascorbic acid is surrounded by other analytes in the tape strip sample leading to matrix-related effects. In HPLC, the full 2 cm × 2 cm tape strip area was extracted, whereas in ToF-SIMS, only the central 4mm x 4mm area was analysed. Taking into consideration these differences, it is thought that the 3D analysis with HPLC, and 2D analysis by ToF-SIMS, plays a key role in why the analytical methods show different permeation profiles. The cream and nanoparticle formulations had the same matrix effects (Section 4.4.7) so is unlikely to explain the different permeation profiles. The formulations were rubbed into the skin test site homogeneously, so the area size of the tape strip analysed by ToF-SIMS should theoretically not affect the permeation profile observed.

The ToF-SIMS images contain different overall ascorbic acid ion intensities so it can be difficult to describe the overall permeation behaviour of ascorbic acid from the formulations just by looking at the images alone. Thus, the absolute ascorbic acid concentration, from HPLC, was plotted against ascorbic acid molecular ion intensity, from ToF-SIMS, to obtain a correlation plot as shown in Figure 5-11.

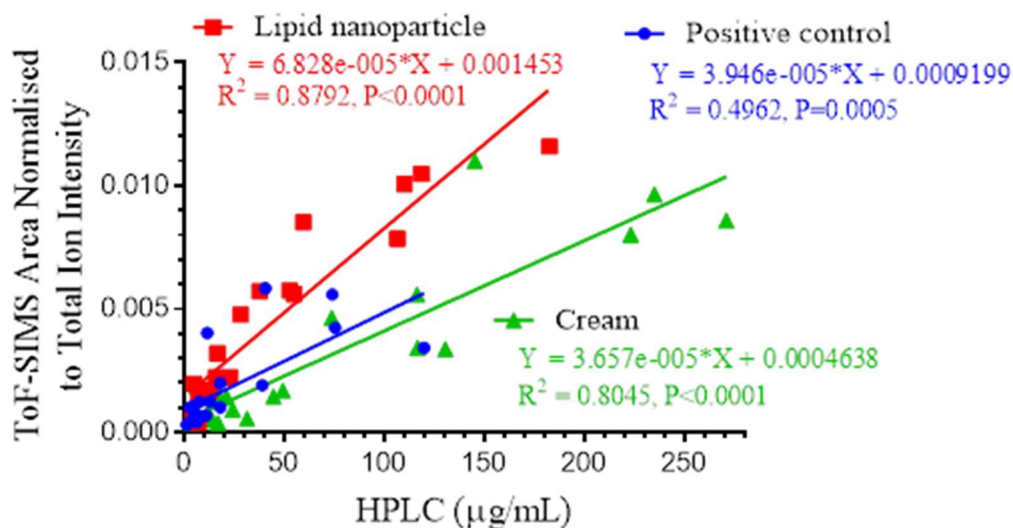


Figure 5-11 HPLC quantification of ascorbic acid correlation with ToF-SIMS ascorbic acid [M-H]- ion intensity from tape strip samples from human skin treated with positive control (blue), lipid nanoparticle (red) and cream (green). n=20 tapes per product.

A low correlation coefficient ($R^2 = 0.4962$) was obtained for tape strips from positive control treated skin because at small ascorbic acid concentration, there was large variability in the ascorbic acid molecular ion intensity, which indicates ToF-SIMS is less sensitive at these smaller concentrations. The steeper gradient of the lipid nanoparticle correlation (Figure 5-11, red) means that for a given ascorbic acid concentration, the measured ascorbic acid $[M-H]^-$ ion intensity increases more than it does for the cream formulation (green). This can be interpreted as the ascorbic acid from the lipid nanoparticle formulation is more laterally spread out than the cream at all concentrations on the tape strip samples. Therefore, more of the ascorbic acid is delivered into the corneocyte cells from the lipid nanoparticle compared to the cream. If both formulations showed the same extent of lateral permeation, then they would have the same gradient.

A skin care product performs best when the active ingredient is delivered into the corneocyte cells (comparatively uniform distribution) and not just localised in the skin furrows (comparatively non uniform distribution) where it has not actually penetrated the *stratum corneum*. Analysis by the conventional approach alone, extraction and HPLC, would have led to a different, inaccurate, conclusion.

The nanoparticle formulation was found to be less viscous than the cream formulation (Section 4.4.7). The higher structural strength of the cream enables it to be pushed into the skin furrows as the formulation is rubbed into the skin, however interaction of ascorbic acid with the thickening agent, xanthan gum, retards its lateral permeation into the surrounding corneocytes. This would agree with Gallagher *et al.*²⁸⁴ who found ketoprofen permeation into the skin was reduced as viscosity of the formulation increased and this was attributed to binding of the drug to the thickening agent.

It is generally accepted that viscous formulations retard dermal absorption of the permeant if the formulation does not form an occlusive layer,²⁸⁵ however in this work it was also found to affect the distribution uniformity of the permeant in the skin. The lipid nanoparticle formulation, which showed the highest lateral permeation into the corneocytes, is considered most efficacious for the

antioxidant properties of ascorbic acid as a uniform distribution in the *stratum corneum* is desired to protect against UV radiation. On the other hand, the cream formulation, which showed more furrow deposition, may have applications where a slow release of the active ingredient over a longer period of time is desired.

At the present time it is not known if a more uniform distribution of the active ingredient in the *stratum corneum* is associated with improvement in the therapeutic effects observed in the skin. This would require a long-term efficacy study to evaluate if one formulation provides more skin care benefit than the other.

The correlation between ToF-SIMS and HPLC analysis of tape strip samples is unprecedented. Whilst the former is considered a 2D analysis, the latter is considered a 3D analysis: this combination enabled the opportunity to reveal new insights into ascorbic acid skin permeation that would not be possible with one analytical technique alone. For example, it would not be possible to replicate this work with CRM with HPLC. CRM has a z-depth resolution of about 1 μm , greater than the height of one corneocyte layer on the tape strip and more than ToF-SIMS z-depth resolution of about 5 nm.⁹¹ So it would not be possible to analyse tape strip samples with the 2D specificity of ToF-SIMS with CRM.

5.4.6 Formulation effects on skin hydration

TEWL measurements show that 1 hour after application of the formulation, the hydration of the skin treated with ascorbic acid containing formulations increased compared to the negative control containing no ascorbic acid (Figure 5-11 A). Ascorbic acid is known to have a hydrating effect on the skin,¹⁶⁵ because it is a hygroscopic ingredient so retains water from the formulation at the *stratum corneum*.

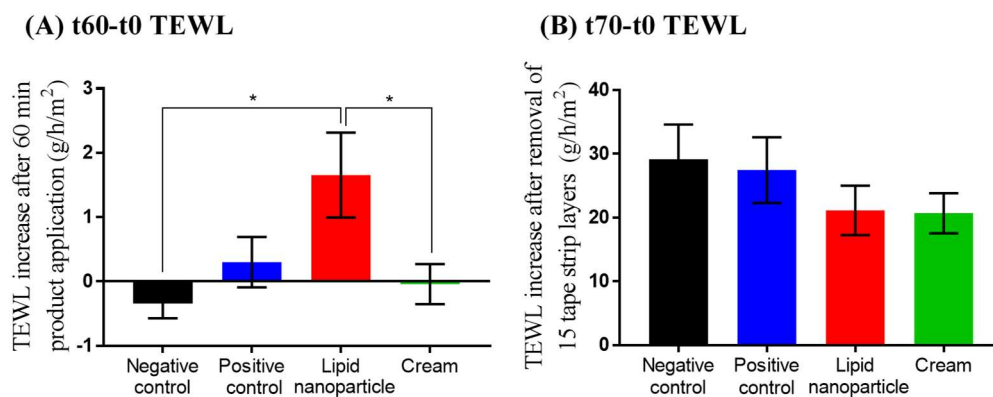


Figure 5-12 TEWL increase 60 minutes after product application (A) and after removal of 15 sequential tape strip layers (B) from in vivo human skin. Mean \pm SEM, $n \geq 10$.

The lipid nanoparticle formulation showed the most significant hydrating effect (Figure 5-11 A), because even after 1 hour, not all of the water from the formulation had evaporated. On the contrary, Jennings *et al.* (2000)²⁸⁶ investigated TEWL from lipid nanoparticle dispersions, applied on a glass surface, and found the nanoparticle preparations lost their own water completely within 1 hour. The inclusion of hygroscopic ascorbic acid may explain these differences. An increased hydration of the skin, is known to cause corneocyte cells to swell, increasing the permeation of hydrophilic molecules through the *stratum corneum* barrier,^{64,65} which would agree with the increased lateral permeation observed in Section 5.4.5. Increased skin hydration is in agreement with Pardeike *et al.*²⁸⁷ who found daily application of NLC formulation, for 28 days, resulted in increased skin hydration, compared to a cream formulation, in a single-blind study of 31 volunteers.

It is evident that the cream did not increase TEWL value after application to the skin (Figure 5-11 A). This is because water is entrapped in the xanthan gum network structure; hence its use as a thickening agent in topical products.^{288,289} Water from the cream formulation therefore does not evaporate as readily and is also locked away from swelling surrounding corneocytes. The cream may increase skin hydration from within, by having an occlusive effect on the skin, however it would not be possible to determine this from a TEWL measurement which measures water loss.

No significant differences were found in the TEWL measurements after tape stripping (Figure 5-11 B). TEWL measurements after tape stripping had large variability since tape stripping removes variable amounts of corneocytes from one site to another, subjects have different *stratum corneum* thicknesses and the permeated ascorbic acid could influence water retention, rather than evaporation. The lipid nanoparticle and cream formulations did show smaller increases in TEWL after tape stripping even though a similar depth of the *stratum corneum* was sampled (Figure 5-1). Lipidic formulations are associated with maintenance of the *stratum corneum* barrier which would result in lower increase in TEWL.²⁶⁴

5.5 Conclusions

In this chapter, both the lipid nanoparticle and cream were demonstrated to increase skin permeation of ascorbic acid compared to a positive control solution. Moreover, this chapter has demonstrated that the analytical method used to evaluate skin permeation, from tape strip samples, can radically influence the permeation profile that is measured. Analysis of tape strip samples by conventional extraction and HPLC showed the cream formulation to deliver the most ascorbic acid into the *stratum corneum*. However, analysis by ToF-SIMS showed the ascorbic acid on the cream treated skin to be mainly localised to the skin furrows whereas more of the ascorbic acid from the lipid nanoparticle formulation was colocalised with the corneocyte material on the tape strips. A more accurate permeation profile was deemed to be obtained by ToF-SIMS because ascorbic acid in the furrows was not considered to have penetrated the *stratum corneum*.

A correlation between ascorbic acid concentration, from HPLC, and ascorbic acid molecular ion intensity, from ToF-SIMS, further revealed the ascorbic acid from the lipid nanoparticle formulation to be more laterally spread over the corneocytes at all concentrations than the cream formulation. In order for ascorbic acid to have therapeutic effect in the *stratum corneum*, it needs to be delivered into the corneocyte cells and not just deposited in the skin furrows. This insight would not have been possible with one analytical technique alone.

In contrast, permeation experiments performed on *ex vivo* porcine skin showed no significant difference between the nanoparticle and cream formulations, despite their particle size and rheological differences, either by HPLC method or ToF-SIMS method. The porcine skin *ex vivo* experiment was conducted for a longer time however a previous finite dose experiment of 4 hours was found not to significantly change permeation amount and depth in porcine skin *ex vivo* compared to 1 hour. Although a time effect cannot be ignored, it is thought that the deeper and wider skin furrows found on porcine skin may influence the interaction of the formulation with the *stratum corneum* barrier as it is rubbed into the skin test site. In future, further consideration should be made when assessing skin permeation on porcine skin due to its different

furrow structure to human skin when assessing skin permeation with tape stripping procedure.

Uncovering the spatial distribution, and localisation, of the permeant in the skin barrier has facilitated identification of the nanoparticle formulation to deliver a more uniform distribution of ascorbic acid in the *stratum corneum*. This could be explained by the increased skin hydration even 1 hour after the lipid nanoparticle formulation was rubbed into the skin. The use of imaging techniques, such as ToF-SIMS, is therefore highly recommended in the analysis of tape strip samples to accurately characterise skin permeation and to understand the mechanism of permeation such that new and more effective formulations can be designed.

Chapter 6: Conclusions and general discussion

6.1 General conclusions

The role of ascorbic acid in skin health is well understood however its instability in aqueous solution presents challenges for formulation. Therefore, in recent times focus has shifted to stable derivatives of ascorbic acid, but these require conversion in the skin back to ascorbic acid to observe efficacy. Accordingly, current knowledge regarding skin permeation of ascorbic acid is limited, with *in vivo* human skin permeation data unavailable. For ascorbic acid to show its beneficial therapeutic effects, it must be able to permeate the skin barrier.

The standard approach to assessing skin permeation typically involves HPLC methods. Although HPLC results in absolute quantitative data, it does not have any imaging capability so cannot provide information about the spatial distribution of an active ingredient within the skin. In contrast, imaging mass spectrometry techniques, such as ToF-SIMS, are increasingly being used to show the spatial distribution of molecules within biological tissue specimens. In addition, ToF-SIMS analysis can be performed without the need for fluorescent reporter tags, which can alter the physiochemical properties of the permeant, or radiolabelling, which is highly expensive and requires additional safety controls. Uncovering the spatial distribution of ascorbic acid in the skin can reveal new information about its permeation that cannot be obtained with chromatography based methods.

There is increased interest in using CRM to non-invasively examine skin permeation in skin tissue, including *in vivo* in humans. However, the work in chapter 2 shows that CRM is not suitable for monitoring ascorbic acid in biological tissue due to a photobleaching effect on the Raman spectrum. In contrast, ToF-SIMS showed a good level of sensitivity and chemical specificity for ascorbic acid in the skin cross sections, after application of a clinically relevant dose to the skin. ToF-SIMS is generally considered to provide semi-quantitative results, so it was necessary to use absolute

quantification methods, namely HPLC and UV-Vis, to study ascorbic acid permeation.

Franz diffusion cells are widely used to study *in vitro* skin permeation since their setup can be replicated easily in any lab across the world. However, previous studies have highlighted their limitations compared to the *in vivo* situation particularly when determining permeant localisation in the skin layers. The work in chapter 3 shows that for hydrophilic ingredients, and when using full thickness porcine skin, no significant differences was observed in permeant localisation between skin exposed to a liquid acceptor medium and not. Therefore, the use of Franz cells or whole intact ear, may be suitably used in this case for skin permeation experiment.

Gel formulations are very common vehicles for the delivery of cosmetic ingredients into the skin. They are almost always rubbed into the skin which is important for distributing the formulation and ensuring a close contact between the gel and the skin. Usually *in vitro* permeation experiments do not specify the application conditions of the product onto the skin. To mimic in use conditions, ascorbic acid and caffeine gels were rubbed into *ex vivo* porcine skin tissue. After 24 hours permeation time, it was found that the gel significantly enhanced the permeation of caffeine compared to cosolvent control. On the other hand, the gel formulation did not enhance the delivery of ascorbic acid into the skin. This is thought to be due to a stronger interaction with the thickening agent.

When examining the spatial distribution, ascorbic acid and caffeine were found primarily localised to the epidermis and non-uniformly. Despite previous reports that the follicular route contributes approximately 50% of the total *in vitro* skin permeation, no localisation of caffeine was observed in the hair follicle. Some ascorbic acid and caffeine were found close to the hair follicle orifices (~ 0.1 mm depth) but this was not considered to have penetrated the hair follicle. Thus, transepidermal routes of permeation contribute largely to skin permeation of ascorbic acid and caffeine.

Lipid nanoparticle based formulations have been described to increase permeation of active ingredients into the skin since their small size ensures a

close contact with the *stratum corneum*. NLC formulation of ascorbic acid was therefore investigated for its potential to enhance ascorbic acid permeation. The work in chapter 4, shows that the developed NLC formulation was the most suitable for topical application in comparison to the previously reported formulations. NLC formulations are widely reported to increase the stability of encapsulated cargo however it was found the stability of ascorbic acid in NLC formulation was not improved compared to aqueous control. It is thought that this is due to the high concentration of ascorbic acid in the formulation, that is required to observe topical efficacy, and the low encapsulation efficiency.

A cream formulation was developed alongside the NLC formulation. A large number of permeation studies compare these formulation types, however, using different lipids and surfactants. In this work the cream formulation was prepared with the exact same composition of lipids and surfactants as the NLC. Therefore, a study comparing permeation between these two formulations would be unique since no additional chemical penetration enhancer effects are expected and the physical properties of the formulation would explain any permeation differences. More importantly, the NLC and cream contain the same matrix composition, so no matrix-related effects were found in the ToF-SIMS reference spectra of the formulations. This would allow comparison of permeation with ToF-SIMS matrix-related effects minimised.

The permeation study in chapter 3 showed ascorbic acid to be mainly localised to the epidermis, so a tape stripping protocol was used to assess skin permeation of the NLC and cream formulation. In chapter 5, both formulations were applied to human skin *in vivo*. Analysis of tape strip samples by conventional HPLC approach showed the cream formulation to deliver the most ascorbic acid into the *stratum corneum*. However, analysis by ToF-SIMS showed the ascorbic acid mainly localised in the furrows of the skin on the tape strips collected from cream treated skin. Conversely tape strips collected from NLC formulation treated skin showed more lateral permeation of the ascorbic acid into the surrounding corneocytes and not just localised in the furrows of the skin.

The extent of lateral permeation was explored further by plotting a correlation between ascorbic acid concentration, determined by HPLC, and ascorbic acid molecular ion intensity, determined by ToF-SIMS. Whilst HPLC can be considered a 3D extraction and analysis, ToF-SIMS is a 2D surface analytical technique. It was most interesting to find that for tape strip samples, collected from NLC treated skin, the correlation shows ascorbic acid is more laterally spread out over the corneocytes than the cream formulation at all concentrations.

Thresholding of the ToF-SIMS data, to exclude ions from the skin furrows, showed the NLC formulation to have a *stratum corneum* permeation profile higher than that of the cream. It could therefore be argued, that since more ascorbic acid was found co-localised with *stratum corneum* corneocytes, the NLC delivers more ascorbic acid into the skin compared to the cream. The cream formulation delivers more ascorbic acid into the furrows of the skin, but this is not able to permeate laterally into the surrounding corneocytes which is where ascorbic acid needs to be delivered to exhibit its antioxidant effects. Analysis by standard HPLC approach alone would have concluded that the cream delivered the most ascorbic acid into the skin. This study represents the first direct correlation between HPLC and ToF-SIMS for the analysis of *stratum corneum* tape strip samples.

TEWL measurements showed the NLC formulation to have the most hydrating effect on the skin. This together with the NLC formulation being less viscous than the cream formulation would explain why more lateral permeation of ascorbic acid was observed. In finite dose studies, with no skin occlusion, it is generally accepted that viscosity thickening agents retard skin permeation however in these studies, it was also found to affect the distribution of the permeant in the skin.

A topical formulation that showed improved ascorbic acid skin permeation and distribution into the corneocytes was developed. This has the potential to increase the therapeutic efficacy observed in the skin, particularly the antioxidant benefits, however, further long-term efficacy studies would be

advised to show improved permeation distribution is linked to improved efficacy.

The standard approach of using HPLC, as advised by regulatory bodies, provides limited information about skin permeation due to a lack of imaging capability. The application of imaging techniques, such as ToF-SIMS, in this work has shown unequivocally permeation behaviour different from current literature understanding and a permeation profile different from conventional chromatography based methodology. It was therefore demonstrated that information regarding spatial distribution of the permeant in the skin barrier is essential to gaining a more holistic understanding of the mechanisms and routes of skin permeation when evaluating the effectiveness of topically applied formulations.

6.2 Future work and recommendations

In recent years, ToF-SIMS has shown its ability to visualise the spatial distribution of endogenous and exogenous molecules in the skin. The work herein builds on that foundation, providing new and important insights into ascorbic acid skin permeation, that would not have been possible with the more established analytical methods currently employed. Moving forward, the outcomes of this work can be used to direct recommendations for future skin permeation studies with the view of improving and expanding the scope of information gained.

The *in vivo* human skin permeation study involved application of 10-12.5 mg/cm² of formulation. Whilst this was considered a finite dose, typical in-use application involves smaller dosage of 2-5 mg/cm². Smaller, but more clinically relevant, dosage requires more sensitive analytical methodologies. In this work ascorbic acid could be detected in all 15 tape strip layers of the skin with the HPLC being more sensitive than ToF-SIMS at the smaller concentration range. Analysis of tape strips from a further *stratum corneum* depth, or smaller formulation dosage, would provide greater information but would require increased analytical method sensitivity.

Increased sensitivity for ascorbic acid could be obtained by using an electrochemical detector in the HPLC. There are various methods which report an ascorbic acid limit of detection of 0.02 µg/mL²⁹⁰⁻²⁹², much lower than the 0.5 µg/mL obtained by using a UV-Vis detector. Electrochemical detectors measure the electrical current generated from oxidation or reduction reactions, so would be suitable for ascorbic acid. However, electrochemical detectors are prone to contamination, and have limited lifetimes, so are not widely used in HPLCs.²⁹³ Other detectors, such as mass spectrometers, should also be explored because it was not possible to determine the native levels of ascorbic acid in the tape strip samples.

More recently, a ToF-SIMS instrument with increased mass-resolving power, the “3D OrbiSIMS” instrument has been developed. It contains an OrbitrapTM mass analyser, with a mass-resolving power of >240,000 at m/z 200 and mass accuracy <1 p.p.m, that would allow detection of ions with enhanced sensitivity (in the region of two orders of magnitude) and specificity than the instrument used in this work. Passarelli *et al.*²⁹⁴ has demonstrated the utility of 3D Orbisims by imaging the distribution of neurotransmitters in single mouse hippocampus cells with a spatial resolution of under 2 µm. This approach could be extended to single cell corneocytes to establish transcellular permeation of active ingredients.

In this work, ToF-SIMS analysis was performed in HCBU mode, as opposed to burst alignment mode. Burst alignment mode should also be investigated, as it offers improved lateral resolution (~ 250 nm), but at the expense of mass resolution (specificity). This approach could be used to study the localisation of active ingredients in more close detail, particularly at the edges of the skin furrows.

This work involved analysis of a large number of skin cross sections and tape strip samples in order to get a reliable perspective of the distribution of the permeant. It was recognised that the distribution of topically applied exogenous molecules is more variable than endogenously found molecules. It is therefore recommended future studies analyse a similarly large number of samples when reaching a conclusion on the distribution patterns. However,

ToF-SIMS analysis currently requires manual alignment of the ion beam, stage height and positioning, analyser and electron flood gun. This is time-consuming, so more sample automation would be helpful. In comparison HPLC, a widely used and established technique, contains an autosampler so many samples can be programmed to be analysed overnight.

The registered clinical trial (Chapter 5), is the first of its kind to analyse tape strip samples by ToF-SIMS to monitor a topically applied substance. It is considered that imaging mass spectrometry techniques, such as ToF-SIMS, should have an increased role in skin permeation studies due to the influence of skin furrows on removal of corneocytes by tape strips. This study involved use of HPLC together with ToF-SIMS because the latter technique does not provide absolute quantification. For ToF-SIMS to generate more definite quantitative data, matrix effects need to be taken into account. This could be achieved, for example, by the use of an isotopically labelled internal standard.²³⁵ Theoretically the same degree of ion suppression or enhancement will be observed for the target analyte and its isotopically labelled analogue. The ratio of the two signals can be used for quantification. This would avoid the need to extract tape strip samples for HPLC. This approach would also be useful for studying formulations, with different excipient compositions and therefore different matrix-related effects.

The study comparing ascorbic acid and caffeine permeation is the first of its kind and shows how a gel formulation can retard the permeation of ascorbic acid but enhance the permeation of caffeine through the skin. The interaction between ascorbic acid and various viscosity thickening agents could be explored to find an ideal thickening agent that did not hinder ascorbic acid partitioning from formulation to *stratum corneum*.

The latter study demonstrates how an NLC formulation can result in more uniform permeation distribution for *in vivo* human skin, with more ascorbic acid delivered into the corneocytes compared to a cream formulation. The NLC formulation contained double emulsion particles in order to encapsulate ascorbic acid. This double emulsion structure could be investigated further by cryo-TEM to determine the size of the inner aqueous phase droplets in order to

maximise encapsulation. Artefacts in the TEM images were observed when using plunge freezing with liquid ethane so high-pressure induced freezing method could be explored as it is reported to result in less damage to nanoparticles and liposomes in the freezing process.²⁹⁵

It is known that smaller lipid nanoparticle sizes can increase occlusion and therefore skin hydration.¹⁴⁰ Smaller nanoparticles often result in low encapsulation efficiencies. In this work, the NLC formulation was found to improve lateral permeation of ascorbic acid despite ~ 80% of the ascorbic acid being non-encapsulated. It is not known whether encapsulation is necessary to deliver ascorbic acid into the corneocytes. Nanoparticle formulations, with non-encapsulated ascorbic acid, should be investigated as a formulation strategy to see if enhanced permeation is also observed. If encapsulation is not important, single emulsion NLCs could be prepared instead of complex double emulsion NLCs. This would afford more flexibility in the use of lipids and surfactants that could be used.

It was found that NLCs did not significantly stabilise ascorbic acid compared to aqueous solution. This would limit the shelf life of this formulation. It is known that other antioxidants, for example ferulic acid and vitamin E, can stabilise ascorbic acid in aqueous solution.²⁹⁶ Effort should be made to incorporate these into the formulation to extend the shelf life of the formulation.

The *in vivo* human permeation study was performed for 1 hour which may be considered a short timeframe. Longer permeation times should be investigated, for example participants applying the formulation to the skin daily for a number of weeks and then assessing skin permeation and distribution. This would better reflect the in-use scenario. In addition, nanoparticles are reported to target the follicular route of permeation.²⁹⁷ This could not be investigated on the volar forearm but could be studied by differential tape stripping on a more hairy skin test site.

Cosmetic and skin care formulations may contain efficacy claims, for example antiaging, after they have been tested in long term clinical trials. These clinical trials are expensive and require large number of volunteers willing to apply the

product over several weeks and months. At the present time, it is not known if more uniform permeant distribution in the skin, as opposed to just increased permeation, can be correlated to improved efficacy. This should be explored for the developed ascorbic acid formulations. At the present time, there has been no previous *in vivo* human study examining the antioxidant effect of topically applied ascorbic acid in the skin.¹⁵⁰ This is of current interest because oxidation of skin lipids, for example by environmental pollution, may lead to cytotoxic, pro-inflammatory, immunological events that speed up the skin ageing process.

Chapter 7: References

- 1 H. A. E. Benson, in *Transdermal and Topical Drug Delivery: Principles and Practice*, 2012, pp. 1–22.
- 2 K. W. Ng and W. M. Lau, in *Percutaneous Penetration Enhancers. Chemical Methods in Penetration Enhancement*, eds. N. Dragicevic and H. I. Maibach, Springer Berlin, Heidelberg, 2015, pp. 3–18.
- 3 H. Maibach and G. Honari, *Skin Structure and Function*, Academic Press, 2014.
- 4 A. C. Williams, *Transdermal and Topical Drug Delivery. From Theory to Clinical Practice*, 2003.
- 5 J. Hadgraft and M. E. Lane, Skin: The ultimate interface, *Phys. Chem. Chem. Phys.*, 2011, **13**, 5215–5222.
- 6 M. Stucker, M. Licht and H. M. Heise, Surface Ultra-Structure and Size of Human Corneocytes from Upper Stratum Corneum Layers of Normal and Diabetic Subjects with Discussion of Cohesion Aspects, *J. Diabetes Metab.*, , DOI:10.4172/2155-6156.1000603.
- 7 P. M. Elias, Structure and function of the stratum corneum permeability barrier, *Drug Dev. Res.*, 1988, **13**, 97–105.
- 8 A. S. Michaels, S. K. Chandrasekaran and J. E. Shaw, Drug permeation through human skin: Theory and invitro experimental measurement, *AIChE J.*, 1975, **21**, 985–996.
- 9 P. R. Bergstresser and J. Richard Taylor, Epidermal ‘turnover time’—a new examination, *Br. J. Dermatol.*, 1977, **96**, 503–506.
- 10 A. Z. Alkilani, M. T. C. McCrudden and R. F. Donnelly, Transdermal drug delivery: Innovative pharmaceutical developments based on disruption of the barrier properties of the stratum corneum, *Pharmaceutics*, 2015, **7**, 438–470.
- 11 M. Boncheva, The physical chemistry of the stratum corneum lipids, *Int. J. Cosmet. Sci.*, 2014, **36**, 505–515.
- 12 J. Van Smeden and J. A. Bouwstra, Stratum Corneum Lipids: Their Role for the Skin Barrier Function in Healthy Subjects and Atopic Dermatitis Patients, *Curr. Probl. Dermatology*, 2016, **49**, 8–26.
- 13 M. yu, A. Finner, J. Shapiro, B. lo, A. Berekatain and K. J. Mcelwee, Hair follicles and their role in skin health, *Expert Rev. Dermatol.*, 2006, **1**, 855–871.
- 14 M. E. Lane, Skin penetration enhancers, *Int. J. Pharm.*, 2013, **447**, 12–21.
- 15 M. Roohnikan, E. Laszlo, S. Babity and D. Brambilla, A Snapshot of Transdermal and Topical Drug Delivery Research in Canada, *Pharmaceutics*, 2019, **11**, 256.
- 16 L. T. Fox, M. Gerber, J. Du Plessis and J. H. Hamman, Transdermal drug delivery enhancement by compounds of natural origin, *Molecules*, 2011, **16**, 10507–10540.
- 17 H. Trommer and R. H. H. Neubert, Overcoming the stratum corneum: The modulation of skin penetration. A review, *Skin Pharmacol. Physiol.*, 2006, **19**, 106–121.
- 18 A. C. Williams and B. W. Barry, Penetration enhancers., *Adv. Drug Deliv. Rev.*, 2004, **56**, 603–18.

- 19 T. M. Sweeney and D. T. Downing, The role of lipids in the epidermal barrier to water diffusion, *J. Invest. Dermatol.*, 1970, **55**, 135–140.
- 20 H. I. Labouta, L. K. El-Khordagui, T. Kraus and M. Schneider, Mechanism and determinants of nanoparticle penetration through human skin, *Nanoscale*, 2011, **3**, 4989–4999.
- 21 M. Bhowmick and T. Sengodan, Mechanisms, Kinetics and Mathematical Modelling of Transdermal Permeation - An Updated Review, *Int. J. Res. Dev. Pharm. Life Sci.*, 2013, **2**, 636–641.
- 22 J. Lademann, F. Knorr, H. Richter, S. Jung, M. C. Meinke, E. Rühl, U. Alexiev, M. Calderon and A. Patzelt, Hair follicles as a target structure for nanoparticles, *J. Innov. Opt. Health Sci.*, 2015, **8**, 1530004.
- 23 X. Liu, J. E. Grice, J. Lademann, N. Otberg, S. Trauer, A. Patzelt and M. S. Roberts, Hair follicles contribute significantly to penetration through human skin only at times soon after application as a solvent deposited solid in man, *Br. J. Clin. Pharmacol.*, 2011, **72**, 768–774.
- 24 S. Trauer, A. Patzelt, N. Otberg, F. Knorr, C. Rozycki, G. Balizs, R. Büttemeyer, M. Linscheid, M. Liebsch and J. Lademann, Permeation of topically applied caffeine through human skin - A comparison of in vivo and in vitro data, *Br. J. Clin. Pharmacol.*, 2009, **68**, 181–186.
- 25 F. Knorr, J. Lademann, A. Patzelt, W. Sterry, U. Blume-Peytavi and A. Vogt, Follicular transport route - Research progress and future perspectives, *Eur. J. Pharm. Biopharm.*, 2009, **71**, 173–180.
- 26 B. D. Anderson, W. I. Higuchi and P. V Raykar, Heterogeneity effects on permeability-partition coefficient relationships in human stratum corneum, *Pharm. Res.*, 1988, **5**, 566–573.
- 27 G. L. Flynn and S. H. Yalkowsky, Correlation and prediction of mass transport across membranes I: Influence of alkyl chain length on flux-determining properties of barrier and diffusant, *J. Pharm. Sci.*, 1972, **61**, 838–852.
- 28 W. J. Pugh, I. T. Degim and J. Hadgraft, Epidermal permeability-penetrant structure relationships: 4, QSAR of permeant diffusion across human stratum corneum in terms of molecular weight, H-bonding and electronic charge, *Int. J. Pharm.*, 2000, **197**, 203–211.
- 29 A. Naik, Y. N. Kalia and R. H. Guy, Transdermal drug delivery: overcoming the skin's barrier function, *Pharm. Sci. Technol. Today*, 2000, **3**, 318–326.
- 30 B. Finnin, K. Walters and T. J. Franz, in *Transdermal and Topical Drug Delivery: Principles and Practice*, 2012, pp. 85–108.
- 31 J. R. Heylings, D. J. Davies and R. Burton, Dermal absorption of testosterone in human and pig skin in vitro, *Toxicol. Vitr.*, 2018, **48**, 71–77.
- 32 Organisation for Economic Co-operation and Development (OECD), Guidance notes on dermal absorption No. 156, 2011, 1–72.
- 33 Organisation for Economic Co-operation and Development (OECD), Guidance Document for the Conduct of Skin Absorption Studies. No. 28, *OECD Ser. Test. Assess.*, 2004, 31.
- 34 Organisation for Economic Co-operation and Development (OECD), OECD GUIDELINE 428 FOR THE TESTING OF CHEMICALS: Skin Absorption: in vitro Method, 2004, 1–8.
- 35 Scientific Committee on Consumer Safety, Basic criteria for the in vitro

- assessment of dermal absorption of cosmetic ingredients, *Eur. Comm.*, 2010, **SCCS/1358**, 1–14.
- 36 Scientific Committee on Consumer Safety (SCCS), The sccs’s notes of guidance for the testing of cosmetic substances and their safety evaluation - 9th revision, 2016, **SCCS/1564/**, 1–137.
- 37 U. Jacobi, M. Kaiser, R. Toll, S. Mangelsdorf, H. Audring, N. Otberg, W. Sterry and J. Lademann, Porcine ear skin: An in vitro model for human skin, *Ski. Res. Technol.*, 2007, **13**, 19–24.
- 38 E. Abd, S. A. Yousef, M. N. Pastore, K. Telaprolu, Y. H. Mohammed, S. Namjoshi, J. E. Grice and M. S. Roberts, Skin models for the testing of transdermal drugs, *Clin. Pharmacol. Adv. Appl.*, 2016, **8**, 163–176.
- 39 J. Caussin, G. S. Gooris, M. Janssens and J. A. Bouwstra, Lipid organization in human and porcine stratum corneum differs widely, while lipid mixtures with porcine ceramides model human stratum corneum lipid organization very closely, *Biochim. Biophys. Acta - Biomembr.*, 2008, **1778**, 1472–1482.
- 40 K. Sato, K. Sugibayashi and Y. Morimoto, Species differences in percutaneous absorption of nicorandil, *J. Pharm. Sci.*, 1991, **80**, 104–107.
- 41 S. Singh, K. Zhao and J. Singh, In vitro permeability and binding of hydrocarbons in pig ear and human abdominal skin, *Drug Chem. Toxicol.*, 2002, **25**, 83–92.
- 42 I. P. Dick and R. C. Scott, Pig Ear Skin as an In-vitro Model for Human Skin Permeability, *J. Pharm. Pharmacol.*, 1992, **44**, 640–645.
- 43 A. K. Dabrowska, G. M. Rotaru, S. Derler, F. Spano, M. Camenzind, S. Annaheim, R. Stämpfli, M. Schmid and R. M. Rossi, Materials used to simulate physical properties of human skin, *Ski. Res. Technol.*, 2016, **22**, 3–14.
- 44 H. Wagner, K.-H. Kostka, C.-M. Lehr and U. F. Schaefer, Drug distribution in human skin using two different in vitro test systems: Comparison with in vivo data, *Pharm. Res.*, , DOI:10.1023/A:1007648807195.
- 45 A. Patzelt, H. Richter, R. Buettemeyer, H. J. R. Huber, U. Blume-Peytavi, W. Sterry and J. Lademann, Differential stripping demonstrates a significant reduction of the hair follicle reservoir in vitro compared to in vivo, *Eur. J. Pharm. Biopharm.*, 2008, **70**, 234–238.
- 46 J. D’Alvise, R. Mortensen, S. H. Hansen and C. Janfelt, Detection of follicular transport of lidocaine and metabolism in adipose tissue in pig ear skin by DESI mass spectrometry imaging, *Anal. Bioanal. Chem.*, 2014, **406**, 3735–3742.
- 47 K. Guth, M. Schäfer-Korting, E. Fabian, R. Landsiedel and B. van Ravenzwaay, Suitability of skin integrity tests for dermal absorption studies in vitro, *Toxicol. Vitro.*, 2015, **29**, 113–123.
- 48 D. J. Davies, R. J. Ward and J. R. Heylings, Multi-species assessment of electrical resistance as a skin integrity marker for in vitro percutaneous absorption studies, *Toxicol. Vitro.*, 2004, **18**, 351–358.
- 49 K. Myer and H. Maibach, Stratum corneum evaluation methods: Overview, *Ski. Res. Technol.*, 2013, **19**, 213–219.
- 50 Q. Zhang, M. Murawsky, T. LaCount, G. B. Kasting and S. K. Li, Transepidermal water loss and skin conductance as barrier integrity

- tests, *Toxicol. Vitr.*, 2018, **51**, 129–135.
- 51 M. P. Vinardell and M. Mitjans, Alternative Methods to Animal Testing for the Safety Evaluation of Cosmetic Ingredients : An Overview, *Cosmetics*, 2017, **4**, 1–14.
- 52 World Medical Association, World Medical Association Declaration of Helsinki Ethical Principles for Medical Research Involving Human Subjects, *Clin. Rev. Educ.*, 2013, **310**, 2191–2194.
- 53 C. Herkenne, I. Alberti, A. Naik, Y. N. Kalia, F. X. Mathy, V. Pr eat and R. H. Guy, In vivo methods for the assessment of topical drug bioavailability, *Pharm. Res.*, 2008, **25**, 87–103.
- 54 S. Wiedersberg and S. Nicoli, in *Transdermal and Topical Drug Delivery: Principles and Practice*, eds. H. A. E. Benson and A. C. Watkinson., John Wiley & Sons, Hoboken, New Jersey, 2nd edn., 2012, p. 109.
- 55 J. Lademann, U. Jacobi, C. Surber, H. J. Weigmann and J. W. Fluhr, The tape stripping procedure - evaluation of some critical parameters, *Eur. J. Pharm. Biopharm.*, 2009, **72**, 317–323.
- 56 A. Rougier, D. Dupuis, C. Lotte, R. Roguet and H. Schaefer, In vivo correlation between stratum corneum reservoir function and percutaneous absorption, *J. Invest. Dermatol.*, 1983, **81**, 275–278.
- 57 A. Bunge, in *Skin Forum EU*, 2010.
- 58 W. L. Au, M. Skinner and I. Kanfer, Comparison of tape stripping with the human skin blanching assay for the bioequivalence assessment of topical clobetasol propionate formulations, *J. Pharm. Pharm. Sci.*, 2010, **13**, 11–20.
- 59 R. G. Van Der Molen, F. Spies, J. M. Van 'T Noordende, E. Boelsma, A. M. Mommaas and H. K. Koerten, Tape stripping of human stratum corneum yields cell layers that originate from various depths because of furrows in the skin, *Arch. Dermatol. Res.*, 1997, **289**, 514–518.
- 60 V. Klang, J. C. Schwarz, A. Hartl and C. Valenta, Facilitating in vitro tape stripping: Application of infrared densitometry for quantification of porcine stratum corneum proteins, *Skin Pharmacol. Physiol.*, 2011, **24**, 256–268.
- 61 R. Holmgaard, J. B. Nielsen and E. Benfeldt, in *Transdermal and Topical Drug Delivery: Principles and Practice*, 2012, pp. 131–153.
- 62 D. Selzer, M. M. A. Abdel-Mottaleb, T. Hahn, U. F. Schaefer and D. Neumann, Finite and infinite dosing: Difficulties in measurements, evaluations and predictions, *Adv. Drug Deliv. Rev.*, 2013, **65**, 278–294.
- 63 S. E. Cross, R. Jiang, H. A. E. Benson and M. S. Roberts, Can increasing the viscosity of formulations be used to reduce the human skin penetration of the sunscreen oxybenzone?, *J. Invest. Dermatol.*, 2001, **117**, 147–150.
- 64 R. R. Warner, K. J. Stone and Y. L. Boissy, Hydration disrupts human stratum corneum ultrastructure, *J. Invest. Dermatol.*, 2003, **120**, 275–284.
- 65 J. A. Bouwstra, A. De Graaff, G. S. Gooris, J. Nijssse, J. W. Wiechers and A. C. Van Aelst, Water distribution and related morphology in human stratum corneum at different hydration levels, *J. Invest. Dermatol.*, 2003, **120**, 750–758.
- 66 E. Chatelain, B. Gabard and C. Surber, Skin penetration and sun

- protection factor of five UV filters: Effect of the vehicle, *Skin Pharmacol. Appl. Skin Physiol.*, 2003, **16**, 28–35.
- 67 H. A. Benson, V. Sarveiya, S. Risk and M. S. Roberts, Influence of anatomical site and topical formulation on skin penetration of sunscreens., *Ther. Clin. Risk Manag.*, 2005, **1**, 209–18.
- 68 Organisation for Economic Co-operation and Development (OECD), OECD Guidelines 427 Skin Absorption: in vivo Method, 2004, 1–8.
- 69 H. Ishii, H. Todo and K. Sugibayashi, Effect of sebum and ointment rubbing on the skin permeation of triamcinolone acetonide from white petrolatum ointment, *Biol. Pharm. Bull.*, 2010, **33**, 876–880.
- 70 H. X. Nguyen, A. Puri and A. K. Banga, Methods to simulate rubbing of topical formulation for in vitro skin permeation studies, *Int. J. Pharm.*, 2017, **519**, 22–33.
- 71 C. H. Salamanca, A. Barrera-Ocampo, J. C. Lasso, N. Camacho and C. J. Yarce, Franz Diffusion Cell Approach for Pre-Formulation Characterisation of Ketoprofen Semi-Solid Dosage Forms, *Pharmaceutics*, 2018, **10**, 1–10.
- 72 I. Dapic, I. Jakasa, N. L. H. Yau, S. Kezic and A. Kammeyer, Evaluation of an HPLC Method for the Determination of Natural Moisturizing Factors in the Human Stratum Corneum, *Anal. Lett.*, 2013, **46**, 2133–2144.
- 73 M. Paz-Alvarez, P. D. A. Pudney, J. Hadgraft and M. E. Lane, Topical delivery of climbazole to mammalian skin, *Int. J. Pharm.*, 2018, **549**, 317–324.
- 74 F. Mohd, H. Todo, M. Yoshimoto, E. Yusuf and K. Sugibayashi, Contribution of the hair follicular pathway to total skin permeation of topically applied and exposed chemicals, *Pharmaceutics*, , DOI:10.3390/pharmaceutics8040032.
- 75 S. Tampucci, S. Burgalassi, P. Chetoni, C. Lenzi, A. Pirone, F. Mailland, M. Caserini and D. Monti, Topical formulations containing finasteride. part II: Determination of finasteride penetration into hair follicles using the differential stripping technique, *J. Pharm. Sci.*, 2014, **103**, 2323–2329.
- 76 J. Lademann, H.-J. Weigmann, S. Schanzer, H. Richter, H. Audring, C. Antoniou, G. Tsikrikas, H. Gers-Barlag and W. Sterry, Optical investigations to avoid the disturbing influences of furrows and wrinkles quantifying penetration of drugs and cosmetics into the skin by tape stripping, *J. Biomed. Opt.*, 2005, **10**, 054015.
- 77 J. E. Seto, B. E. Polat, B. Vanveller, R. F. V. Lopez, R. Langer and D. Blankschtein, Fluorescent penetration enhancers for transdermal applications, *J. Control. Release*, 2012, **158**, 85–92.
- 78 C. S. Cerqueira-Coutinho, V. E. B. De Campo, A. L. Rossi, V. F. Veiga, C. Holandino, Z. M. F. Freitas, E. Ricci-Junior, C. R. E. Mansur, E. P. Santos and R. Santos-Oliveira, Comparing in vivo biodistribution with radiolabeling and Franz cell permeation assay to validate the efficacy of both methodologies in the evaluation of nanoemulsions: A safety approach, *Nanotechnology*, 2015, **27**, 15101.
- 79 Y. Y. Grams, L. Whitehead, P. Cornwell and J. A. Bouwstra, Time and depth resolved visualisation of the diffusion of a lipophilic dye into the hair follicle of fresh unfixed human scalp skin, *J. Control. Release*,

- 2004, **98**, 367–378.
- 80 G. Chen, C. Ji, M. Miao, K. Yang, Y. Luo, M. Hoptroff, L. Z. Collins and H. G. Janssen, Ex-vivo measurement of scalp follicular infundibulum delivery of zinc pyrithione and climbazole from an anti-dandruff shampoo, *J. Pharm. Biomed. Anal.*, 2017, **143**, 26–31.
- 81 M. E. M. J. Van Kuijk-Meuwissen, L. Mougín, H. E. Junginger and J. A. Bouwstra, Application of vesicles to rat skin in vivo: A confocal laser scanning microscopy study, *J. Control. Release*, 1998, **56**, 189–196.
- 82 S. Zsikó, E. Csányi, A. Kovács, M. Budai-Szucs, A. Gácsi and S. Berkó, Methods to Evaluate Skin Penetration In Vitro, *Sci. Pharm.*, 2019, **87**, 1–21.
- 83 P. J. Caspers, G. W. Lucassen, E. A. Carter, H. A. Bruining and G. J. Puppels, In vivo confocal raman microspectroscopy of the skin: Noninvasive determination of molecular concentration profiles, *J. Invest. Dermatol.*, 2001, **116**, 434–442.
- 84 V. K. Tippavajhala, T. de Oliveira Mendes and A. A. Martin, In Vivo Human Skin Penetration Study of Sunscreens by Confocal Raman Spectroscopy, *AAPS PharmSciTech*, 2018, **19**, 753–760.
- 85 B. G. Saar, L. R. Contreras-Rojas, X. S. Xie and R. H. Guy, Imaging drug delivery to skin with stimulated raman scattering microscopy, *Mol. Pharm.*, 2011, **8**, 969–975.
- 86 L. Chrit, P. Bastien, B. Biatry, J. -T. Simonnet, A. Potter, A. M. Minondo, F. Flament, R. Bazin, G. D. Sockalingum, F. Leroy, M. Manfait and C. Hadjur, In vitro and in vivo confocal Raman study of human skin hydration: Assessment of a new moisturizing agent, pMPC, *Biopolymers*, 2006, **85**, 359–369.
- 87 L. Chrit, P. Bastien, G. D. Sockalingum, D. Batisse, F. Leroy, M. Manfait and C. Hadjur, An in vivo randomized study of human skin moisturization by a new confocal Raman fiber-optic microprobe: Assessment of a glycerol-based hydration cream, *Skin Pharmacol. Physiol.*, 2006, **19**, 207–215.
- 88 M. Förster, M. A. Bolzinger, G. Montagnac and S. Briançon, Confocal raman microspectroscopy of the skin, *Eur. J. Dermatology*, 2011, **21**, 851–863.
- 89 K. Buckley and A. G. Ryder, Applications of Raman Spectroscopy in Biopharmaceutical Manufacturing: A Short Review, *Appl. Spectrosc.*, 2017, **71**, 1085–1116.
- 90 S. Wartewig and R. H. H. Neubert, Pharmaceutical applications of Mid-IR and Raman spectroscopy, *Adv. Drug Deliv. Rev.*, 2005, **57**, 1144–1170.
- 91 National Physical Laboratory, Commercial services from NPL - Surface , Nano and Biophysical characterisation, <http://www.npl.co.uk/upload/pdf/surface-nano-biophys-char-comm-services.pdf%0A>.
- 92 B. Enthaler, M. Trusch, M. Fischer, C. Rapp, J. K. Pruns and J. P. Vietzke, MALDI imaging in human skin tissue sections: Focus on various matrices and enzymes, *Anal. Bioanal. Chem.*, 2013, **405**, 1159–1170.
- 93 P. J. Hart, S. Francese, E. Claude, M. N. Woodroffe and M. R. Clench,

- MALDI-MS imaging of lipids in ex vivo human skin, *Anal. Bioanal. Chem.*, 2011, **401**, 115–125.
- 94 C. S. De Macedo, D. M. Anderson, B. M. Pascarelli, J. M. Spraggins, E. N. Sarno, K. L. Schey and M. C. V. Pessolani, MALDI imaging reveals lipid changes in the skin of leprosy patients before and after multidrug therapy (MDT), *J. Mass Spectrom.*, 2015, **50**, 1374–1385.
- 95 G. Hochart, F. Farcette, D. Bonnel, J. Stauber and G. Stamatias, Biomarker mapping on skin tape strips using MALDI-MSI, *J. Am. Soc. Mass Spectrom.*, , DOI:10.1016/j.jid.2018.03.697.
- 96 J. Bunch, M. R. Clench and D. S. Richards, Determination of pharmaceutical compounds in skin by imaging matrix-assisted laser desorption/ionisation mass spectrometry, *Rapid Commun. Mass Spectrom.*, 2004, **18**, 3051–3060.
- 97 J. Dong, W. Ning, D. J. Mans and J. D. Mans, A binary matrix for the rapid detection and characterization of small-molecule cardiovascular drugs by MALDI-MS and MS/MS, *Anal. Methods*, 2018, **10**, 572–578.
- 98 N. Winograd and A. Bloom, in *Mass spectrometry imaging of small molecules, Methods in Molecular Biology*, ed. L. He, Springer, New York, 2014, vol. 1203, pp. 9–19.
- 99 J. C. Vickerman, in *Surface analysis: the principal techniques*, eds. J. C. Vickerman and I. Gilmore, John Wiley & Sons, West Sussex, 2nd edn., 2009, pp. 113–206.
- 100 National Institute of Standard and Technology (NIST), <https://www.nist.gov/mml/materials-measurement-science-division/surface-and-trace-chemical-analysis-group/time-flight>.
- 101 J. Vickerman and N. Winograd, in *Cluster Secondary Ion Mass Spectrometry: Principles and Applications*, 2013, pp. 269–312.
- 102 N. Tanji, M. Okamoto, Y. Katayama, M. Hosokawa, N. Takahata and Y. Sano, Investigation of the cosmetic ingredient distribution in the stratum corneum using NanoSIMS imaging, *Appl. Surf. Sci.*, 2008, **255**, 1116–1118.
- 103 A. M. Judd, D. J. Scurr, J. R. Heylings, K. W. Wan and G. P. Moss, Distribution and visualisation of chlorhexidine within the skin using ToF-SIMS: A potential platform for the design of more efficacious skin antiseptic formulations, *Pharm. Res.*, 2013, **30**, 1896–1905.
- 104 T. Kezutyte, N. Desbenoit, A. Brunelle and V. Briedis, Studying the penetration of fatty acids into human skin by ex vivo TOF-SIMS imaging, *Biointerphases*, 2013, **8**, 3.
- 105 A. Kubo, I. Ishizaki, A. Kubo, H. Kawasaki, K. Nagao, Y. Ohashi and M. Amagai, The stratum corneum comprises three layers with distinct metal-ion barrier properties, *Sci. Rep.*, 2013, **3**, 1–11.
- 106 P. Sjovall, T. M. Greve, S. K. Clausen, K. Moller, S. Eirefelt, B. Johansson and K. T. Nielsen, Imaging of distribution of topically applied drug molecules in mouse skin by combination of time-of-flight secondary ion mass spectrometry and scanning electron microscopy, *Anal. Chem.*, 2014, **86**, 3443–3452.
- 107 N. J. Starr, D. J. Johnson, J. Wibawa, I. Marlow, M. Bell, D. A. Barrett and D. J. Scurr, Age-related changes to human stratum corneum lipids detected using ToF-SIMS following in vivo sampling, *Anal. Chem.*, 2016, **88**, 4400–4408.

- 108 V. Čižinauskas, N. Elie, A. Brunelle and V. Briedis, Skin Penetration Enhancement by Natural Oils for Dihydroquercetin Delivery, *Molecules*, 2017, **22**, 1–16.
- 109 V. Čižinauskas, N. Elie, A. Brunelle and V. Briedis, Fatty acids penetration into human skin ex vivo : A TOF-SIMS analysis approach , *Biointerphases*, 2017, **12**, 011003.
- 110 A. M. Holmes, D. J. Scurr, J. R. Heylings, K. W. Wan and G. P. Moss, Dendrimer pre-treatment enhances the skin permeation of chlorhexidine digluconate: Characterisation by in vitro percutaneous absorption studies and Time-of-Flight Secondary Ion Mass Spectrometry, *Eur. J. Pharm. Sci.*, 2017, **104**, 90–101.
- 111 P. Sjövall, L. Skedung, S. Gregoire, O. Biganska, F. Clément and G. S. Luengo, Imaging the distribution of skin lipids and topically applied compounds in human skin using mass spectrometry, *Sci. Rep.*, 2018, **8**, 1–14.
- 112 N. J. Starr, K. Abdul Hamid, J. Wibawa, I. Marlow, M. Bell, L. Pérez-García, D. A. Barrett and D. J. Scurr, Enhanced vitamin C skin permeation from supramolecular hydrogels, illustrated using in situ ToF-SIMS 3D chemical profiling, *Int. J. Pharm.*, 2019, **563**, 21–29.
- 113 M. H. Al-Mayahy, A. H. Sabri, C. S. Rutland, A. Holmes, J. McKenna, M. Marlow and D. J. Scurr, Insight into imiquimod skin permeation and increased delivery using microneedle pre-treatment, *Eur. J. Pharm. Biopharm.*, 2019, **139**, 33–43.
- 114 H. Marwah, T. Garg, A. K. Goyal and G. Rath, Permeation enhancer strategies in transdermal drug delivery, *Drug Deliv.*, 2016, **23**, 564–578.
- 115 V. Mathur, Y. Satrawala and M. S. Rajput, Physical and chemical penetration enhancers in transdermal drug delivery system, *Asian J. Pharm.*, 2010, **4**, 173–183.
- 116 T. Waghule, G. Singhvi, S. K. Dubey, M. M. Pandey, G. Gupta, M. Singh and K. Dua, Microneedles: A smart approach and increasing potential for transdermal drug delivery system, *Biomed. Pharmacother.*, 2019, **109**, 1249–1258.
- 117 K. B. Ita, Chemical Penetration Enhancers for Transdermal Drug Delivery- Success and Challenges, *Curr. Drug Deliv.*, 2015, **12**, 645–651.
- 118 K. Walkley, Bound water in stratum corneum measured by differential scanning calorimetry., *J. Invest. Dermatol.*, 1972, **59**, 225–227.
- 119 D. Bucks and H. I. Maibach, in *Percutaneous Absorption; Drugs—Cosmetics—Mechanisms—Methodology*, eds. R. L. Bronaugh and H. I. Maibach, Marcel Dekker, New York, 3rd edn., 1999, p. Chapter 4.
- 120 P. B. Patil, S. K. Datir and R. B. Saudagar, A Review on Topical Gels as Drug Delivery System P.B., *J. drug Deliv. Ther.*, 2019, **3**, 989–994.
- 121 P. Chittodiya, R. S. Tomar, U. Ramchandani, N. Manocha and S. Agrawal, Topical Gel:-a Review, *Int. J. Pharm. Biol. Arch.*, 2013, **4**, 603–613.
- 122 Cosmetics & Toiletries,
<https://www.cosmeticsandtoiletries.com/formulating/function/viscosity/mod/2672031.html#close-olyticsmodal>.
- 123 G. Sworn, Xanthan gum, *Handb. Hydrocoll. Second Ed.*, 2009, 186–203.

- 124 J. N. Mayba and M. J. Gooderham, A guide to topical vehicle formulations, *J. Cutan. Med. Surg.*, 2018, **22**, 207–212.
- 125 Y. S. Cheng, K. W. Lam, K. M. Ng, R. K. M. Ko and C. Wibowo, An integrative approach to product development-A skin-care cream, *Comput. Chem. Eng.*, 2009, **33**, 1097–1113.
- 126 F. Spada, T. M. Barnes and K. A. Greive, Skin hydration is significantly increased by a cream formulated to mimic the skin's own natural moisturizing systems, *Clin. Cosmet. Investig. Dermatol.*, 2018, **11**, 491–497.
- 127 A. Mitchell, <https://www.skincarebyalana.com/blog/im-sharing-love-lipids-skincare/>.
- 128 J. Pardeike, A. Hommoss and R. H. Müller, Lipid nanoparticles (SLN, NLC) in cosmetic and pharmaceutical dermal products, *Int. J. Pharm.*, 2009, **366**, 170–184.
- 129 R. Costa and L. Santos, Delivery systems for cosmetics - From manufacturing to the skin of natural antioxidants, *Powder Technol.*, 2017, **322**, 402–416.
- 130 Q. Li, T. Cai, Y. Huang, X. Xia, S. P. C. Cole and Y. Cai, A review of the structure, preparation, and application of NLCs, PNP, and PLN, *Nanomaterials*, 2017, **7**, 1–25.
- 131 S. Das, W. K. Ng and R. B. H. Tan, Are nanostructured lipid carriers (NLCs) better than solid lipid nanoparticles (SLNs): Development, characterisations and comparative evaluations of clotrimazole loaded SLNs and NLCs?, *Eur. J. Pharm. Sci.*, 2012, **47**, 139–151.
- 132 J. Jose and G. Netto, Role of solid lipid nanoparticles as photoprotective agents in cosmetics, *J. Cosmet. Dermatol.*, , DOI:10.1111/jocd.12504.
- 133 M. Üner, S. A. Wissing, G. Yener and R. H. Müller, Skin moisturizing effect and skin penetration of ascorbyl palmitate entrapped in Solid Lipid Nanoparticles (SLN) and Nanostructured Lipid Carriers (NLC) incorporated into hydrogel, *Pharmazie*, 2005, **60**, 751–755.
- 134 S. Ghanbarzadeh, R. Hariri, M. Kouhsoltani, J. Shokri, Y. Javadzadeh and H. Hamishehkar, Enhanced stability and dermal delivery of hydroquinone using solid lipid nanoparticles, *Colloids Surfaces B Biointerfaces*, 2015, **136**, 1004–1010.
- 135 R. H. Müller and J. Pardeike, Coenzyme Q10 - loaded NLCs : preparation , occlusive properties and penetration enhancement, *Pharm Technol Eur.*, 2007, **19**, 46–49.
- 136 V. Jennings, M. Schäfer-Korting and S. Gohla, Vitamin A-loaded solid lipid nanoparticles for topical use: Drug release properties, *J. Control. Release*, 2000, **66**, 115–126.
- 137 J. Liu, W. Hu, H. Chen, Q. Ni, H. Xu and X. Yang, Isotretinoin-loaded solid lipid nanoparticles with skin targeting for topical delivery, *Int. J. Pharm.*, 2007, **328**, 191–195.
- 138 R. H. Müller, M. Radtke and S. A. Wissing, Solid lipid nanoparticles (SLN) and nanostructured lipid carriers (NLC) in cosmetic and dermatological preparations, *Adv. Drug Deliv. Rev.*, 2002, **54**, 131–155.
- 139 S. Jain, M. A. Mistry and N. K. Swarnakar, Enhanced dermal delivery of acyclovir using solid lipid nanoparticles, *Drug Deliv. Transl. Res.*, 2011, **1**, 395–406.
- 140 S. A. Wissing and R. H. Müller, The influence of solid lipid

- nanoparticles on skin hydration and viscoelasticity - In vivo study, *Eur. J. Pharm. Biopharm.*, 2003, **56**, 67–72.
- 141 E. S. Farboud, S. A. Nasrollahi and Z. Tabbakhi, Novel formulation and evaluation of a Q10-loaded solid lipid nanoparticle cream: in vitro and in vivo studies., *Int. J. Nanomedicine*, 2011, **6**, 611–617.
- 142 C. M. R. R. Nastiti, T. Ponto, E. Abd, J. E. Grice, H. A. E. Benson and M. S. Roberts, Topical nano and microemulsions for skin delivery, *Pharmaceutics*, 2017, **9**, 1–25.
- 143 M. S. Roberts, Y. Mohammed, M. N. Pastore, S. Namjoshi, S. Yousef, A. Alinaghi, I. N. Haridass, E. Abd, V. R. Leite-Silva, H. A. E. Benson and J. E. Grice, Topical and cutaneous delivery using nanosystems, *J. Control. Release*, 2017, **247**, 86–105.
- 144 B. C. Palmer and L. A. DeLouise, Nanoparticle-enabled transdermal drug delivery systems for enhanced dose control and tissue targeting, *Molecules*, 2016, **21**, 7–9.
- 145 J. Dreier, J. A. Sørensen and J. R. Brewer, Superresolution and fluorescence dynamics evidence reveal that intact liposomes do not cross the human skin barrier, *PLoS One*, 2016, **11**, 1–15.
- 146 S. A. Wissing, A. Lippacher and R. H. Müller, Investigations on the occlusive properties of solid lipid nanoparticles (SLN), *J. Cosmet. Sci.* , 2001, **52**, 313–324.
- 147 E. B. Souto and R. H. Müller, Cosmetic features and applications of lipid nanoparticles (SLN, NLC), *Int. J. Cosmet. Sci.*, 2008, **30**, 157–165.
- 148 M. Manela-Azulay and E. Bagatin, Cosmeceuticals vitamins, *Clin. Dermatol.*, 2009, **27**, 469–474.
- 149 K. E. Burke, Interaction of vitamins C and E as better cosmeceuticals, *Dermatol. Ther.*, 2007, **20**, 314–321.
- 150 N. P. J. Stamford, Stability, transdermal penetration, and cutaneous effects of ascorbic acid and its derivatives, *J. Cosmet. Dermatol.*, 2012, **11**, 310–317.
- 151 L. Robitaille and L. J. Hoffer, A simple method for plasma total vitamin C analysis suitable for routine clinical laboratory use, *Nutr. J.*, , DOI:10.1186/s12937-016-0158-9.
- 152 H. Masaki, Role of antioxidants in the skin: Anti-aging effects, *J. Dermatol. Sci.*, 2010, **58**, 85–90.
- 153 H. Nazar, A. Nazar and M. Nazar, Beauty is now more than skin deep — the emergence of cosmeceuticals, *Pharm. J.*, 2014, **292**, 380.
- 154 T. Quan, Z. Qin, W. Xia, Y. Shao, J. J. Voorhees and G. J. Fisher, Matrix-degrading metalloproteinases in photoaging, *J. Investig. Dermatology Symp. Proc.*, 2009, **14**, 20–24.
- 155 P. S. Telang, Vitamin C in dermatology, *Indian Dermatol. Online J.*, 2013, **4**, 143–146.
- 156 C. M. Lee, Fifty years of research and development of cosmeceuticals: a contemporary review, *J. Cosmet. Dermatol.*, 2016, **15**, 527–539.
- 157 F. Al-Niaimi and N. Y. Z. Chiang, Topical Vitamin C and the Skin: Mechanisms of Action and Clinical Applications., *J. Clin. Aesthet. Dermatol.*, 2017, **10**, 14–17.
- 158 D. Darr, S. Combs, S. Dunston, T. Manning and S. Pinnell, Topical vitamin C protects porcine skin from ultraviolet radiation-induced damage, *Br. J. Dermatol.*, 1992, **127**, 247–253.

- 159 K. I. Kivirikko and R. Myllyla, Post-Translational Processing of Procollagens, *Ann. N. Y. Acad. Sci.*, 1985, **460**, 187–201.
- 160 K. Maeda and M. Fukuda, Arbutin: mechanism of its depigmenting action in human melanocyte culture., *J. Pharmacol. Exp. Ther.*, 1996, **276**, 765–769.
- 161 V. Nobile, Guidelines on Cosmetic Efficacy Testing on Humans. Ethical, Technical, and Regulatory Requirements in the Main Cosmetics Markets, *J. Cosmetol. Trichology*, 2016, **02**, 1–10.
- 162 My Awesome Beauty, Best vitamin c serum for face reviews 2017, <https://myawesomebeauty.com/best-vitamin-c-serum/>.
- 163 MakingCosmetics, Vitamin C (L-ascorbic acid), http://www.makingcosmetics.com/Vitamin-C-L-ascorbic-acid_p_321.html.
- 164 R. E. Fitzpatrick and E. F. Rostan, Double-blind, half-face study comparing topical vitamin C and vehicle for rejuvenation of photodamage, *Dermatologic Surg.*, 2002, **28**, 231–236.
- 165 P. Humbert, P. Creidi, A. Richard and A. Rougier, Efficacy of a 5% ascorbic acid cream on skin aging induced by UVA, *J Am Acad Dermatol*, 2005, **28**, 209.
- 166 D. Crisan, I. Roman, M. Crisan, K. Scharffetter-Kochanek and R. Badea, The role of vitamin C in pushing back the boundaries of skin aging: An ultrasonographic approach, *Clin. Cosmet. Investig. Dermatol.*, 2015, **8**, 463–470.
- 167 A. R. Elmore, Final report of the safety assessment of L-Ascorbic Acid, Calcium Ascorbate, Magnesium Ascorbate, Magnesium Ascorbyl Phosphate, Sodium Ascorbate, and Sodium Ascorbyl Phosphate as used in cosmetics., *Int. J. Toxicol.*, 2005, **24**, 51–111.
- 168 J. M. Pullar, A. C. Carr and M. C. M. Vissers, The roles of vitamin C in skin health, *Nutrients*, , DOI:10.3390/nu9080866.
- 169 J. Fuchs and H. Kern, Modulation of UV-light-induced skin inflammation by D-alpha-tocopherol and L-ascorbic acid: A clinical study using solar simulated radiation, *Free Radic. Biol. Med.*, 1998, **25**, 1006–1012.
- 170 F. McArdle, L. E. Rhodes, R. Parslew, C. I. A. Jack, P. S. Friedmann and M. J. Jackson, UVR-induced oxidative stress in human skin in vivo: effects of oral vitamin c supplementation, *Free Radic. Biol. Med.*, 2002, **33**, 1355–1362.
- 171 S. R. Pinnell, H. Yang, M. Omar, N. M. Riviere, H. V Debuys, L. C. Walker, Y. Wang and M. Levine, Topical L-Ascorbic Acid : Percutaneous Absorption Studies, *Dermatol Surg*, 2001, **27**, 137–142.
- 172 A.-R. Cho Lee and K. Tojo, Characterisation of Skin Permeation of Vitamin C: Theoretical Analysis of Penetration Profiles and Differential Scanning Calorimetry Study, *Chem. Pharm. Bull.*, 1998, **46**, 174–177.
- 173 N. Leveque, P. Muret, S. Makki, S. Mac-Mary, J. P. Kantelip and P. Humbert, Ex vivo cutaneous absorption assessment of a stabilized ascorbic acid formulation using a microdialysis system, *Skin Pharmacol. Physiol.*, 2004, **17**, 298–303.
- 174 W. R. Lee, S. C. Shen, K. H. Wang, C. H. Hu and J. Y. Fang, Lasers and Microdermabrasion Enhance and Control Topical Delivery of Vitamin C, *J. Invest. Dermatol.*, 2003, **121**, 1118–1125.

- 175 G. K. Heber, B. Markovic and A. Hayes, An immunohistological study of anhydrous topical ascorbic acid compositions on ex vivo human skin, *J. Cosmet. Dermatol.*, 2006, **5**, 150–156.
- 176 W. Zhou, W. Liu, L. Zou, W. Liu, C. Liu, R. Liang and J. Chen, Storage stability and skin permeation of vitamin C liposomes improved by pectin coating, *Colloids Surfaces B Biointerfaces*, 2014, **117**, 330–337.
- 177 S. Duarah, R. D. Durai and V. H. B. Narayanan, Nanoparticle-in-gel system for delivery of vitamin C for topical application, *Drug Deliv. Transl. Res.*, 2017, **7**, 750–760.
- 178 L. Maione-Silva, E. G. de Castro, T. L. Nascimento, E. R. Cintra, L. C. Moreira, B. A. S. Cintra, M. C. Valadares and E. M. Lima, Ascorbic acid encapsulated into negatively charged liposomes exhibits increased skin permeation, retention and enhances collagen synthesis by fibroblasts, *Sci. Rep.*, 2019, **9**, 1–14.
- 179 US 7,179,841 B2, 2007.
- 180 G. Güney, H. M. Kutlu and L. Genç, Preparation and characterization of ascorbic acid loaded solid lipid nanoparticles and investigation of their apoptotic effects, *Colloids Surfaces B Biointerfaces*, 2014, **121**, 270–280.
- 181 F. C. Su, S. H. Wang and M. L. Yeh, 1st Global Conference on Biomedical Engineering & 9th Asian-Pacific Conference on Medical and Biological Engineering: October 9–12, 2014, Tainan, Taiwan, *IFMBE Proc.*, 2015, **47**, 5–6.
- 182 D. de Britto, M. R. de Moura, F. A. Aouada, F. G. Pinola, L. M. Lundstedt, O. B. G. Assis and L. H. C. Mattoso, Entrapment characteristics of hydrosoluble vitamins loaded into chitosan and N,N,N-trimethyl chitosan nanoparticles, *Macromol. Res.*, 2014, **22**, 1261–1267.
- 183 Y. Cho, J. T. Kim and H. J. Park, Size-controlled self-aggregated N-acetyl chitosan nanoparticles as a vitamin C carrier, *Carbohydr. Polym.*, 2012, **88**, 1087–1092.
- 184 X. Yang, S. Patel, Y. Sheng, D. Pal and A. K. Mitra, Statistical design for formulation optimization of hydrocortisone butyrate-loaded PLGA nanoparticles, *AAPS PharmSciTech*, 2014, **15**, 569–587.
- 185 A. Herman and A. P. Herman, Caffeine's Mechanisms of Action and Its Cosmetic Use, *Skin Pharmacol. Physiol.*, 2013, **26**, 8–14.
- 186 L. Luo and M. E. Lane, Topical and transdermal delivery of caffeine, *Int. J. Pharm.*, 2015, **490**, 155–164.
- 187 N. Otberg, A. Patzelt, U. Rasulev, T. Hagemeister, M. Linscheid, R. Sinkgraven, W. Sterry and J. Lademann, The role of hair follicles in the percutaneous absorption of caffeine, *Br. J. Clin. Pharmacol.*, 2008, **65**, 488–492.
- 188 Leica Biosystems Nussloch GmbH, An introduction to specimen preparation, <https://www.leicabiosystems.com/pathologyleaders/an-introduction-to-specimen-preparation/>, (accessed 20 September 2019).
- 189 U. Lindemann, K. Wilken, H.-J. Weigmann, H. Schaefer, W. Sterry and J. Lademann, Quantification of the horny layer using tape stripping and microscopic techniques, *J. Biomed. Opt.*, 2003, **8**, 601.
- 190 N. Raj, R. Voegeli, A. V. Rawlings, S. Gibbons, M. R. Munday, B. Summers and M. E. Lane, Variation in stratum corneum protein content

- as a function of anatomical site and ethnic group, *Int. J. Cosmet. Sci.*, 2016, **38**, 224–231.
- 191 W. Meyer and N. Zschemisch, Skin layer thickness at the ear of the domesticated pig, with special reference to the use of the ear integument for human dermatological research, *Berl Munch Tierarztl Wochenschr.*, 2002, **115**, 401–6.
- 192 G. Rolls and C. Sampias, H&E Staining Overview: A Guide to Best Practices, <https://www.leicabiosystems.com/pathologyleaders/hc-staining-overview-a-guide-to-best-practices/>, (accessed 20 September 2019).
- 193 M. L. Clausen, H. C. Slotved, K. A. Krogfelt and T. Agner, Tape Stripping Technique for Stratum Corneum Protein Analysis, *Sci. Rep.*, 2016, **6**, 1–8.
- 194 A. M. Maia, A. R. Baby, W. J. Yasaka, E. Suenaga, T. M. Kaneko and M. V. R. Velasco, Validation of HPLC stability-indicating method for Vitamin C in semisolid pharmaceutical/cosmetic preparations with glutathione and sodium metabisulfite, as antioxidants, *Talanta*, 2007, **71**, 639–643.
- 195 R. Voegeli, J. Heiland, S. Doppler, A. V. Rawlings and T. Schreier, Efficient and simple quantification of stratum corneum proteins on tape strippings by infrared densitometry, *Ski. Res. Technol.*, 2007, **13**, 242–251.
- 196 R. L. Anderson and J. M. Cassidy, Variations in physical dimensions and chemical composition of human stratum corneum, *J. Invest. Dermatol.*, 1973, **61**, 30–32.
- 197 N. Accart, F. Sergi and R. Rooke, Revisiting Fixation and Embedding Techniques for Optimal Detection of Dendritic Cell Subsets in Tissues, *J. Histochem. Cytochem.*, 2014, **62**, 661–671.
- 198 M. A. Lampe, A. L. Burlingame, J. Whitney, M. L. Williams, B. E. Brown, E. Roitman and P. M. Elias, Human stratum corneum lipids: characterization and regional variations., *J. Lipid Res.*, 1983, **24**, 120–30.
- 199 C. Alonso, V. Carrer, C. Barba and L. Coderch, Caffeine delivery in porcine skin: a confocal Raman study, *Arch. Dermatol. Res.*, 2018, **310**, 657–664.
- 200 B. D. Beier and A. J. Berger, Method for automated background subtraction from Raman spectra containing known contaminants, *Analyst*, 2009, **134**, 1198–1202.
- 201 C. Wright, Investigation of near-infrared fluorescence and photobleaching of human volar side fingertips in vivo : antioxidants and melanin, *Syracuse Univ. Honor. Progr. Capstone Proj.* 346.
- 202 R. Root-Bernstein, J. Fewins, T. Rhinesmith, A. Koch and P. F. Dillon, Enzymatic recycling of ascorbic acid from dehydroascorbic acid by glutathione-like peptides in the extracellular loops of aminergic G-protein coupled receptors, *J. Mol. Recognit.*, 2016, **29**, 296–302.
- 203 B. Rozman and M. Gašperlin, Stability of vitamins C and E in topical microemulsions for combined antioxidant therapy, *Drug Deliv.*, 2007, **14**, 235–245.
- 204 C. Lyman, M. Schultze and C. King, The effect of metaphosphoric acid and some other inorganic acids on the catalytic oxidation of ascorbic

- acid, *J. Biol. Chem.*, 1937, 757–764.
- 205 G. B. Golubitskii, E. V. Budko, E. M. Basova, a. V. Kostarnoi and V. M. Ivanov, Stability of ascorbic acid in aqueous and aqueous--organic solutions for quantitative determination, *J. Anal. Chem.*, 2007, **62**, 742–747.
- 206 AOAC International, *AOAC Official Method 967.21 Ascorbic Acid in Vitamin Preparations and Juices*, 1968.
- 207 Ü. Şengül, Comparing determination methods of detection and quantification limits for aflatoxin analysis in hazelnut, *J. Food Drug Anal.*, 2016, **24**, 56–62.
- 208 U.S. Department of Health and Human Services, Guidance for Industry, Bio- analytical Method Validation.
- 209 G. R. Kelm, Stability Testing for Topical Formulation Development, *Handb. Formul. Dermal Appl.*, 2016, 425–462.
- 210 Q. V. Vuong and P. D. Roach, Caffeine in green tea: Its removal and isolation, *Sep. Purif. Rev.*, 2014, **43**, 155–174.
- 211 A. K. Nayak and P. P. Panigrahi, Solubility Enhancement of Etoricoxib by Cosolvency Approach, *ISRN Phys. Chem.*, 2012, **2012**, 1–5.
- 212 D. W. Lachenmeier, Safety evaluation of topical applications of ethanol on the skin and inside the oral cavity, *J. Occup. Med. Toxicol.*, 2008, **3**, 1–16.
- 213 M. Reichel, P. Heisig, T. Kohlmann and G. Kampf, Alcohols for Skin Antisepsis at Clinically Relevant Skin Sites, *Antimicrob. Agents Chemother.*, 2009, **53**, 4778–4782.
- 214 World Health Organization, WHO Guidelines on Hand Hygiene in Health Care, *World Heal. Organ.*, 2017, 1–259.
- 215 M. S. M. Pires-e-Campos, G. R. Leonardi, M. Chorilli, R. C. Spadari-Bratfisch, M. L. O. Polacow and D. M. Grassi-Kassisse, The effect of topical caffeine on the morphology of swine hypodermis as measured by ultrasound, *J. Cosmet. Dermatol.*, 2008, **7**, 232–237.
- 216 L. Duracher, L. Blasco, J. C. Hubaud, L. Vian and G. Marti-Mestres, The influence of alcohol, propylene glycol and 1,2-pentanediol on the permeability of hydrophilic model drug through excised pig skin, *Int. J. Pharm.*, 2009, **374**, 39–45.
- 217 American Chemistry Council, Studies Regarding the Safety of Propylene Glycol Use in Cosmetic Products, 1994, **13**, 1–3.
- 218 P. L. Gould, M. Goodman and P. A. Hanson, Investigation of the solubility relationships of polar, semi-polar and non-polar drugs in mixed co-solvent systems, *Int. J. Pharm.*, 1984, **19**, 149–159.
- 219 M. A. L. I. Sheraz, M. F. Khan, S. Ahmed, S. H. Kazi and I. Ahmad, Stability and Stabilization of Ascorbic Acid A Review, 2015, **10**, 22–25.
- 220 A. Shalmashi and F. Golmohammad, Solubility of caffeine in water, ethyl acetate, ethanol, carbon tetrachloride, methanol, chloroform, dichloromethane, and acetone between 298 and 323 K, *Lat. Am. Appl. Res.*, 2010, **40**, 283–285.
- 221 A. Shalmasi and A. Eliassi, Solubility of L-(+)-Ascorbic Acid in Water, Ethanol, Methanol, Propan-2-ol, Acetone, Acetonitrile, Ethyl Acetate, and Tetrahydrofuran from (293 to 323) K, *J. Chem. Eng. Data*, 2008, **53**, 1332–1334.
- 222 L. Luo and M. E. Lane, Topical and transdermal delivery of caffeine,

- Int. J. Pharm.*, 2015, **490**, 155–164.
- 223 D. Kilian, H. J. R. Lemmer, M. Gerber, J. L. Du Preez and J. Du Plessis, Exploratory data analysis of the dependencies between skin permeability, molecular weight and log P, *Pharmazie*, 2016, **71**, 311–319.
- 224 R. L. McMullen, *Antioxidants and the Skin: Second Edition*, 2018.
- 225 D. J. Davies, J. R. Heylings, H. Gayes, T. J. McCarthy and M. C. Mack, Further development of an in vitro model for studying the penetration of chemicals through compromised skin, *Toxicol. Vitr.*, 2017, **38**, 101–107.
- 226 R. Iswandana, W. Chalista and E. S. Sitepu, Formulation and Penetration Enhancement Activity of Sticks Containing Caffeine, *J. Appl. Pharm. Sci.*, 2018, **8**, 043–049.
- 227 E. C. Jung and H. I. Maibach, in *Topical Drug Bioavailability, Bioequivalence, and Penetration*, ed. V. P. Shah, Springer, New York, 2014, pp. 21–30.
- 228 I. Brinkmann and C. C. Müller-Goymann, An attempt to clarify the influence of glycerol, propylene glycol, isopropyl myristate and a combination of propylene glycol and isopropyl myristate on human stratum corneum., *Pharmazie.*, 2005, **60**, 215–220.
- 229 J. Bettinger, M. Gloor, C. Peter, P. Kleesz, J. Fluhr and W. Gehring, Opposing effects of glycerol on the protective function of the horny layer against irritants and on the penetration of hexyl nicotinate, *Dermatology*, 1998, **197**, 18–24.
- 230 X. J. Cai, P. Mesquida and S. A. Jones, Investigating the ability of nanoparticle-loaded hydroxypropyl methylcellulose and xanthan gum gels to enhance drug penetration into the skin, *Int. J. Pharm.*, 2016, **513**, 302–308.
- 231 R. L. Bronaugh and R. F. Stewart, Methods for in vitro percutaneous absorption studies III: Hydrophobic compounds, *J. Pharm. Sci.*, 1984, **73**, 1255–1258.
- 232 T. Ogiso, T. Shiraki, K. Okajima, T. Tanino, M. Iwaki and T. Wada, Transfollicular drug delivery: Penetration of drugs through human scalp skin and comparison of penetration between scalp and abdominal skins in vitro, *J. Drug Target.*, 2002, **10**, 369–378.
- 233 E. Abd, M. S. Roberts and J. E. Grice, A Comparison of the Penetration and Permeation of Caffeine into and through Human Epidermis after Application in Various Vesicle Formulations, *Skin Pharmacol. Physiol.*, 2016, **29**, 24–30.
- 234 M. P. Seah and A. G. Shard, The matrix effect in secondary ion mass spectrometry, *Appl. Surf. Sci.*, 2018, **439**, 605–611.
- 235 P. Panuwet, R. E. H. Jr, P. E. D. Souza, X. Chen, A. Radford, J. R. Cohen, M. E. Marder, K. Kartavenka, P. Barry and D. B. Barr, Biological Matrix Effects in Quantitative Tandem Mass Spectrometry-Based Analytical Methods: Advancing Biomonitoring, *Crit Rev Anal Chem*, 2016, **46**, 93–105.
- 236 S. Soares, P. Fonte, A. Costa, J. Andrade, V. Seabra, D. Ferreira, S. Reis and B. Sarmiento, Effect of freeze-drying, cryoprotectants and storage conditions on the stability of secondary structure of insulin-loaded solid lipid nanoparticles, *Int. J. Pharm.*, 2013, **456**, 370–381.
- 237 Guinama SLU, <https://www.guinama.com/euxyl-pe-9010.html>,

- <https://www.guinama.com/euxyl-pe-9010.html>, (accessed 9 February 2019).
- 238 T. Fürtjes, K. T. Weiss, A. Filbry, F. Rippke and S. Schreml, Impact of a pH 5 Oil-in-Water Emulsion on Skin Surface pH, *Skin Pharmacol. Physiol.*, 2018, **30**, 292–297.
- 239 F. Rodrigues, A. C. Alves, C. Nunes, B. Sarmento, M. H. Amaral, S. Reis and M. B. P. P. Oliveira, Permeation of topically applied caffeine from a food by-product in cosmetic formulations: Is nanoscale in vitro approach an option?, *Int. J. Pharm.*, 2016, **513**, 496–503.
- 240 L. Dekić and M. Primorac, Microemulsions and Nanoemulsions as Carriers for Delivery of NSAIDs, *Microsized Nanosized Carriers Nonsteroidal Anti-inflamm. Drugs Formul. Challenges Potential Benefits*, 2017, 69–94.
- 241 M. Danaei, M. Dehghankhold, S. Ataei, F. Hasanzadeh Davarani, R. Javanmard, A. Dokhani, S. Khorasani and M. R. Mozafari, Impact of particle size and polydispersity index on the clinical applications of lipidic nanocarrier systems, *Pharmaceutics*, 2018, **10**, 1–17.
- 242 K. Mingard, R. Morrell, P. Jackson, S. Lawson, S. Patel and R. Buxton, Good Practice Guide for Improving the Consistency of Particle Size Measurement, *Natl. Phys. Lab.*, 2009, 66.
- 243 H. Rauscher, K. Rasmussen and B. Sokull-Klüttgen, Regulatory Aspects of Nanomaterials in the EU, *Chemie-Ingenieur-Technik*, 2017, **89**, 224–231.
- 244 European Commission, Cosmetic ingredient database (CosIng), https://ec.europa.eu/growth/sectors/cosmetics/cosing_en, (accessed 9 February 2019).
- 245 E. Joseph and G. Singhvi, *Multifunctional nanocrystals for cancer therapy: a potential nanocarrier*, Elsevier Inc., 2019.
- 246 S. Honary and F. Zahir, Effect of Zeta Potential on the Properties of Nano - Drug Delivery Systems - A Review (Part 2), *Trop. J. Pharm. al Res.*, 2013, **12**, 265–273.
- 247 P. A. Grabnar, N. Zajc and J. Kristl, Improvement of ascorbyl palmitate stability in lipid nanoparticle dispersions for dermal use, *J. Drug Deliv. Sci. Technol.*, 2006, **16**, 443–448.
- 248 A. Dingler, R. P. Blum, H. Niehus, R. H. Müller and S. Gohla, Solid lipid nanoparticles (SLNTM/LipopearlsTM) a pharmaceutical and cosmetic carrier for the application of vitamin E in dermal products, *J. Microencapsul.*, 1999, **16**, 751–767.
- 249 V. Teeranachaideekul, R. H. Müller and V. B. Junyaprasert, Encapsulation of ascorbyl palmitate in nanostructured lipid carriers (NLC)-Effects of formulation parameters on physicochemical stability, *Int. J. Pharm.*, 2007, **340**, 198–206.
- 250 The Boots Company PLC, No7 Youthful Vitamin C Fresh Radiance Essence 10ml, <https://www.boots.com/no7-youthful-vitamin-c-fresh-radiance-essence-10228255>, (accessed 9 February 2019).
- 251 T. G. F. Souza, V. S. T. Ciminelli and N. D. S. Mohallem, A comparison of TEM and DLS methods to characterize size distribution of ceramic nanoparticles, *J. Phys. Conf. Ser.*, , DOI:10.1088/1742-6596/733/1/012039.
- 252 M. Üner, in *Handbook of Nanoparticles*, ed. M. Aliofkhazraei, 2016, pp.

- 117–141.
- 253 R. Cortesi, G. Valacchi, X. M. Muresan, M. Drechsler, C. Contado, E. Esposito, A. Grandini, A. Guerrini, G. Forlani and G. Sacchetti, Nanostructured lipid carriers (NLC) for the delivery of natural molecules with antimicrobial activity: production, characterisation and in vitro studies, *J. Microencapsul.*, 2017, **34**, 63–72.
- 254 J. A. Hanson, C. B. Chang, S. M. Graves, Z. Li, T. G. Mason and T. J. Deming, Nanoscale double emulsions stabilized by single-component block copolypeptides, *Nature*, 2008, **455**, 85–88.
- 255 R. Bernewitz, G. Guthausen and H. P. Schuchmann, in *Imaging Technologies and Data Processing for Food Engineers*, ed. N. Sozer, 2016, vol. 1, pp. 69–98.
- 256 L. E. Franken, E. J. Boekema and M. C. A. Stuart, Transmission Electron Microscopy as a Tool for the Characterization of Soft Materials: Application and Interpretation, *Adv. Sci.*, 2017, **4**, 1–9.
- 257 C. Parmenter, Senior Research Fellow in Electron Microscopy, Nanoscale and Microscale Research Centre (nmRC), University of Nottingham, Personal Communication.
- 258 K. L. McDonald, A review of high-pressure freezing preparation techniques for correlative light and electron microscopy of the same cells and tissues, *J. Microsc.*, 2009, **235**, 273–281.
- 259 Anton Paar, Rheology of Creams and Lotions, <https://blog.anton-paar.com/rheology-of-creams-and-lotions/>, (accessed 9 February 2019).
- 260 M. Chaplin, Xanthan Gum, http://www1.lsbu.ac.uk/water/xanthan_gum.html, (accessed 9 February 2019).
- 261 J. Lademann, A. Patzelt, H. Richter, S. Schanzer, W. Sterry, A. Filbry, K. Bohnsack, F. Rippke and M. Meinke, Comparison of two in vitro models for the analysis of follicular penetration and its prevention by barrier emulsions, *Eur. J. Pharm. Biopharm.*, 2009, **72**, 600–604.
- 262 A. Alikhan and H. I. Maibach, in *Textbook of Aging Skin*, eds. M. A. Farage, K. W. Miller and H. I. Maibach, Springer-Verlag, Berlin, 2010, pp. 401–408.
- 263 U. Jacobi, N. Meykadeh, W. Sterry and J. Lademann, Effect of the vehicle on the amount of stratum corneum removed by tape stripping, *JDDG - J. Ger. Soc. Dermatology*, 2003, **1**, 884–889.
- 264 V. Klang, J. C. Schwarz, B. Lenobel, M. Nadj, J. Auböck, M. Wolzt and C. Valenta, In vitro vs. in vivo tape stripping: Validation of the porcine ear model and penetration assessment of novel sucrose stearate emulsions, *Eur. J. Pharm. Biopharm.*, 2012, **80**, 604–614.
- 265 C. S. Choe, J. Schleusener, J. Lademann and M. E. Darvin, Human skin in vivo has a higher skin barrier function than porcine skin ex vivo—comprehensive Raman microscopic study of the stratum corneum, *J. Biophotonics*, , DOI:10.1002/jbio.201700355.
- 266 C. Herkenne, A. Naik, Y. N. Kalia, J. Hadgraft and R. H. Guy, Pig ear skin ex vivo as a model for in vivo dermatopharmacokinetic studies in man, *Pharm. Res.*, 2006, **23**, 1850–1856.
- 267 H.-J. Weigmann, S. Schanzer, A. Patzelt, V. Bahaban, F. Durat, W. Sterry and J. Lademann, Comparison of human and porcine skin for characterization of sunscreens, *J. Biomed. Opt.*, 2009, **14**, 024027.

- 268 A. Nair, S. Jacob, B. Al-Dhubiab, M. Attimarad and S. Harsha, Basic considerations in the dermatokinetics of topical formulations, *Brazilian J. Pharm. Sci.*, 2013, **49**, 423–434.
- 269 M. Breternitz, M. Flach, J. Präbller, P. Elsner and J. W. Fluhr, Acute barrier disruption by adhesive tapes is influenced by pressure, time and anatomical location: Integrity and cohesion assessed by sequential tape stripping; A randomized, controlled study, *Br. J. Dermatol.*, 2007, **156**, 231–240.
- 270 C. Herkenne, A. Naik, Y. N. Kalia, J. Hadgraft and R. H. Guy, Dermatopharmacokinetic prediction of topical drug bioavailability in vivo, *J. Invest. Dermatol.*, 2007, **127**, 887–894.
- 271 W. Navidi, A. Hutchinson, B. N’Dri-Stempfer and A. Bunge, Determining bioequivalence of topical dermatological drug products by tape-stripping, *J. Pharmacokinet. Pharmacodyn.*, 2008, **35**, 337–348.
- 272 S. Nallagundla, S. Patnala and I. Kanfer, Application of an Optimized Tape Stripping Method for the Bioequivalence Assessment of Topical Acyclovir Creams, *AAPS PharmSciTech*, 2018, **19**, 1567–1573.
- 273 S. Hoeller, V. Klang and C. Valenta, Skin-compatible lecithin drug delivery systems for fluconazole: effect of phosphatidylethanolamine and oleic acid on skin permeation, *J. Pharm. Pharmacol.*, 2008, **60**, 587–591.
- 274 V. Klang, J. C. Schwarz, N. Matsko, E. Rezvani, N. El-Hagin, M. Wirth and C. Valenta, Semi-solid sucrose stearate-based emulsions as dermal drug delivery systems, *Pharmaceutics*, 2011, **3**, 275–306.
- 275 T. Hakozaki, H. Takiwaki, K. Miyamoto, Y. Sato and S. Arase, Ultrasound enhanced skin-lightening effect of vitamin C and niacinamide, *Ski. Res. Technol.*, 2006, **12**, 105–113.
- 276 U. Jacobi, H. J. Weigmann, M. Baumann, A. I. Reiche, W. Sterry and J. Lademann, Lateral Spreading of Topically Applied UV Filter Substances Investigated by Tape Stripping, *Skin Pharmacol. Physiol.*, 2004, **17**, 17–22.
- 277 R. V. Pelchrzim, H. J. Weigmann, H. Schaefer, T. Hagemeister, M. Linscheid, V. P. Shah, W. Sterry and J. Lademann, Determination of the formation of the stratum corneum reservoir for two different corticosteroid formulations using tape stripping combined with UV/VIS spectroscopy, *JDDG - J. Ger. Soc. Dermatology*, 2004, **2**, 914–919.
- 278 P. Creidi, B. Faivre and P. Agoche, Assessment of skin hydration and softening effects of colloidal oat fraction containing cream, *J. Appl. Cosmetol.*, 1992, **6**, 1–5.
- 279 A. Mavon, C. Miquel, O. Lejeune, B. Payre and P. Moretto, In vitro percutaneous absorption and in vivo stratum corneum distribution of an organic and a mineral sunscreen, *Skin Pharmacol. Physiol.*, 2006, **20**, 10–20.
- 280 J. Lademann, H. J. Weigmann, C. Rickmeyer, H. Barthelmes, H. Schaefer, G. Mueller and W. Sterry, Penetration of titanium dioxide microparticles in a sunscreen formulation into the horny layer and the follicular orifice, *Skin Pharmacol. Appl. Skin Physiol.*, 1999, **12**, 247–256.
- 281 F. Pflücker, H. Hohenberg, E. Hölzle, T. Will, S. Pfeiffer, R. Wepf, W. Diembeck, H. Wenck and H. Gers-Barlag, The outermost stratum

- corneum layer is an effective barrier against dermal uptake of topically applied micronized titanium dioxide, *Int. J. Cosmet. Sci.*, 1999, **21**, 399–411.
- 282 C. Adlhart and W. Baschong, Surface distribution and depths profiling of particulate organic UV absorbers by Raman imaging and tape stripping, *Int. J. Cosmet. Sci.*, 2011, **33**, 527–534.
- 283 R. Alvarez-Román, A. Naik, Y. N. Kalia, R. H. Guy and H. Fessi, Skin penetration and distribution of polymeric nanoparticles, *J. Control. Release*, 2004, **99**, 53–62.
- 284 S. J. Gallagher and C. M. Heard, Solvent content and macroviscosity effects on the in vitro transcutaneous delivery and skin distribution of ketoprofen from simple gel formulations, *Skin Pharmacol. Physiol.*, 2005, **18**, 186–194.
- 285 V. R. Leite-Silva, M. M. De Almeida, A. Fradin, J. E. Grice and M. S. Roberts, Delivery of drugs applied topically to the skin, *Expert Rev. Dermatol.*, 2012, **7**, 383–397.
- 286 V. Jennings, A. Gysler, M. Schäfer-Korting and S. H. Gohla, Vitamin A loaded solid lipid nanoparticles for topical use: Occlusive properties and drug targeting to the upper skin, *Eur. J. Pharm. Biopharm.*, 2000, **49**, 211–218.
- 287 J. Pardeike, K. Schwabe and R. H. Müller, Influence of nanostructured lipid carriers (NLC) on the physical properties of the Cutanova Nanorepair Q10 cream and the in vivo skin hydration effect, *Int. J. Pharm.*, 2010, **396**, 166–173.
- 288 D. Saha and S. Bhattacharya, Hydrocolloids as thickening and gelling agents in food: A critical review, *J. Food Sci. Technol.*, 2010, **47**, 587–597.
- 289 M. Chaplin, Water Structure and Science: Hydrocolloid Rheology, <http://www1.lsbu.ac.uk/water/rheology.html> [Accessed May 2016].
- 290 H. Iwase, Routine high-performance liquid chromatographic determination of ascorbic acid in foods using L-methionine for the pre-analysis sample stabilization, *Talanta*, 2003, **60**, 1011–1021.
- 291 H. Iwase, Use of nucleic acids in the mobile phase for the determination of ascorbic acid in foods by high-performance liquid chromatography with electrochemical detection, *J. Chromatogr. A*, 2000, **881**, 327–330.
- 292 H. Iwase, Use of an amino acid in the mobile phase for the determination of ascorbic acid in food by high-performance liquid chromatography with electrochemical detection, *J. Chromatogr. A*, 2000, **881**, 317–326.
- 293 R. J. Flanagan, D. Perrett and R. Whelpton, *Electrochemical detection in HPLC*, Royal Society of Chemistry, Cambridge, 2005.
- 294 M. K. Passarelli, A. Pirkl, R. Moellers, D. Grinfeld, F. Kollmer, R. Havelund, C. F. Newman, P. S. Marshall, H. Arlinghaus, M. R. Alexander, A. West, S. Horning, E. Niehuis, A. Makarov, C. T. Dollery and I. S. Gilmore, The 3D OrbiSIMS - Label-free metabolic imaging with subcellular lateral resolution and high mass-resolving power, *Nat. Methods*, 2017, **14**, 1175–1183.
- 295 M. J. Choi, G. P. Hong, S. Briancon, H. Fessi, M. Y. Lee and S. G. Min, Effect of a high-pressure-induced freezing process on the stability of freeze-dried nanocapsules, *Dry. Technol.*, 2008, **26**, 1199–1207.

- 296 F. H. Lin, J. Y. Lin, R. D. Gupta, J. A. Tournas, J. A. Burch, M. A. Selim, N. A. Monteiro-Riviere, J. M. Grichnik, J. Zielinski and S. R. Pinnell, Ferulic acid stabilizes a solution of vitamins C and E and doubles its photoprotection of skin, *J. Invest. Dermatol.*, 2005, **125**, 826–832.
- 297 P. R. Desai, P. P. Shah, P. Hayden and M. Singh, Investigation of follicular and non-follicular pathways for polyarginine and oleic acid-modified nanoparticles, *Pharm. Res.*, 2013, **30**, 1037–1049.

Chapter 8: Appendix I - Supplementary figures

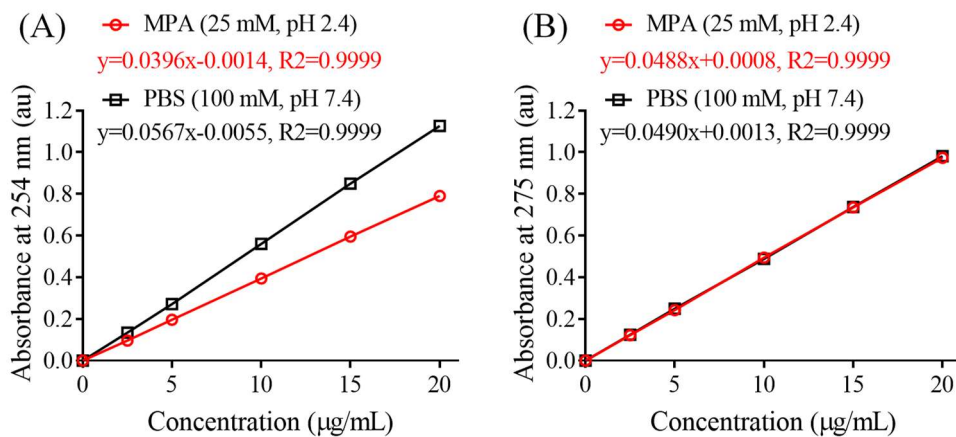


Figure A-1 UV-vis spectroscopy calibration curve of (A) ascorbic acid and (B) caffeine. Data shown as mean \pm SD, $n=3$.

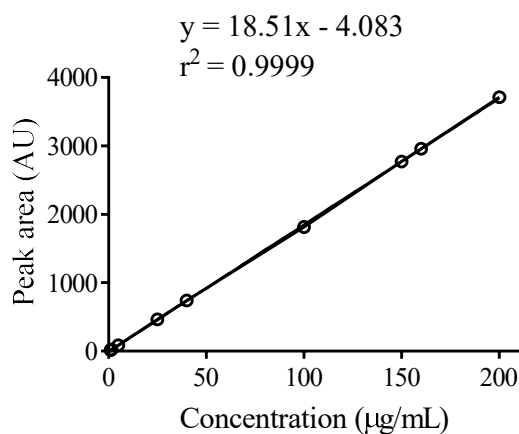


Figure A-2 HPLC calibration curve of ascorbic acid. Data shown as mean \pm SD, $n=6$.

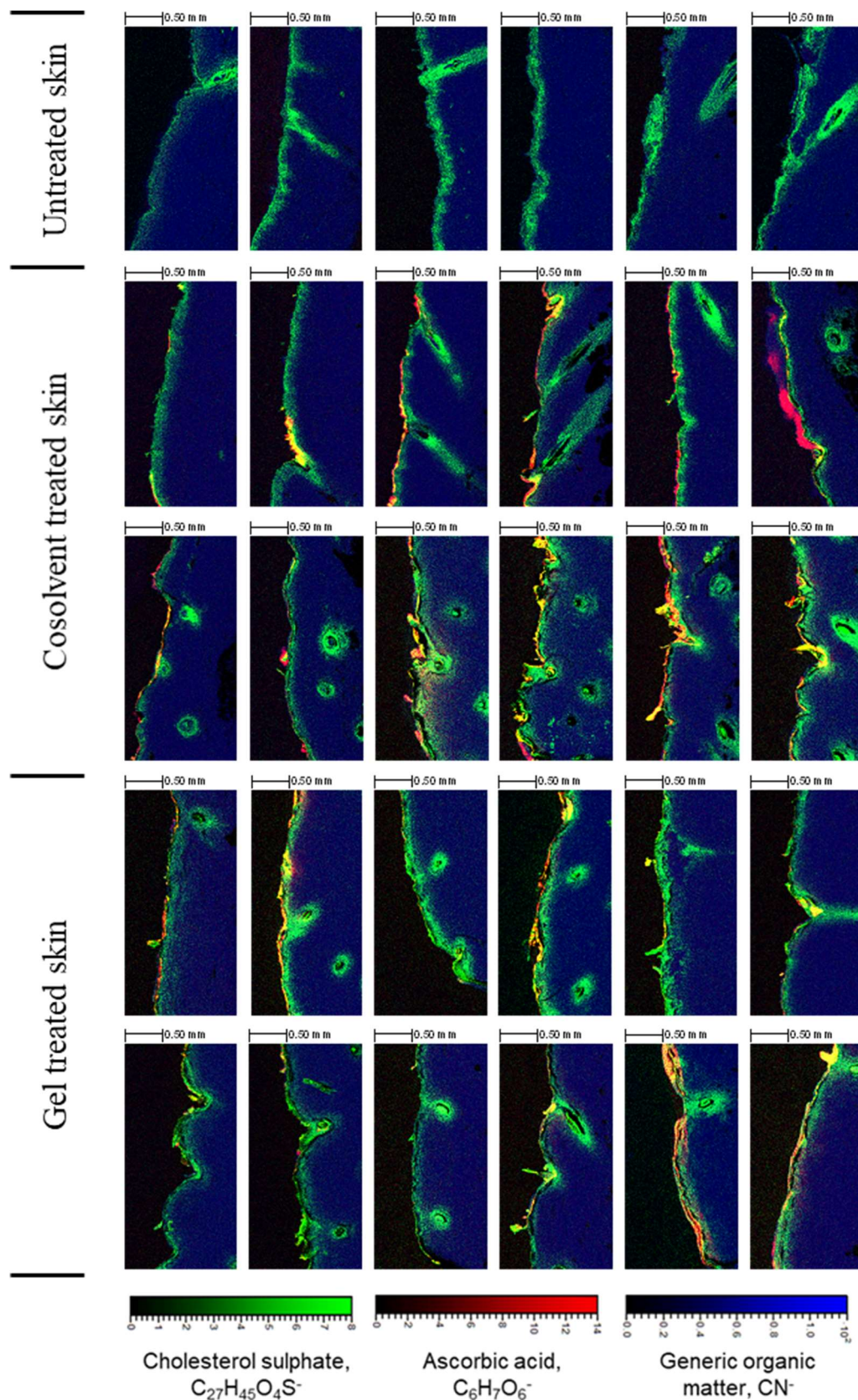


Figure A-3 ToF-SIMS images of excised skin cross sections, highlighting the spatial distribution of ascorbic acid ion $C_6H_7O_6^-$ (red) after treatment with cosolvent and gel formulation ($n=6$ biological donors).

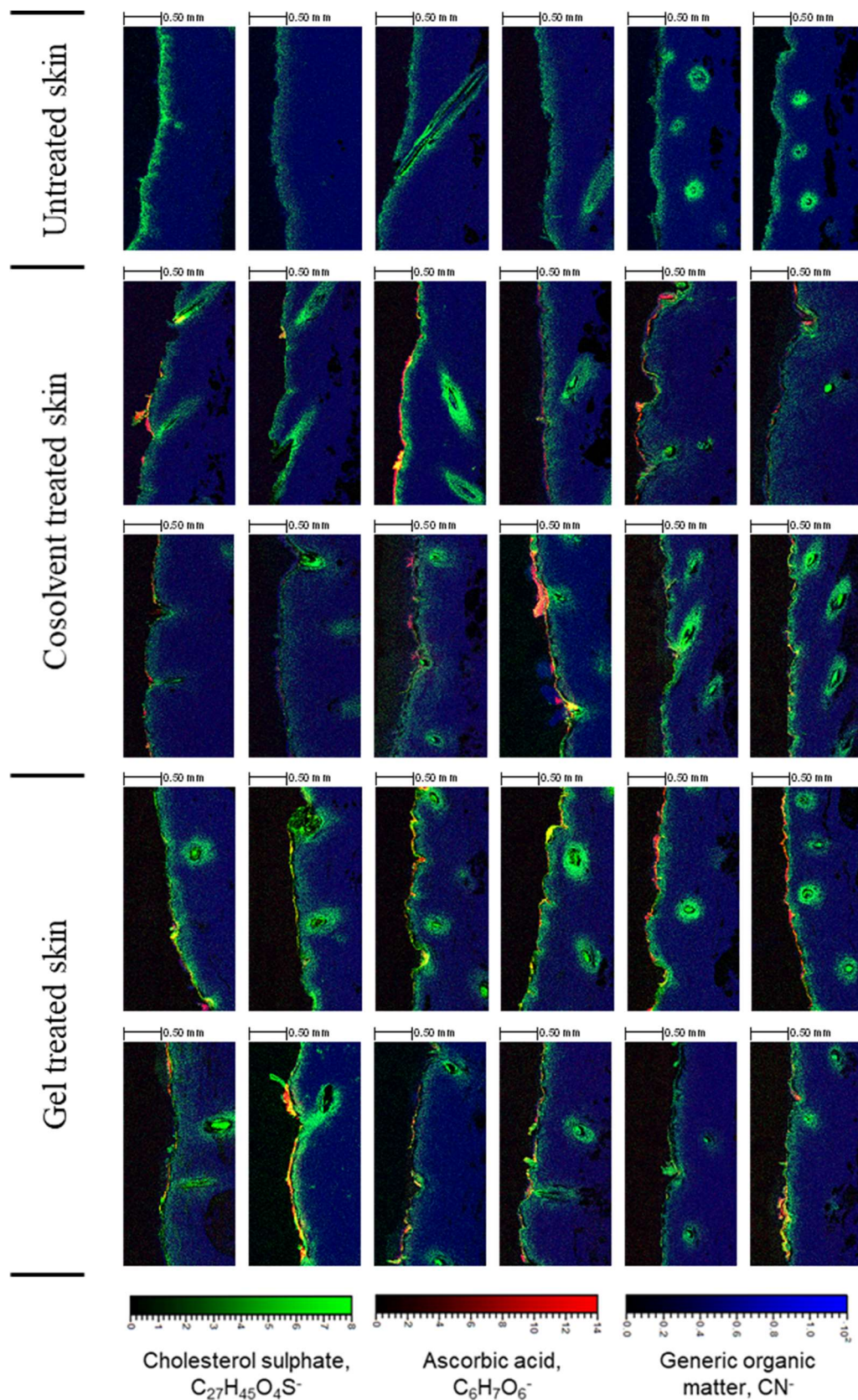


Figure A-4 ToF-SIMS images of intact skin cross sections, highlighting the spatial distribution of ascorbic acid ion $C_6H_7O_6^-$ (red) after treatment with cosolvent and gel formulation ($n=6$ biological donors).

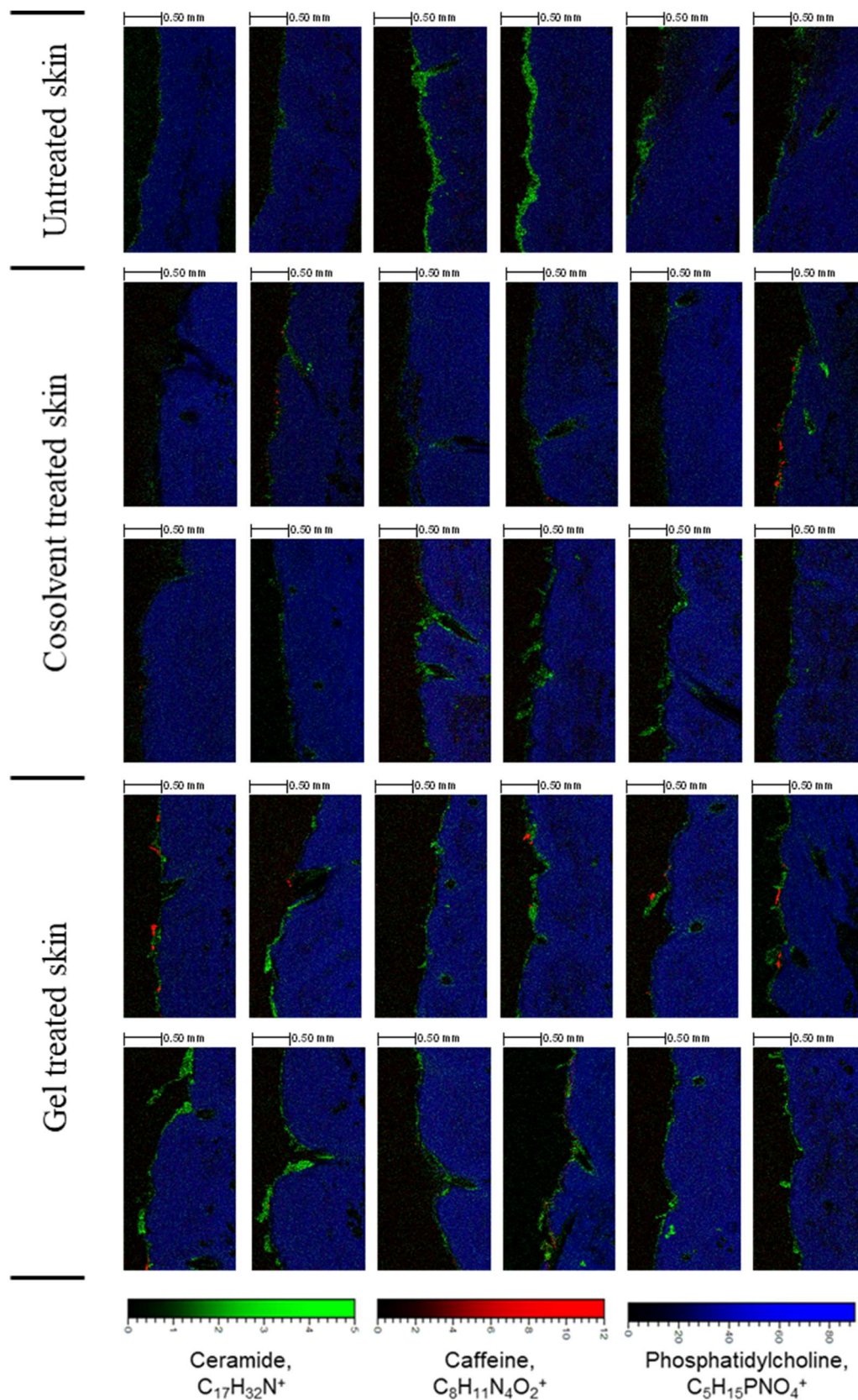


Figure A-5 ToF-SIMS images of excised skin cross sections, highlighting the spatial distribution of ascorbic acid ion $C_8H_{11}N_4O_2^+$ (red) after treatment with cosolvent and gel formulation ($n=6$ biological donors).

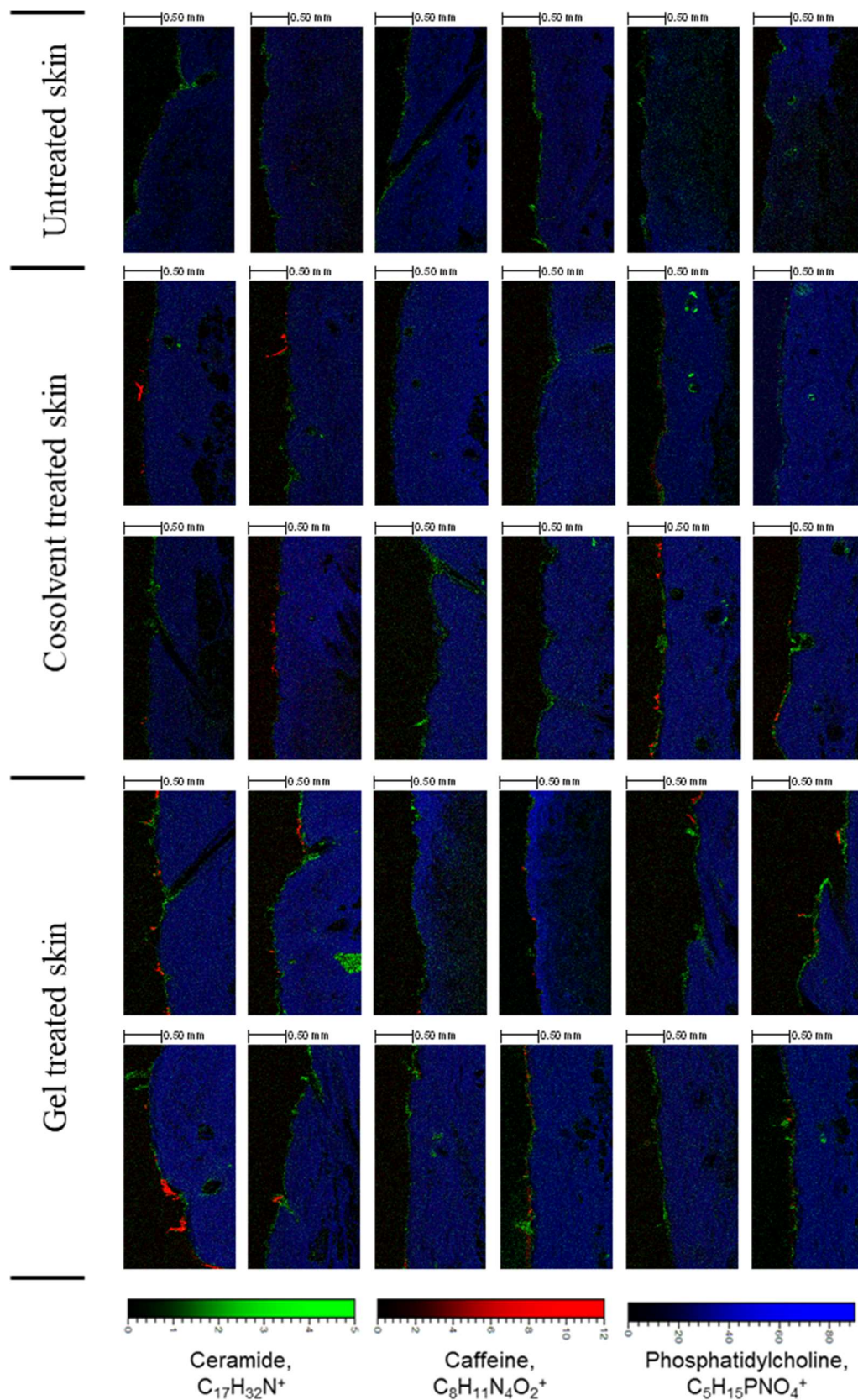


Figure A-6 ToF-SIMS images of intact skin cross sections, highlighting the spatial distribution of ascorbic acid ion $C_8H_{11}N_4O_2^+$ (red) after treatment with cosolvent and gel formulation ($n=6$ biological donors).

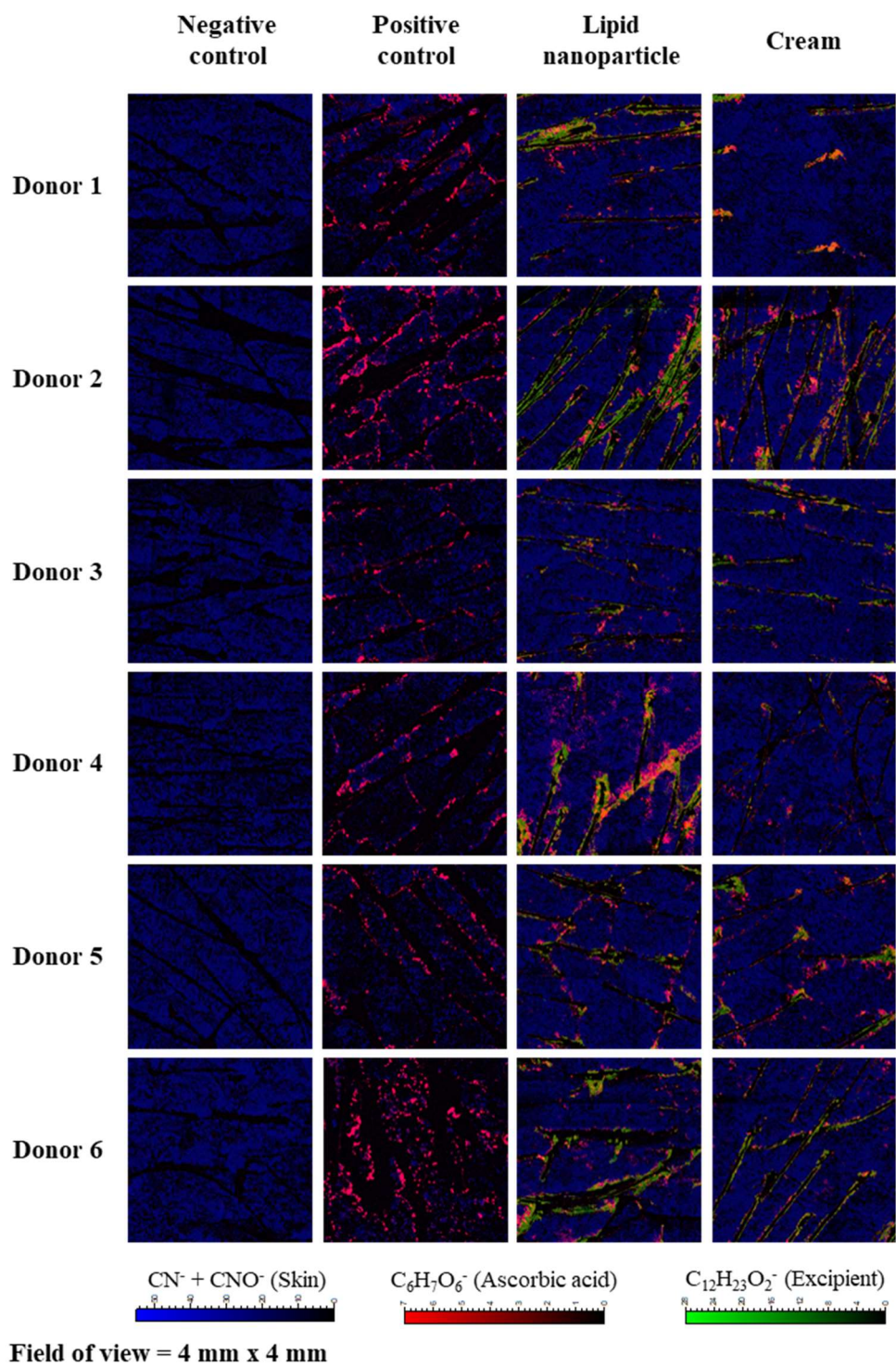


Figure A-7 ToF-SIMS images of porcine tape strips collected at a SC depth of approximately $3.2 \mu\text{m}$ highlighting the distribution of ascorbic acid ($\text{C}_6\text{H}_7\text{O}_6^-$, red) from test formulations.

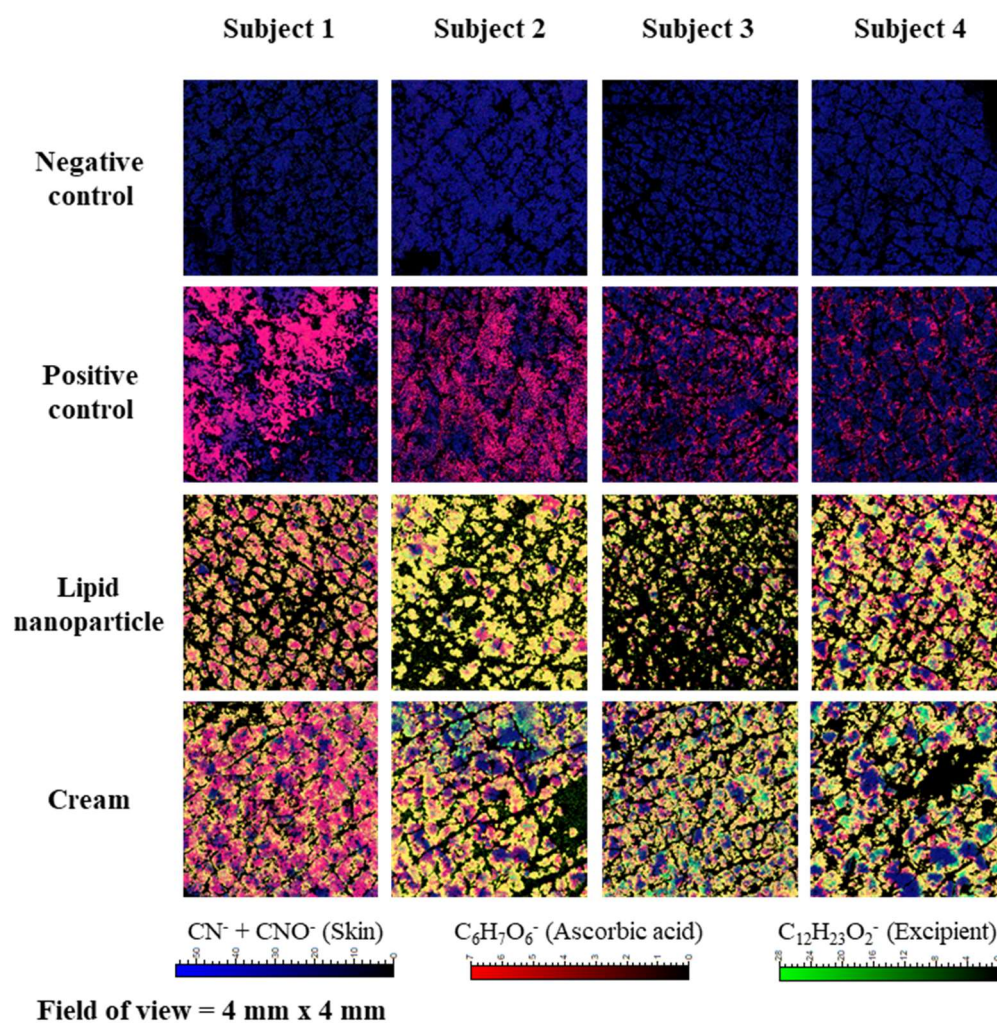


Figure A-8 Thresholded ToF-SIMS images of human tape strips collected at a SC depth of approximately $0.7 \mu\text{m}$ (tape strip no. 3) highlighting the distribution of ascorbic acid ($\text{C}_6\text{H}_7\text{O}_6^-$, red) from test formulations.

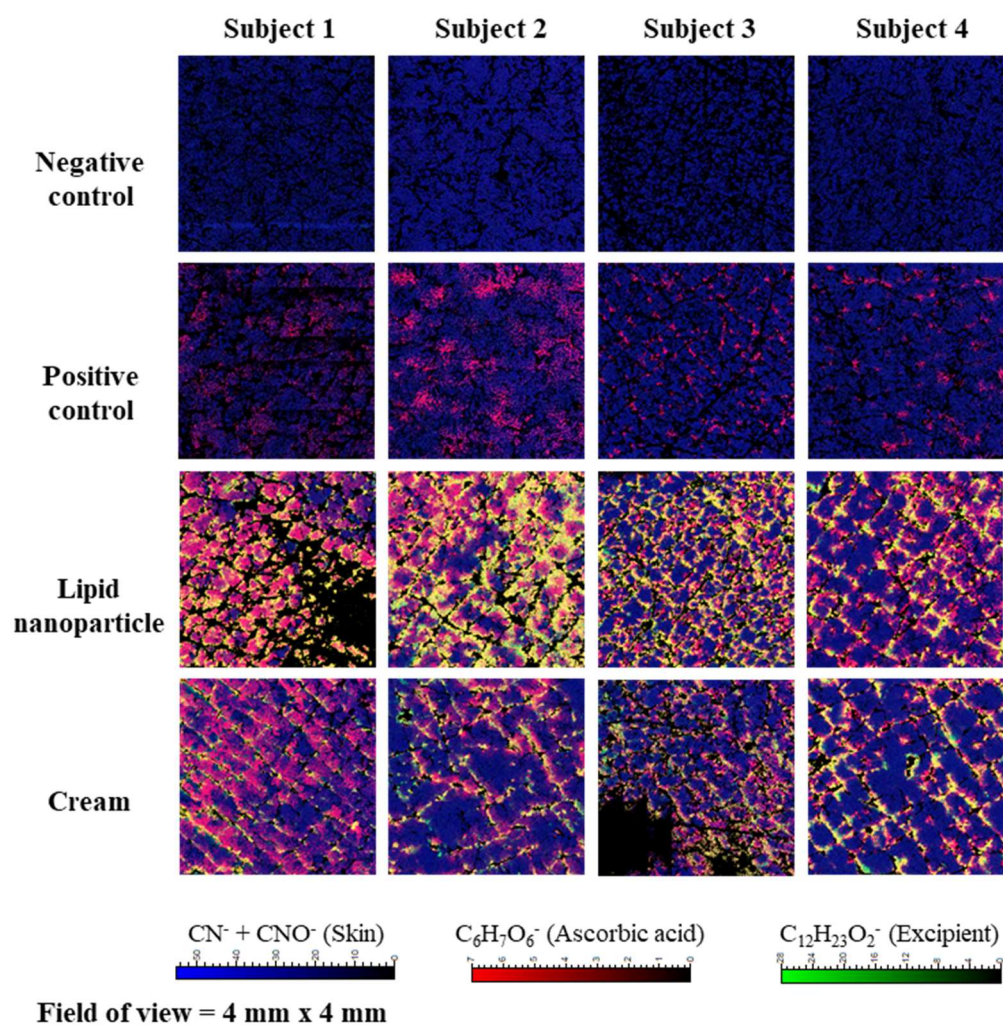


Figure A-9 Thresholded ToF-SIMS images of human tape strips collected at a SC depth of approximately 1.5 μm (tape strip no. 6) highlighting the distribution of ascorbic acid ($\text{C}_6\text{H}_7\text{O}_6^-$, red) from test formulations.

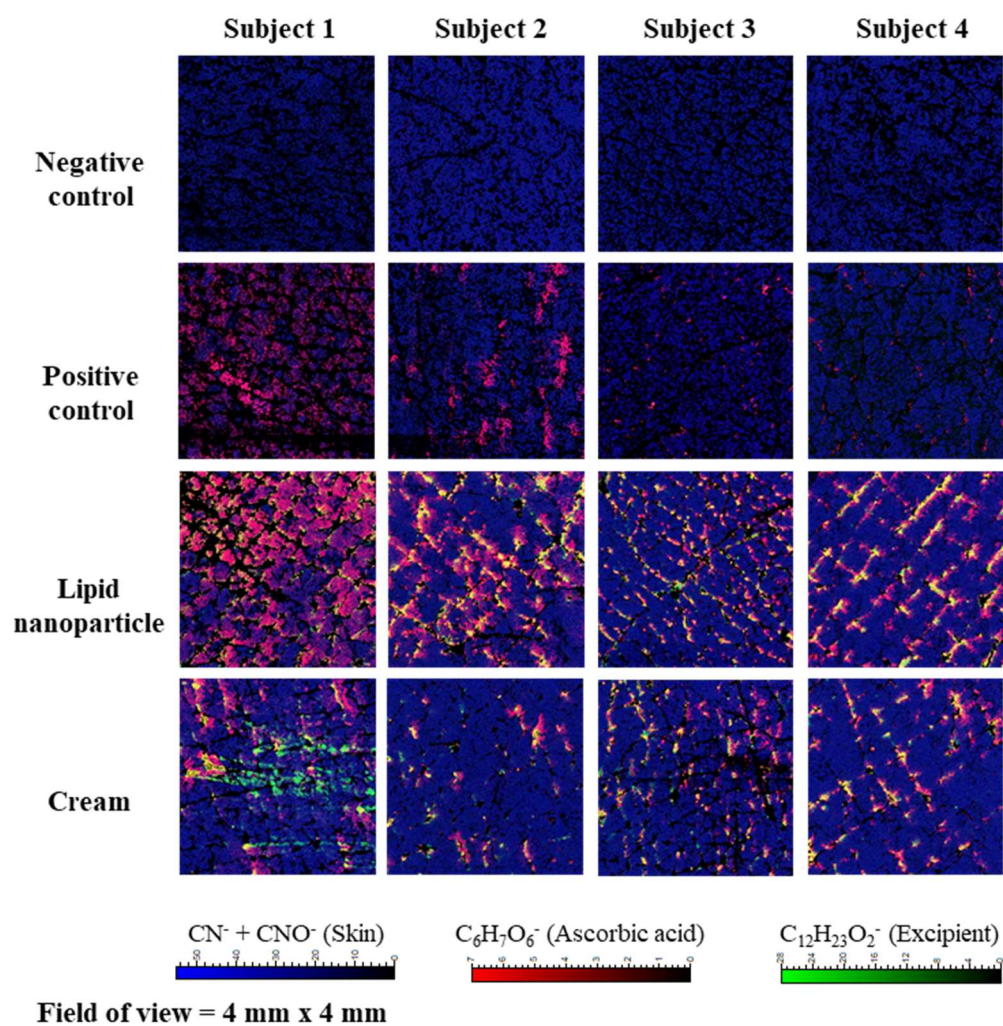


Figure A-10 Thresholded ToF-SIMS images of human tape strips collected at a SC depth of approximately $2.1 \mu\text{m}$ (tape strip no. 9) highlighting the distribution of ascorbic acid ($\text{C}_6\text{H}_7\text{O}_6^-$, red) from test formulations.

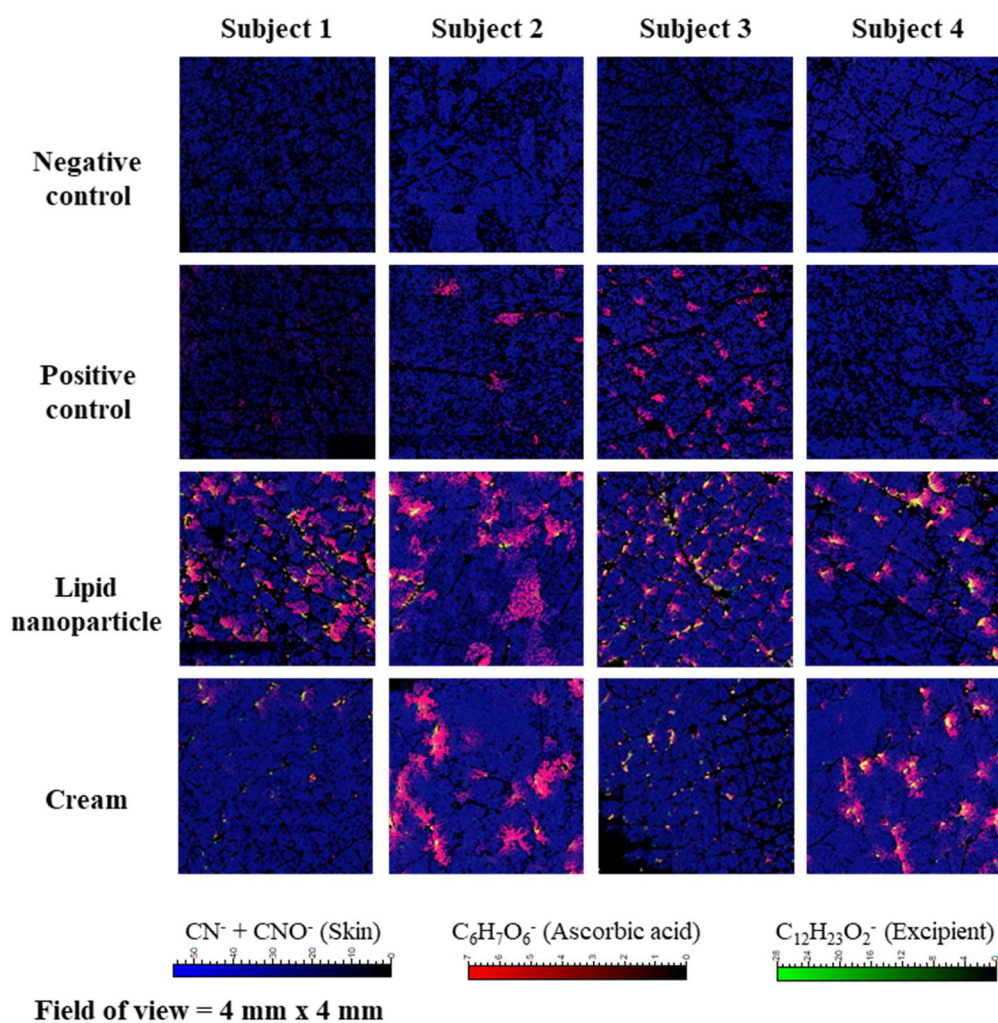


Figure A-11 Thresholded ToF-SIMS images of human tape strips collected at a SC depth of approximately 2.7 μm (tape strip no. 12) highlighting the distribution of ascorbic acid ($\text{C}_6\text{H}_7\text{O}_6^-$, red) from test formulations.

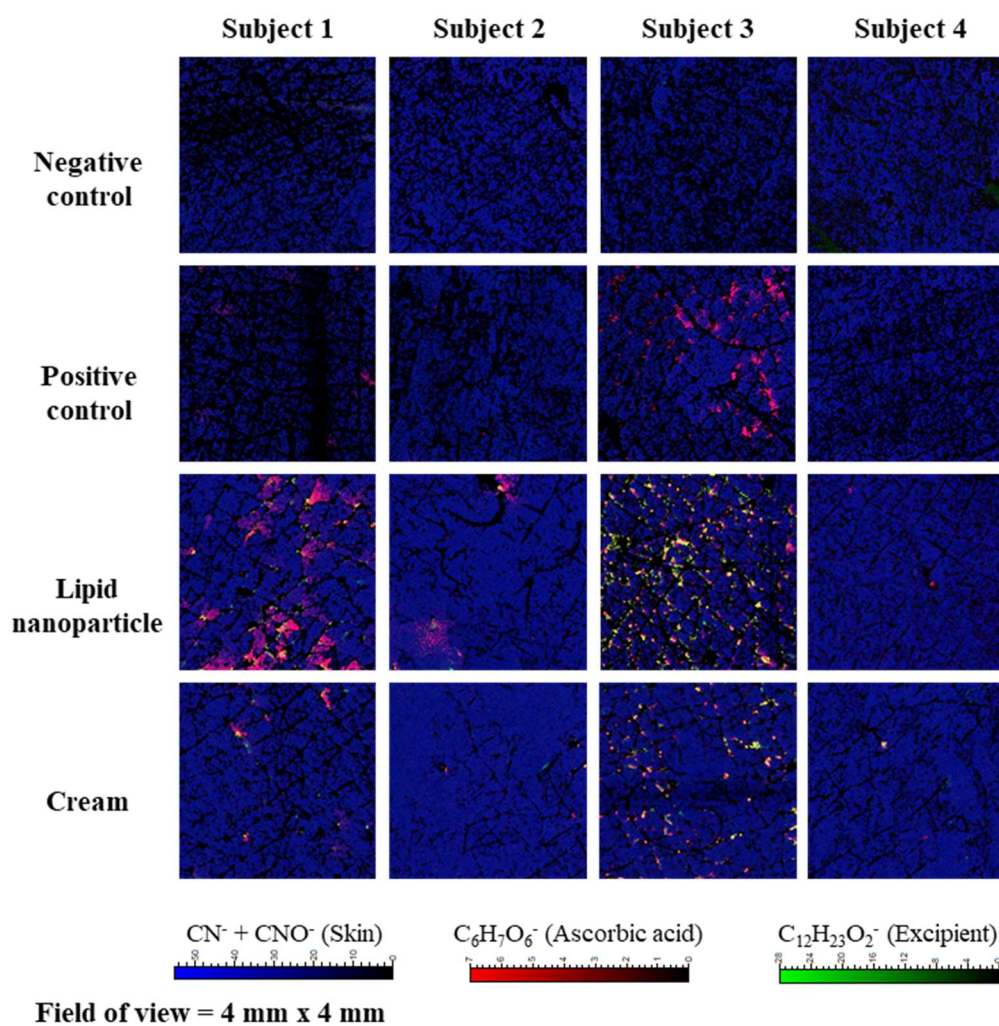


Figure A-12 Thresholded ToF-SIMS images of human tape strips collected at a SC depth of approximately 3.4 μm (tape strip no. 15) highlighting the distribution of ascorbic acid ($\text{C}_6\text{H}_7\text{O}_6^-$, red) from test formulations.

Chapter 9: Appendix II - *In vivo* study ethical approval

Informed consent form:



Informed Consent form

VERSION (01, 18-10-2018)

N ° INOVAPOTEK OF STUDY: PPF7A17

N ° STUDY OF PROMOTOR: NA

SINGLE BLIND STUDY TO COMPARE APPEARANCE OF ASCORBIC ACID (VITAMIN C) IN SKIN WITH DIFFERENT COSMETIC FORMULATIONS

Inovapotek, as sponsor of study PPF7A17 under the title Single blind study to compare appearance of ascorbic acid (vitamin C) in skin with different cosmetic formulations, invites you to participate in this clinical study.

The objectives, the mode of application, methodologies, risks and benefits are described in the following table and will also be transmitted orally.

Summary description	<p>The aim of this study is to compare how different type of cosmetic formulations, containing ascorbic acid (vitamin C), behave across the outermost layer of the skin. The secondary objective is to evaluate the occlusive (barrier) effect of the same formulations.</p> <p>In this study, all participants will test 2 control products, 1 investigational product and 1 comparator product.</p>
Area of application	Inner side of both forearms
Mode of application of the product	A single application (40-50 mg) of each product will be done in the test area by an Inovapotek Research Assistant / Technical Assistant.
Methodology	<p>The test is performed according to the following methodology:</p> <p><u>a) 1st visit (recruitment)</u></p> <p>- Study explanation and verification of inclusion and exclusion criteria.</p> <p><u>b) Day 1 (2nd Visit)</u></p> <p>- Participants should go to Inovapotek facilities where they will be accommodated in a controlled temperature and humidity room for 20 minutes. On this visit, participants will have to stay at Inovapotek facilities for about 2h 30min.</p>

	<ul style="list-style-type: none"> - After acclimatization time, 4 locations (skin test sites) will be marked inside the participants' forearms using a self-adhesive plastic covering (Sadipal®). - Initial measurements (see Measurements) will be performed at the 4 designated locations. - In the 4 marked places will be applied by the investigator, or by someone designated, the different products to be tested (see Mode of application of the product). - 1 hour after application of the products will be made new measurements on site. - After 1h application of the products, the remaining product on the skin surface will be wiped off with a sponge. - Tape stripping will be performed using Corneofix® tapes, taking up to 15 sequential tape strip layers from each test site. The tape strips collected will then be analysed to determine the amount of ascorbic acid present in the outermost layer of the skin. - After the previous procedure, new measurements will be taken in the same skin location.
Measurements	<p>To evaluate the effectiveness of the test products the following evaluations will be made:</p> <ul style="list-style-type: none"> - Evaluation of transepidermal water loss with Tewameter® equipment before product application, 1 hour after product application and after removal of 15 tape strip layers - Skin surface temperature measurement using an infrared camera (FLIR® E60) 20 minutes after the start of the acclimatization period.
Risks	<p>The occurrence of adverse reactions is not expected, although it may occur.</p> <p>Irritation reactions may occur after the tape stripping which will be confined to the area of the test site locations and be of low intensity. Expected redness of the skin, burning and stinging sensation where skin damage is caused. During the first 24-48 hours after damage, erythema can be increased, and later the skin will begin to recover. Darkening, peeling and / or scabbing of the skin could be expected during the period of skin recovery. Complete skin recovery may take 7 to 28 days. Transient and mild intensity irritation may be induced by the product ingredients</p> <p>Any appropriate medical follow-up will be provided if any serious adverse reaction.</p>
Benefits	<p>The expected benefit to society is better knowledge of the degree of effectiveness of the cosmetic products under study.</p>
Instructions	<p>- Participants will not be able to apply any other topical product to the inner forearms within 24 hours prior to the study and until the end of the study. Not even cosmetic products like moisturizers, body lotions, shower gel, soaps, etc.</p>

	<p>- Participants should not have applied topical products containing vitamin C to their forearms in the two weeks preceding the beginning of the study and until the end of the study.</p> <p>- Participants should not expose forearms to sun and solariums for the following month after end of study.</p> <p>- In case of adverse reactions, participants should inform the physician to provide all necessary medical support.</p> <p>- Participants should inform the responsible investigators if there are any change in your health or your medication.</p> <p>- Participants should inform investigators if they become pregnant during participation in the study.</p> <p>- Participants should attend the Inovapotek facilities on the scheduled days and times.</p>
Data handling	Each participant is encoded by a numeric key so that their data is kept confidential (no ability to associate data with names).
Safety	The sponsor of the study assumes the responsibility to cover any damages that may be caused to the participant arising from participation in the study (when applicable).
Conflict of interests	Inovapotek is the study sponsor.

Informed consent

By signing this informed consent form, I volunteer to participate in the above experimental study described (Study no. PPF7A17), which will be performed / supervised by the principal investigator (s) Rita Matias.

I declare that the purpose, conditions, procedures and duration of the study have been explained to me, as well as the possibility of adverse reactions and that I was free to ask questions related to the study. I commit to abide by the protocol described above, to apply the study product as described previously, attending the study site at the scheduled time and day. However, I understand that I have all freedom to leave the study at any time without giving any clarification to Inovapotek about the reasons that led me to do so.

I will be able to ask any questions during the course of the study as well as report any adverse effects at any time by calling 91 647 59 55 or 22 030 15 31. I agree to inform Inovapotek if my health or medication changes during the study.

I understand that under certain circumstances the researcher may terminate my participation in the study without my prior consent.

I declare that "I"/" my partner "(depending on whether the participant is female or male) is not" I am "/" is " pregnant, breastfeeding and not "have" / "intends" to become pregnant during my participation in this study.

I understand that I, the study participant, will be identified by a specific code so as not to allow immediate identification. I agree that the data collected during the study can be subjected to computer and statistical treatment by Inovapotek for scientific research purposes and I am aware of that I can access, rectify and / or delete

personal data with respect to me at any time by requesting it from Inovapotek via telephone (22 030 15 31) or email (geral@inovapotek.com), and of which I can report to the Commission National Data Protection Agency (CNPD) any situation in which I believe there is a violation of my rights as the data subject according to Regulation (EU) 2016/679 of 27 April (General Data Protection Regulation, GDPR). Study results related to my participation can be published, however, any information that can identify me will be kept confidential with the study records.

If required by the study methodology, I authorize the capture of photos, videos and audio by Inovapotek, as well as taking biological samples (for example: skin corneocytes, hair, nails, saliva) from me, under conditions that ensure both confidentiality and anonymity, which means no one can recognize me at all.

I consent to inovapotek and / or the sponsor of the study to use in any form, including the dissemination, reproduction, processing of this data for scientific, technical and / or commercial research purposes. I acknowledge that such authorizations are made free of charge. I understand that security measures are taken in archiving and transmitting data (including biological data) to the study sponsor and that only a limited number of contributors will have access to my data. I understand that biological samples will not leave the Inovapotek, except for a laboratory specifically designated for analysis.

I allow non-biological data collected during my participation in the study to be stored for 10 years after the end of the study. I understand that at the end of this time, the documents that allow my identification will be deleted. Other documentation that does not allow data to be associated with me will be destroyed or sent to the study sponsor as agreed. I agree that the data collected during my participation are eliminated at the end of the study.

At the end of this study, I will be compensated for expenses incurred in the amount of _____ (as applicable). If I give up during the study period or if the researcher terminates my participation in the study, I will not receive any compensation, except where this exclusion is directly related to the test product. The bonus will be commensurate with the time of my participation and should be observed on the same day you give up.

Medical expenses not reimbursed, not covered by insurance or other third party will be reimbursed by Inovapotek for the medical treatment of an injury which, in the opinion of the study investigator and the prosecutor, is caused directly by the study trial product or procedures required by the study protocol that would not have been performed as part of my regular medical treatment.

I undertake not to disclose any information whatsoever in connection with this study and the product.

I declare that I have been allowed 24 hours to reflect on my participation in this study before signing this informed consent form.

I agree to participate in this study under the conditions specified above.

I have received a copy of this document and have been informed that a copy will be kept by inovapotek under conditions guaranteeing confidentiality.

Done in duplicate (one copy for the participant)

Participant:

Write: "Read, Approved and Understood"

Full name: _____

Signature: _____ Date: _____

Inovapotek Investigator/ Technical Assistant:

First and last name: _____

Signature: _____ Date: _____

Ethical approval of the clinical study:

 PHARMACEUTICAL RESEARCH ANALYZE. OPTIMIZE	ETHICS COMMITTEE FOR HEALTH – OPINION		
OPINION			
IDENTIFICATION OF THE STUDY			
Title of the Clinical Study:	SINGLE BLINDED STUDY TO COMPARE APPEARANCE OF ASCORBIC ACID IN SKIN FROM DIFFERENT TYPES OF COSMETIC FORMULATION	No. of identification of the Clinical Investigation Plan	FFP7A17
Date of Opinion	27/11/2017		

Upon request of opinion on the above identified Clinical Study, The Ethics Committee for Health of inovapotek has evaluated the following items:

- a) The relevance of the Clinical Study and its Conception;
- b) The evaluation of the benefits and potential risks;
- c) The Protocol, including the study dissemination plans;
- d) The aptitude of the principal investigator and other team members;
- e) The human and material conditions necessary to the performance of the clinical study;
- f) The amounts and modalities of eventual retribution to the investigators and compensations to the study subjects and the pertinent elements of any financial contract established between the promoter and the clinical study centre, when applicable;
- g) The subjects' recruitment modalities;
- h) The existence or not of conflict of interests either from the promoter's side or the investigator involved in the study;
- i) The term and the conditions of the subjects' clinical follow-up after conclusion of the clinical study as well as, when applicable, the term of presumption if higher than the one predicted in nº3 of the article 15 from Lei nº 21/2014 de 16 de Abril;
- j) The procedure to obtain the Informed Consent form, as well as the information to be communicated to the subjects;
- k) The investigator's brochure, when applicable;
- l) The quality of the facilities;
- m) The insurances for promoter's and investigator's liability, if applicable;
- n) The reasoning for the performance of the clinical study in which participate children or adults incapable of giving consent, in the terms of no.2 of article 7 and no.3 of article 8 from Lei nº 21/2014 de 16 de Abril;

Mod.080.01

The Ethics Committee for Health of inovapotek, after the appreciation of all the above mentioned requirements, as well as the answers and additional elements provided by the principal investigator (where applicable), has observed their compliance, and therefore, decides to give a

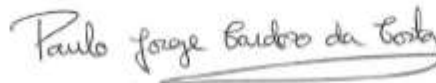
Favourable

Unfavourable

opinion about this investigation.

Inovapotek's Ethics Committee for Health, Porto, 27, November, 2017

Rapporteur Signature



(Paulo Jorge Cardoso da Costa)

All documents and records supporting the clinical investigation are archived at
Inovapotek, Pharmaceutical Research and Development Lda.,
UPTEC, Science and Technology Park of University of Porto, Rua Alfredo
Allen N.º455/461 4200-135 PORTO, PORTUGAL.
for at least 10 years following study end.